GALLIUM SOLVENT EXTRACTION FROM SULPHATE SOLUTIONS USING ORGANOPHOSPHORIC ACID REAGENTS (D2EHPA, OPAP)

by

Indje O. Mihaylov

Department of Mining and Metallurgical Engineering
McGill University
Montreal, Quebec, Canada
September 1991

A Thesis submitted to the Faculty of Graduate
Studies and Research in partial fulfillment
of the requirements for the degree of
Doctor of Philosophy

To my wonderful

family there

Abstract

The subject of this work is gallium extraction from sulphate solutions – an additional source of this metal from hydrometallurgical zinc production – with organophosphorus acid reagents: di-2-ethyl hexyl phosphoric acid (D2EHPA) and OPAP, a mixed extractant consisting of mono- and di-octyl phenyl phosphoric acids. Extraction proceeds *via* cation-exchange and Ga^{3+} is the reacting species. Gallium is extracted with D2EHPA mostly as $GaR_3 \cdot HR$. The results for OPAP suggest existence of four reactions, which form GaM_3, GaM_2D, $GaMD_2$, and GaD_3, this explains and allows prediction of behaviour over a wide range of OPAP compositions. Sulphate complexation causes decrease in concentration of the reacting species, and thus lower D_{Ga} values and extraction rates. Prior knowledge on gallium aqueous complexes is used, and an algorithm developed, to allow quantitative prediction of complexation effects on extraction. The model of mass-transfer with chemical reaction, verified with several known criteria for reaction site determination, describes well the kinetic data for the Ga-D2EHPA system. The model is further developed to account for the stronger acidity and the monomer/dimer equilibria typical for the kind of extractants used. A detailed reaction mechanism is proposed and the first organic ligand addition is found as rate-limiting. The model parameters, estimated from extraction kinetic data, are reasonable, when compared with those obtained for other metals elsewhere. The model's predictions agree with the results from stripping kinetics; the equilibrium conditions (zero rate) can also be satisfactorily predicted, as found by comparisons with the equilibrium data. Ga-D2EHPA and Ga-OPAP systems are compared with an emphasis given to the potential for metal separation; the importance of the ligand exchange rate constant is illustrated with the example of Ga and Al extraction/stripping and their separation based on different rates with D2EHPA.

Résumé

L'éxtraction du gallium de solutions sulphate compose le sujet de ce tr vail—une autre source de ce métal provenant de la production hydrométallurgique du zinc—avec l'utilisation de réactifs d'acides organophosphoriques: acide phosphorique di-2-éthyl héxyl (D2EHPA) et OPAP, un réactif composé d'un mélange d'acides phosphoriques mono- et di-octyl phényl. L'éxtraction est par échange cationique et l'espèce réactive est le Ga^{3+}. Le gallium est éxtrait par le D2EHPA surtout par la formation du $GaR_3 \cdot HR$ Les résultats pour l'OPAP suggére l'existence de quatre reactions formant le GaM_3, GaM_2D, $GaMD_2$, et GaD_3; ce qui explique et permet de prédire la conduite sur une grande variation de composition d'OPAP. La complexation sulphate crée une diminution en concentration de l'espèce réactive, baissant ainsi les valeurs D_{Ga} et les cours d'éxtractions. Des connaissances antérieures sur les complexes aqueux du gallium, ainsi qu'un algorithme composé, sont utilisés pour permettre une prédiction quantitative d'effets de complexation sur l'éxtraction. Le modèle de transfer de masse avec réaction chimique, vérifié par plusieurs critères connus pour le décelage des sites réactifs, décrit bien les données de cinétique du système Ga-D2EHPA. Le modèle est plus développé pour tenir compte de plus fortes concentrations acides et d'équilibres monomères/dimères typique pour les types de réactifs utilisés. Un méchanisme de réaction détaillé et proposé et l'addition du premier ligand et limité par le cours de la réaction. Les paramètres du modèle évalué des données de cinétique de réaction sont raisonnables lorsqu'elles sont comparées avec celles obtenues pour d'autres métaux ailleurs. Les prédictions du modèle sont en accord avec les résultats de cinétique de rééxtraction; les conditions d'équilibre (au cours nul) peuvent aussi être bien prédit, selon des comparaisons avec des données d'équilibre. Les systèmes Ga-D2EHPA et Ga-OPAP sont comparé avec un intérêt particulier pour la séparation des métaux; l'importance du constant de cours d'échange de ligand est illustré avec l'example du Ga et l'éxtraction/rééxtraction de l'Al et leur séparation basée sur des régime différents avec le D2EHPA.

Acknowledgements

First, and foremost, I would like to express my sincere thanks to Professor P.A. Distin, my supervisor, for the encouragement, advice and support he has given me in his own gentle way, throughout the course of this study.

I would like also to thank Professor G.P. Demopoulos for his continuous interest, comments and questions, and his ability to 'up-lift the spirits'.

I am very much indebted to Professor G.D. Kyuchoukov, of the Institute of Chemical Engineering in Sofia, for his trust and support; without his assistance, my coming to study at McGill would have been hardly possible

The National Council for Research and Technologies (Bulgaria) and the National Sciences and Engineering Research Council of Canada are acknowledged for providing financial support.

Thanks are also due to Mr. M. Knoepfel for the precision in making the RDC assembly, and to Professor W.C. Cooper, of the Department of Metallurgical Engineering at Queen's University then, for sharing with me his practical experience with the cell.

I would like also to thank Mr. V. Aprahamian for his invaluable help in translating the abstract in French.

Last, but not least, I thank Mr. V.G. Papangelakis, now a professor at the University of Toronto, who was always present to listen or answer my numerous questions, to ask his difficult ones and to argue, to criticize first and first to encourage—during all these blessed years of sharing WM258.

Contents

List of Figures

List of Tables

Nomenclature

Symbols

A	intercept of line in log D *vs* pH coordinates, eqn (4.9)
A_x	parameter, defined by eqn (4.30) and eqn (4.47)
A_D	Debye-Hückel constant (eqn 5.3)
a	activity [(mol)(length)$^{-3}$]
B_D	Debye-Hückel constant (eqn 5.3)
b_e	empirical constant in the Debye-Hückel equation (eqn 5.3)
b	empirical parameter in eqn (5.9)
C	concentration [(mol)(length)$^{-3}$]
C^{CMC}	critical micelle concentration [(mol)(length)$^{-3}$]
C^{MIN}	minimum surfactant concentration [(mol)(length)$^{-3}$]
C_T	total formal concentration of OPAP [(mol)(length)$^{-3}$]
c	molar concentration [(mol)(length)$^{-3}$]
D	distribution coefficient
$\mathcal{D}$	diffusion coefficient [(length)(time)$^{-2}$]
$\mathcal{D}'$	parameter, defined by eqn (C.37)
d_a	mean distance of approach of ions [length]
E	percent extraction
E_a	activation energy [(energy)(mol)$^{-1}$]
F	formal concentration [(mol)(length)$^{-3}$]
HM	mono-octyl phenyl phosphoric acid (mono-OPAP)
HD	di-octyl phenyl phosphoric acid (di-OPAP)
h	hydration number
I	ionic strength
J_i	flux through interface [(mol)(time)$^{-1}$(length)$^{-2}$]
K_{ex}	thermodynamic equilibrium constant
K'_{ex}	apparent equilibrium constant

K^*	adsorption/desorption equilibrium constant
K_I, K_{II}, K_{III}	equilibrium constants of elementary steps (eqns 6.13 6.15)
K_G	equilibrium constant (eqn 6.16)
K_{eq}	equilibrium constant (eqn 6.17)
K'	equilibrium constant (eqn 6.20)
K_a	acid dissociation constant of extractant [(mol)(length)$^{-3}$]
K_2	second dissociation constant of H_2SO_4 [(mol)(length)$^{-3}$]
K_w	dissociation constant of water [(mol)^2(length)$^{-6}$]
K_d	dimerization constant of extractant [(mol)$^{-1}$(length)^3]
k_f	forward (extraction) chemical reaction rate constant [(length)^3(mol)$^{-1}$(time)$^{-1}$]
k_b	backward (stripping) chemical reaction rate constant [(time)$^{-1}$]
k_w	rate constant of water ligand exchange [(time)$^{-1}$]
M	formula weight
m	molal concentration [(mol)(mass)$^{-1}$]
N_a	Avogadro number [(mol)$^{-1}$]
n	g-ions of H^+ released per g-ion of metal extracted
P	partition coefficient
$\mathcal{P}$	percent of metal transferred to organic phase
R	universal gass constant [(energy)(mol)$^{-1}$(temperature)$^{-1}$]
r	rate of chemical reaction
S_F	separation factor
$\Delta S^\ddagger$	entropy of activation [(energy)(mol)$^{-1}$(temperature)$^{-1}$]
s	solvation number
T	temperature (absolute scale) [temperature]
t	temperature (Celcius scale) [temperature]
t	time [time]
$\vec{u}$	velocity vector
V_B	molar volume of solute at boiling point [length^3]
$\Delta V^\ddagger$	activation volume [(length)^3(mol)$^{-1}$]

x	mole fraction of mono-OPAP
x	distance from interface [length]
z	ionic charge
[ ]	concentration [(mol)(length)$^{-3}$]

Greek Symbols

α	probability for occupation of a ligand site
β	mass-stability constant
Γ	surface excess [(mol)(length)$^{-2}$]
γ	activity coefficient
δ	thickness of diffusion layer [length]
δ_m	thickness of membrane [length]
κ^0	physical mass-transfer coefficient [(length)(time)$^{-1}$]
κ	mass-transfer coefficient in presence of chemical reaction [(length)(time)$^{-1}$]
μ	viscosity [(force)(time)(length)$^{-2}$]
Θ	rate parameter (eqn 6.43)
θ	fraction of occupied adsorption sites at interface [(length)^2(time)$^{-2}$]
ρ	density [(mass)(length)$^{-3}$]
σ	interfacial tension [(force)(length)$^{-1}$]

Subscripts

i	interfacial property
0	bulk phase property
j	component
aq	aqueous phase
org	organic phase
ads	adsorbed species

init	initial value

Superscripts

overbar	organic phase property
T	total value
0	value at zero ionic strength

Chapter 1

Introduction

Gallium belongs to the group of so-called 'electronic metals'—used primarily for various electronic devices. The reason is in the specific band structure of its crystalline compounds (mostly gallium arsenide). Such structure provides efficient optical transitions as well as high electron mobilities [1]. Hence, applications of gallium-based devices range from semiconductor lasers and light-emitting diodes to superconducting magnets and digital integrated circuits. The growing importance of these devices in today's technology explains the increased interest in gallium sources, supply, and recovery techniques.

Despite the fact that gallium is relatively abundant element in the earth's crust (more than tin or lead, for example) it is always present in extremely small amounts compared to common metals (especially aluminum, zinc, iron) coexisting in all primary and most secondary sources. This makes gallium recovery a difficult and challenging task.

Solvent extraction is one of the established methods for metal recovery. Its ability to concentrate metals and to perform necessary separations has been extensively demonstrated in process development work and commercial applications.

The most important source of gallium is the sodium aluminate solutions (from Bayer process for aluminum from bauxite ores) which account for about 90 % of its production [2]. Much of the efforts for gallium recovery have been focused in that

area. Here, solvent extraction is used to recover gallium from highly alkaline medium.

Other important sources of gallium are leach residues and flue dusts. Although their contribution in the overall supply of gallium is much less than from bauxites, they are significant as an additional, supplementary source [3]. Sulphuric acid is the common leaching reagent used and gallium, among other metals, reports into the sulphate solution. Solvent extraction is employed for metal recovery and the general suitability of carboxylic and organophosphorus extractants has been recognized.

A major problem here is low gallium extraction at acidity levels of these leach solutions. One approach is to neutralize the solution up to a suitable pH. The other is to try to find extractants and conditions which would result in better extraction This requires understanding the mechanism of the extraction process and the main factors affecting it. Gallium extraction from sulphate solutions has been reported in several studies. There are, however, important questions linking mechanism and performance, which need be addressed. Among them are the following

- What is the effect of the aqueous phase composition and complexation phenomena on the equilibrium metal distribution and on the rates of metal phase transfer
- What are the rates of extraction and stripping and how do they relate to the nature of the metal in question and the extractant
- How this information can be applied to improve metal separation in this type of systems

Given the increasing importance of gallium, it is timely and appropriate to address these questions. Hence, this project was initiated with the purpose of studying the equilibrium and kinetic aspects of gallium extraction from acidic sulphate solutions which will help in understanding the mechanism and phenomena involved and in selecting extractants and conditions for improved gallium recovery.

Two organophosphorus extractants were selected for this study—di-2-ethyl hexyl phosphoric acid (D2EHPA) and octyl phenyl acid phosphate (OPAP), a mixture of mono- and di-octyl phenyl phosphoric acids. Both are commercially available and cheap (approximately US $3 per pound in large quantities). In addition, D2EHPA is perhaps one of the most studied and used reagents for solvent extraction, its physico-chemical properties are relatively well known and comparative data for related extraction systems are available in the literature.

The material will be presented in the following order—in Chapter 2 published research on gallium solvent extraction will be reviewed with an emphasis on extraction from acidic solutions pertinent to hydrometallurgy. Chapter 3 covers details on experimentation while Chapter 4 is where the experimental results will be given and the equilibrium aspects of extraction discussed. In Chapter 5 gallium complexation in sulphate solutions and its effect on extraction performance will be described. Results from the kinetic experiments will then be used in elucidating the mechanism of extraction, viewed as a sum of mass-transfer and sequential chemical reaction steps (Chapter 6). The proposed model will be discussed, its predictions compared with experimental data, and the implications for extractant selection and improved selectivity presented. Finally, in Chapter 7 the overall conclusions from this work will be given and suggestions for further investigations outlined.

Chapter 2

Literature survey

2.1 Introduction

In this Chapter, a general overview on gallium solvent extraction, from the perspective of hydrometallurgical practice, will be presented. First, sources of this metal along with relevant solutions into which gallium is transferred will be described, and existing recovery processes will be noted. Secondly, extraction from alkaline solutions, which has attracted the most attention, will be described. The rest of this Chapter will be devoted to extraction from acidic solutions—chloride, sulphate and nitrate.

2.2 Sources of Gallium and Recovery Processes

Minerals, rich in gallium, are few and very rare. This requires gallium to be recovered as a by-product of other processes. There is only one exception—the Apex Mine in Utah, USA. This old copper mine was reopened in 1985 particularly for Ga and Ge production [4]. Here jarosite is the main host for Ga, containing up to 0.7 wt%, and the average concentration in the ore is 0.030–0.045 wt% [5].

Being similar to aluminum, gallium exists in most aluminum-containing ores and minerals [6], with bauxites being of primary significance. Here, the amount of gallium varies from 0.003 to 0.008 wt% [3]. It is also found in sphalerite within a very wide concentration range depending on the origin of the deposit—from 0.001-

0.005 up to 0.1 wt% [6]. Gallium tends to accumulate in flue dusts, generated during elemental phosphorus production from phosphate rocks (0.03–0.05 wt% Ga [7]), or aluminum electrolysis (0.13 % Ga as Ga_2O_3 [8]), or from coal burning [4].

As a by-product, the potential for gallium recovery from a particular source depends on the demand for the main product. This is the case with both bauxites—for Al, and sphalerites—for Zn.

Bauxites

In the Bayer process for aluminum production, the bauxite ore is first digested with hot 3.5–4.0 M NaOH. Depending on the chemical and mineralogical composition of the ore, this step is carried out at 90–95 °C or at higher temperatures (230–240 °C) in autoclaves [6]. Aluminum and gallium go into solution as sodium aluminate and gallate, respectively. Upon cooling, spontaneous precipitation of $Al(OH)_3$ occurs, accelerated by seed addition of previously produced hydroxide. The remaining so-called 'decomposed' solution is fed back to the digestion step.

Although some gallium coprecipitation takes place, the metal as a whole remains in the alkaline solution due to the higher stability of gallate.[1] In this way the recycling solution is gradually concentrated in gallium and at 0.15–0.25 g/l Ga (as Ga_2O_3) is taken to the gallium recovery unit.

At this point, various methods for gallium separation and recovery have been proposed—those based on partial destruction of the alkaline process solution in order to decrease the aluminum content thus making selective gallium recovery more viable, and those based on direct recovery, so avoiding the disadvantage of producing a non-recyclable solution. One example of the former is the carbonation method [10], involving selective precipitation of part of the aluminum content first, and then gallium concentration by precipitation followed by redissolution in NaOH and electrolysis.

[1] The reason is that gallium is more electronegative than aluminum [9] and as a result $Ga(OH)_3$ is more acidic than $Al(OH)_3$

Direct recovery, without modification to the solution composition, has been proven feasible in two cases—electrolysis using agitated mercury cathode [11], and solvent extraction with an alkylated 8-hydroxy quinoline as an extractant [12]. The key element in the electrolysis method is to use agitated mercury as a cathode because firstly, as soon as gallium is deposited it is dissolved into mercury thus forming a dilute amalgam in such a way that gallium concentration on the cathode surface is kept low allowing continued metal deposition.[2] Secondly, the different solubility of metals in mercury contributes to increased overall selectivity of the process. Disadvantages of the method are the high price of mercury (considerable amount is necessary for the cathode), its poisonous vapours, and sensitivity to the presence of organic material transferred from the ore to the process solution to the extent that this method has been found inapplicable in processing North American bauxites [10].

Sphalerites

Gallium recovery from zinc leach residues is a more complicated process than from Bayer solutions and the reason is that many other elements are present—iron, aluminum, tin, cadmium, germanium, indium, vanadium, arsenic, etc.

Zinc calcine, produced from roasting the sulphide concentrate, is first subjected to the so-called 'neutral' leach—with weakly acidic sulphuric acid solution [13]. Most of the soluble zinc and other elements dissolve. The pH is raised to about 5 so that ferric iron precipitates as hydroxide—thus removing, either by coprecipitation or adsorption, most of the impurities including gallium. This precipitate is the starting material for gallium recovery.

In the current gallium recovery practice, subsequent solubilization and precipitation steps [14] are first carried out in order to obtain more concentrated gallium precipitates and remove impurities as much as possible. The last solubilization is

[2] In order to have net metal accumulation, gallium concentration in solution must be above 0.3 g/l if solid cathodes are to be used [10], this is more than the actual concentration of 0.15–0.25 g/l

with H_2SO_4, and SO_2 is added so that all iron be maintained as Fe(II):

$$H_2O + SO_2 \longrightarrow H_2SO_3 \tag{2.1}$$

$$2Fe(OH)_3 + H_2SO_3 + H_2SO_4 \longrightarrow 2FeSO_4 + 5H_2O \tag{2.2}$$

The solution is neutralized to pH of about 3 with sodium or ammonium hydroxide and metal hydroxides (presumably not gallium) which precipitate are filtered off. Solvent extraction with Versatic 10 reagent (a carboxylic acid extractant, Shell Chemical) is carried out, followed by stripping of the loaded organic with concentrated HCl. Under these conditions, gallium is in the solution as $GaCl_4^-$, thus readily extracted in the next step by a tertiary amine. The metal is then stripped into NaOH solution and finally recovered by electrolysis.

This process has overcome a number of difficulties previously encountered—tedious filtrations, considerable loss of product, extraction with highly flammable reagents like ethyl ether, etc. Among the disadvantages is the need for neutralizing the solution to a relatively high pH for efficient extraction [15].

Other sources

As mentioned earlier, the Apex Mine is the first and so far only mine primarily for gallium (and germanium) production although not yet fully operational. The process flowsheet [5] involves leaching with sulphuric acid in three counter-current stages during which the elements initially present—Fe, Cu, Zn, As, Ga, and Ge report into a 20–80 g/l H_2SO_4 solution. In the following metal recovery copper is first cemented out with scrap iron, then Ge, As, and any residual Cu are precipitated as sulphides by purging with H_2S. Soda ash is added for neutralization. The filtrate contains almost all of the gallium as well as Fe, Zn, and Al. Solvent extraction is used for gallium recovery from the filtrate. The extractant is D2EHPA in kerosene with tributyl phosphate (TBP) as modifier. In order to prevent simultaneous extraction of iron, SO_2 is sparged to reduce Fe(III) to Fe(II) (cf. reactions 2.1, 2.2). Sulphuric acid

(approx. 80 g/l) is used to strip gallium. This solution is further refined, and final electrolysis yields gallium metal.

Using HCl, Baldwin *et al.* [16] attempted to leach gallium from the mica fraction (400 ppm to 800 ppm Ga) of certain pegmatite tailings. Acid consumption was high, because gallium could not be leached selectively over the aluminum (and potassium) content of the mica. Recently, gallium recovery from coal fly ash and separation from vanadium was reported [17]. Sulphuric acid was used for leaching, while solvent extraction with quaternary ammonium salt, and subsequently D2EHPA, was employed for solution purification and metals separation.

Gallium recovery from flue dust generated in phosphorus production was tried using a sodium carbonate fusion-water leach procedure [7]. Apart from gallium, this material contains mostly alkali and alkaline-earth metals, and also Zn, Al, and Fe. Upon leaching iron was not dissolved, but the solution contained up to 50 times more Al than gallium. This aqueous system is therefore roughly analogous to Bayer solutions, but with very different sodium hydroxide concentrations.

Flue dusts generated in aluminum plants were the subject of another study for gallium recovery [8]. Here, the major metals that gallium has to be separated from, include Al, Fe, and vanadium. Several acids were investigated as leaching reagents, and H_2SO_4 and HNO_3 were found to be superior to HCl. D2EHPA along with two amine extractants—tri-*iso*-octyl amine and Amberlite LA-1 (a secondary amine), were used for extraction and separation.

It should be emphasized that both studies on recovery from flue dusts were on laboratory scale only, and no consideration was given to economic feasibility and industrial implementation. Nevertheless, together with the other processes described, they serve to illustrate the place and important role of solvent extraction among the various unit operations involved in gallium recovery in general.

2.3 Extraction of Gallium from Alkaline Solutions

It is generally accepted that Kelex 100 (Schering/Sherex) and Lix 26 (Henkel Corp.), with alkylated derivatives of 8-hydroxy quinoline as the active component, are the only commercially available extractants suited to direct gallium recovery from the highly alkaline Bayer solutions for aluminum production. Here, solvent extraction must separate small (100 ppm to 300 ppm) amounts of gallium from a large quantity of chemically similar aluminum (40 g/l), these elements being present as $Ga(OH)_4^-$ and $Al(OH)_4^-$ in the roughly 3.6 M NaOH solution.

Leveque and Helgorsky [12, 18] were the first to demonstrate gallium recovery from Bayer solutions into Kelex 100 (HL):

$$Ga(OH)_4^- + 3HL_{(org)} \rightleftharpoons GaL_{3\,(org)} + OH^- + 3H_2O \qquad (2.3)$$

Simultaneously, aluminum and sodium are extracted:

$$Al(OH)_4^- + 3HL_{(org)} \rightleftharpoons AlL_{3\,(org)} + OH^- + 3H_2O \qquad (2.4)$$

$$Na^+ + OH^- + HL_{(org)} \rightleftharpoons NaL_{(org)} + H_2O \qquad (2.5)$$

Under equilibrium conditions, partial selectivity toward gallium loading over that of Al and Na results from relatively high distribution coefficients for gallium (D_{Ga}). Nevertheless only 3-4 % of the extractant's loading capacity is then taken up by this metal, and the reaction is slow. In a typical 'shake-out' test with 8.5 % Kelex 100 and 10 % decanol in kerosene, about 80 % of the gallium was extracted from a 270 ppm feed, this requiring about 3 hours at 28 °C. Here, metal was loaded from 'decomposed' Bayer solution with an Al/Ga ratio of 147, which became about 6.5 in loaded organic [18]. The decanol modifier was needed to avoid third phase formation during acid stripping.

In a series of equilibrium and kinetic studies, Sato *et al.* [19, 20, 21, 22, 23] confirmed the validity of reaction 2 3. Under non-equilibrium conditions, the preferential loading of Ga over Al from Bayer-type solutions has been attributed to relatively

slow aluminum extraction [19], although an alternative interpretation is that Al is extracted first, then stripped by gallium in approaching an equilibrium ratio [24]. D_{Ga} values decrease with increasing temperature [18, 19, 20, 21], and a slight reduction results from 10 % decanol addition [18].

It has been suggested [20, 23] that the reaction path followed for gallium recovery depends on sodium hydroxide level. The rate-limiting step, in absence of mass-transfer limitations,has been attributed to the slow interfacial formation of intermediate activated species such as $Na^+Ga(OH)_3\ OH^-$ at below 1 M total sodium, or $Na_2^+Ga(OH)_3$ at high sodium levels, where gallium extraction is extremely slow. As demonstrated by Pesic and Zhou [26] using synthetic and real Bayer solutions, recovery rates also depend strongly on choice of diluent and modifier.

Given the relatively high Al and Na contents of the loaded organic, production of a high purity gallium strip solution is promoted if Na and Al are selectively acid stripped before gallium [18]. While several acid stripping procedures were investigated, the best method is to strip first with 6 M HCl leaving only Ga in the organic, held by protonated Kelex 100 as $LH_2^+GaCl_4^-$. Subsequently, Ga can be stripped with 2 M HCl. This procedure avoids gallium loss into the primary strip solution, and gives the lowest impurity levels in the secondary strip solution.

Over the years, there have been numerous improvements to the original solvent extraction method for gallium from alkaline solutions with respect to long-term extractant stabilility and improved kinetics To prevent gradual degradation of Kelex 100 due to the high basicity of the medium, Helgorsky and Leveque suggested [27] that alkyl- rather than alkenyl-substituted (as Kelex 100) 8-hydroxy quinolines be used instead. Tests, carried out with a 7-alkyl substituted ($R = C_{11}H_{23}$) 8-hydroxy quinoline showed stable and constant extractant performance even after 1000 hours of operation. However, the rate of gallium extraction with the suggested extractant was not mentioned.

Oxidation of the substituted 8-hydroxy quinoline by atmospheric oxygen was

another reason for decreasing extractant performance. Thus, it was proposed that at least the extraction step be carried out under an inert (e.g., nitrogen) atmosphere [28]. A remarkable 90 % loss of hydroxy quinoline resulted after 500 hours continuous stirring with Bayer solution under air *versus* only 7 % loss under nitrogen. These findings, however, are somewhat confusing since no detectable degradation was reported in the previous patent [27], when using the same extractant (7-alkyl substituted 8-hydroxy quinoline, R = $C_{11}H_{23}$) for a longer time, and presumably, under air.

A relatively new method for increasing reaction rates, based on deliberate creation of a 'water-in-oil' microemulsion in the organic phase, has been studied for this system [24, 25, 29, 30]. Working with a pure, synthetic analogue of Kelex 100 in kerosene, Fourré *et al.* [29, 30] have shown that a microemulsion is produced by adding a long chain alcohol (e.g., butanol) and the sodium salt of a long chain carboxylic acid (e.g., octanoate). These additives, acting as surfactants, promote solubilization in the organic phase of large amounts of 50-100 Å water microdroplets with a skin of alcohol, carboxylate and extractant molecules. Factors contributing to increased recovery rates may include increase in interfacial area and, around the skin of the water droplets, a higher local concentration of extractant molecules with more favourable orientation towards extraction than exists in the continuous organic phase [29, 30]. Loading rates up to 20 times faster than obtained by conventional means were reported. Microemulsion formation and enhanced recovery from Bayer solutions has also been demonstrated using Kelex 100, dodecanol and Versatic 911 in kerosene [24].

Most probably, the formation of microemulsions was also the reason for accelerated gallium recovery in several other reported cases of Kelex 100 being used in a mixture with various carboxylic [31] or organophosphorus acids [32, 33], organic sulphates or sulfonates [34], together with a long-chain alcohol. However, use of organic acids in contact with highly alkaline Bayer solutions raises the question of increased aqueous solubility and substantial organic losses, which in turn would lead to changes

in composition of the mixture during continuous operation.

Attempts to find a reagent which loads gallium from Bayer solution both more rapidly and with better selectivity than Kelex 100 have been unsuccessful. Uhlemann and Mickler [35] have studied extraction by various bidentate ligands (e.g., β-diketones, 8-quinolinols), and concluded that only 7-alkyl 8-hydroxy quinolines (Kelex 100) are suitable for highly alkaline solutions. Other work has focused on changing the nature or substituent position of the alkyl group (from 7- to 5-) on the 8-quinoline structure [36, 37, 38]. When compared with Kelex 100, most of these alternatives showed poorer selectivity for gallium recovery over that of aluminum, while all were slower extractants.

Apart from 8-hydroxy quinoline extractants, others have also been proposed. In the early 1970's, Bretèque and Beerli [39] patented a process where acetylacetone is used to extract gallium. The results showed fast and high gallium recovery from Bayer solutions. However, possible aluminum co-extraction as well as extractant losses due to aqueous solubility were not discussed.

2.4 Extraction of Gallium from Acidic Solutions

2.4.1 Chloride System

It has long been recognized that gallium is readily extracted from strongly acidic chloride solutions. The reason is the formation of $GaCl_4^-$ complex, extractable *via* ion-pair association (anion-exchange), or by solvation as $HGaCl_4$ with several groups of organic reagents—ethers, ketones, amines. Ferric iron forms analogous chloro complexes and therefore is co-extracted if present. Aluminum forms $AlCl_4^-$ but this complex can exist only in non-aqueous media because of hydrolysis [9]. Hence, aluminum would remain unextracted.

In probably the first ever report on gallium solvent extraction, Swift [40] showed that, from 6 M HCl, gallium can be loaded selectively into di-ethyl ether over

virtually any probable co-existing elements, except Ge and Fe(III). Several ethers (di-ethyl, *iso*-propyl, butyl, amyl, etc.) have been studied [41] for gallium extraction, and maximum recovery is obtained at 6–7 M HCl. Beyond this acidity level, recovery decreases due to competitive acid extraction [42, 43].

The high distribution coefficients achieved for gallium, fast kinetics and the relatively good selectivity made ethers the first extractants introduced in commercial operations in the 1940's [44, 45, 46]. Di-ethyl ether extraction was also used in early processes for treatment of zinc leach residues [14,46]. However, the high flammability of ethers, low boiling point, and considerable aqueous solubility especially in strong acids make them an unattractive choice as commercial extractants.

Gallium extraction with amines is in many respects similar to extraction by ethers but without most of the disadvantages. In studies with several common alkyl amines (e.g., tri-*iso*-octyl amine), Good *et al.* [47, 48], and Sato *et al.* [49] have deduced from extraction isotherms and analyses of fully loaded organic phases, that gallium is loaded in the form of $R_3NHGaCl_4$. Both $GaCl_3$ and $GaCl_4^-$ have been postulated as being the principal extracted species although the latter is the most probable alternative. Analysis of extraction equilibria in these systems is complicated by simultaneous acid co-extraction and resulting polymerization in the organic phase [50].

Gallium is also extracted [47, 49, 51] as $GaCl_4^-$ into quaternary ammonium salts (e.g., tri-capryl mono methyl ammonium chloride—Aliquat 336):

$$GaCl_4^- + R_3R'NCl_{(org)} \rightleftharpoons R_3R'NGaCl_{4\ (org)} + Cl^- \qquad (2.6)$$

For both types of reagent, extraction is rapid, and increases with increasing chloride concentration, D_{Ga} reaching a maximum at between 6 M and 10 M chloride depending on the extractant used. Of the reagents studied by Good and Holland [47], tri-*n*-hexyl amine gave the highest recovery with $D_{Ga} \approx 100$ at an optimum 6 M chloride when extracting into 0.2 M tri-*n*-hexyl amine (in toluene).

The high distribution coefficients that can be achieved in extraction with

amines, and therefore the opportunity to concentrate gallium, have made these extractants suitable for application in gallium recovery circuits. Such an example is T2EHA (tri-2-ethyl hexyl amine) used for gallium extraction as a final purification step before electrowinning in recovery from zinc residues. Here, D_{Ga} values of about 101 in 5 M HCl have been achieved [14]. For the same purpose, MIBK (methyl *iso*-butyl ketone) was used in the gallium recovery process from Apex Mine ore [5].

Gallium is extracted with organophosphorus compounds by solvation, while additionally, at low HCl concentrations, the acidic reagents among them extract *via* cation exchange. Studies using tri-butyl phosphate (TBP) [19, 52, 53, 54] established that, with increasing hydrochloric acid level, D_{Ga} rises to a maximum beyond which a decrease is observed. Values of the optimum acidity and associated D_{Ga} depend on gallium and TBP concentrations in the aqueous and organic phases respectively. At low acidity or neutral solutions, the extracted species is $GaCl_3$ in the form of hydrated solvates:

$$GaCl_3 + hH_2O + sTBP_{(org)} \rightleftharpoons GaCl_3.hH_2O\ sTBP_{(org)} \qquad (2.7)$$

where $h \leq 2$, while $s = 1$ under conditions of organic saturation and $s = 2$ at low extractant loading [55]. The rise in extraction with increasing acidity is due to the additional formation of $HGaCl_4$ extracted as a tri-solvate [52, 53, 56]. At above optimum acidity, acid extraction reduces availability of TBP for gallium.

Recovery can also be enhanced by adding a chloride salt such as LiCl or $AlCl_3$ [52, 49]. The effectiveness of the addition increases with increasing charge of the cation, and, for cations of the same charge, with decrease in ionic radius [52]. Recognizing the importance of the free chloride concentration, Reznik and Zekel [56], and Judin and Bautista [57] have developed models allowing D_{Ga} to be predicted over a wide range of conditions for the gallium chloride/aluminum chloride/hydrochloric acid/TBP system.

Gallium extraction with tri-octyl phosphine oxide (TOPO) [58, 59, 49] is similar to TBP regarding dependence on acidity, although at a given level, D_{Ga} for

TOPO is greater than for TBP [49]. At low acidity, the principal extracted species is $GaCl_3$.sTOPO where $s = 1$ or 2 depending on extent of extractant loading, while $HGaCl_4$.3TOPO forms at high acidity [58].

With organophosphoric acids, the dependence of gallium extraction on HCl concentration shows the opposite behaviour to that with TBP. As acidity increases from low values, D_{Ga} decreases to a minimum then rises with further acid addition [60, 61, 49, 63]. In studies at low acidity (0.01 M to 2 M) with D2EHPA, Kimura [64, 65] found that extraction was by cation exchange, a conclusion confirmed by Levin *et al.* [60, 61] with supportive evidence from infrared spectra of the organic phase and its very low chloride content. Subsequently, Sato *et al.* [49, 63] showed that reactions in the low and high acid regions were, respectively:

$$Ga^{3+} + 1.5(HR)_{2\ (org)} \rightleftharpoons GaR_{3\ (org)} + 3H^+ \qquad (< 1\ M\ HCl) \qquad (2.8)$$

$$Ga^{3+} + 3Cl^- + 1.5(HR)_{2\ (org)} \rightleftharpoons GaCl_3.3HR_{\ (org)} \qquad (> 1\ M\ HCl) \qquad (2.9)$$

Solvation reaction 2.9 is promoted by chloride salt addition. It has also been suggested that, at above about 4 M acid, gallium may be extracted as $HGaCl_4$.sD2EHPA complex [60, 61].

Similar extraction behaviour has been observed when carboxylic acids are used [66, 67]. Cation exchange, with selectivity over many common metals, has been demonstrated, but from very dilute acid solutions only (pH > 2.5). Due primarily to the adverse relationship between D_{Ga} and acid concentration, there have been no actual or proposed processes involving gallium recovery from acid chloride solutions using acidic organophosphorus compounds or carboxylic acids.

2.4.2 Sulphate and Nitrate System

Contrary to extraction from HCl solutions, the conditions in H_2SO_4 and HNO_3 solutions are much different. Extractants that are successfully used in acid chloride medium perform poorly here. This is due to the large aquophilic tendency of sulphate and very weak metal-complex formation (if any) with nitrate ions [50]. The

fact that gallium does not form extractable complexes with sulphate as readily as with chloride has been indicated by analytical procedures that require prior chloride addition [68, 69, 70].

Nevertheless, the capability for recovery from acidic sulphate solutions, without chloride, is necessary if solvent extraction is to be compatible with the sulphate systems in the processing of gallium sources. Without a complexing additive, solvent extraction in the sulphate system, using common metallurgical extractants, must rely on cation exchange reaction where a major problem is low D_{Ga} values at acid levels of relevant process solutions. In addition, gallium recovery from nitrate solutions may soon become important with increasing availability of scrapped GaAs chips.[3]

Levin *et al.* [60, 61, 62] have studied the potential of mono-2-ethyl hexyl phosphoric acid (M2EHPA), pyro-2-ethyl hexyl phosphoric acids (P2EHPA), and D2EHPA as analytical reagents for separating gallium from a wide range of elements. M2EHPA and P2EHPA were found to extract gallium at much higher acidities than D2EHPA. Studies on extraction from nitrate solutions with several acidic organophosphorus reagents [71, 72, 74], including D2EHPA in kerosene or toluene, have shown that gallium is loaded by cation exchange with extractant dimers forming $GaR_3.sHR$:

$$Ga^{3+} + \frac{3+s}{2}(HR)_{2\ (org)} \rightleftharpoons GaR_3.sHR_{\ (org)} + 3H^+ \qquad (2.10)$$

where s depends on the organophosphorus acid used and the loading level. The absence of nitrate in the organic phase and the insensitivity of D_{Ga} values to lithium nitrate addition suggested that gallium is not extracted as nitrate complexes [74].

Tian Run-cang *et al.* [75] have described a series of solvent extraction steps, tested in continuous operation, for recovering In, Ge, and Ga from H_2SO_4 solution, containing about 0.16 g/l Ga, and derived from the treatment of a zinc leach residue. Here, P204 (a compound similar to D2EHPA) first selectively extracts indium at relatively high acidity, giving a raffinate at pH 0.3. Germanium is then loaded using

[3]With nitric acid solution to dissolve their gallium content, the highly oxidizing leach conditions would advantageously promote fixation of associated arsenic in insoluble forms.

20 % P204 with 1 % of a synergist (YW 100) in kerosene, YW100 not being identified. After neutralization of this second raffinate to about pH 1.4, and with a slight increase in YW 100 concentration, gallium is recovered into germanium loaded organic. Subsequently, gallium can be selectively stripped using 2.5 M H_2SO_4. Problems with co-extraction of iron can be avoided with prior Fe(III) reduction.

Kikuchi and Kamagami [76, 77] have reported gallium loading from 1 g/l solutions into octyl phenyl acid phosphate (OPAP) and nonyl phenyl acid phosphate (NPAP) in benzene with equilibration completed in about 10 minutes. The potential for practical application of OPAP has recently been shown by Judd and Harbuck [78] who operated a continuous solvent extraction system to process 0.32 g/l Ga (20 g/l iron) solutions at pH 0–0.5, and produced from the leaching of a zinc residue. Here, 0.3 M OPAP in kerosene with *iso*-decanol modifier was used, and the 'milky turbidity' and phase separation problems reported by Kikuchi and Kamagami were apparently not encountered. It was also found that OPAP would load gallium at higher acidity than was possible using D2EHPA. Despite prior ferric reduction with iron powder, a small amount of residual Fe(III) was co-extracted but not totally removed by the 1.5 M H_2SO_4 strip solution used. A phosphoric acid scrub of stripped organic controlled its Fe(III) content to < 0.5 g/l at which efficient gallium loading into recycled organic could be maintained.

There have been only a few attempts to use chelating reagents for gallium extraction from these acidic media. Inoue and Nakayama [73] found that recovery from nitrate solutions into Kelex 100 was by cation exchange, but reaction rates are even slower (several days to equilibrium at 30 °C) than with extraction from Bayer solutions. A probable explanation is that Kelex 100 is a very weak acid.

It appears that these problems can be overcome by using as chelating reagents various aryl- and alkyl- substituted hydroxamic acids.[4] Zhou *et al.* [15] have proposed a process for metal recovery and separation from zinc leach solution. Here a number

[4]This class of reagents has a $O = C - NH - OH$ group responsible for chelation through oxygen from the hydroxy group and nitrogen [50].

of specially synthesized substituted hydroxamic acids were tried as extractants for gallium. Among them, a compound named H106 (a mixture of *neo*-tri-decyl and *neo*-penta-decyl hydroxamic acids) in kerosene showed close to a 100 % Ga extraction (at pH 1.0), and fast kinetics. Extractant stability was improved with a modifier addition, and no degradation was found after 8 hours contact with 6 M HNO_3. However, when contacted with 0.2 M $KMnO_4$ solution (strong oxidant) for the same duration, degradation did occur resulting in about 30 % loss of extractant. This indicates that longer contact times with the solutions of practical significance may be necessary in order to reliably estimate the long-term stability of this class of extractants.

2.5 Summary

Concluding this overview Chapter, the following remarks are presented:

- For gallium, the most important aqueous processing solutions are the alkaline Bayer and the acidic sulphate solutions. Hydrochloric acid solutions are in some instances used in intermediate purification stages. Increasing importance of acidic nitrate solutions is anticipated.

- Solvent extraction plays a significant role in gallium recovery and for each of these media requires a specific type of extractants; those which work well in one system would not do so in another—e.g., amine extractants.

- Alkylphosphoric (mostly D2EHPA) and carboxylic acids are currently used in industrial practice for recovery from sulphate solutions. The potential of OPAP extractant has recently been indicated.

- Despite its significance, few studies exist on the fundamentals of extraction from sulphate (and nitrate) solutions. Little or no attention has been paid to gallium extraction equilibria, kinetics and various associated aspects. This is the subject of the present work.

Chapter 3

Experimental Methodology

3.1 Introduction

The various chemical reagents and the methods of analysis that have been used will be described in this Chapter. Detailed information on the experimental procedures will also be given.

3.2 Reagents

All inorganic chemicals were of analytical grade. Stock aqueous solutions of Ga(III) were prepared by dissolving a given amount of $Ga_2(SO_4)_3$ or $Ga(NO_3)_3$ in distilled water. Both salts were from Aldrich Chemical Co., with at least 99.99 % purity. Because they are hygroscopic the resulting gallium concentration in solution had always to be determined. The respective concentrations of sulphates or nitrates were then found from the stoichiometric formulae. In order to prevent possible hydroxide precipitation, known amounts of acid were added.

Di-2-ethyl hexyl phosphoric acid (D2EHPA) was purchased from BDH Inc. The product information sheet[1] gives 100 % purity. Analysis of several samples from extractant 'as received', by potentiometric titration, showed 97.5–98.0 % D2EHPA and 0.5–0.6 % M2EHPA content by weight. The very low M2EHPA content of

[1]Material Safety Data Sheet, Technical Services, BDH Inc , Toronto, Ontario, November 1988

the BDH-supplied reagent has been noted by Slater [80]. Also, the densities found for purified D2EHPA [81] (973 kg/m^3 at 20 °C and 969 kg/m^3 at 25 °C) agree well with the value of 971 kg/m^3 at 21 °C determined here. Thus, it was felt that special purification steps (e.g., the copper-salt technique [81]) were not needed and the conditioning of the stock extractant solutions was limited only to contacting several times with sulphuric acid solution, then washing with distilled water, and finally filtration through Whatman PS (silicone-treated) filter. Analysis of the extractant solution then gave 0.2–0.3 % M2EHPA, which value is close to the error level of determination. Comparative experiments, carried out several times in the course of this work, showed no noticeable difference in the results obtained with newly prepared and conditioned, or with recycled, extractant solutions.

Octyl phenyl acid phosphate (OPAP) was supplied by Albright & Wilson Americas Inc. This reagent comes as a mixture of mono- and di-octyl phenyl phosphoric acids abbreviated in this work as mono-OPAP and di-OPAP (fig 3.1). From the analysis by potentiometric titration it was found that OPAP consists of 61.5–62.0 mol % mono-OPAP and 38.5–38.0 mol % di-OPAP. As a mixed extractant, changes in its composition during continuous operation are likely to occur. Hence, it was necessary to be able to distinguish between individual contributions from each component to extraction, and a method to separate mono- from di-OPAP was needed. A method has been recently developed [82] for separation of M2EHPA and D2EHPA based on selective precipitation of the barium salt of M2EHPA. With some modifications, this method was adopted here to separate mono- from di-OPAP. Detailed description of the procedure is given in Appendix A.

Kerosene (Fisher Scientific) was used as a solvent for the organic solutions throughout this work. While there were no problems with phase-separation or a third phase formation for D2EHPA-kerosene solutions, such were experienced with OPAP extractants in kerosene. Addition of a modifier was thus necessary and *n*-decanol from Eastman Kodak Co. was used.

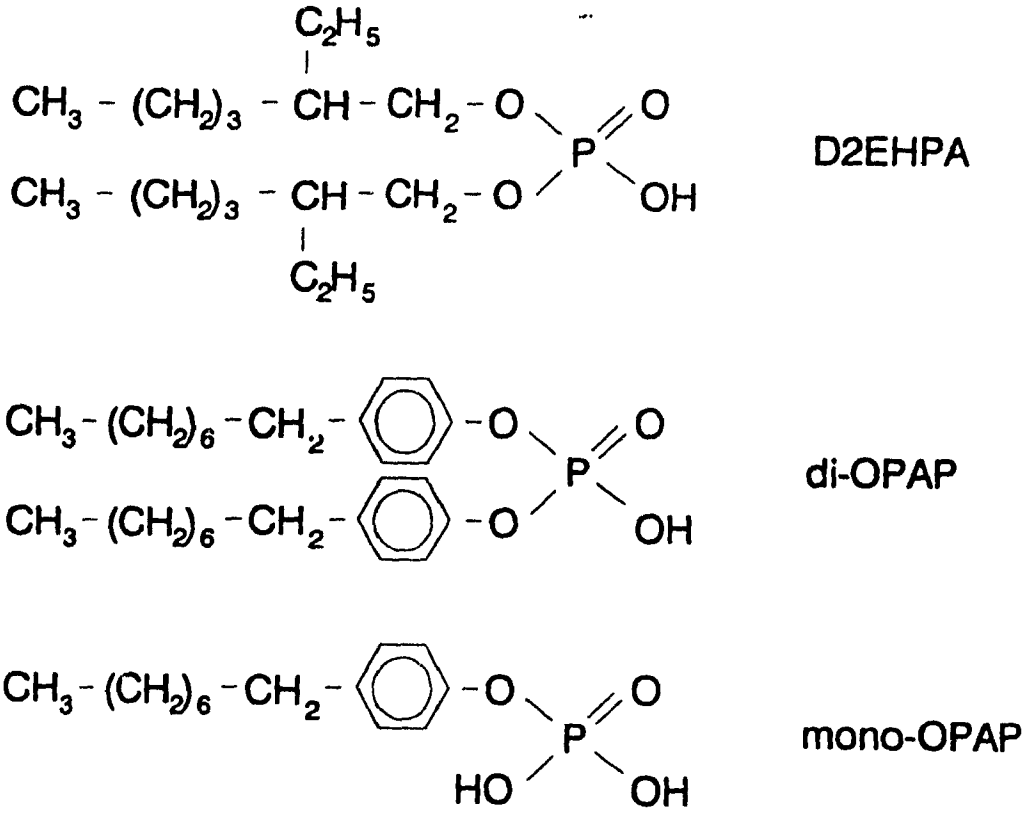

Figure 3.1: Structural formulae of D2EHPA (formula weight: 322), di-OPAP (formula weight: 474), and mono-OPAP (formula weight: 286).

3.3 Analytical Methods

Acidity of the aqueous solutions was determined either by titration with NaOH or in the pH-range—with a pH electrode. Standard solution of 0.1 N NaOH (Fisher Certified) was used for acid-base titrations and was periodically checked against standard 0.1 N HCl (Fisher Certified) solution. All these titrations were carried out with a 10 ml ABU 80 autoburette from Radiometer Copenhagen (three decimal digits, precision ± 2.5 μl). Phenolphthalein was the indicator used in most cases. The pH was measured with a PHM 84 Research pH meter from Radiometer Copenhagen and an ORION ROSS combination pH electrode. The fast response, minimal drift, and the stable, accurate and reproducible readings of the ROSS series of electrodes, according to the manufacturer's specifications,[2] were of primary importance in minimizing the inherent lower accuracy of measurements in the region of pH 1. Calibrations of the electrode were performed regularly with standard buffer solutions (Fisher Scientific, Radiometer, or BDH) of pH values 1.00 and 4.01 for measurements in low pH region (around pH of one), and buffers 7.00 and 4.01 for higher pH and potentiometric titration. The slope was usually 98–101 % of the theoretical response (the Nernst equation).

The pH measurement is very sensitive to even slight temperature variations particularly in the low pH region. Care was taken, especially when measuring in small sample volumes, not to heat the solution from unexpected sources—e.g., from the magnetic stirrer. In general, corrections for temperature were done manually, if necessary, according to the readings from a thermometer immersed into the sample solution.

Metal concentrations in the aqueous solution were determined by flame atomic absorption on a Instrumentation Laboratory spectrophotometer. The flame was nitrous oxide-acetylene mixture. Calibration solutions for gallium were prepared from 995 ppm gallium standard solution in 0.1 % HNO_3 for atomic absorption, from Aldrich

[2]ROSS pH electrode, Instruction manual, Orion Research Inc , 1988

Ga standards (ppm)	measured absorbance	Fitting equation:
Y	A_b	
0.0	0.001	$Y = x_0 + x_1.A_b + x_2.A_b^2$
1.99	0.023	
4.98	0.055	$x_0 = 0.1218$
7.96	0.091	$x_1 = 79.7438$
9.95	0.115	$x_2 = 57.0270$
19.90	0.217	
29.85	0.305	corr. coeff. = 0.9998

Table 3-1: Typical measured absorbance values of gallium standards.

Chemical Co. According to the specifications,[3] the linear response range (concentration *vs* absorbance) for Ga is up to 60 ppm. It was found, however, that in the upper end of this range (above 35–40 ppm) significant deviation from linearity occurred, thus requiring polynomial regression curve fitting. At the same time, stable and linear response was observed for gallium concentrations below 10 ppm down to 1 ppm. Therefore, standard solutions of up to 30 ppm Ga were prepared and used throughout this work. All samples for analysis were prepared to match this range by appropriate dilutions into 0.1 N HNO_3. Nevertheless, a second-order polynomial regression was still used for the standard curve. A typical example of absorbance readings and curve fitting parameters is given in Table 3-1. Background (blank sample) absorbance was monitored during analysis, and if exceeding ± 0.002 units, recalibration was performed and samples were reanalyzed. As a general rule, samples were analyzed at least twice and readings of the standard solutions were taken at the beginning and at the end of the session. Tests for possible interferences and matrix effects were also carried out. Specifically, the presence and concentration levels of up to: 2.5 M H_2SO_4, or 8 M HNO_3, or 2000 ppm Na, or 2000 ppm Al, were checked. Of these, slight suppression of gallium absorbance was noted at 2 M H_2SO_4 and the readings at high sodium concentrations were not very stable. Therefore, for those gallium samples in strongly

[3]Gallium Determination by Flame Atomization, Instrumentation Laboratory Inc., July 1979.

acidic sulphate solutions, standards with a similar matrix were prepared.

Extractant concentrations in the organic phase were determined by potentiometric titration with standard 0.1 N NaOH solution. The autoburette, the pH meter and electrode used are described above. The sample (usually 1 ml) was dissolved in 120 ml acetone (reagent grade) and 22 ml H_2O was added. The titrant was slowly added in small portions under continuous stirring. After each addition, readings of the stable pH and volume of base were taken. In this manner, the well-known S-shape titration curves were obtained when plotted in pH *vs* volume of base coordinates. The equivalent point was determined from the respective first-derivative curve. The obtained results were highly reproducible. Presence of kerosene in the sample had no effect, except that it required a relatively large amount of acetone (120 ml), with regard to the sample volume, because of mutual solubility problems (kerosene-acetone-water). The presence of *n*-decanol in samples of OPAP extractant also had no effect on the titration result. Since mono-OPAP is a di-basic acid, two equivalent points are observed—the first one corresponding to the total concentration of mono- and di-OPAP, the second one being proportional to the mono-OPAP content. Figures 3.2 and 3.3 illustrate characteristic titration curves for D2EHPA and OPAP extractants, respectively.

3.4 Experimental Procedures

Equilibrium experiments

These experiments were carried out in tightly stoppered Erlenmeyer conical flasks (125 ml volume) placed on a wrist-action shaker and at room temperature (21 $\pm$1 °C). Thus, possible losses of solution due to leakage during shaking were prevented. Most of the experiments were performed at O/A (organic-to-aqueous) phase ratio of one. In this case, the sample volume of each phase was 20–25 ml.

A few tests at specifically chosen conditions (two different levels of metal and

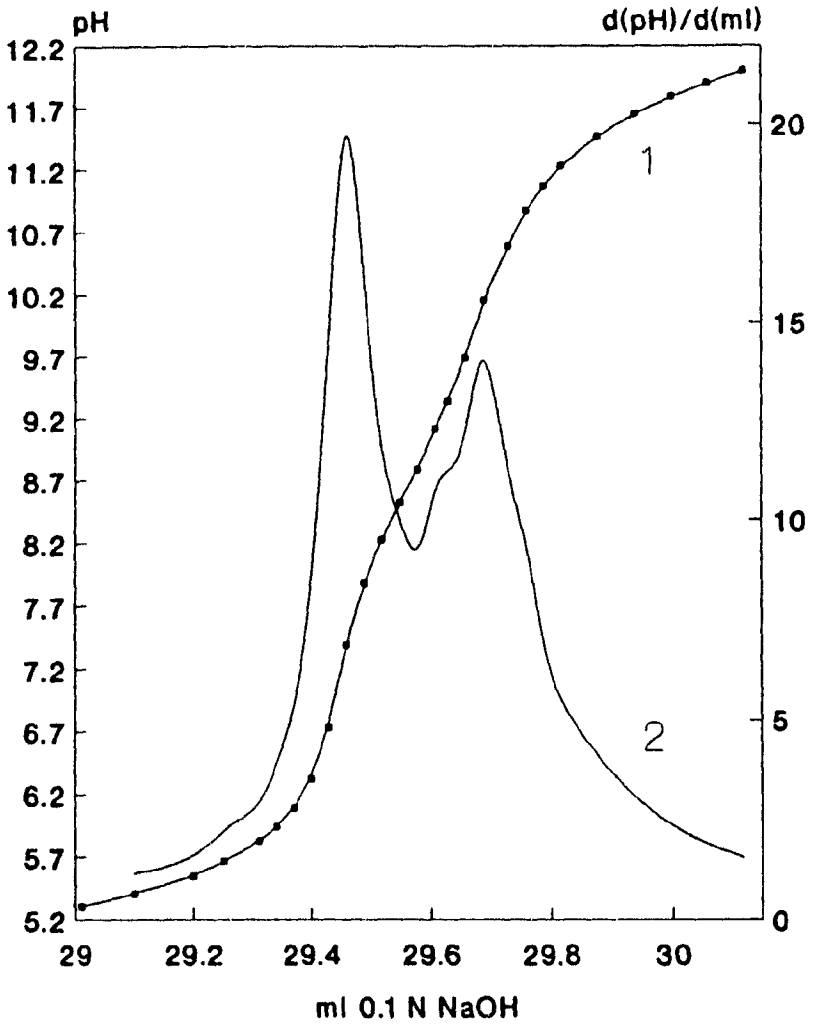

Figure 3.2: Determination of D2EHPA concentration in the organic phase. Titration curve (1), First derivative curve (2).

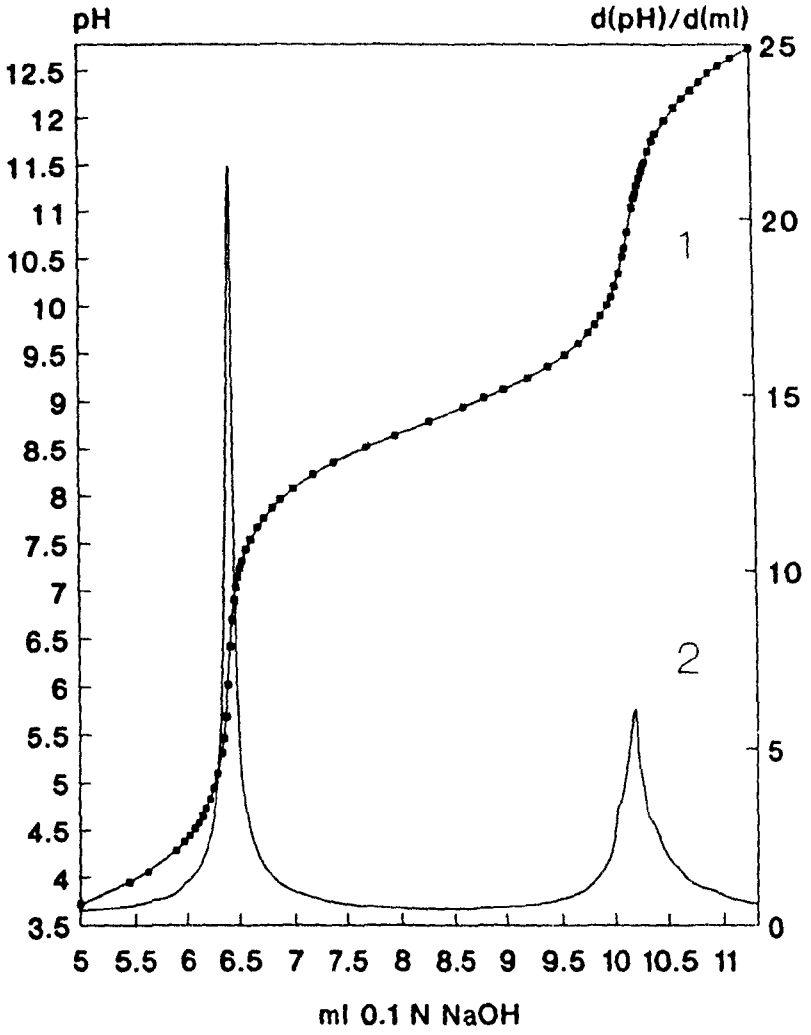

Figure 3.3: Determination of mono-OPAP and di-OPAP concentrations in the organic phase. Titration curve (1), First derivative curve (2).

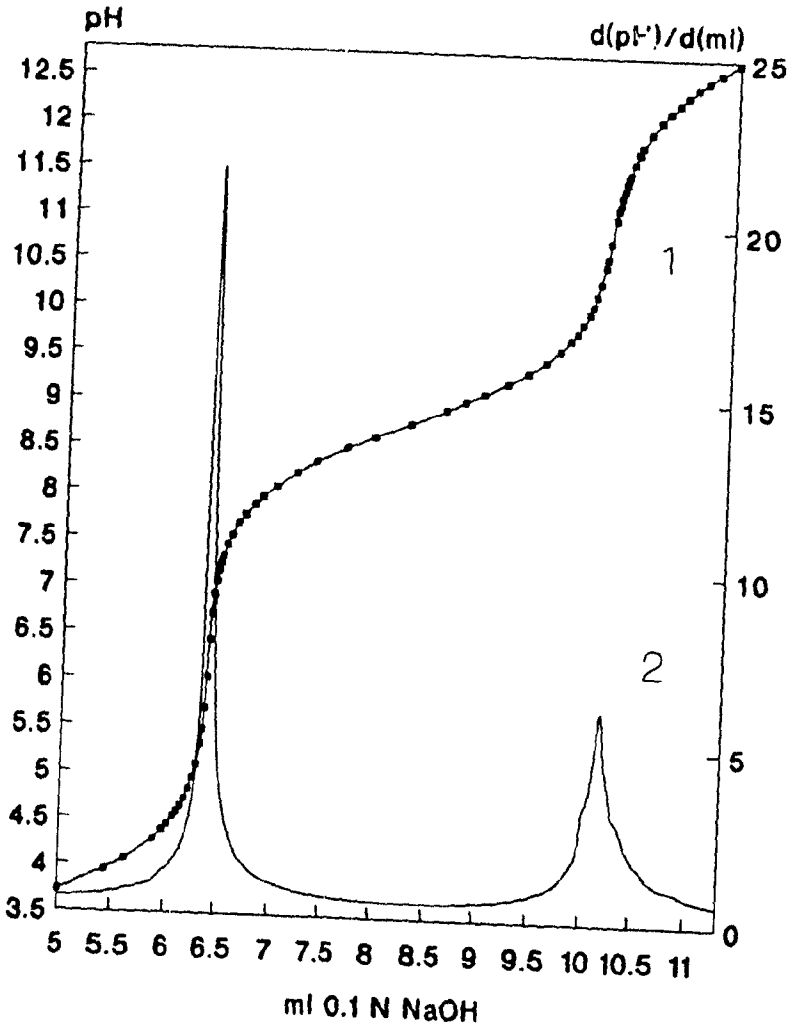

Figure 3.3: Determination of mono-OPAP and di-OPAP concentrations in the organic phase. Titration curve (1), First derivative curve (2).

extractant concentrations, and pH) were carried out in order to check whether change in volume of a given phase during equilibration would occur. No measurable difference was detected.[4] Thus, for the most part, metal concentrations were determined only in the aqueous phase—before and after extraction—and then the respective concentration in the organic phase was calculated from the difference. Occasionally, metal in the organic phase was analyzed after complete stripping into H_2SO_4 solution. The results were in agreement with the mass-balance requirements within the experimental error limits.

Problems with phase disengagement after mixing were not encountered.[5] Nevertheless, care was taken to ensure full separation before analysis. In particular, it is obvious that for highly loaded extractant and low metal concentration in the raffinate, the presence of small droplets of organic material in the aqueous phase may lead to quite erroneous results. Normally, after an experiment, the content of the flask was transferred into a separatory funnel, then the raffinate was filtered through Whatman 2 and Whatman 42 filter paper, with the organic phase filtered through Whatman PS.

Preliminary experiments showed that equilibrium was approached after 15 to 20 minutes mixing time. Considering, however, the strong dependence of rate on the particular conditions, and especially pH, the flasks were usually left shaking for at least 12 hours.

Kinetic experiments

Kinetic studies in this work were performed with a rotating diffusion cell (RDC). This technique was developed and first applied for solvent extraction kinetics by Albery and Fisk [83]. It has been used since for studies in several solvent extraction systems—e.g., copper extraction with oxime [84], nickel, cobalt, and zinc extraction with organophosphoric acid extractants [86, 87, 88, 89].

[4]The minimum detectable volume difference was estimated to be 0.100–0.150 ml

[5]Provided that OPAP is used with addition of *n*-decanol

Here, the two liquid phases come into contact through a thin porous membrane glued to a rotating acrylic cylinder containing one of them and immersed into the other. Part of the membrane may be rendered impermeable, thus producing an inner circle with the desired interfacial area. Inside the cylinder is a specially designed stationary cylindrical baffle made of teflon.

During an experiment, the baffle imposes the hydrodynamics of rotating disc in the vicinity of the inside membrane surface [84, 85]. The flow of the inner liquid is shown schematically with arrows on fig. 3.4, which also gives a general picture of the cell assembly used in this work.

At the beginning of each experiment, a new membrane (Millipore, 0.22 μm pore size) is mounted on the clean and dry cylinder with acrylic glue (made of acrylic turnings dissolved in benzene). Except for a small central circular area (from 8 to 15 mm for most experiments), the rest of the membrane is 'cleared' with solution [85] containing 33 % 1,4 dioxane, 33 % hexane, 33 % 1,2 di-chloroethane, and 1 % water by volume, and becomes transparent when dry. It is essential that this small uncleared area is indeed a well formed and centered circle. The aqueous solution is placed in the thermostated beaker, then the non-cleared area of the filter is wetted with a drop or two of the solvent (kerosene), any excess removed, then the cylinder is lowered until just touching the aqueous surface. The organic phase is added slowly to the cylinder which is gradually immersed into the aqueous solution. The exact position is adjusted so that the hydrostatic pressure of the two liquids is equal at the membrane surface.[6]

The RDC technique has been applied to extraction kinetics of reactions involving cation exchange, i.e., where for every g-ion of metal Me^{n+}, extracted into the organic phase, n g-ions of H^+ enter, in return, the aqueous solution:

$$Me^{n+} + nHR_{(org)} \rightleftharpoons MeR_{n\ (org)} + nH^+ \qquad (3.1)$$

[6]Determined by the difference in densities of the two solutions. The level of the lighter phase—the organic, should be higher. The exact height difference was found by trial and error. The change in pressure when stirred was neglected

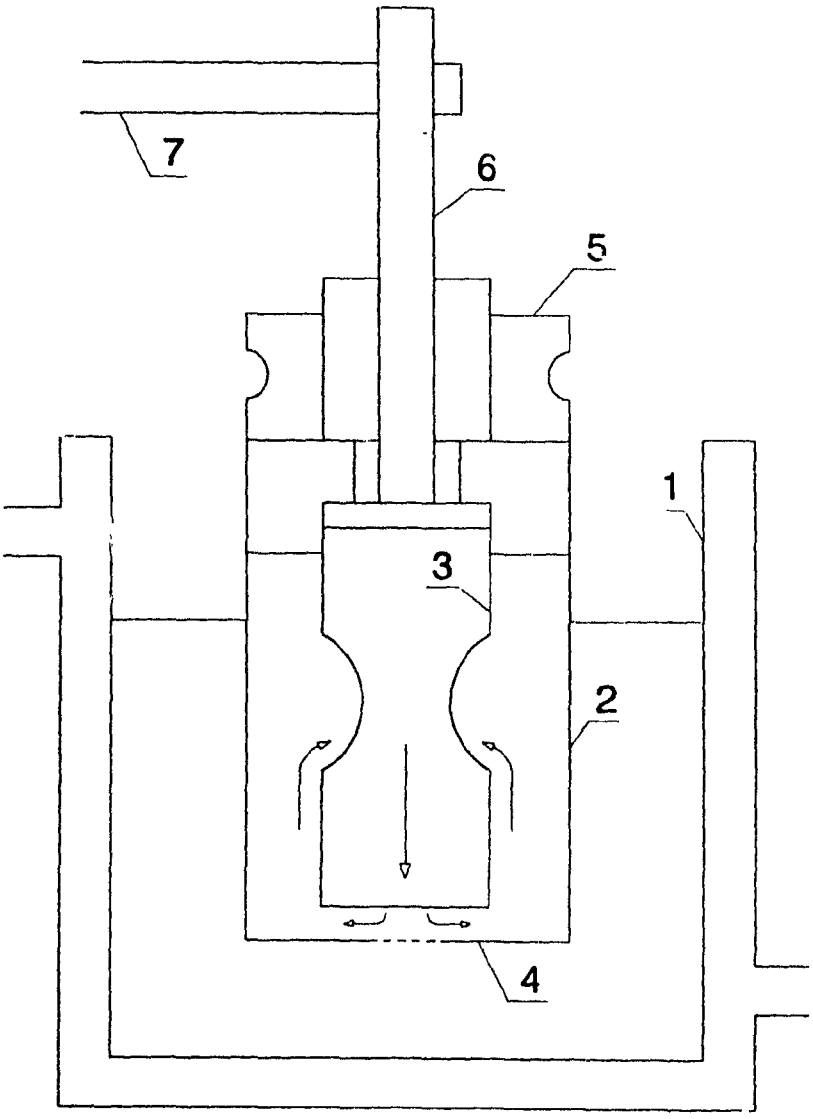

Figure 3.4: Schematic picture of the rotating diffusion cell. 1-thermostated beaker; 2-acrylic cylinder; 3-baffle; 4-Millipore membrane; 5-teflon pulley; 6-hollow steel rod; 7-mounting rod.

Hence, the rate of the reaction is directly related to the pH change with time during the experiment. The pH may be maintained constant by base addition (e.g., NaOH solution) with a pH-stat. In this way, the rate of the extraction reaction can be determined from the recorded rate of base added. This is the idea used in the kinetic studies cited above. There, the pH was continuously measured, the signal fed to a pH-stat, which in turn activated an autoburette for base solution delivery whenever the pH fell below a preset value.

In order to use successfully this fairly simple and straightforward procedure, the following conditions should be met:

- The maintained pH should be high enough so that very small changes in H^+ activity are readily detected.
- The observed pH change should result only from the extraction reaction and not be due to other chemical or physical phenomena.
- The solution chemistry of the aqueous phase should be known as to whether the H^+ activity is (or may possibly be) affected by any reaction other than (3.1).

The first condition is well satisfied if pH is above 3.5–4.0. Problems with the second condition may come from simultaneous physical distribution of the extractant to the aqueous phase and dissociation therein; another one may result from unpredictable change in the liquid-junction potential of the pH electrode due to prolonged continuous use and contamination, thus leading to erroneous readings.

Complications in connection with the third condition can be illustrated with the example of sulphate/bisulphate equilibrium:

$$H^+ + SO_4^{2-} \rightleftharpoons HSO_4^- \qquad (3.2)$$

Clearly, some of H^+ entering the aqueous phase will react to produce HSO_4^-. The situation may be complicated even further if the metal extracted is itself involved in various complexation reactions in the aqueous solution.

For the particular purpose here—kinetics of gallium extraction from acidic sulphate and nitrate solutions—the first and the third condition could not be satisfied. The pH range was from pH 0.6 to pH 1.9, and not only reaction 3.2 would take place but also gallium would be involved in complex formation reactions in the aqueous phase.[7] Only the second condition could be met satisfactorily—because of relatively high acidity the effect of possible extractant dissociation in the aqueous phase on pH would be negligible, as would also be the effect of CO_2 coming from the air and dissolving in the solution—a problem, recognized and solved by purging nitrogen in the case of higher pH [86].

Due to these considerations, the procedure employed here had to be changed. First, there was no need to purge nitrogen into the solution because of the low pH. Second, the idea of following the extraction rate through the base addition had to be abandoned—instead, reaction rate was determined from the amount of metal extracted into the organic phase for a given period of time.

Each experiment was carried out under constant conditions—stirring, interfacial area, pH, metal and extractant concentrations, volume of the two phases (for most experiments—50 ml organic and 250 ml aqueous phase), and temperature--for a specified time, usually 2400 or 3600 seconds.

After the experiment, an exact measured volume of the organic phase (48 ml) was contacted with 2 M H_2SO_4 (usually 30 ml) for complete stripping of the metal. Tests have shown that this stripping with sulphuric acid indeed gave complete back-extraction. The metal concentration in the strip solution was determined by atomic absorption either directly or after proper dilution, when necessary. From the result, the total amount (in moles) of metal extracted was calculated and then divided by the known interfacial area and time to yield the flux of metal (moles per surface area per time) through the interface for the particular experiment.

This procedure, however, will only be correct if the rate of metal extraction

[7]To be discussed in Chapter 5

(i.e., the flux through the interface) is constant for the duration of the experiment. In other words, regardless of the time period (up to a certain limit, of course), the flux must be the same under otherwise identical conditions. This was verified by carrying out several experiments for times ranging from 20 minutes to 2 hours and plotting metal extracted per surface area *vs* time. The result must be a straight line with zero intercept, and a slope equal to the flux.

Such experiments, which will be called here 'linearity' tests, have been carried out on several occasions under different conditions, and acceptably good straight lines with practically zero intercepts have been obtained. Results from one typical example are shown on fig. 3.5.

This linearity is not surprising, since during an experiment the amounts of metal extracted and H^+ produced are very small when compared with their initial amounts present in the aqueous phase.[8] In fact, because of the low pH, there was no need to add base for pH correction. This constancy of reagent concentrations (also in the organic phase) was a prerequisite for the observed linearity. In addition, such tests served as proof of reproducibility of the RDC results. Viewed from another angle, the information obtained by the described RDC method is gained with little disturbance of the system, thus allowing it to remain in a quasi steady-state. This is considered as one of its main advantages.

In the present work, the RDC method was also employed to study the stripping kinetics of gallium from loaded D2EHPA. The initial primary purpose of these experiments was to check the model developed based on the results for the extraction kinetics. The RDC technique has not so far been applied to studies of stripping kinetics with one exception [84]. There, copper stripping kinetics were studied by following the reduction of incoming Cu^{2+} on a ring-disc electrode and measuring the resulting current.

A similar procedure to that described for the extraction kinetics was used

[8] In the most favourable cases—high pH and high extraction rates—the change is no more that 1–1.5 % with respect to the initial

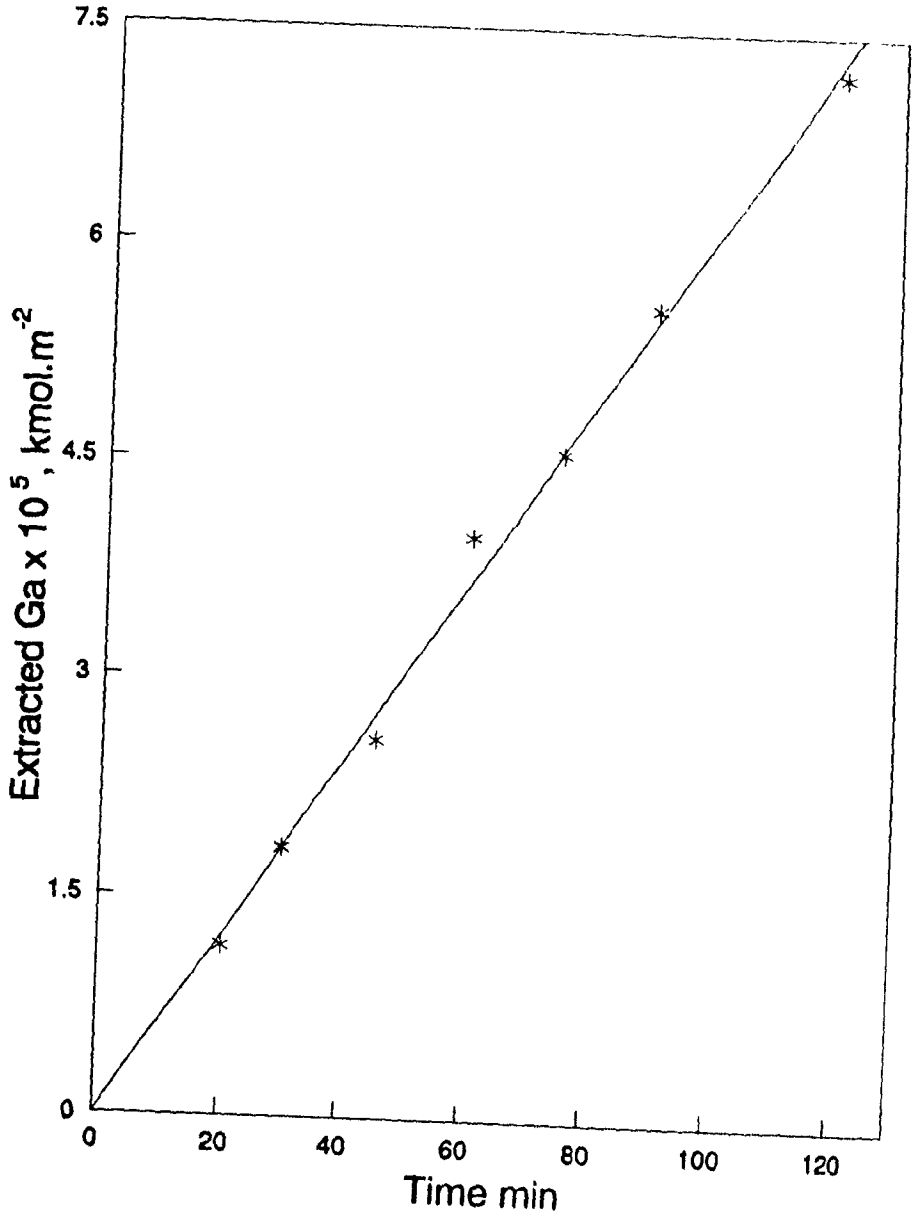

Figure 3.5: RDC: Test for constant extraction rate. $Ga_{(aq)} = 2.29 \times 10^{-2}$ g-ion/l, D2EHPA = 0.28 F, pH = 1.48, t = 22 °C.

also for the stripping experiments. Here, the acidic strip solution was placed in the thermostated beaker with the pre-loaded organic with known metal concentration in the rotating cylinder. The main difference—and problem—was with the analysis of the stripped metal. The resulting metal concentrations in the aqueous strip solution were very low even for direct analysis by atomic absorption. Smaller volumes of the aqueous phase and longer times (for the most part, 180 ml and 5400 seconds, resp.) than in the extraction experiments were used, but these changes still were not sufficient to obtain metal concentrations high enough for reliable analysis.

One option was to use solvent extraction as a pre-concentration step. However, such analytical techniques would require HCl medium or chloride addition (see pages 12, 16). Spectrometric determination with rhodamine B, at these low metal concentrations, would also require extraction prior to analysis [90]. Thus, it was decided at this point to do the simplest thing possible—to obtain more concentrated solution by slow evaporation of part of the water.

After an experiment, two parallel samples of 80 ml each were taken, placed in two beakers, and left on a laboratory heater at a very low heating mode. During evaporation, some of the water vapour was condensing on the cold walls of the beaker and re-entering the solution. After about 4 hours, the volume was reduced to approximately 6–8 ml. The exact volume was measured by an Eppendorf digital pipette (three digits, range 0.100–1.000 ml, imprecision less than 0.2 %). Metal determination in these samples was now possible. The results for the two parallel samples were usually in good agreement, and if so, the average value was used in the subsequent calculations. Although this technique is open to criticism, yet through both reproduction of some of the experiments and successful application of 'linearity' tests (see page 32), which were also carried out here, a satisfactory degree of confidence was gained. Nevertheless, a better analytical method should be found and used to provide lower detection levels, such as, for example, inductively coupled plasma spectroscopy (ICP).

Chapter 4

Experimental Results

4.1 Introduction

The results from experimental work are the subject of this Chapter. First, those regarding extraction equilibria will be presented and discussed. Based on them, stoichiometry of the reactions and respective equilibrium constants will be determined, and the two extractants—D2EHPA and OPAP—compared. Then, the results from kinetic experiments will be presented.

4.2 Gallium–D2EHPA Extraction Equilibria

4.2.1 Basic Elements and Concepts

The overall gallium extraction reaction can be represented as:

$$Ga^{3+} + \frac{n+s}{2}(HR)_{2\ (org)} \rightleftharpoons GaR_n \cdot sHR_{\ (org)} + nH^+ \qquad (4.1)$$

where s, the solvation number, depends on the nature of the organophosphoric acid, HR, as well as on the loading level. The solvated metal-organic complexes follow formation of extractant dimers through hydrogen bonds in non-polar solvents [92, 93]. However, the extractant exists mainly as monomer if solvents capable of hydrogen bonding, such as alcohols, are present—due to strong solute-solvent interactions. In methyl alcohol, for example, both D2EHPA and M2EHPA are fully monomerized [94].

The same has also been reported for M2EHPA in *n*-decanol [95]. The thermodynamic equilibrium constant of reaction 4.1 is given by:

$$K_{ex} = \frac{a_{GaR_n \cdot sHR} a_{H^+}^n}{a_{Ga^{3+}} a_{(HR)_2}^{\frac{n+s}{2}}} \tag{4.2}$$

or

$$K_{ex} = \frac{\gamma_{GaR_n \cdot sHR} \gamma_{H^+}^n}{\gamma_{Ga^{3+}} \gamma_{(HR)_2}^{\frac{n+s}{2}}} \frac{[GaR_n \cdot sHR][H^+]^n}{[Ga^{3+}][(HR)_2]^{\frac{n+s}{2}}} \tag{4.3}$$

where a denotes activities and γ—activity coefficients. If the experimental conditions are such that the product of activity coefficients is kept constant, then the so-called 'apparent' equilibrium constant, K'_{ex}—

$$K'_{ex} = K_{ex} \frac{\gamma_{Ga^{3+}} \gamma_{(HR)_2}^{\frac{n+s}{2}}}{\gamma_{GaR_n \cdot sHR}} = \frac{[GaR_n \cdot sHR]\, a_{H^+}^n}{[Ga^{3+}][(HR)_2]^{\frac{n+s}{2}}} \tag{4.4}$$

can be used to describe the extraction equilibrium. Since activity coefficients depend on the ionic strength (I) of the solution, K'_{ex} will always refer to a particular value of I, at which it has been determined. Under such conditions, the distribution of metal between the two phases—aqueous and organic—can be described by the distribution coefficient, defined as the ratio of total concentrations at equilibrium:

$$D_{Ga} = \frac{[Ga]^T_{org}}{[Ga]^T_{aq}} \tag{4.5}$$

If the only gallium species in the respective phases are $GaR_n \cdot sHR$ and Ga^{3+}, then from eqns (4.4) and (4.5) follows that

$$K'_{ex} = D_{Ga} \frac{a_{H^+}^n}{[(HR)_2]^{\frac{n+s}{2}}} \tag{4.6}$$

or, in the form of logarithms:[1]

$$\log D_{Ga} = \log K'_{ex} + \frac{n+s}{2} \log [(HR)_2] + n\text{pH} \tag{4.7}$$

Equation (4.7) is well known and has been used for determination of reactions stoichiometry and equilibrium constants [96]. When $\log D_{Ga}$ is plotted *vs* pH at constant

[1]Throughout this work, it is adopted that $\log a$ refers to the logarithm of a with base 10, and $\ln a$—to the natural logarithm of a

free extractant concentration in the organic phase $[(HR)_2]$, a line with a slope equal to n should result—if no change in the mechanism occurs within the given pH range. Similarly, when $\log D_{Ga}$ is plotted vs $\log[(HR)_2]$, at constant pH, the resulting line should have a slope equal to $(n+s)/2$. In order to correctly apply this method several conditions should be satisfied or taken into account. Firstly, the ionic strength has to be same for all of the employed aqueous solutions and kept constant, so that the activity coefficients of the species in the aqueous phase remain unchanged (and K'_{ex} to be constant indeed). Estimation of activity coefficients of the species in the organic phase is also needed. For solutions of D2EHPA in aliphatic diluents, deviations from ideality have been attributed to weak dimer dimer interactions [97], which are not affected by the particular aliphatic diluent, and the following relationship linking $\gamma_{(HR)_2}$ and formal extractant concentration[2] has been proposed:

$$\log \gamma_{(HR)_2} = -0.83\sqrt{F/2} \tag{4.8}$$

Secondly, eqn (4.7) assumes (by inclusion of D_{Ga}) that no gallium species other than Ga^{3+} exist in the aqueous phase, and accordingly, in the organic phase gallium is in the form of $GaR_n \cdot sHR$ only. If this does not hold, then eqn (4.7) has to be modified to account for the existence of other species. Thirdly, the extractant term in eqn (4.7) refers to the *free* concentration at equilibrium. It can be assumed equal to the initial concentration only if the latter is sufficiently large with the metal concentration low, so that changes due to the metal extracted are negligibly small.

4.2.2 Preliminary Tests

The initial experiments showed that gallium is well extracted with D2EHPA. When 125 ml solution containing 9.61×10^{-3} g-ion/l Ga with pH of 2.16 was contacted with 125 ml 10 vol % D2EHPA in kerosene, gallium concentration in the raffinate was only 0.57×10^{-4} g-ion/l after 40 seconds contact time (Table 4-1). In order to estimate the time necessary to establish equilibrium, under given conditions, a similar test

[2]Formal concentration, or formality, F, is the number of formula weights, per litre of solution

contact time seconds	Ga in raffinate $\times 10^4$ g-ion/l	pH of raffinate	E %
10	6.45	1.67	93.3
20	1.29	1.65	98.7
30	0.72	1.64	99.3
40	0.57	1.59	99.4

Table 4-1: Gallium extraction with D2EHPA. $Ga_{init} = 9.61 \times 10^{-3}$ g-ion/l, 10 vol % D2EHPA, O/A=1, t = 21 °C.

contact time minutes	Ga in raffinate $\times 10^2$ g-ion/l	pH of raffinate	E %
5	2.35	1.06	58.7
10	2.10	1.02	63.1
15	1.95	1.01	65.7
20	1.87	1.01	67.0
25	1.86	1.00	67.3
30	1.86	1.00	67.3

Table 4-2: Gallium extraction with D2EHPA. $Ga_{init} = 5.68 \times 10^{-2}$ g-ion/l, 10 vol % D2EHPA, O/A=1, t = 21 °C.

was carried out, but with higher gallium concentration in the aqueous phase. The results (Table 4-2) showed that in this particular case approximately 25 minutes were needed.

Samples from the loaded organic from these tests were contacted with solution of 1.5 M H_2SO_4 for different times, and it was found that in 20 minutes, all gallium was stripped.

Two loading tests for two different concentrations of D2EHPA—0.045 and 0.086 F, were performed. Small volume (15 ml) of the organic phase was contacted several times with portions of 100 ml 0.06 g-ion/l gallium solution. Gallium loading in the organic phase reached a level of 0.140 and 0.251 g-ion/l for the two D2EHPA concentrations, respectively. These values represent approximately 3:1 metal:extractant molar ratio. Thus, it can be concluded that in fully loaded D2EHPA, the stoichio-

metric formula of gallium complex is GaR_3.[3]

For several samples of gallium-loaded D2EHPA, 1 M HCl solution was used to strip the metal. Gallium was stripped but no sulphates were found in the resulting solutions (test reaction with Ba^{2+}). This showed that sulphates were not co-extracted.

4.2.3 Dependence on pH and D2EHPA Concentration. Reaction Stoichiometry

A series of equilibrium experiments were carried out at different aqueous acidities and constant extractant concentration in order to determine the dependence of gallium distribution on pH (fig. 4.1). When $\log D_{Ga}$ was plotted *vs* pH a straight line with a slope of 3.47 resulted (correlation coefficient of 0.9947). This showed that there is no change in the extraction mechanism within the pH interval. On the other hand, the value of the slope was unexpected—as for a tri-valent metal, n should be equal to 3. The difference was too large to be attributed solely to experimental uncertainties.

Eventually, the reason was found to be the following: the aqueous solutions of gallium were prepared from $Ga_2(SO_4)_3$, so that the metal concentrations for all of them were the same, and H_2SO_4 was added to obtain solutions with increasing acidity. Thus, the solutions prepared would have had not only different acidities but also different sulphate concentrations. If gallium could form complexes with sulphates, as was later found to be the case, then eqn (4.7) would be no longer applicable—increased sulphate concentration would mean lower concentration of free Ga^{3+} and therefore less metal extracted, according to the equilibrium reaction 4.1. Hence, these first extraction results served to stress the importance of gallium complexation in sulphate solutions.

In order to avoid, at this point, additional complications arising from sulphate complexation, gallium nitrate solutions were prepared and their acidity was varied

[3]This, however, does not exclude possible existence under such conditions of polynuclear species with the same monomer formula

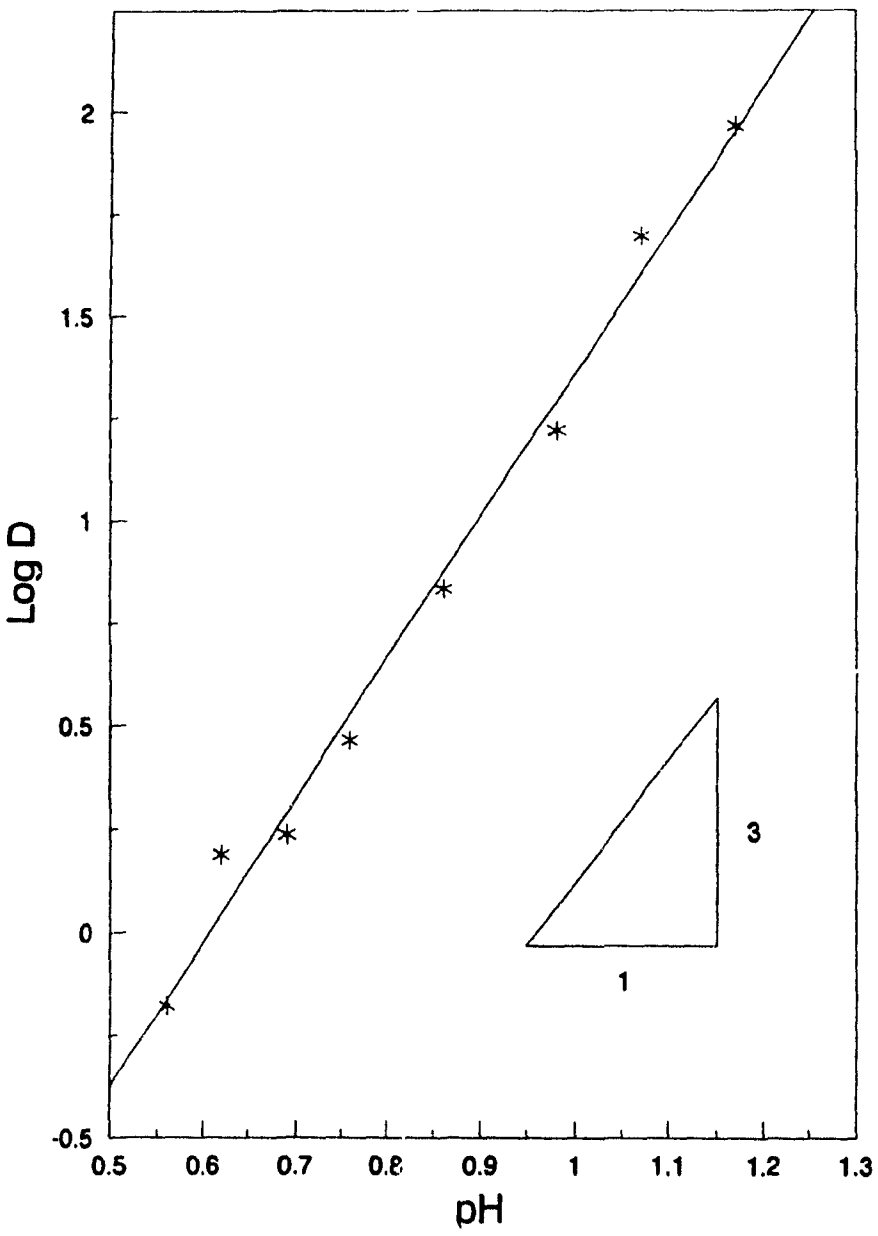

Figure 4.1: Extraction equilibrium with D2EHPA. Conditions: $Ga_{init} = 1.05 \times 10^{-2}$ g-ion/l; 20 vol % D2EHPA; O/A=1; t = 22 °C; the acidity is varied by H_2SO_4 addition, i.e., the total sulphate concentration increases with decreasing the pH.

by addition of HNO_3.[4] The ionic strength was maintained with $NaNO_3$ at $I = 0.5$. The results for several concentrations of D2EHPA are shown on fig. 4.2. The slopes of all lines were from 2.94 to 3.05, as determined by the least-squares method, with correlation coefficients ranging from 0.9961 to 0.9995. Thus, the value of n was accepted to be equal to 3.

The dependence of gallium distribution on D2EHPA concentration can be determined from the results on fig. 4.2 as well. It is clear, that any vertical line through the graph, crossing the pH axis at a given point, will give values of $\log D_{Ga}$ for that particular pH. Also, the intercept, A, of each line is equal, according to eqn (4.7), to:

$$A = \log K'_{ex} + \frac{n+s}{2} \log [(HR)_2] \tag{4.9}$$

Therefore, when the values of A are plotted as a function of $\log[(HR)_2]$, a line with a slope of $(n+s)/2$ and intercept equal to $\log K'_{ex}$ should be obtained. The results from this are shown on fig. 4.3. The obtained line has a slope equal to 2.04 and intercept of -0.121 (correlation coefficient of 0.9982).

Based on these results it was concluded that the value of s is equal to one and K'_{ex} is equal to 0.757 mol/l (for $I = 0.5$). Thus, the stoichiometry of the overall extraction reaction was determined to be:

$$Ga^{3+} + 2(HR)_{2\ (org)} \rightleftharpoons GaR_3 \cdot HR_{\ (org)} + 3H^+ \tag{4.10}$$

Recently, the same stoichiometry was also reported by Inoue *et al* [71].

Another way to determine the reaction stoichiometry is based on the following considerations: Assuming that a given gallium complex—$GaR_n \cdot sHR$—forms in the

[4] In all reviewed sources for gallium complexation in aqueous solutions (e.g., references [118] [125]) there was no evidence of possible existence of nitrate complexes. For most metals, for which stability constants, β, are available, $\log \beta$ is less than 0.5, and for many this value is negative—e.g., Ni^{2+}, Co^{2+}, Fe^{3+} [104]. For In^{3+}, the only metal similar to Ga^{3+} for which data are available, $\log \beta_1 = -0.43$ (at $I = 4$) is given. This low value implies that the effects of any possible nitrate complexation will be very small.

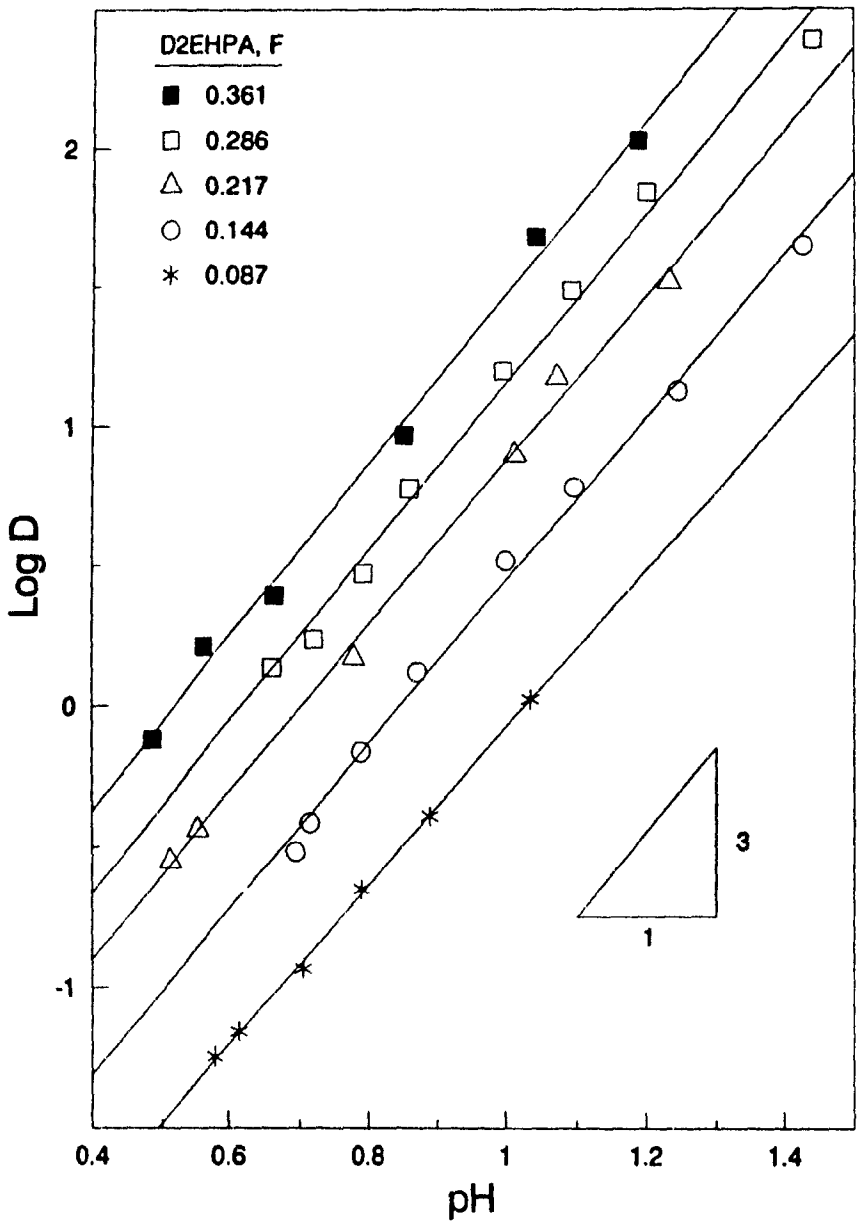

Figure 4.2: Extraction equilibrium with D2EHPA. Effect of pH. Conditions: Ga_{init} = 5.59×10^{-3} g-ion/l; O/A=1; t = 21 °C; the aqueous solutions are nitrate-based (do not contain sulphates) and the acidity is varied by HNO_3 addition.

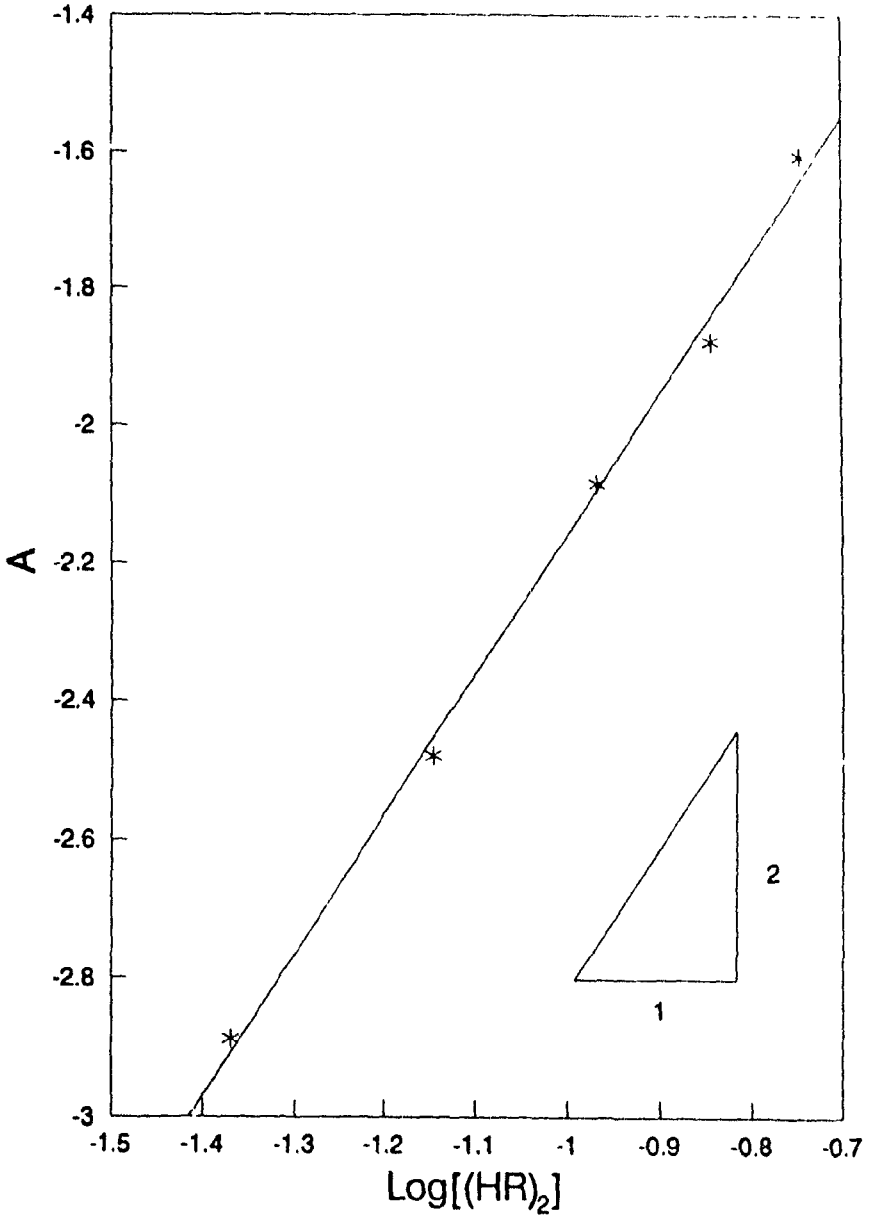

Figure 4.3: Extraction equilibrium with D2EHPA. Effect of extractant concentration.

organic phase,[5] then the free extractant concentration at equilibrium will be:

$$[(HR)_2] = [(HR)_2]_{init} - \frac{n+s}{2}[GaR_n \cdot sHR] \tag{4.11}$$

Provided that the experiments have been carried out at O/A ratio of one, then from

$$[Ga^{3+}] = [Ga^{3+}]_{init} - [GaR_n \cdot sHR] \tag{4.12}$$

it follows that

$$[GaR_n \cdot sHR] = \frac{D_{Ga}}{D_{Ga}+1}[Ga^{3+}]_{init} \tag{4.13}$$

When $[GaR_n \cdot sHR]$ from eqn (4.13) is substituted into (4.11):

$$[(HR)_2] = [(HR)_2]_{init} - \frac{n+s}{2}\frac{D_{Ga}}{D_{Ga}+1}[Ga^{3+}]_{init} \tag{4.14}$$

After substituting $[(HR)_2]$—from eqn (4.14) into (4.7), and final rearranging, the following expression is obtained:

$$\log D_{Ga} = \log K'_{ex} + p \log \left(\frac{[(HR)_2]_{init} - p\frac{D_{Ga}}{D_{Ga}+1}[Ga^{3+}]_{init}}{a_{H+}^{n/p}} \right) \tag{4.15}$$

where $p = (n+s)/2$. This equation differs from (4.7) in that here the free extractant concentration, at equilibrium, is expressed with the known initial values.

The unknowns, n and s, can be determined by assuming for them, and therefore p, certain integer numbers, then calculating with these values the second term on the right-hand side in eqn (4.15), and finally plotting the result *vs* $\log D_{Ga}$. If the assumed values are the correct ones, the obtained slope should be equal to p. An advantage of this procedure is the account of the *free* $[(HR)_2]$. Unless the experimental conditions are such that it can be assumed equal to $[(HR)_2]_{init}$, $[(HR)_2]$ can be found only if the stoichiometry of the extraction reaction is known.

This technique was applied to the gallium-D2EHPA equilibrium data (fig. 4.2) for different values of n and s. The resulting slopes, as found by the least square method, for $n = 3$ and for s from 0 to 3, are given in Table 4-3.

[5] Formation of polynuclear complexes in the organic phase is not considered here because of the low metal concentrations in the aqueous phase and low loading levels used in the experiments

assumed values for s, p	initial D2EHPA (as dimer), F				
	0.013	0.072	0.108	0.113	0.180
	obtained values for p				
$s = 0, p = 1.5$	1.59	1.62	1.64	1.65	1.67
$s = 1, p = 2.0$	2.02	2.04	2.03	2.03	2.05
$s = 2, p = 2.5$	2.71	2.70	2.68	2.69	2.66
$s = 3, p = 3.0$	3.46	3.38	3.30	3.27	3.22

Table 4-3: Calculated slope ($p = \frac{n+s}{2}$) values, $n = 3$. Data from fig. 4.2.

The results show that for all extractant concentrations the closest match between assumed and found values of p is for $n = 3$ and $s = 1$, therefore confirming the stoichiometry of the extraction reaction 4.10. For the case of $s = 0$, the obtained values for p are relatively close to the assumed, and the difference increases with extractant concentration. The opposite trend is observed with the case of $s = 3$. These two trends can be possibly explained by the following considerations. It is known that the large excess of extractant with respect to the metal in the organic phase favours formation of complexes of the type $MeR_n \cdot nHR$. On the other hand, when the loading capacity of the extractant is approached, the molar extractant:metal ratio is then close to n.1 [98, 99, 100]. Therefore, in the transition from low to high metal loadings, there will be a gradual change in the distribution of several possibly existing metal-extractant complexes.

The results from gallium equilibrium extraction with D2EHPA lead to the conclusion that gallium is extracted as $GaR_3 \cdot HR$, according to the overall reaction 4.10. This complex, however, should be viewed only as the predominant one (for the range of experimental conditions) and not the only one that may exist in the organic phase. The two trends, observed in the results in Table 4-3, appear to support the fact that at very low metal loadings the predominant complex will be $GaR_3 \cdot 3HR$, while at high loadings—GaR_3. The latter was also indicated in the loading capacity tests.

4.2.4 Effect of Sulphate Concentration

As it was noted earlier, gallium complexation in sulphate solutions appeared to have a significant effect on gallium distribution between the two phases. Several series of experiments were carried out at different sulphate concentrations. The amount of sulphates were controlled by addition of Na_2SO_4, while acidity and ionic strength ($I = 0.5$) were adjusted with HNO_3 and $NaNO_3$. The obtained results for two different extractant concentrations and gallium solutions with and without sulphates are given on fig. 4.4.

The results clearly show that the presence of sulphates in the aqueous solution leads to a significant decrease in gallium distribution coefficients. Also, the apparent slope of the lines for those experiments with sulphates is noticeably less than three. Least-square curve fitting gave slopes close to 2.3 for lines 4 and 5 (2.36 and 2.25, resp.), and slopes of 2.50 and 2.74—for lines 6 and 7, respectively.

The fact that linear dependence of $\log D_{Ga}$ on pH is again observed with the results for extraction from sulphate solutions means that there is no change in extraction mechanism as compared with the case when no sulphates are present in the aqueous phase. Thus the reason for lower extraction is probably due to gallium sulphate complexation. Given the practical significance of sulphate-based process solutions for gallium recovery, gallium complexation and implications for extraction clearly become important.

Due to complexation, eqn (4.7) will no longer be applicable since the total gallium concentration in the aqueous phase, $[Ga]^T_{aq}$, will not be equal to the concentration of free Ga^{3+}, which is supposedly the reacting species.[6] Hence, from eqns (4.4) and (4.5) it follows that

$$K'_{ex} = D_{Ga}\frac{[Ga]^T_{aq}}{[Ga^{3+}]}\frac{a^3_{H+}}{[(HR)_2]^2} \tag{4.16}$$

[6] In fact, Ga^{3+} is hydrated and exists as $[Ga(H_2O)_6]^{3+}$ in aqueous solutions [9]

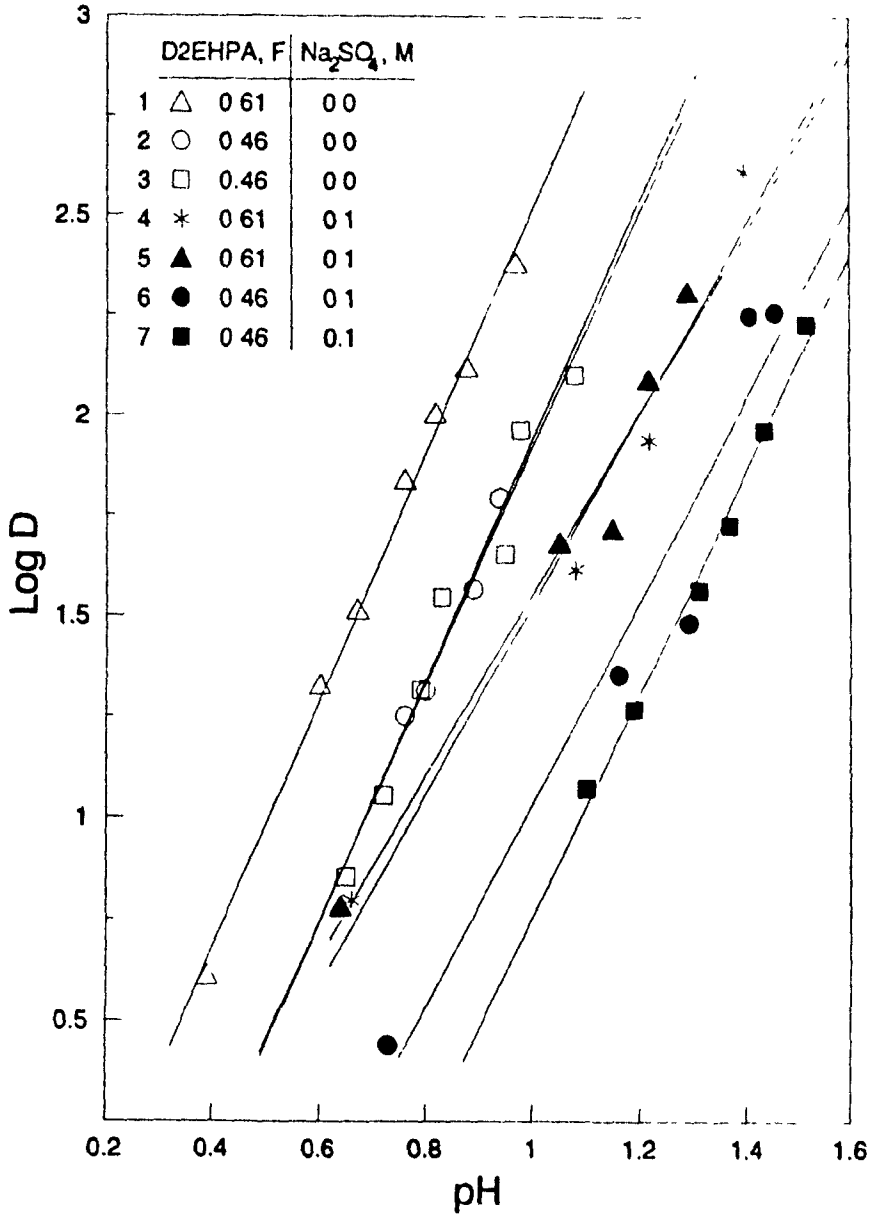

Figure 4.4: Extraction equilibrium with D2EHPA. Effect of sulphate concentration. line 1: $Ga_{init} = 9.61 \times 10^{-3}$ g-ion/l, line 2: $Ga_{init} = 4.02 \times 10^{-3}$ g-ion/l, line 3: $Ga_{init} = 9.32 \times 10^{-3}$ g-ion/l, line 4: $Ga_{init} = 6.17 \times 10^{-3}$ g-ion/l, line 5: $Ga_{init} = 10.47 \times 10^{-3}$ g-ion/l, line 6: $Ga_{init} = 5.74 \times 10^{-3}$ g-ion/l, line 7: $Ga_{init} = 9.32 \times 10^{-3}$ g-ion/l, O/A=1, t = 21 °C. The acidity is varied by HNO_3 addition, i e., the total sulphate concentration (from Na_2SO_4) remains constant and does not change with pH.

and accordingly

$$\log D_{Ga} = \log K'_{ex} + 2\log[(HR)_2] + 3pH - \log \frac{[Ga]^T_{aq}}{[Ga^{3+}]} \tag{4.17}$$

Equation (4.17) can also be written as

$$\log D_{Ga} = \log D_{Ga_0} - \log \frac{[Ga]^T_{aq}}{[Ga^{3+}]} \tag{4.18}$$

where D_{Ga_0} is the distribution coefficient of gallium obtained in absence of sulphates and under otherwise the same conditions. Equation (4.18) shows that the decrease of $\log D_{Ga}$ in comparison with $\log D_{Ga_0}$ is due to the always positive $\log\left([Ga]^T_{aq}/[Ga^{3+}]\right)$ term. Obviously, it will be equal to zero—and therefore $\log D_{Ga}$ equal to $\log D_{Ga_0}$—only when no gallium complexation in the aqueous phase takes place, i.e., $[Ga]^T_{aq} = [Ga^{3+}]$. On the other hand, this term does not depend on the particular extractant but only on solution chemistry and complex equilibria in the aqueous phase. Thus, eqn (4.18) implies that the relative effect[7] of sulphate complexation on extraction will be the same regardless of the particular extractant as long as the extraction mechanism remains the same.

In order to correctly predict how D_{Ga} will be affected by gallium complexation in aqueous solutions, it is necessary to be able to find $[Ga^{3+}]$ as functions of the total (analytical) gallium, $[Ga]^T_{aq}$, and the total sulphate concentrations as well as other properties of the aqueous solution—acidity, presence and concentrations of other elements, ionic strength. These will be further discussed in Chapter 5.

4.3 Gallium–OPAP Extraction Equilibria

When considering gallium extraction with OPAP, it is important to remember that OPAP is a mixture of two extractants—the di-basic mono-OPAP and the mono-basic di-OPAP (fig. 3.1). The former may be regarded as analogous to M2EHPA and the latter—to D2EHPA, with the difference being only in the nature of the hydrocarbon

[7] For D_{Ga} compared to D_{Ga_0}

radical. Due to similarities in structure, the physico chemical properties of mono OPAP and di-OPAP will be close to those of M2EHPA and D2EHPA, resp., while the differences will be due to the different radicals

As mentioned earlier, addition of an alcohol modifier to OPAP, dissolved in kerosene, is necessary for improved phase separation. In this work, the concentration of the alcohol, *n*-decanol, in the organic phase was 12.6 vol %, which corresponds to approximately 0.66 mol/l.[8] Although direct evidence about formation of OPAP dimers in non-polar solvents and existence as monomers in the presence of alcohols is not available from the literature,[9] it is assumed this is the case, as is with other alkyl and aryl mono- and di-basic organophosphorus acidic extractants [50, 94].

4.3.1 Aqueous Solubility of OPAP

Of the two OPAP components, mono-OPAP is expected to have the higher aqueous solubility, and this will have an effect on long-term performance and extractant composition.

Parallel samples of OPAP in kerosene (containing 12.6 % *n*-decanol) were contacted several times at O/A ratio of 1/2 with successive equal portions of 0.1546 M HNO_3 solution with constant ionic strength of 0.5, maintained with $NaNO_3$. After each contact the aqueous acidity and OPAP concentration in the organic were determined. The results, given on fig. 4.5, show that the gradual decrease in extractant concentration is mainly due to the mono-OPAP component. The drop, as expected, is most significant after the first contact caused probably in part by water-soluble impurities, since the samples were intentionally taken from the non-conditioned 'as received' extractant. In the following contacts, however, the decrease is slight

The effect of pH on extractant solubility is shown on fig. 4.6. Here, samples of

[8] This is almost three times more than the highest total (mono- plus di-) OPAP concentrations used in the experiments

[9] In fact, no data on any physico-chemical properties of the OPAP components were found in the available literature sources

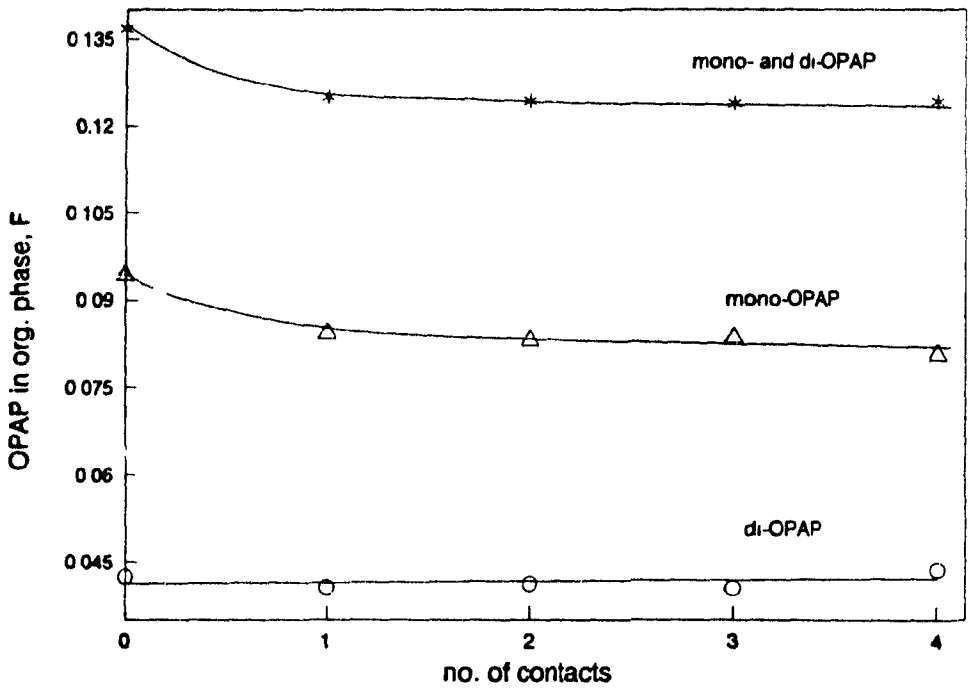

Figure 4.5: Aqueous solubility of OPAP, 'as received'. O/A=1/2, 0.1546 M HNO_3, t = 21 °C.

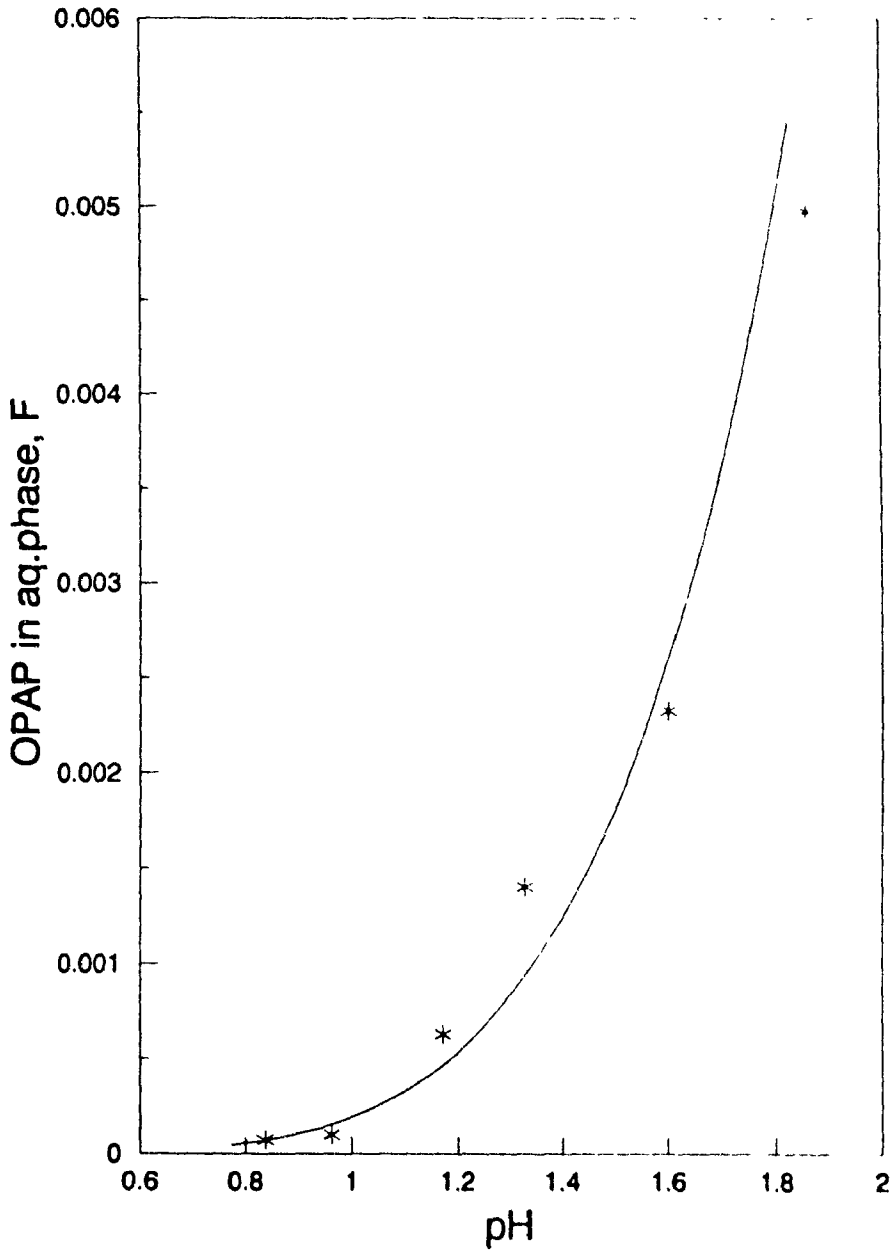

Figure 4.6: Aqueous solubility of OPAP. Effect of pH. O/A=1/2, t = 21 °C.

the conditioned extractant were used and the aqueous solutions were with the same composition as in the previous experiments, but with varying acidities. The results are consistent with the two-phase distribution of a weak acid [50], HR:

$$HR_{(aq)} \rightleftharpoons H^+ + R^- \tag{4.19}$$

and accordingly

$$[HR]^T_{(aq)} = [HR]_{(aq)} + \frac{K_a[HR]_{(aq)}}{[H^+]} \tag{4.20}$$

where $[HR]^T_{(aq)}$ is the total acid concentration in the aqueous phase and K_a is the acid dissociation constant.

The scatter of experimental data was found, however, to be significant because of the very small differences in extractant concentrations involved. Hence, any quantitative interpretation based on these results would be uncertain and was therefore not attempted.

4.3.2 Equilibrium Distribution of Gallium

Results for the obtained $\log D_{Ga}$ values as a function of pH at different extractant concentrations for four compositions of OPAP are given on figures 4.7–4.10, respectively.[10] The gallium aqueous solutions—compositions and ionic strength—were the same as those used for the extraction equilibria with D2EHPA (fig. 4.2).

The results showed a linear dependence of $\log D_{Ga}$ on pH. The slopes of the lines were found to be close to three, though in some cases slightly higher—even up to 3.22. No relation, however, was observed between these higher slope values and extractant concentration and/or composition.

When comparing different extractant compositions under otherwise the same conditions, the results clearly show increased extraction with increasing mole fraction, x, of mono-OPAP in the extractant.

[10]The values of extractant concentrations, shown on the graphs, represent the sums of the formalities of mono- and di-OPAP, i.e., the total concentration, C_T

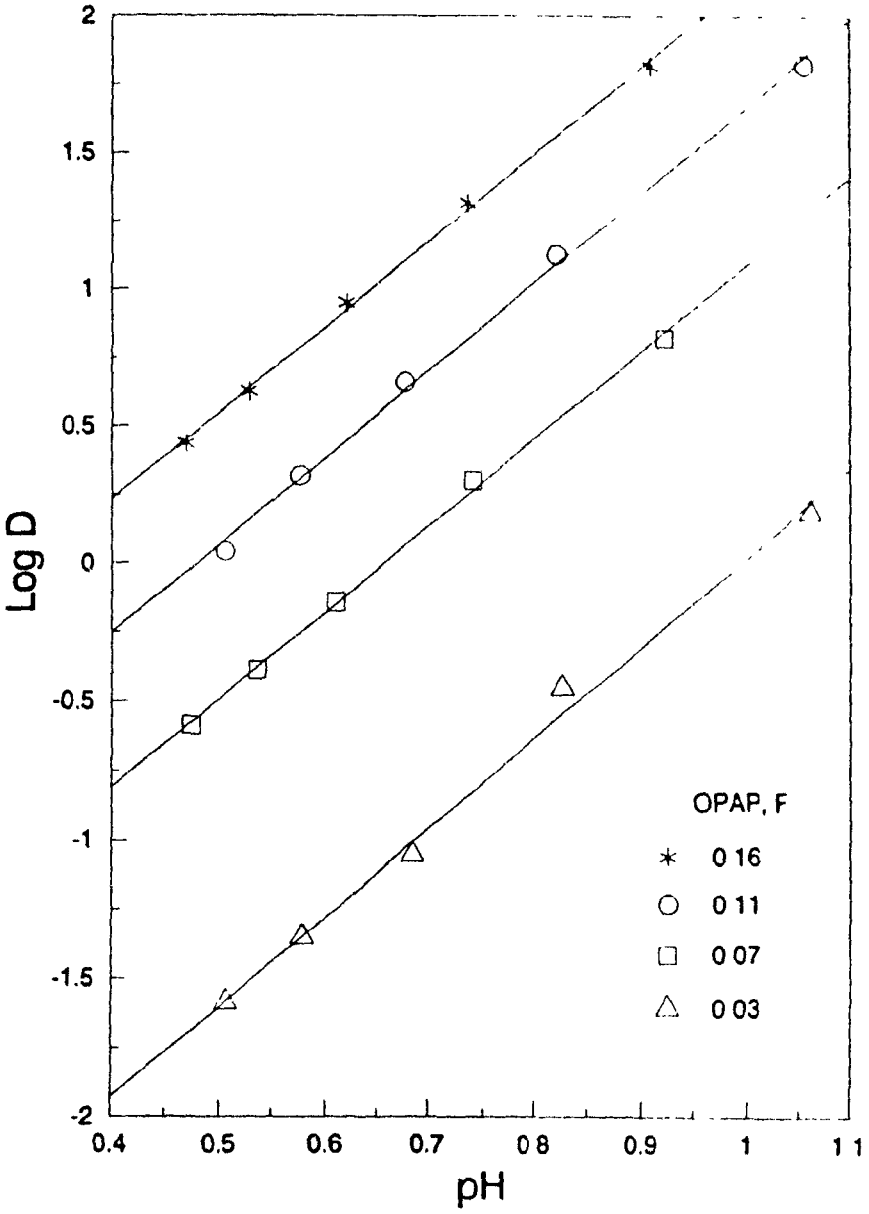

Figure 4.7: Extraction equilibrium with OPAP. Effect of pH. Mole fraction of mono-OPAP: $x = 0.22$. $Ga_{init} = 3.93 \times 10^{-3}$ g-ion/l, O/A=1, t = 21 °C; nitrate-based aqueous solutions, acidity is varied by HNO_3 addition.

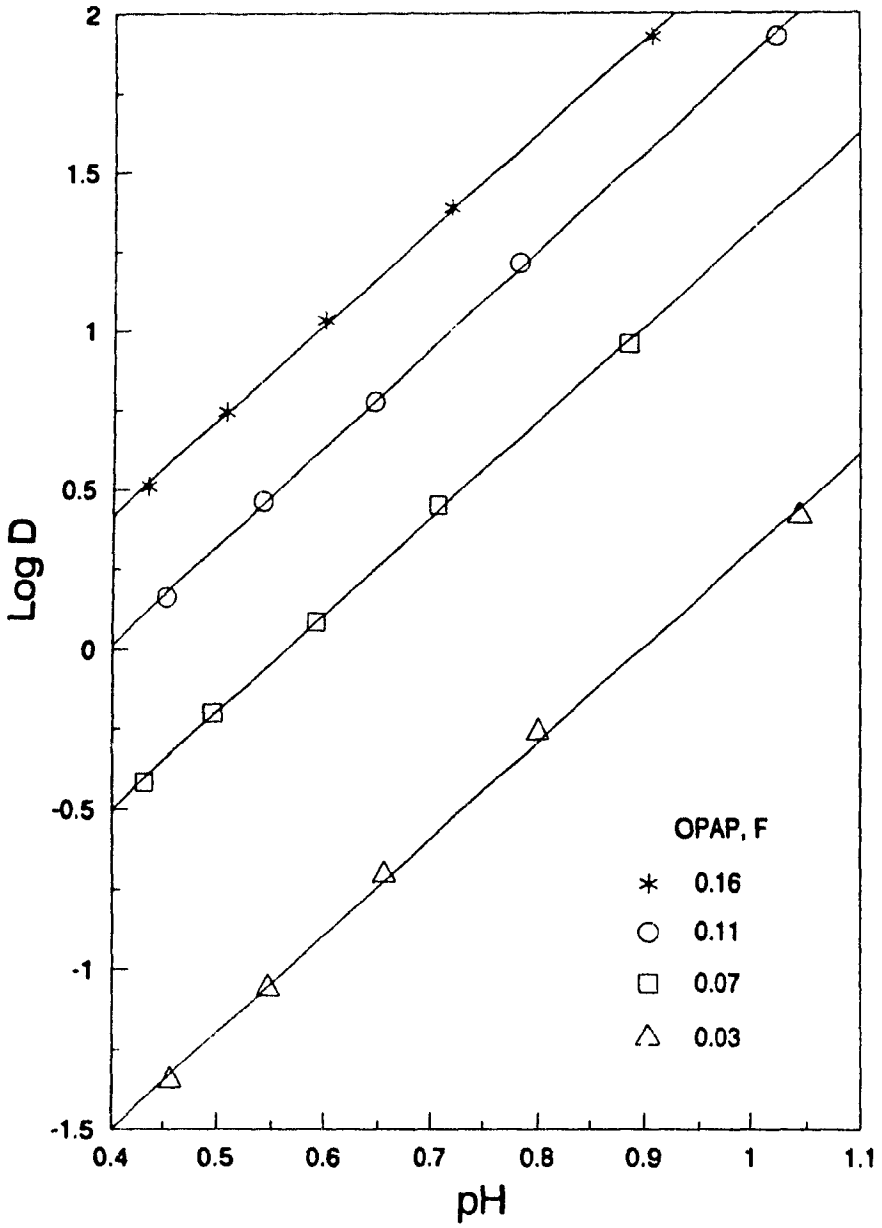

Figure 4.8: Extraction equilibrium with OPAP. Effect of pH. Mole fraction of mono-OPAP: $x = 0.43$. $Ga_{init} = 3.79 \times 10^{-3}$ g-ion/l, O/A=1, t = 21 °C; nitrate-based aqueous solutions, acidity is varied by HNO_3 addition.

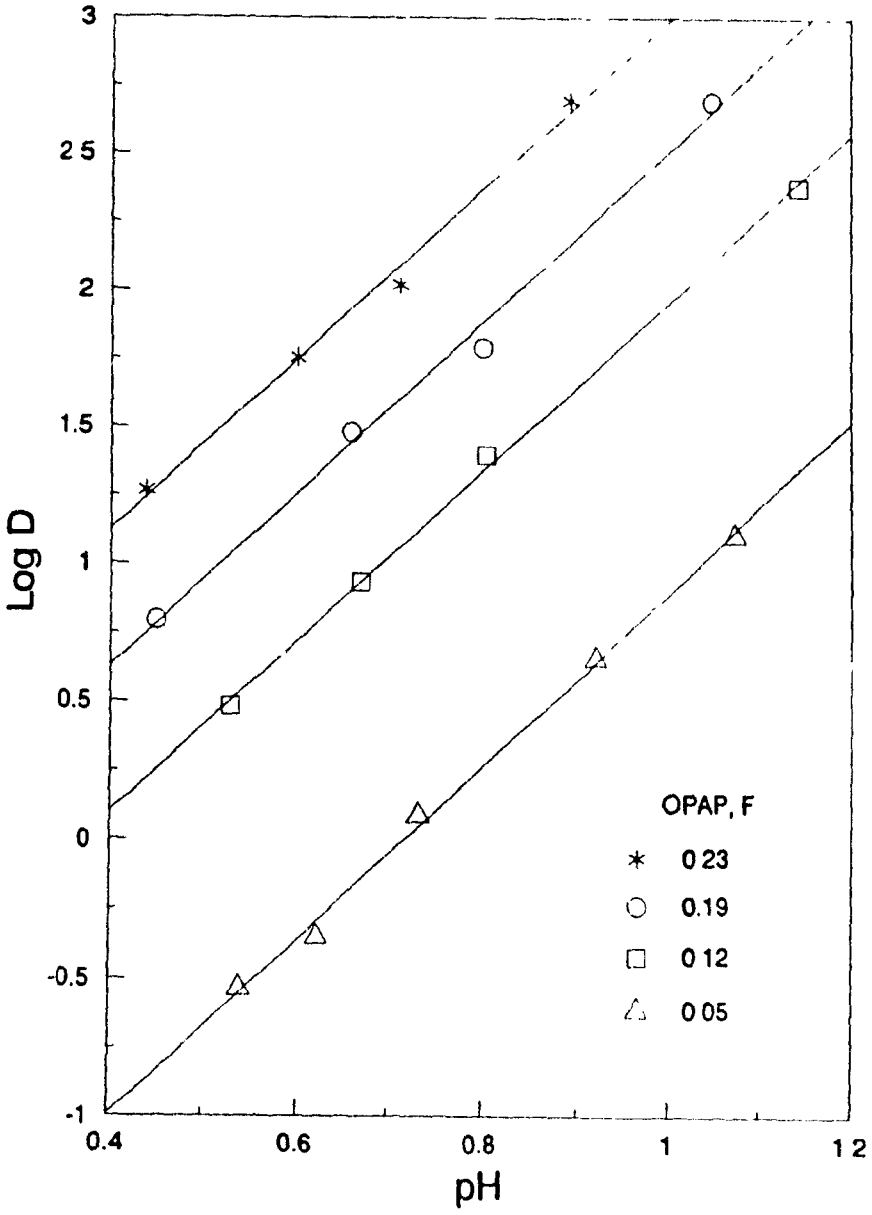

Figure 4.9: Extraction equilibrium with OPAP. Effect of pH. Mole fraction of mono-OPAP: $x = 0.62$. $Ga_{init} = 3.63 \times 10^{-3}$ g-ion/l, O/A=1, t = 21 °C; nitrate-based aqueous solutions, acidity is varied by HNO_3 addition.

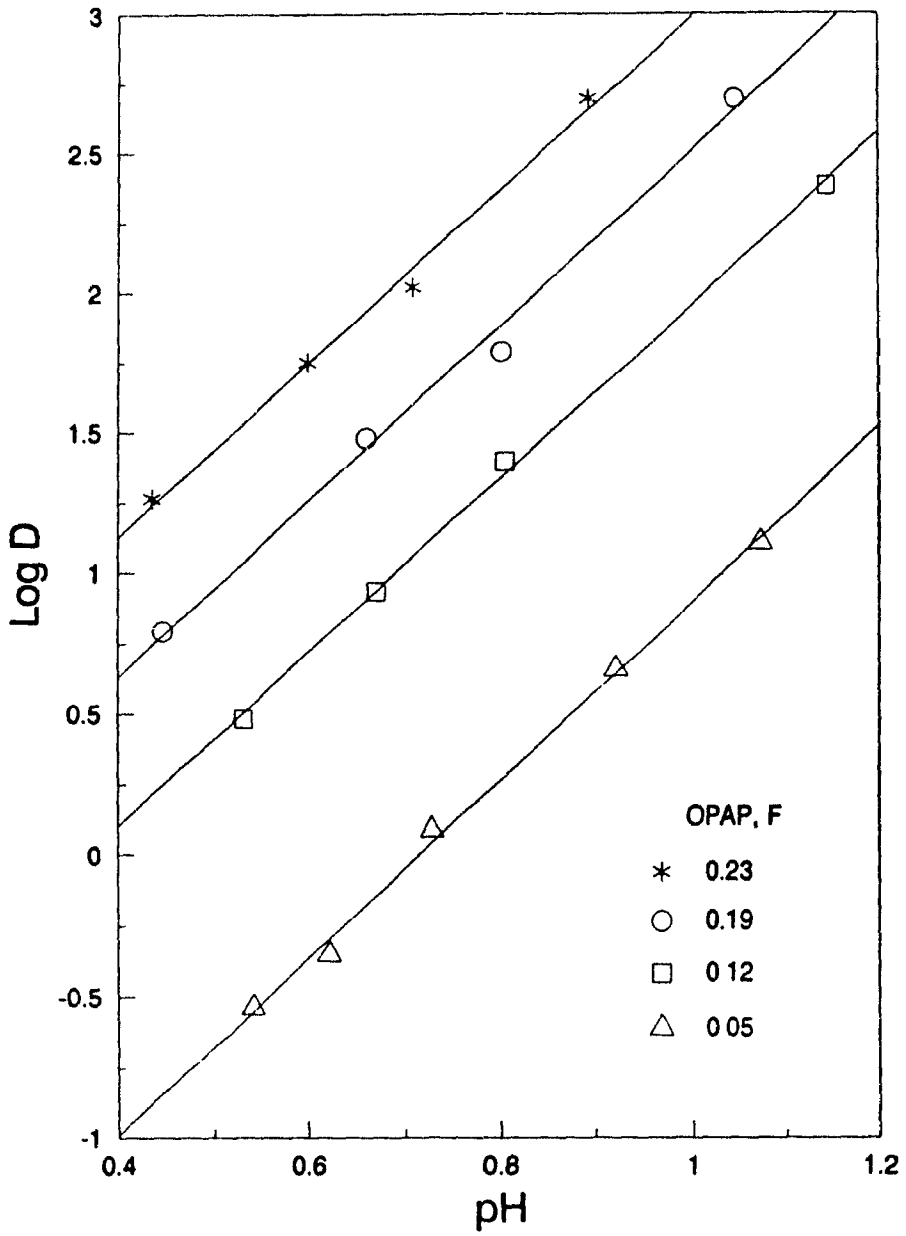

Figure 4.9: Extraction equilibrium with OPAP. Effect of pH. Mole fraction of mono-OPAP: $x = 0.62$. $Ga_{init} = 3.63 \times 10^{-3}$ g-ion/l, O/A=1, t = 21 °C; nitrate-based aqueous solutions, acidity is varied by HNO_3 addition.

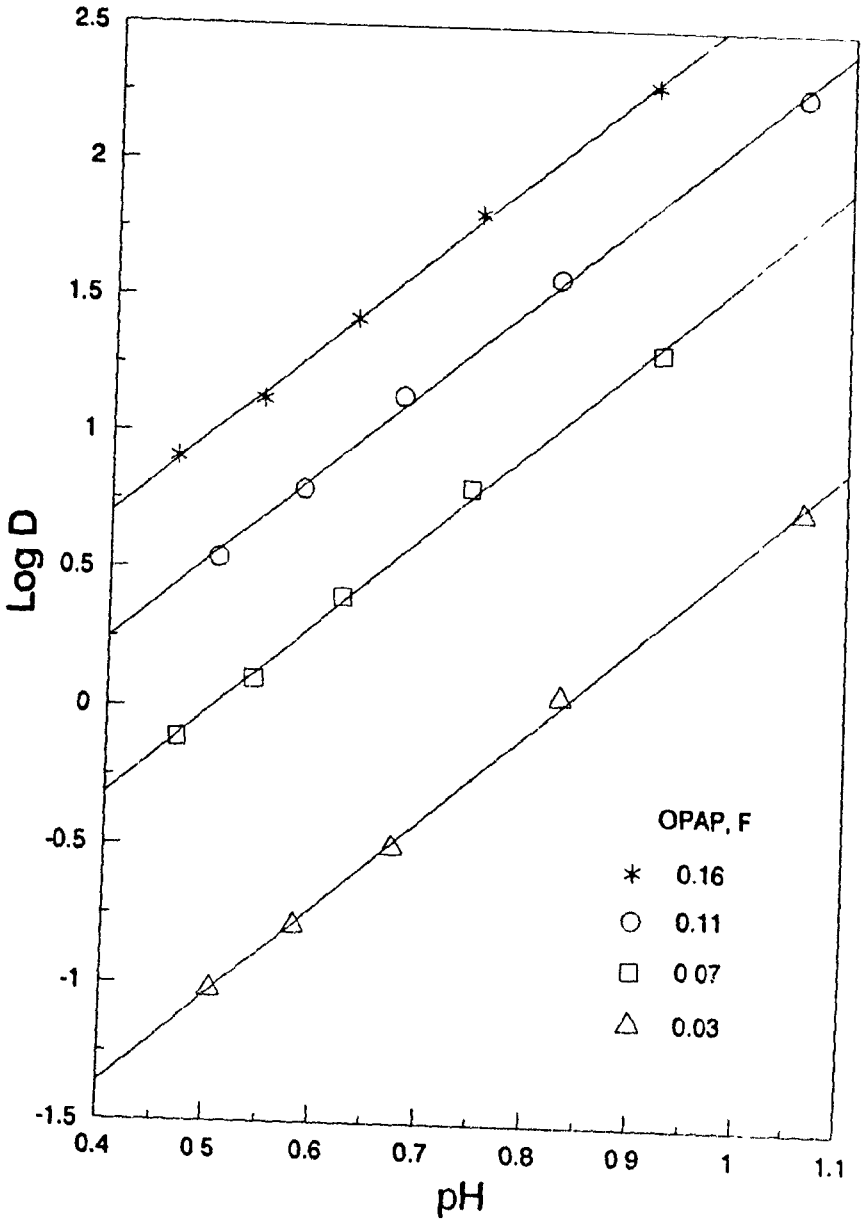

Figure 4.10: Extraction equilibrium with OPAP. Effect of pH. Mole fraction of mono-OPAP: $x = 0.95$. $Ga_{init} = 4.00 \times 10^{-3}$ g-ion/l, O/A=1, t = 21 °C; nitrate-based aqueous solutions, acidity is varied by HNO_3 addition.

4.3.3 Extraction Reactions with OPAP Extractants

Case of two parallel reactions

Gallium extraction with OPAP may be represented by two parallel reactions—for the two components, assuming, at this point, that only the complexes with general formulae $GaM_3 \cdot s_1HM$ and $GaD_3 \cdot s_2HD$ can form, respectively:[11]

$$Ga^{3+} + (3 + s_1)HM_{(org)} \rightleftharpoons GaM_3 \cdot s_1HM_{(org)} + 3H^+ \tag{4.21}$$

$$Ga^{3+} + (3 + s_2)HD_{(org)} \rightleftharpoons GaD_3 \cdot s_2HD_{(org)} + 3H^+ \tag{4.22}$$

where HM denotes mono-OPAP (M = $ROP(O)(OH)O^-$) and HD—di-OPAP (D = $(RO)_2P(O)O^-$). Accordingly, the apparent equilibrium constants for reactions 4.21 and 4.22 will be:

$$K'_{M,ex} = K_{M,ex}\frac{\gamma_{Ga^{3+}}\gamma_{HM}^{3+s_1}}{\gamma_{GaM_3 \cdot s_1HM}} = \frac{[GaM_3 \cdot s_1HM]\, a_{H^+}^3}{[Ga^{3+}][HM]^{3+s_1}} \tag{4.23}$$

for mono-OPAP, and

$$K'_{D,ex} = K_{D,ex}\frac{\gamma_{Ga^{3+}}\gamma_{HD}^{3+s_2}}{\gamma_{GaD_3 \cdot s_2HD}} = \frac{[GaD_3 \cdot s_2HD]\, a_{H^+}^3}{[Ga^{3+}][HD]^{3+s_2}} \tag{4.24}$$

for di-OPAP. The distribution coefficient of gallium is then:

$$D_{Ga} = \frac{[GaM_3 \cdot s_1HM] + [GaD_3 \cdot s_2HD]}{[Ga^{3+}]} \tag{4.25}$$

Thus, from eqns (4.23), (4.24), and (4.25), it follows.

$$\log D_{Ga} = \log\left(K'_{M,ex}[HM]^{3+s_1} + K'_{D,ex}[HD]^{3+s_2}\right) + 3pH \tag{4.26}$$

Since the total OPAP concentration in the organic phase, C_T, is the sum of [HM] and [HD], and also $[HM] = xC_T$ and $[HD] = (1 - x)C_T$, eqn (4.26) can be written as:

$$\log D_{Ga} = \log\left(K'_{M,ex}x^{3+s_1}C_T^{3+s_1} + K'_{D,ex}(1 - x)^{3+s_2}C_T^{3+s_2}\right) + 3pH \tag{4.27}$$

In this eqn (4.27), the respective equilibrium constants as well as the values of s_1 and s_2 are unknown. Once they are determined, gallium extraction can then be predicted

[11] The two components are considered fully monomerized in the organic phase (see page 49).

based on extractant composition and concentration and pH. It should be also noted here, that the possibility for mono-OPAP to act as a bi-dentate ligand for the metal, i.e., to have hydrogens from both OH-groups exchanged, is unlikely. The fact that the second equivalent point in potentiometric titrations of OPAP is around pH 11 (cf fig. 3.3 and Appendix A) suggests that the second dissociation constant of mono-OPAP is much smaller than the first dissociation constant. Therefore, in extraction reactions from acidic solutions mono-OPAP is likely to act as a mono basic acid, as is the case also with M2EHPA [95].

As a first approximation, s_1 and s_2 can be assumed equal, to s, and then eqn (4.27) becomes.

$$\log D_{Ga} = \log \left(K'_{M,ex} x^{3+s} + K'_{D,ex} (1-x)^{3+s} \right) + (3+s) \log C_I + 3pH \qquad (4.28)$$

When the values of $(\log D_{Ga} - 3pH)$ from the equilibrium data (fig. 4.7-4.10) are plotted *vs* $\log C_T$, the slope should be equal to $(3+s)$ and the intercept to the logarithmic term, containing the equilibrium constants and the mole fraction (eqn 4.28). The results are shown on fig. 4.11. It appears, from the calculated slope values, that the stoichiometry of the complexes formed is GaM_3 and GaD_3 (i.e., $s = 0$), although this does not explain why the slopes are less than three.

This procedure is similar to the one, followed for the gallium D2EHPA system. There are, however, two important differences concerning the OPAP system: firstly, two extracting reagents are present and the behaviour of one may not be independent of the other. Secondly, because no information on activity coefficients of the OPAP reagents in the organic phase is available, they are assumed equal to one. This is a significant simplification given the complexity of the organic solution: three reagents present with probable strong solute-solute interactions between *n*-decanol and mono- and di-OPAP, and hydrogen bonding. Thus, considerable deviation from ideality in the organic solution can be expected.

If the only gallium complexes in the organic phase are GaM_3 and GaD_3, then

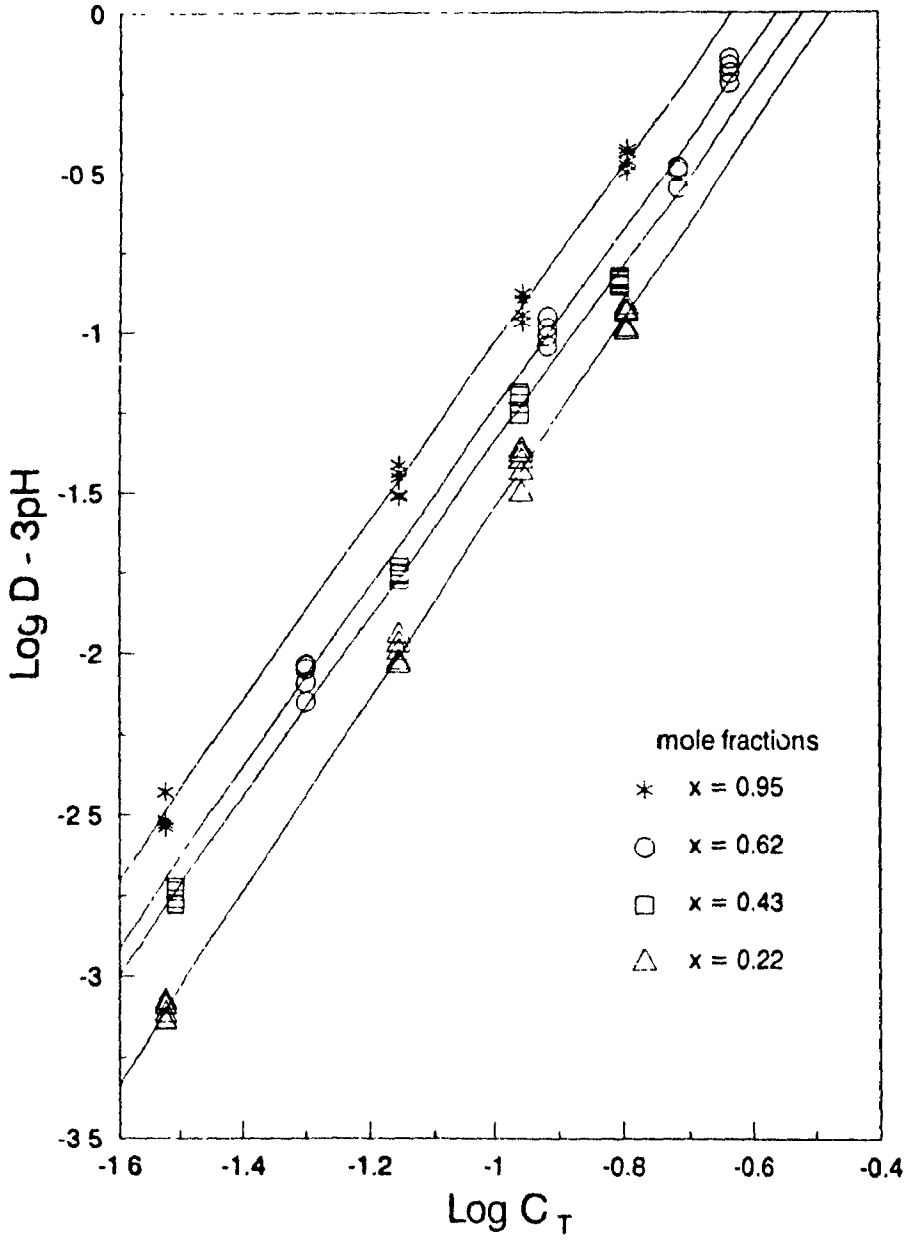

Figure 4.11: Extraction equilibrium with OPAP. Plots of $\log D_{\mathrm{Ga}} - 3\mathrm{pH}$ *vs* $\log C_T$, based on the data from figures 4.7–4.10.

x	A_x
0.22	29.03
0.43	45.32
0.62	62.01
0.95	92.63

Table 4-4: Calculated values of A_x using the experimental data (fig. 4.7 - 4.10) in $D_{Ga}\, a^3_{H+}$ *vs* C_T^3 coordinates.

according to eqn (4.28):

$$D_{Ga}\, a^3_{H+} = A_x C_T^3 \tag{4.29}$$

where

$$A_x = K'_{M,ex} x^3 + K'_{D,ex}(1-x)^3 \tag{4.30}$$

Hence, values of A_x can be calculated from the equilibrium data by plotting, in accordance with eqn (4.29), $D_{Ga}\, a^3_{H+}$ *vs* C_T^3, for each OPAP composition (and, therefore, a given value of x). The results are given in Table 4-4. Contrary to eqn (4.30), however, the obtained values of A_x show clearly a first (and not a third) order dependence on x. The data from Table 4-4 yield the empirical equation

$$A_x = 96.33x + 8.79(1-x)$$

with correlation coefficient of 0.9992. The two numbers, 96.33 and 8.79, would have the physical meaning of being the respective equilibrium constants, $K'_{M,ex}$ and $K'_{D,ex}$, but only for the two limiting cases of $x = 1$ and $x = 0$, in accordance with eqns (4.29) and (4.30). Furthermore, if these two numbers are used as $K'_{M,ex}$ and $K'_{D,ex}$ in eqn (4.30) to calculate A_x for $0 < x < 1$, it is obvious that much lower values of A_x than those calculated from experimental data, and accordingly D_{Ga} from eqn (4.29), will be obtained. This is illustrated on fig. 4.12.

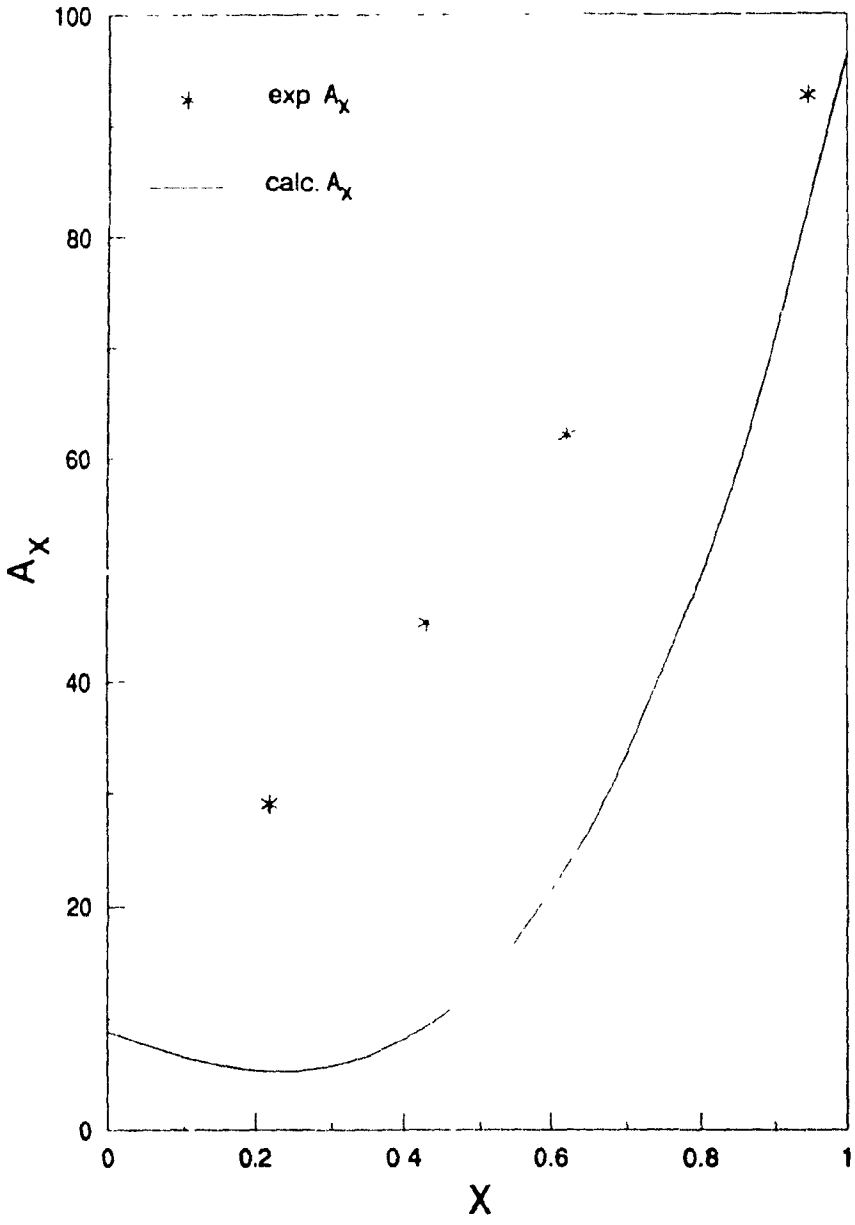

Figure 4.12: Comparison between A_x values from Table 4-4 and those calculated from eqn (4.30) for $K'_{\mathrm{M,ex}} = 96.33$ and $K'_{\mathrm{D,ex}} = 8.79$.

Apparent first order dependency of A_x on x

Clearly now the question is why A_x appears to be first order dependent on x, while, at the same time, D_{Ga} is third order dependent on C_T. In the search for an explanation, a number of probable options have been considered. First, it is possible that s_1 and s_2 are not equal, i.e., the gallium complexes in the organic phase are $GaM_3 \cdot s_1HM$ and $GaD_3 \cdot s_2HD$. Then the appropriate equation, similar to eqn (4.29), will be

$$D_{Ga}\, a_{H+}^3 = K'_{M,ex} x^{3+s_1} C_T^{3+s_1} + K'_{D,ex}(1-x)^{3+s_2} C_T^{3+s_2} \qquad (4.\ldots)$$

From this eqn (4.31), by polynomial regression using the equilibrium data (fig. 4.7-4.10) with C_T being the independent and $D_{Ga}\, a_{H+}^3$ the dependent variable, the two coefficients, $K'_{M,ex} x^{3+s_1}$ and $K'_{D,ex}(1-x)^{3+s_2}$, can be estimated for constant x and given sets of s_1 and s_2. The calculations showed, however, that for all combinations (for values of s_1 and s_2 from 0 to 3), either negative coefficients or very low correlations, or both resulted, with the only exception for $s_1 = s_2 = 0$.

Another possibility is the existence of more than two gallium species, i.e., in addition to GaM_3 and GaD_3, the complexes $GaM_3 \cdot s_1HM$ and $GaD_3 \cdot s_2HD$ are also present. Then an equation analogous to eqns (4.29) and (4.31) can be similarly derived:

$$\begin{aligned} D_{Ga}\, a_{H+}^3 \;=\; & \left(K'_{M,ex} x^3 + K'_{D,ex}(1-x)^3\right) C_T^3 + \\ & K'_{M_1,ex} x^{3+s_1} C_T^{3+s_1} + K'_{D_2,ex}(1-x)^{3+s_2} C_T^{3+s_2} \end{aligned} \qquad (4.32)$$

where $K'_{M_1,ex}$ and $K'_{D_2,ex}$ are the equilibrium constants for the second complexes, $GaM_3 \cdot s_1HM$ and $GaD_3 \cdot s_2HD$, respectively. Again, as in the previous case, the results from polynomial regression indicated that these two additional complexes were not present.

It is appropriate to recall, at this point, that the apparent first order dependence of A_x on x is just that—an apparent order, and it only reflects the overall effect from two or more extraction reactions. The results indicate, by the observed

nearly third order dependence on C_T, that at least the two complexes GaM_3 and GaD_3 do form. On the other hand, the calculated line from eqn (4.30), as shown on fig. 4.12, gives much lower values of A_x than the straight line based on those found (Table 4-4), and the two lines intercept each other at $x = 0$ and $x = 1$. Furthermore, the difference between the A_x values, as they are given from the two lines, changes with x. The change is such that the difference appears to be proportional to the *product* of x and $(1 - x)$, in other words—to the product of mono- and di-OPAP concentrations. This is possible only in case of formation of mixed complexes or adducts.

Formation of mixed complexes

It is known that higher metal loadings with acidic extractants are obtained if the extracted complex involves undissociated molecules of the extractant. Formation of such complexes is common in extraction with organophosphoric and carboxylic acids and they may be considered as adducts [50]. The undissociated molecules are often from a neutral extractant (e.g., TBP, TOPO) present. Various systems containing a chelating, HL, or an organophosphoric acid extractant, HR, and a neutral extractant, E, have been described [50, 96]. The enhanced extraction results from formation of one or more adducts having a general formula $MeL_n \cdot eE$— for the case of a chelating, and $MeR_n \cdot sHR \cdot eE$--for an organophosphoric acid extractant:

$$MeL_{n(org)} + eE_{(org)} \rightleftharpoons MeL_n \cdot eE_{(org)} \tag{4.33}$$

$$MeR_n \cdot sHR_{(org)} + eE_{(org)} \rightleftharpoons MeR_n \cdot sHR \cdot eE_{(org)} \tag{4.34}$$

Adduct formation, in the case of organophosphoric acid, may also proceed by substitution of one or more of the solvated HR molecules:

$$MeR_n \cdot sHR_{(org)} + eE_{(org)} \rightleftharpoons MeR_n \cdot qHR \cdot eE_{(org)} + (s - q)HR_{(org)} \tag{4.35}$$

If two similar extractants are together in the same organic phase, then mixed complexes may form. For example, in the case of two chelating reagents, HL′ and

HL″, formation of mixed $MeL'_aL''_{(n-a)}$ is possible [50].

$$Me^{n+} + aHL'_{(org)} + (n-a)HL''_{(org)} = MeL'_aL''_{(n-a)(org)} + nH^+ \qquad (4.36)$$

On the other hand, if the two similar reagents are organophosphoric or carboxylic acids, then mixed dimers (heterodimerization) in non polar solvents are known to form [50]. It seems, therefore, reasonable to suggest that in the case of mono- and di-OPAP, mixed complexes of the type MeM_nD_{3-n} may form

Four simultaneous extraction reactions

Since n can have values from zero to three for a tri-valent metal like gallium, there are four possible complexes with their extraction reactions and equilibrium constants defined as follows:

$$Ga^{3+} + 3HM_{(org)} = GaM_{3(org)} + 3H^+ \qquad (4.37)$$

$$K'_{30,ex} = \frac{[GaM_3]\,a^3_{H^+}}{[Ga^{3+}][HM]^3} \qquad (4.38)$$

$$Ga^{3+} + 2HM_{(org)} + HD_{(org)} = GaM_2D_{(org)} + 3H^+ \qquad (4.39)$$

$$K'_{21,ex} = \frac{[GaM_2D]\,a^3_{H^+}}{[Ga^{3+}][HM]^2[HD]} \qquad (4.40)$$

$$Ga^{3+} + HM_{(org)} + 2HD_{(org)} = GaMD_{2(org)} + 3H^+ \qquad (4.41)$$

$$K'_{12,ex} = \frac{[GaMD_2]\,a^3_{H^+}}{[Ga^{3+}][HM][HD]^2} \qquad (4.42)$$

$$Ga^{3+} + 3HD_{(org)} = GaD_{3(org)} + 3H^+ \qquad (4.43)$$

$$K'_{03,ex} = \frac{[GaD_3]\,a^3_{H^+}}{[Ga^{3+}][HD]^3} \qquad (4.44)$$

If these four complexes are the only ones, existing in the organic phase, then D_{Ga} will be:

$$D_{Ga} = \frac{[GaM_3] + [GaM_2D] + [GaMD_2] + [GaD_3]}{[Ga^{3+}]} \qquad (4.45)$$

$K'_{30,ex} = 97.01$	$K'_{03,ex} = 12.87$
$K'_{21,ex} = 201.31$	$K'_{12,ex} = 106.99$

Table 4-5: Calculated equilibrium constants of the four complexes.

From eqn (4.45) and eqns (4.38), (4.40), (4.42), and (4.44), after substitution for [HM] and [HD] with C_T and x, the following equation is obtained:

$$D_{Ga}\, a^3_{H+} = A_x C_T^3 \tag{4.46}$$

where

$$A_x = K'_{30,ex}x^3 + K'_{21,ex}x^2(1-x) + K'_{12,ex}x(1-x)^2 + K'_{03,ex}(1-x)^3 \tag{4.47}$$

Equation (4.46) is the same as eqn (4.29) but the expression for A_x, eqn (4.47), is now different. After rearrangement for x, eqn (4.47) becomes:

$$\begin{aligned} A_x \;=\; & \left(K'_{12,ex} + K'_{30,ex} - K'_{03,ex} - K'_{21,ex}\right)x^3 + \left(3K'_{03,ex} + K'_{21,ex} - 2K'_{12,ex}\right)x^2 + \\ & \left(K'_{12,ex} - 3K'_{03,ex}\right)x + K'_{03,ex} \end{aligned} \tag{4.48}$$

Using for A_x the data from Table 4-4, the four coefficients, thence the values of the equilibrium constants, can be determined by polynomial regression.[12] The calculated values for the constants are given in Table 4-5. With them, A_x values are calculated from eqn (4.48) and plotted as a function of x on fig. 4.13 where the data from Table 4-4 are again given for comparison. It is obvious from fig. 4.13 that eqn (4.48) together with the respective values of the four equilibrium constants describes well the data from Table 4-4. An *apparent* first order dependence of A_x on x now becomes clear once eqn (4.48) is written with the values of the constants substituted in it:

$$A_x = -10.18x^3 + 25.94x^2 + 68.38x + 12.87 \tag{4.49}$$

[12] This, strictly speaking, is impossible since for determination of the four coefficients in eqn (4.48) at least five observations are needed, while only four (Table 4-4) are available. The problem was solved by generating a few 'artificial' points between the experimental ones from Table 4-4, which is possible due to the low scatter of data and clearly displayed linearity.

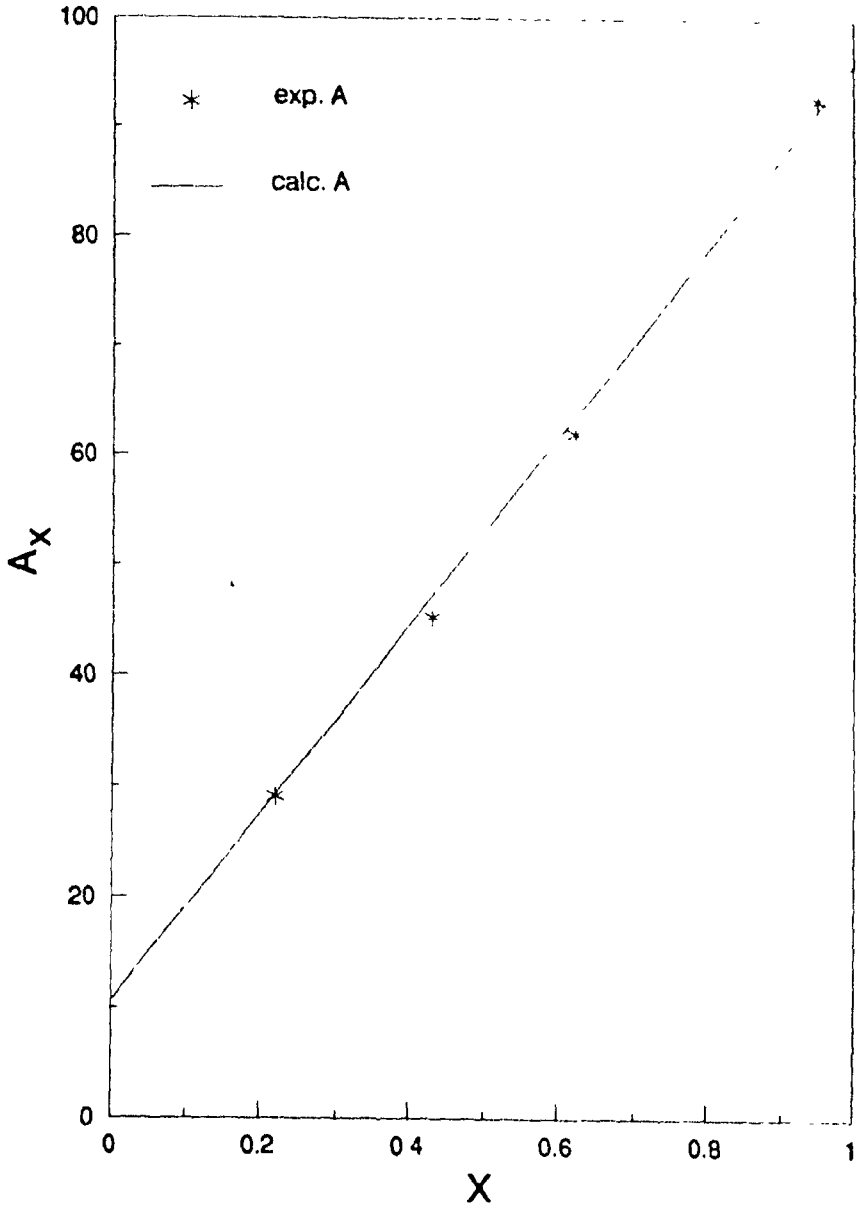

Figure 4.13: Comparison between A_x values from Table 4-4 and those calculated from eqn (4.48).

With these coefficients before x^3 and x^2, and $x < 1$, the contribution of the second and third order terms to the value of A_x will be very small.

Relative to each other, the obtained values for the four equilibrium constants appear reasonable. Due to the higher acidity of di-basic acids (e g., M2EHPA, mono-OPAP), they extract better than their mono-basic analogues –D2EHPA, di-OPAP. This is reflected in the higher values of the extraction equilibrium constants for metal complexes of the former. On the other hand, the constants for the two mixed complexes, $GaMD_2$ and GaM_2D, are higher than those for the 'pure' ones. This can be explained in principle in terms of different probabilities for formation of a particular complex [101, 102].

Probability for a ligand to occupy a given site

It is obvious that the probability for three ligands of the same kind to combine with the central metal cation, thus forming GaM_3 or GaD_3, is less than the probability to form a mixed complex, provided that the occupation of any given ligand site by M or D is equally probable, regardless of whether or not other sites have been already occupied.

If α is the probability of finding M in a given site, then $(1 - \alpha)$ will be the probability of finding D there. Therefore, if $C_{Ga\ (org)}$ is the total metal concentration in the organic phase, then the concentration of each complex can be expressed based on the probability α [102]:

$$[GaM_3] = C_{Ga\ (org)}\alpha^3 \qquad [GaD_3] = C_{Ga\ (org)}(1-\alpha)^3$$
$$[GaM_2D] = 3C_{Ga\ (org)}(1-\alpha)\alpha^2 \qquad [GaMD_2] = 3C_{Ga\ (org)}\alpha(1-\alpha)^2 \qquad (4.50)$$

Hence, the respective equilibrium constants, from eqns (4 38), (4.40), (4.42) and (4.44), can be written, after substitution for complex concentrations from eqn (4.50), as:

$$K'_{30,ex} = \frac{C_{Ga\ (org)}\alpha^3 a^3_{H+}}{[Ga^{3+}][HM]^3} \qquad (4.51)$$

$$K'_{21,ex} = \frac{3C_{Ga\ (org)}(1-\alpha)\alpha^2 a^3_{H+}}{[Ga^{3+}][HM]^2[HD]} \tag{4.52}$$

$$K'_{12,ex} = \frac{3C_{Ga\ (org)}\alpha(1-\alpha)^2 a^3_{H+}}{[Ga^{3+}][HM][HD]^2} \tag{4.53}$$

$$K'_{03,ex} = \frac{C_{Ga\ (org)}(1-\alpha)^3 a^3_{H+}}{[Ga^{3+}][HD]^3} \tag{4.54}$$

From eqn (4.52) it follows that

$$\left(\frac{K'_{21,ex}}{3}\right)^3 = \frac{C^2_{Ga\ (org)}\alpha^6 a^6_{H+}}{[Ga^{3+}]^2[HM]^6} \frac{C_{Ga\ (org)}(1-\alpha)^3 a^3_{H+}}{[Ga^{3+}][HD]^3} \tag{4.55}$$

and therefore, according to eqns (4.51) and (4.51)

$$\left(\frac{K'_{21,ex}}{3}\right)^3 = K'^2_{30,ex} K'_{03,ex} \tag{4.56}$$

Similarly, for $K'_{12,ex}$ is obtained.

$$\left(\frac{K'_{12,ex}}{3}\right)^3 = K'_{30,ex} K'^2_{03,ex} \tag{4.57}$$

It can be proven from eqns (4.56) and (4.57) that the equilibrium constant of a mixed complex will always be greater than the smaller of $K'_{30,ex}$ and $K'_{03,ex}$

When $K'_{21,ex}$ and $K'_{12,ex}$ are calculated using eqns (4.56) and (4.57) with $K'_{30,ex}$ and $K'_{03,ex}$ from Table 4-5, the following values are obtained

$$K'_{21,ex} = 148.43 \quad K'_{12,ex} = 75.70$$

Although smaller than those calculated in Table 4-5, they nevertheless illustrate why higher equilibrium constants apply to the mixed complexes. It is possible that the above values are smaller because the initial assumptions of equal probability may not always be correct—it is reasonable to expect that through available oxygen and hydrogen, for example, attached M and D ligands may interact. There may also be steric reasons that will cause hindrance or preference for a given site and ligand

Furthermore, in systems of two chelating extractants, it is commonly observed that the experimental values of the equilibrium constants for mixed complexes (cf reaction 4.36) are up to ten times higher than those found from probability considerations alone [103]. It has been also observed that the more the two extractants differ in their extraction ability, the higher this difference is. This condition is certainly true for mono- and di-OPAP. Therefore, the values of $K'_{21,ex}$ and $K'_{12,ex}$, found smaller than those in Table 4-5, are not considered an unreasonable exception.

With the obtained values of the four equilibrium constants (Table 4-5) from eqns (4.46) and (4.47), D_{Ga} can be recalculated for given pH and extractant concentration and composition. The results are shown on figures 4.14–4.17 (with dashed lines) and compared with those from the experiments. It is seen that the calculated lines describe the experimental data reasonably well. The greatest deviations are for the case when $x = 0.62$.

One reason for the observed deviations is that the calculated lines follow an exact third order dependence on C_T, according to eqn (4.46), while the experimental data show different order dependencies—from 2.73 to 3.02 for the different extractant compositions (fig. 4.11).

As noted earlier, it is assumed that the activity coefficients of all species in the organic solutions of OPAP are equal to one since no data for this particular system are found in the literature, and this is obviously a considerable simplification. When increasing the concentration of OPAP, the activity coefficients of its components will be expected to drop and, as a result, lower distribution coefficients will be obtained.[13] Thus, the apparent dependence on extraction concentration will be less than three.

The activity coefficients in the OPAP system will depend on the solute-solute interactions between mono-OPAP, di-OPAP, and the alcohol present—*n*-decanol, and also with the solvent. Therefore, as with mixed electrolyte solutions, a precise determination of activity coefficients will be a complicated task.

[13]Provided, however, that the metal loadings are always low, so that the same argument will be less applicable to the activities of extracted species.

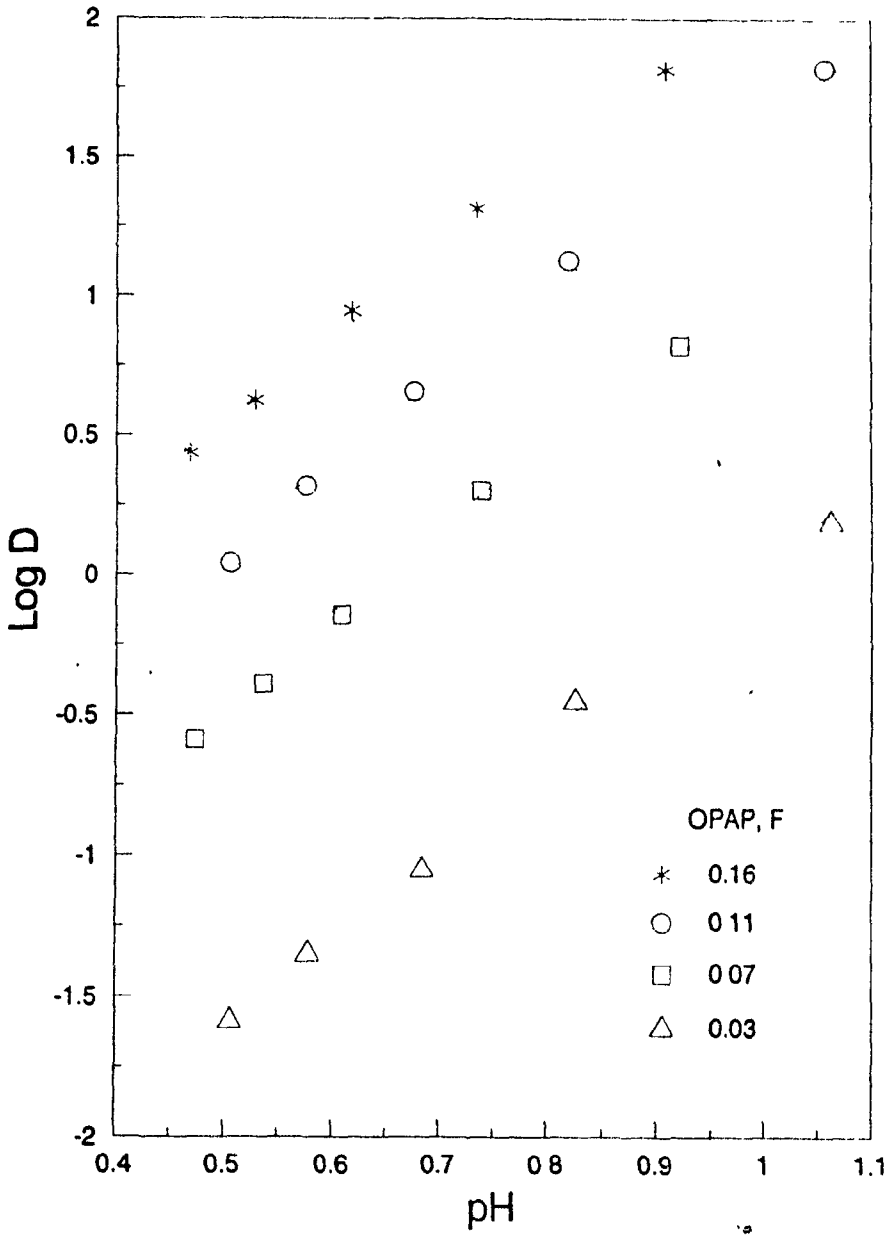

Figure 4.14: Extraction equilibrium with OPAP. Comparison between experimental and calculated data. Experimental conditions of fig. 4.7, $x = 0.22$.

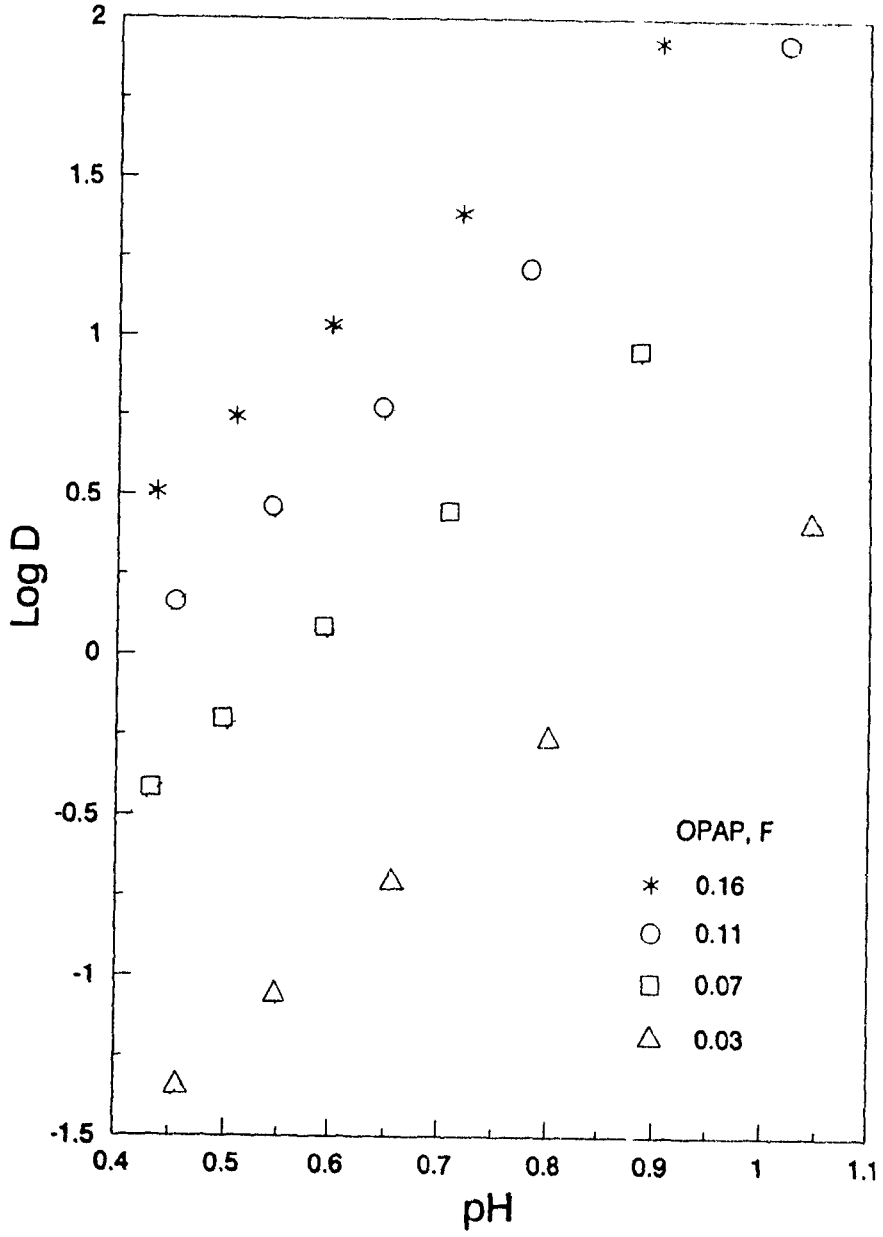

Figure 4.15: Extraction equilibrium with OPAP. Comparison between experimental and calculated data. Experimental conditions of fig. 4.8, $x = 0.43$.

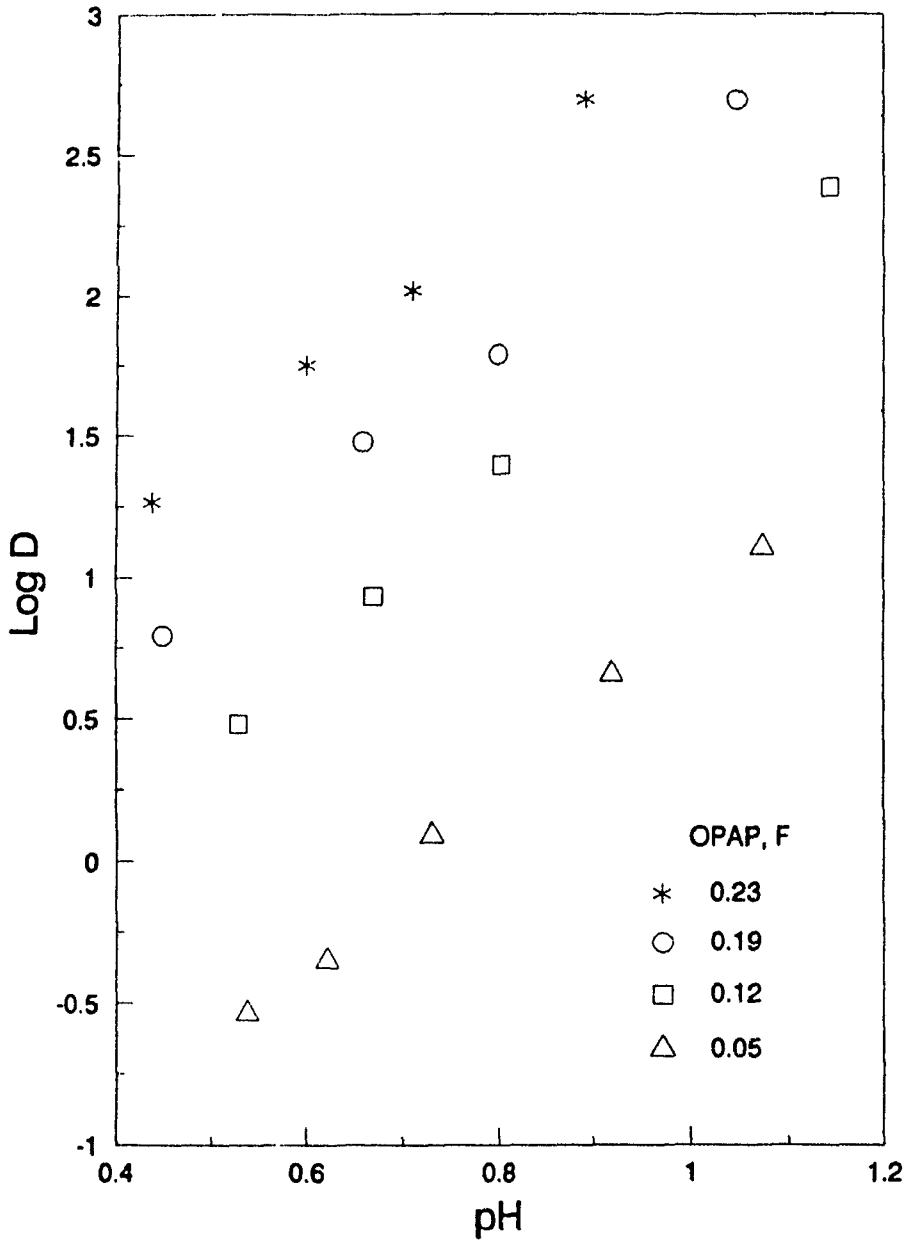

Figure 4.16: Extraction equilibrium with OPAP. Comparison between experimental and calculated data. Experimental conditions of fig. 4.9, $x = 0.62$.

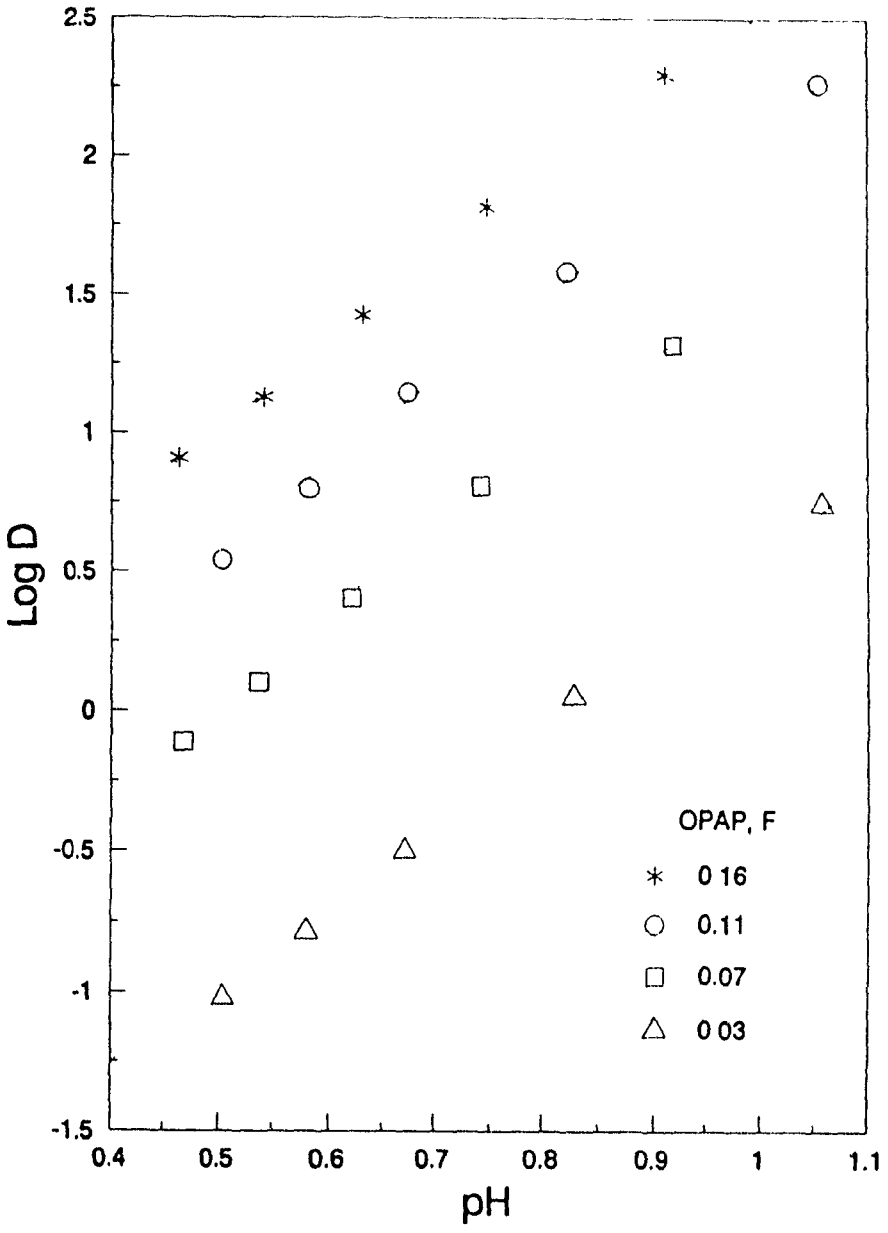

Figure 4.17: Extraction equilibrium with OPAP. Comparison between experimental and calculated data. Experimental conditions of fig. 4.10, $x = 0.95$.

There have been various methods proposed for determination of activity coefficients in organic solutions. One example is the so-called improved Scatchard-Hildebrand model [106, 107, 108], based on one originally developed for binary mixtures [105]. Here, the interactions between any two species, i and j, are accounted for in the expression for activity coefficient by fitting to the experimental data a series of so-called terminal constants A_{ij}. This is necessary because for more than two-component systems, A_{ij} are found to change with extractant concentration [109]. The model has been successfully applied for several extraction systems, with the most complex among them being five-component [108] There are, however, two additional aspects which would require further clarification. The first is with respect to the change of A_{ij} with extractant concentration—linearity is observed (thus it is possible to extrapolate for a particular concentration), but since no precise reasons are given for this, it is by no means certain that the same will hold for other more complex systems. The second question is whether the thermodynamic equilibrium constant for a given metal-extractant complex, determined using this method, remains the same, as it should, regardless of the particular solvent system and other species present.

Another proposed model is the universal functional activity coefficient (UNIFAC) model [110]. As the name suggests, this model regards each organic species as a composition of functional groups, and its activity coefficient is estimated from the structural parameters of the constituent groups and their interactions. Thus, three classes of parameters are needed—volume and surface area of the groups, and energy parameters of their interactions. Unfortunately, for many metal-organic complexes, these parameters are not known [109].

A trend in the observed dependency of D_{Ga} on extractant concentration with composition may be noted. It seems that the order becomes closer to three as x approaches either limit of one or zero (Table 4-6). This may be viewed as an indication of existing mono-OPAP–di-OPAP interactions and their contribution to the overall

mole fraction	slope
0 22	3 02
0.43	2 73
0.62	2.82
0.95	2.91

Table 4-6: Extractant composition (mole fraction) and dependence on extractant concentration (slope values from fig. 4.11).

deviation from ideal behaviour of the organic solution. Therefore, higher deviations will be expected for x close to 0.5.

Following the discussion on mixed complexes and adducts formation (see page 63), it is also possible to suggest that complexes of the type $GaM_3 \cdot s_1HD$ and $GaD_3 \cdot s_2HM$ may form. Such solvates, however, will have equal or almost equal probability of formation compared to $GaM_3 \cdot s_1HM$ or $GaD_3 \cdot s_2HD$ since interactions are mainly electrostatic [50] through hydrogen bonding. On the other hand, the existence of all these solvates will be to some extent hindered due to the presence of alcohol. As shown earlier (discussion on eqn 4.32), the assumption of two additional species being present, namely $GaM_3 \cdot s_1HM$ and $GaD_3 \cdot s_2HD$, does not explain the extraction data. If the above mixed solvates are also included, an equation similar to (4.32) can be derived, but—again—the description of the experimental data is poor. On the other hand, it would be appropriate, once mixed species are considered, to include also in such treatment the two mixed complexes—GaM_2D and $GaMD_2$. However, the assumption of their formation along with GaM_3 and GaD_3 describes the extraction results well with the reasons for observed small deviations (figs 4.14 -4.17) attributed mostly to the non-ideal behaviour of the OPAP solution

4.4 Gallium Extraction Equilibria: Comparison Between D2EHPA and OPAP

As discussed earlier, extraction of metals by organophosphorus acid extractants, including gallium with D2EHPA and OPAP, proceeds *via* cation exchange mechanism. In these systems, the nature of interactions between the metal cation and the organic ligands is mainly electrostatic [50]. Therefore, the stability of a metal-extractant complex, a measure for which is the relevant equilibrium constant, will depend on the size and charge of the metal cation and the organic ligand. These extractants, in regard to their acidic properties, are typical oxo-acids with the active group being P-O-H. The metal cation acts as a Lewis acid, accepting electron density from the donor—a Lewis base—the oxo-acid ion.

The magnitude of the electron density on the donor will be dependent on the nature and the properties, with respect to it, of the adjacent groups in the molecular structure of the extractant. This is directly related to the acidity of the extractant, expressed by its acid dissociation constant in aqueous solution, K_a. The acidity is higher, i.e., the loss of the proton from P-O-H is more favourable, when the positive charge on the central atom in the active group (phosphorus) is higher [9]. In monobasic phosphoric extractants (e g., D2EHPA, di-OPAP), the two hydrocarbon radicals are bound to oxygen which, in turn, is bound to the central atom. Thus, the absence of one such oxygen in the phosphonic, and two in the phosphinic extractants is the reason for decreasing acidity in that order.

The positive charge on the central atom is also affected by the nature of the hydrocarbon radical. It is known that the presence of alkyl groups, which are electron-donating [111], serves to decrease this charge through inductive effects, while aryl groups act oppositely since they are electron-withdrawing due to delocalized (and stabilized through *sp*-hybridization) electron density in the benzene ring [9, 111].

This explains why the di-basic extractants are more acidic than their mono-

basic analogues. Accordingly, mono-OPAP will be more acidic than di-OPAP, and, at the same time, the two OPAP extractants will be more acidic than M2EHPA and D2EHPA, respectively. It is, therefore, not surprising that mono-OPAP is a better extractant for gallium than di-OPAP, and both of them are better than D2EHPA, as found in this work. If, for example, $\log D_{Ga}$ values are calculated using $K'_{03,ex}$ from Table 4-5 for $x = 0$, i.e., extraction with di-OPAP alone, for the same conditions and formal D2EHPA concentrations of fig. 4.2, then significantly higher gallium distribution coefficients than those with D2EHPA are predicted, as illustrated on fig. 4.18.

Similar significant differences between D2EHPA and di-OPAP (toluene used as a diluent) have also been found in studies of promethium and curium extraction [112]. There, the logarithm of the extraction equilibrium constant was approximately 3.5 for both metals in the case of di-OPAP, and about -2.2 in the case of D2EHPA.

The stability of the extracted metal complex will also depend on the space availability around the central (phosphorus) atom in the extractant molecule. It is obvious that increased branching of the hydrocarbon chain may cause steric hindrance. Considering the structural formula of D2EHPA (fig. 3.1) it is possible that the ethyl group may have such an effect. On the other hand, increasing the length and branching of the chain leads to lower aqueous solubility of the reagent, which is beneficial in decreasing extractant losses during continuous operation. Mono- and di-OPAP have higher formula weights (286 and 474, resp.) than M2EHPA and D2EHPA (210 and 322, resp.). Hence, it is expected that the two OPAP reagents will have approximately the same or lower solubility in aqueous solutions than M2EHPA and D2EHPA, respectively. This, combined with the superior extraction performance, would make OPAP preferable to D2EHPA and M2EHPA.

The role of the alcohol, present in the OPAP organic solutions, should also be taken into account. In general, its effect on extraction varies from one extractant to another even if they are of the same class [96], which makes proper selection

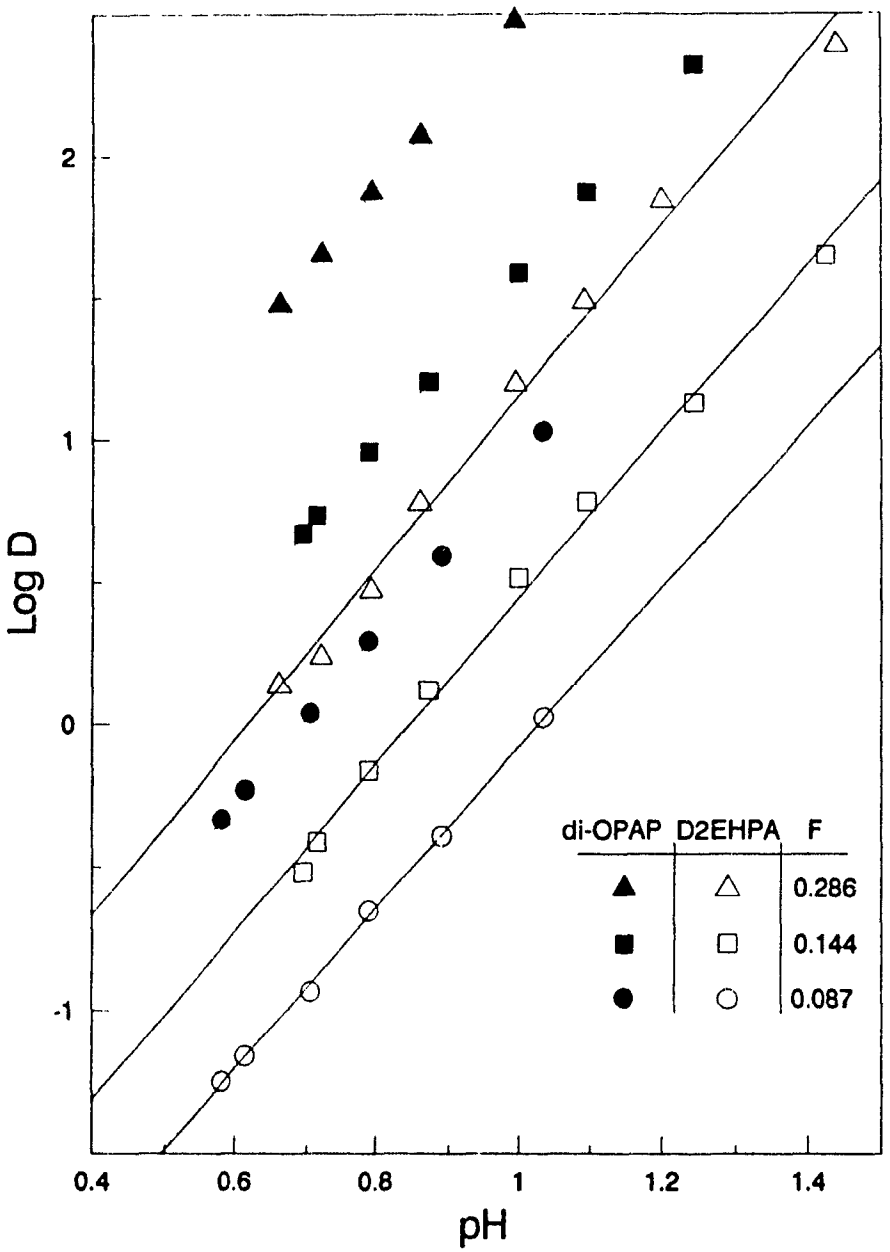

Figure 4.18: Comparison between the experimental results for gallium extraction with D2EHPA (fig. 4.2) and those predicted for di-OPAP ($x = 0$), for the same conditions.

and prediction of side effects difficult In the extraction of rare earth metals with D2EHPA, several modifiers--*iso*-decanol, 2-ethyl hexanol, were found to have a depressant effect [96] On the other hand, it was suggested [113] that the increased extraction with M2EHPA, when alcohol is present, was due to the monomerization of the extractant thus making the hydrogen from the OH-group more available for cation exchange. In that sense, the extraction equilibrium constants reported for the OPAP system (Table 4-5) are conditional--they include the effect of the 12.6 vol% *n*-decanol concentration, which has been kept constant for all experiments, and found to be the minimum required to ensure good phase separation. Increasing the alcohol level above this minimum, even if it leads to improved extraction, will be undesirable because of its relatively high aqueous solubility.

4.5 Kinetic Experiments in the System Gallium-D2EHPA

4.5.1 Extraction Kinetics

As described in Chapter 3, the kinetic experiments were carried out with a rotating diffusion cell (RDC). The effects of the following parameters on the gallium extraction rate were determined:

- pH of the aqueous solution—for pH from 0.78 to 2.10
- Gallium concentration in the aqueous phase—in the range from 7.2×10^{-4} to 2.8×10^{-2} g-ion/l
- Concentration of sulphates in the aqueous phase- ranging from 0 to 0.12 g-ion/l
- D2EHPA concentration in the organic phase—from 0.01 to 0.28 F
- Temperature—from 21 °C to 72 °C

volume, ml		Flux Ga, kmol.m^{-2} s^{-1}	
aq. phase	org. phase	(a)	(b)
300	50	1.63×10^{-8}	5.90×10^{-10}
275	50	1.65×10^{-8}	5.81×10^{-10}
250	50	1.61×10^{-8}	5.83×10^{-10}
225	50	1.57×10^{-8}	5.86×10^{-10}
200	50	1.62×10^{-8}	5.79×10^{-10}

Table 4-7: Gallium extraction kinetics with D2EHPA. Effect of the O/A ratio. (a) Conditions of fig. 4.19. (b) Conditions of fig. 4.20.

Effect of interfacial area, stirring, phase volume ratio

Experiments for different sets of the above parameters were also carried out for the effects of interfacial area, stirring, and volume ratio of the two phases on the extraction rate, in addition to the 'linearity' tests described previously.[14]

The results showed a linear dependence between the amount of metal extracted per given time and the interfacial area (figs. 4.19 and 4.20). In such coordinates, the rate of extraction (flux of Ga) can be obtained directly from the respective slopes. One experiment from each series (fig. 4.19, 4.20) was repeated for several different O/A ratios with the other conditions being kept the same.[15] The results (Table 4-7) showed no apparent dependence on the ratio of the two liquid phases. The results also indicate the reproducibility of the experiments.

Several series of experiments were carried out with different sets of conditions and variations in the rate of stirring. The results (fig. 4.21) gave no clear evidence for the extraction rate being dependent on the rate of stirring within the range of experimental conditions.

[14]See Chapter 3, page 32

[15]Except for very small variations in interfacial areas

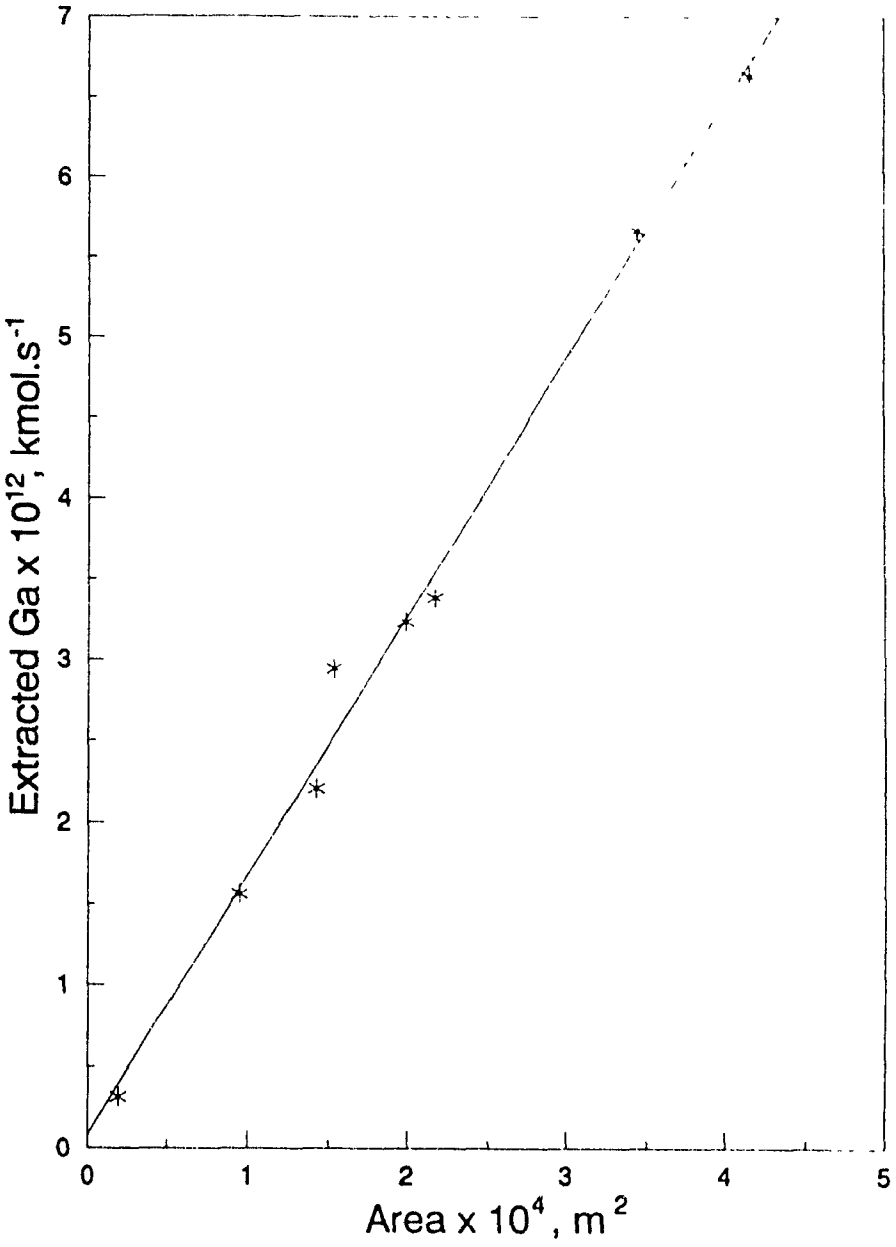

Figure 4.19: Extraction kinetics with D2EHPA. Effect of the interfacial area. $Ga_{(aq)}$ = 1.11 x 10^{-2} g-ion/l, D2EHPA = 0.29 F, pH = 1.88, 250 ml aqueous phase, 50 ml organic phase, rotation = 300 rpm, t = 22 °C.

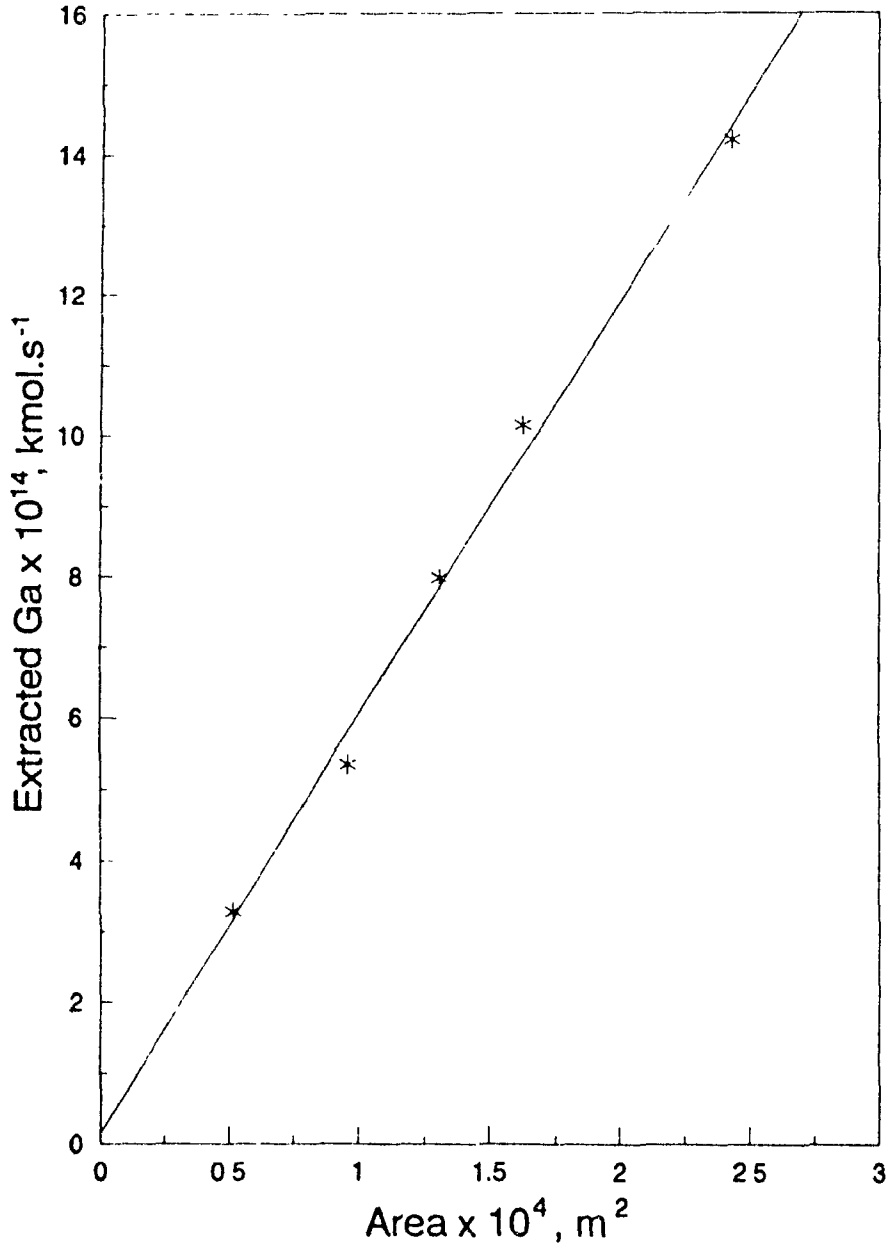

Figure 4.20: Extraction kinetics with D2EHPA. Effect of the interfacial area. $Ga_{(aq)}$ = 5.16 x 10^{-3} g-ion/l, D2EHPA = 0.15 F, pH = 1.14, 250 ml aqueous phase, 50 ml organic phase, rotation = 300 rpm, t = 22 °C.

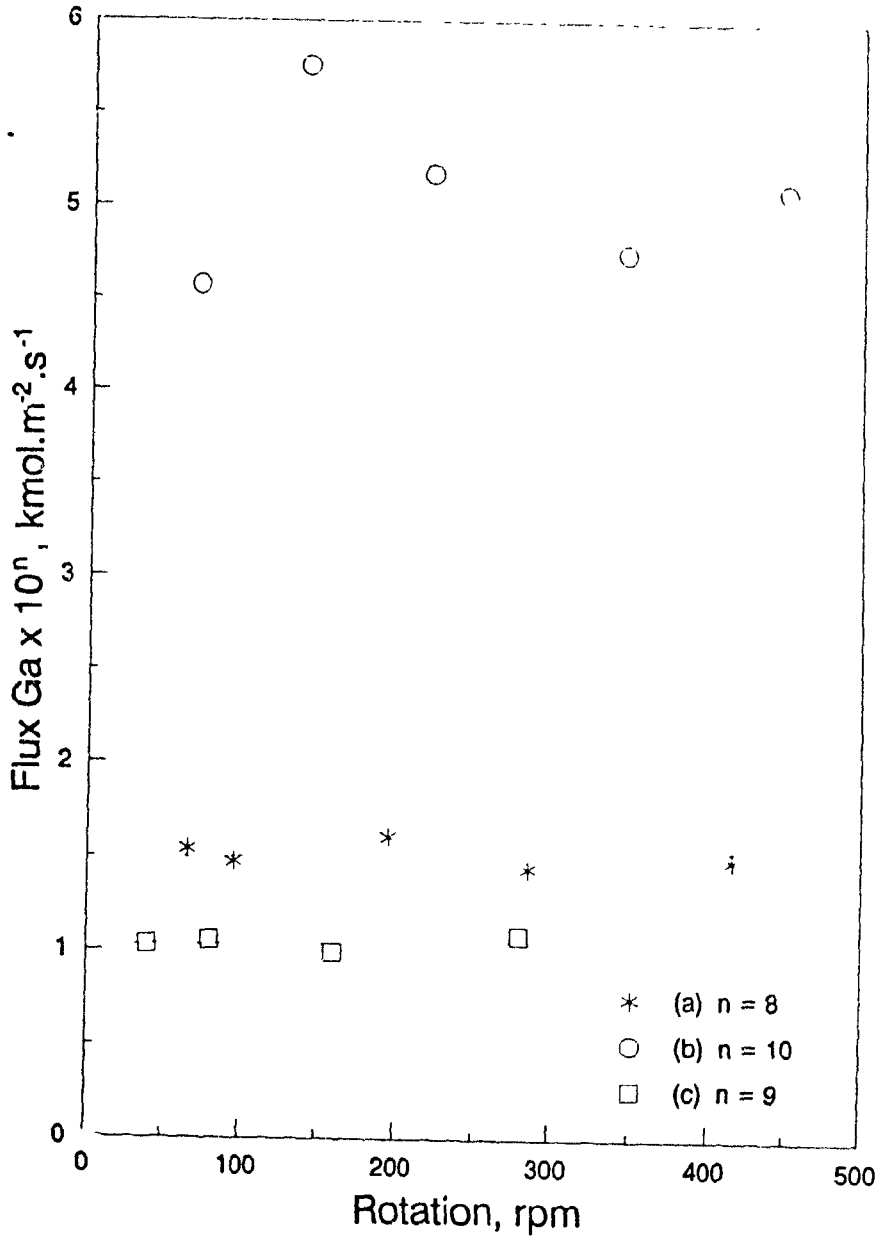

Figure 4.21: Extraction kinetics with D2EHPA Effect of stirring. (a) $Ga_{(aq)}$ = 1.43×10^{-2} g-ion/l, D2EHPA = 0.28 F, pH = 1.80; (b) $Ga_{(aq)} = 1.41 \times 10^{-2}$ g-ion/l, D2EHPA = 0.28 F, pH = 0.79; (c) $Ga_{(aq)} = 1.10 \times 10^{-2}$ g-ion/l, D2EHPA = 0.27 F, pH = 0.98; t = 22 °C.

Effect of pH, metal and extractant concentrations

As expected, the obtained results (figures 4.22, 4.23, 4.24) showed that the rate of gallium extraction increases with increasing pH, metal and extractant concentrations. For each series it is possible to determine the power dependence of gallium flux on the particular parameter, by plotting the data in log-log coordinates. Thus, the following empirical equation is obtained:

$$\text{Flux Ga}\left(\frac{\text{kmol}}{\text{m}^2.\text{s}}\right) = 1.82 \times 10^{-9}\,[\text{Ga}^{3+}]_0^{0.71}\,[(\text{HR})_2]_{0\ (\text{org})}^{0.60}\,[\text{H}^+]_0^{-1.53} \qquad (4.58)$$

where the subscript o refers to bulk values. This equation describes well the experimental data for the region of low extraction rates, but gives higher than the experimental values for relatively high rates. The fact that non-integer numbers are obtained implies that they probably reflect the contribution of both mass-transfer and chemical reaction rates, i.e., neither of the two simultaneous processes can be considered as being the only one rate-controlling step. This will be further discussed in Chapter 6.

Effect of sulphate concentration

In the kinetic experiments described so far, the gallium aqueous solutions were nitrate-based and with the same ionic strength ($I = 0.5$) as in the equilibrium tests. Several series of experiments varying the sulphate concentration under otherwise the same conditions, including the *total* gallium concentration in the aqueous phase, were performed. The results (fig. 4.25) showed that the rate decreases with increasing sulphate concentration. This obviously reflects again the effect of gallium sulphate complexation in aqueous solutions, which will be discussed in more detail in Chapter 5.

Effect of temperature

The results for the temperature effect on gallium extraction rate are shown on fig. 4.26 in the usual Arrhenius plot coordinates. The value of the apparent activation energy,

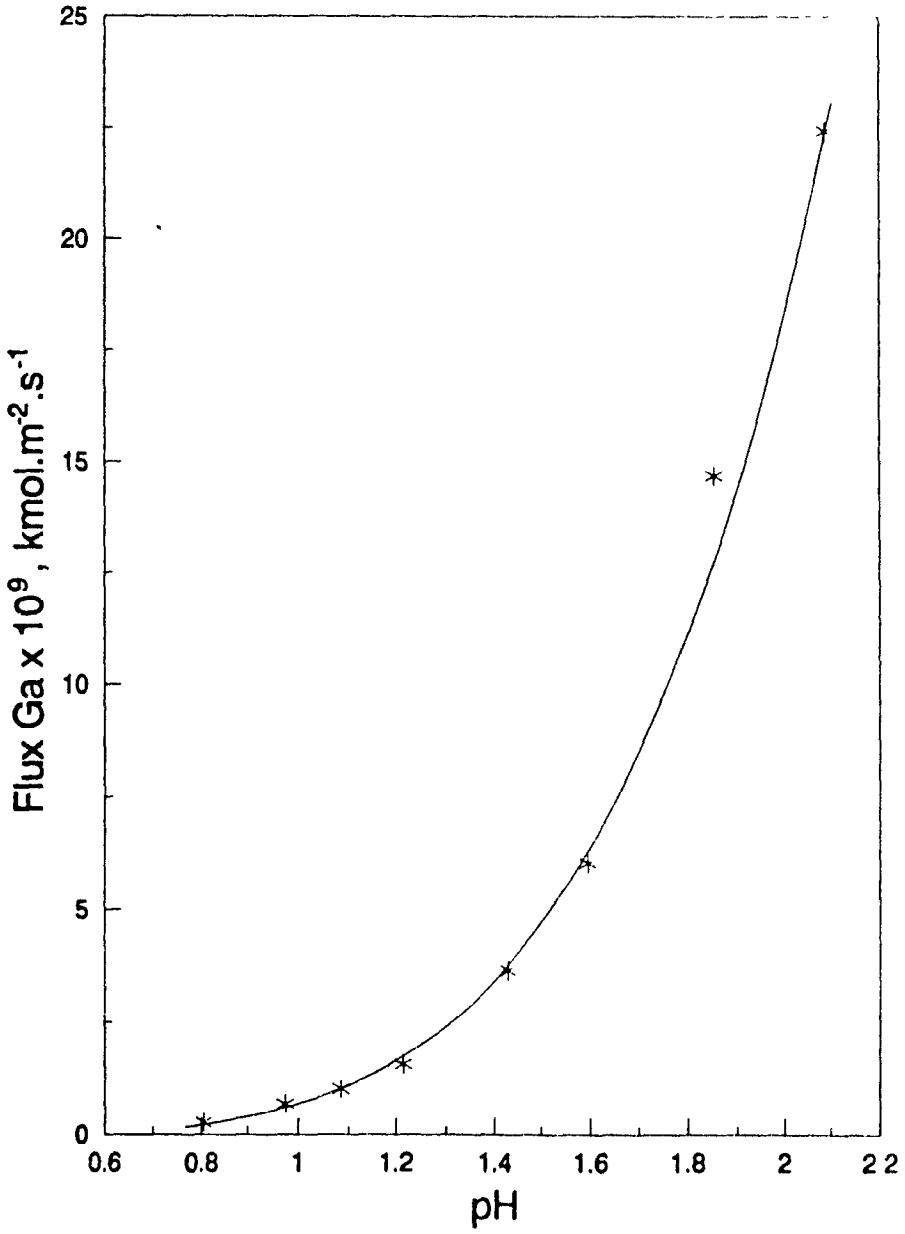

Figure 4.22: Extraction kinetics with D2EHPA. Effect of pH. $Ga_{(aq)} = 1.11 \times 10^{-2}$ g-ion/l, D2EHPA = 0.28 F, t = 21 °C.

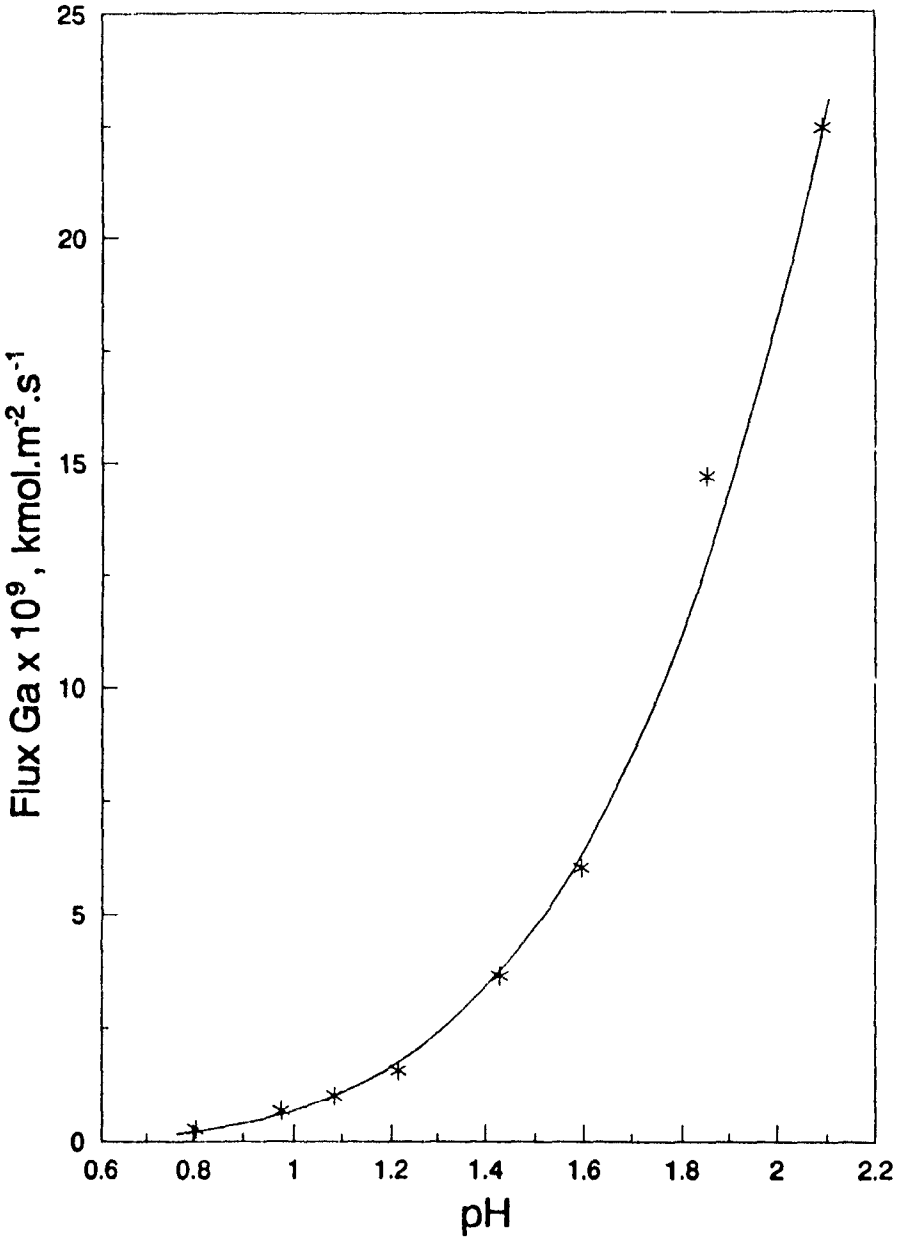

Figure 4.22: Extraction kinetics with D2EHPA. Effect of pH. $Ga_{(aq)} = 1.11 \times 10^{-2}$ g-ion/l, D2EHPA = 0.28 F, t = 21 °C.

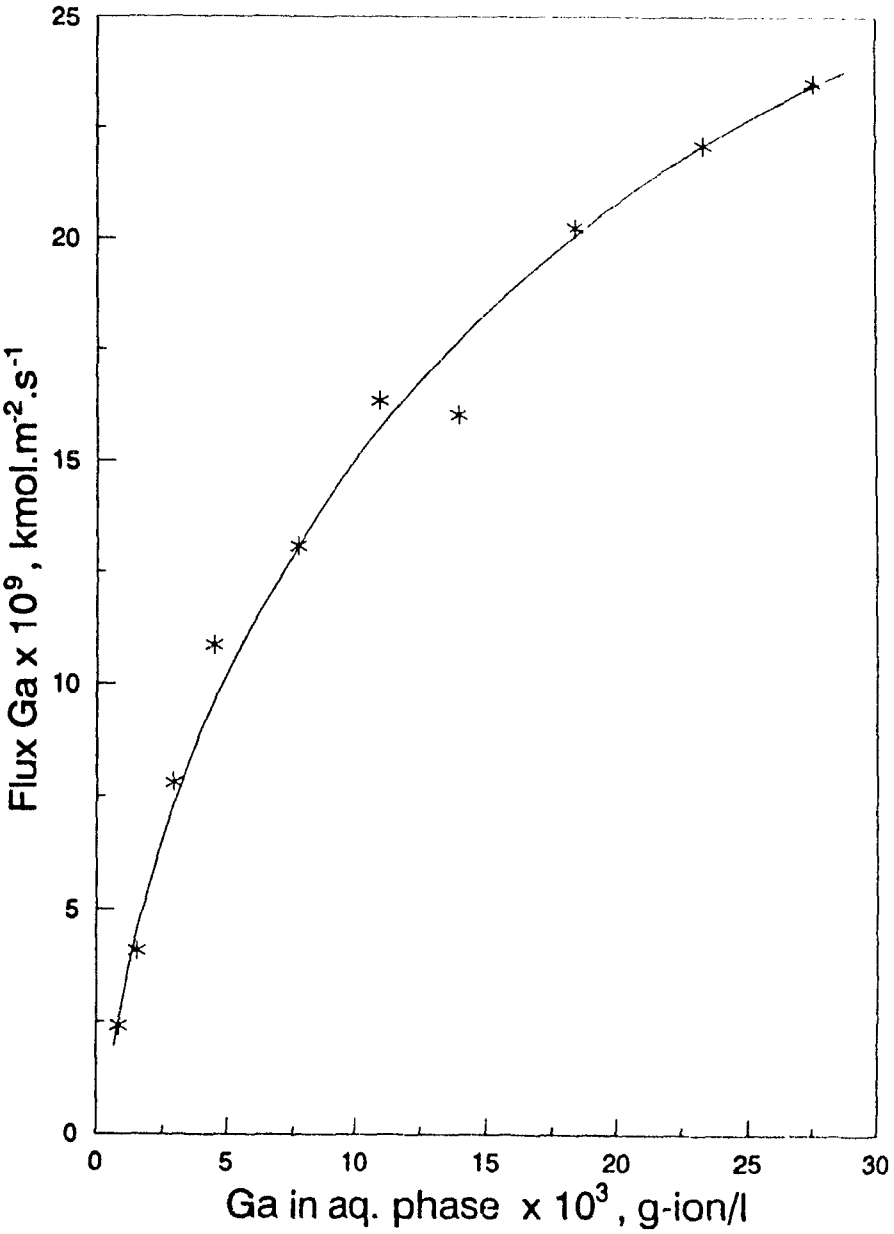

Figure 4.23: Extraction kinetics with D2EHPA. Effect of metal concentration in the aqueous phase. D2EHPA = 0.29 F, pH = 1.89, t = 22 °C.

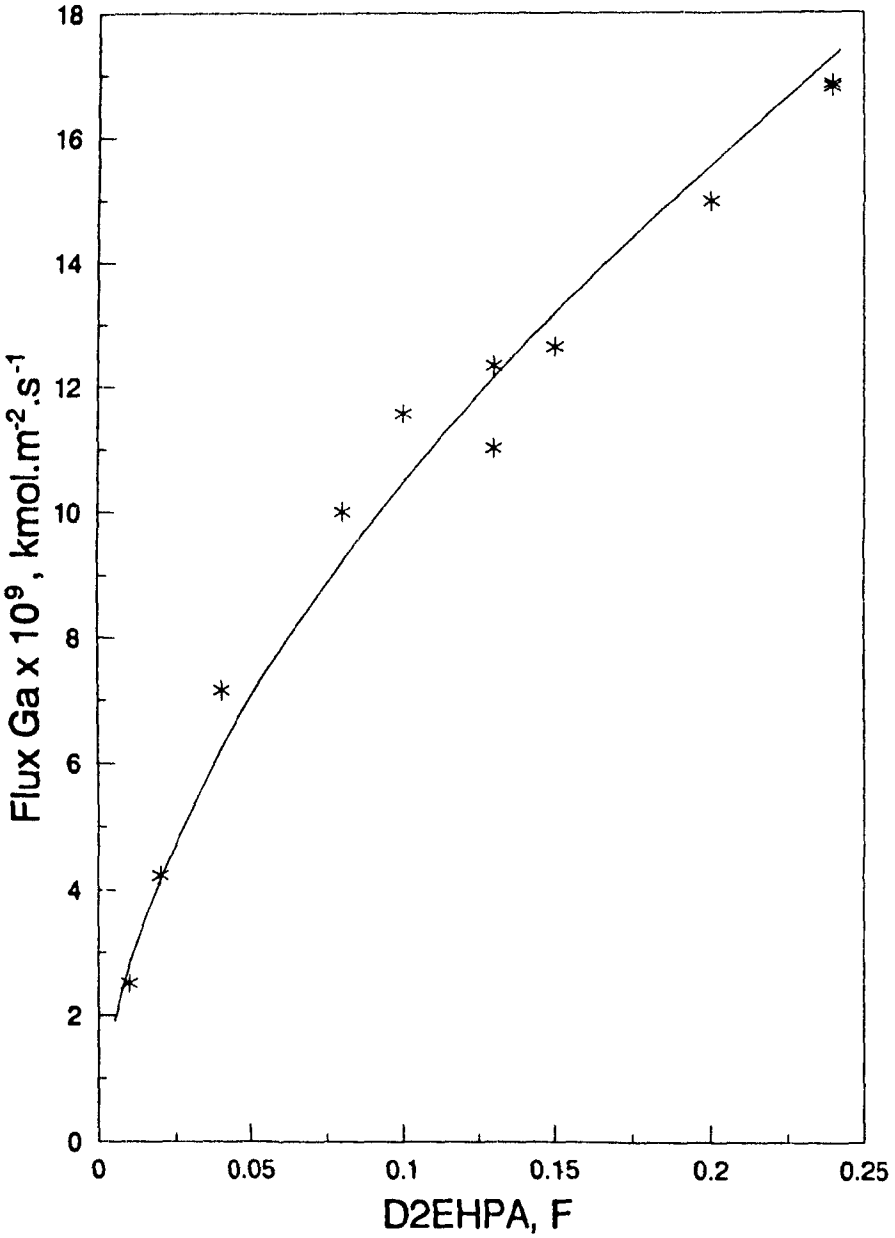

Figure 4.24: Extraction kinetics with D2EHPA. Effect of D2EHPA concentration. $Ga_{(aq)} = 1.26 \times 10^{-2}$ g-ion/l, pH = 1.88, t = 22 °C.

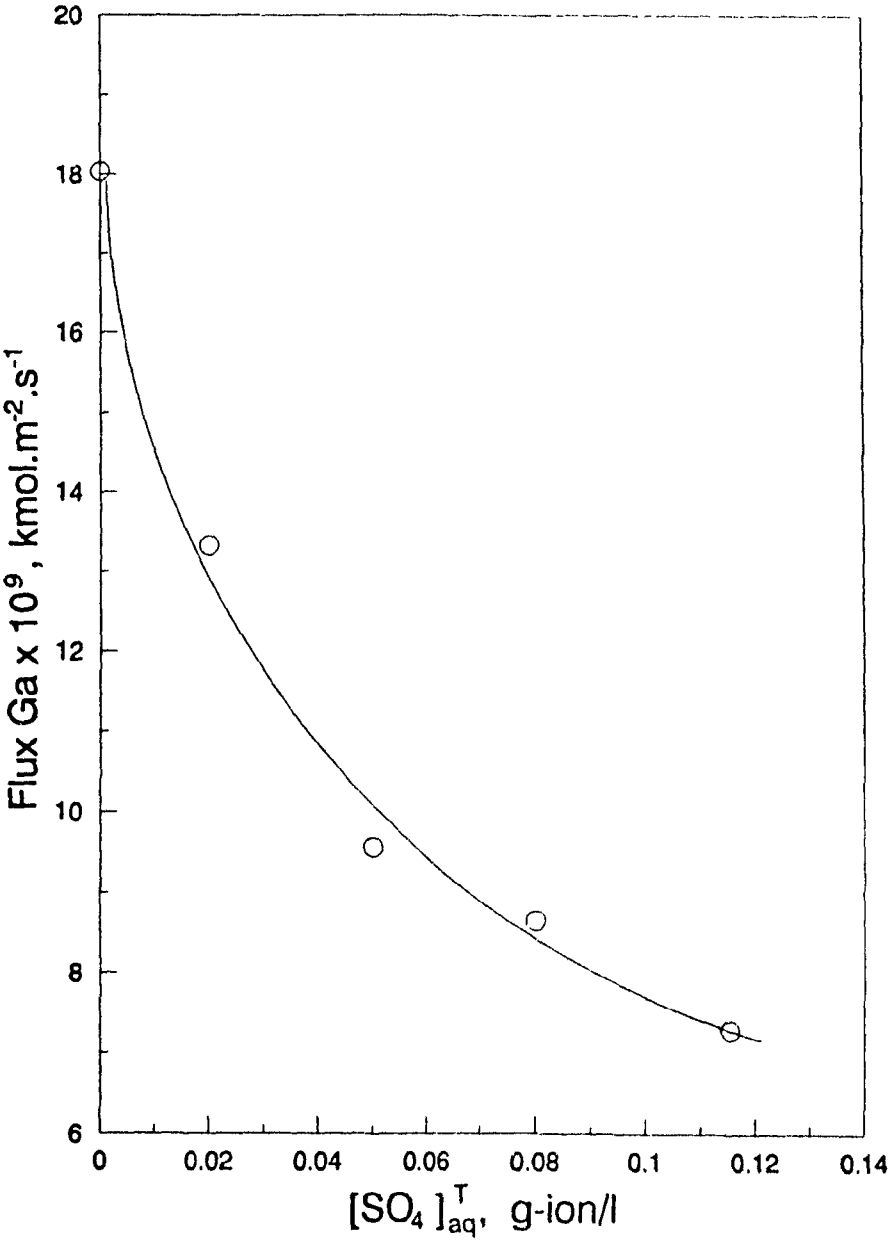

Figure 4.25: Extraction kinetics with D2EHPA. Effect of sulphate concentration. $Ga_{(aq)} = 1.43 \times 10^{-2}$ g-ion/l, D2EHPA = 0.28 F, pH = 1.80, t = 21 °C.

E_a, of the reaction is directly determined from the slopes of the resulting lines.

It is known that for diffusion-controlled processes the values of E_a are low due to the small effect of temperature on diffusion coefficients [114]. On the other hand, for processes controlled by chemical reaction, E_a values are much higher because of the usually strong dependence of the intrinsic rate constant on temperature. Thus, the values of E_a obtained for a given process can serve as an indication whether diffusion or chemical reaction is rate controlling. Usually values of E_a less than 20 kJ/mol imply predominant diffusion control, while for more than 65–70 kJ/mol, chemical control is considered predominant.

The values of E_a obtained here indicate a mixed diffusion-chemical reaction control of the overall process but close to the case of chemical control. In fact, fig. 4.26 reveals that the data for each series of experiments can be better correlated by two straight lines (shown as dashed lines) having slightly different slopes, and therefore E_a values. This is to be expected, taking into account that at higher temperature the diffusion limitations will be more pronounced, thus resulting in deviations from linearity and lower values of E_a [114].

Furthermore, it is readily seen that the values of E_a decrease with increasing pH, other conditions remaining the same. This can be again explained with the effect of diffusion on the overall extraction rate—at higher pH the rate will be higher, as shown on fig. 4.22, and therefore the whole reaction will become more controlled by the mass-transfer. Hence, the value of the true activation energy (i.e., that of the chemical reaction), as distinguished from the apparent activation energy, will be closer to the value of E_a obtained for low pH and low temperature region. There, from line 4 of fig. 4.26, a value of 74.6 kJ/mol is determined.

The obtained values of the apparent activation energy compare well with those reported for aluminum extraction with D2EHPA—79.4, 79.5 and 82.4 kJ/mol for extraction from H_2SO_4, HCl, and HNO_3 solutions, respectively [115, 116]. The higher E_a values for aluminum are probably due to its lower extraction rate with D2EHPA

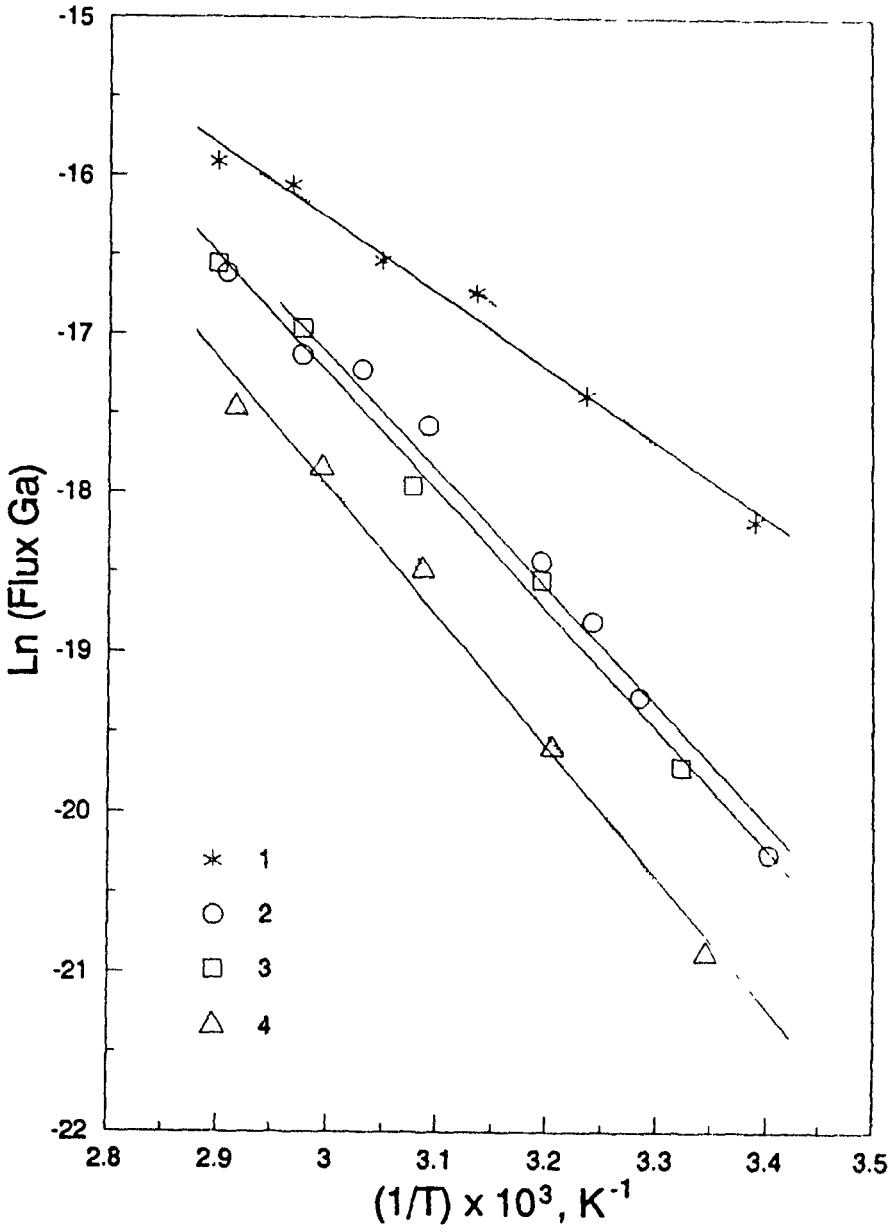

Figure 4.26: Extraction kinetics with D2EHPA. Temperature effect. $Ga_{(aq)} = 1.43 \times 10^{-2}$ g-ion/l, D2EHPA = 0.28 F, line 1: pH = 1.75, E_a = 41.4 kJ/mol; line 2: pH = 1.26, E_a = 60.9 kJ/mol; line 3: pH = 1.23, E_a = 61.9 kJ/mol; line 4: pH = 1.00, E_a = 67.6 kJ/mol.

in comparison to gallium (cf Section 6.5.2). On the other hand, for systems where the extraction is known to be fast, the values of E_a are much lower, indicating diffusion-controlled processes. Such an example is the extraction of copper with hydroxyoximes where E_a of 25.1 kJ/mol was found in the case of Lix 65N and 14.65 kJ/mol for a mixture of Lix 65N and Lix 63 extractants [117].

4.5.2 Stripping Kinetics

In the experiments for kinetics of gallium stripping from loaded D2EHPA, the effect of the following parameters was investigated:

- Gallium concentration in the organic phase—from 7.2×10^{-4} to 7.9×10^{-3} g-ion/l
- Free D2EHPA concentration[16] in the organic phase—from 0.01 to 0.30 F
- Acidity of the aqueous nitrate strip solution—from 0.10 to 0.80 g-ion/l
- Temperature—from 20 °C to 71 °C

Before starting the experiments, the 'linearity' test was performed and the results (fig. 4.27) showed that the rate of stripping remained constant within the specified time interval, as was the case with the rate of extraction.

Tests for the effect of interfacial area and stirring were also carried out. The rate of stripping was found proportional to the interfacial area (fig. 4.28), while a slight dependence on stirring was observed, as shown on fig. 4.29.

Effect of aqueous acidity, free extractant and metal concentrations in the organic phase

The rate of gallium stripping increases with increasing the acidity and the metal concentration in the organic phase (figures 4.30 and 4.31, resp.), and decreases when

[16] Defined as the total formal concentration minus the concentration corresponding to the amount complexed with the metal (see also Appendix C, page 243)

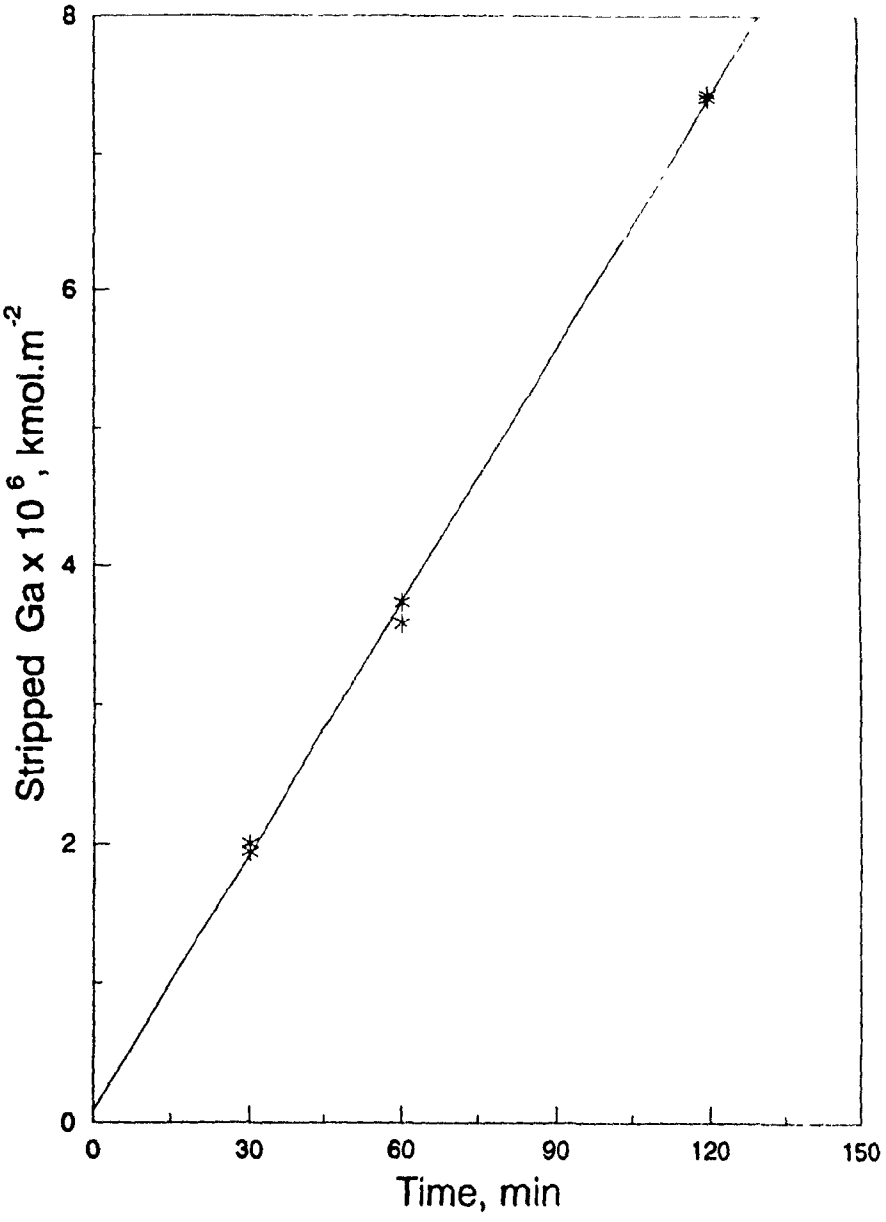

Figure 4.27: Test for constant rate of stripping. $Ga_{(org)} = 3.8 \times 10^{-3}$ g-ion/l, D2EHPA = 0.11 F, $[H^+] = 0.87$ g-ion/l, t = 20 °C.

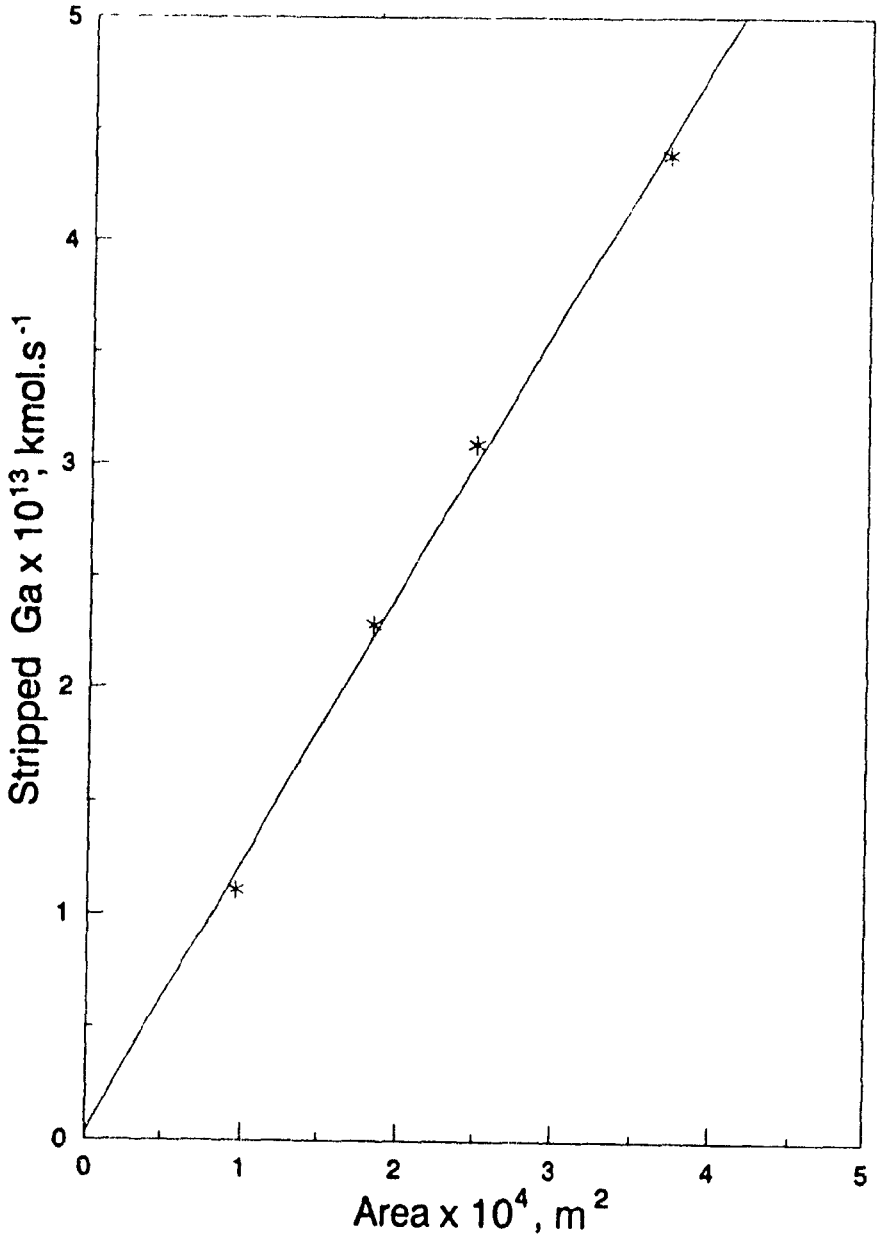

Figure 4.28: Stripping kinetics with D2EHPA. Effect of the interfacial area. $Ga_{(org)}$ = 3.8×10^{-3} g-ion/l, D2EHPA = 0.04 F, $[H^+]$ = 0.87 g-ion/l, t = 20 °C.

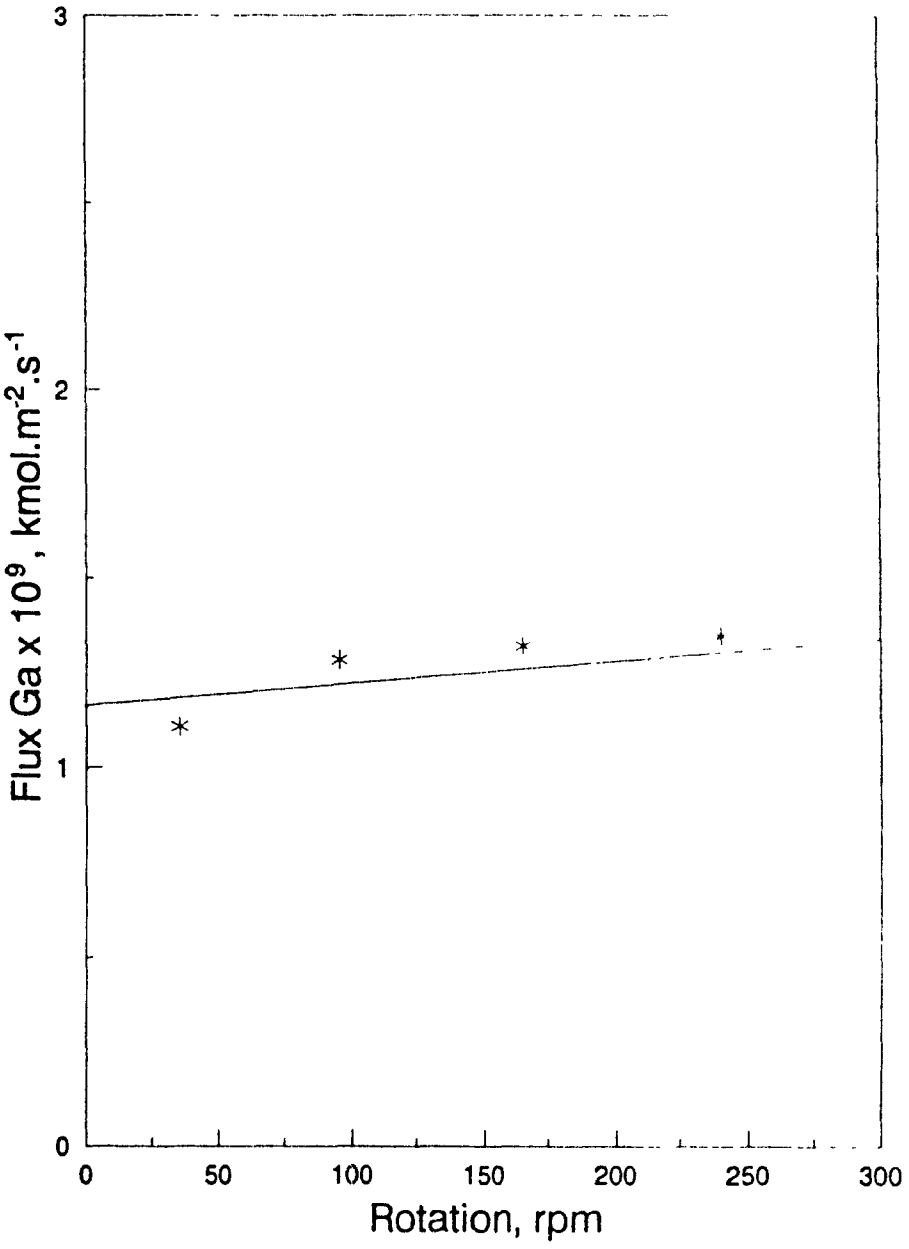

Figure 4.29: Stripping kinetics with D2EHPA. Effect of stirring. $Ga_{(org)} = 3.8 \times 10^{-3}$ g-ion/l, D2EHPA = 0.04 F, $[H^+] = 0.87$ g-ion/l, t = 20 °C.

the extractant concentration increases (fig. 4.32). The results show a very close to a first-order dependence of the rate of stripping on metal concentration in the organic phase and acidity, and an inverse first-order with respect to the concentration of dimeric D2EHPA.

As with eqn (4.58) for the extraction rate, the following empirical equation is obtained here for the rate of stripping:

$$\text{Flux Ga (stripping)} \left(\frac{\text{kmol}}{\text{m}^2.\text{s}}\right) = 0.87 \times 10^{-8} [\text{Ga}]_{0\ (\text{org})}^{1.03} [(\text{HR})_2]_{0\ (\text{org})}^{-1.01} [\text{H}^+]_0^{1.01} \quad (4.59)$$

If the two equations (4.58) and (4.59) were representing the intrinsic kinetics of the extraction and stripping reactions, respectively, then the ratio of the two constants, $(1.82 \times 10^{-8}/0.87 \times 10^{-8}) = 0.21$, should be equal to the equilibrium constant, K'_{ex}, which was found earlier to be 0.757 mol/l (see page 41). Furthermore, the order dependence on the respective terms in the equation for K'_{ex} for the overall reaction 4.10, should coincide with the orders which result when eqns (4.58) and (4.59) are combined under the condition of established equilibrium—the rate of extraction equal to the rate of stripping. The fact that differences are observed implies that the two empirical equations reflect just different overall effects of the simultaneously proceeding mass-transfer and the chemical reaction for the extraction and stripping processes.

Effect of temperature

The results are presented on fig. 4.33 in Arrhenius plot coordinates. The deviation from a straight line at higher temperatures is evident. Hence, the data were correlated by two lines—a value of 41.8 kJ/mol for E_a was determined for the low temperature region, and a value of 14.2 kJ/mol for the range of higher temperature. Both values of E_a are lower than those obtained for the extraction, which means that the rate of stripping is less sensitive to temperature than the extraction rate. Also, the lower values imply a mixed diffusion-chemical reaction control, especially in the higher temperature range.

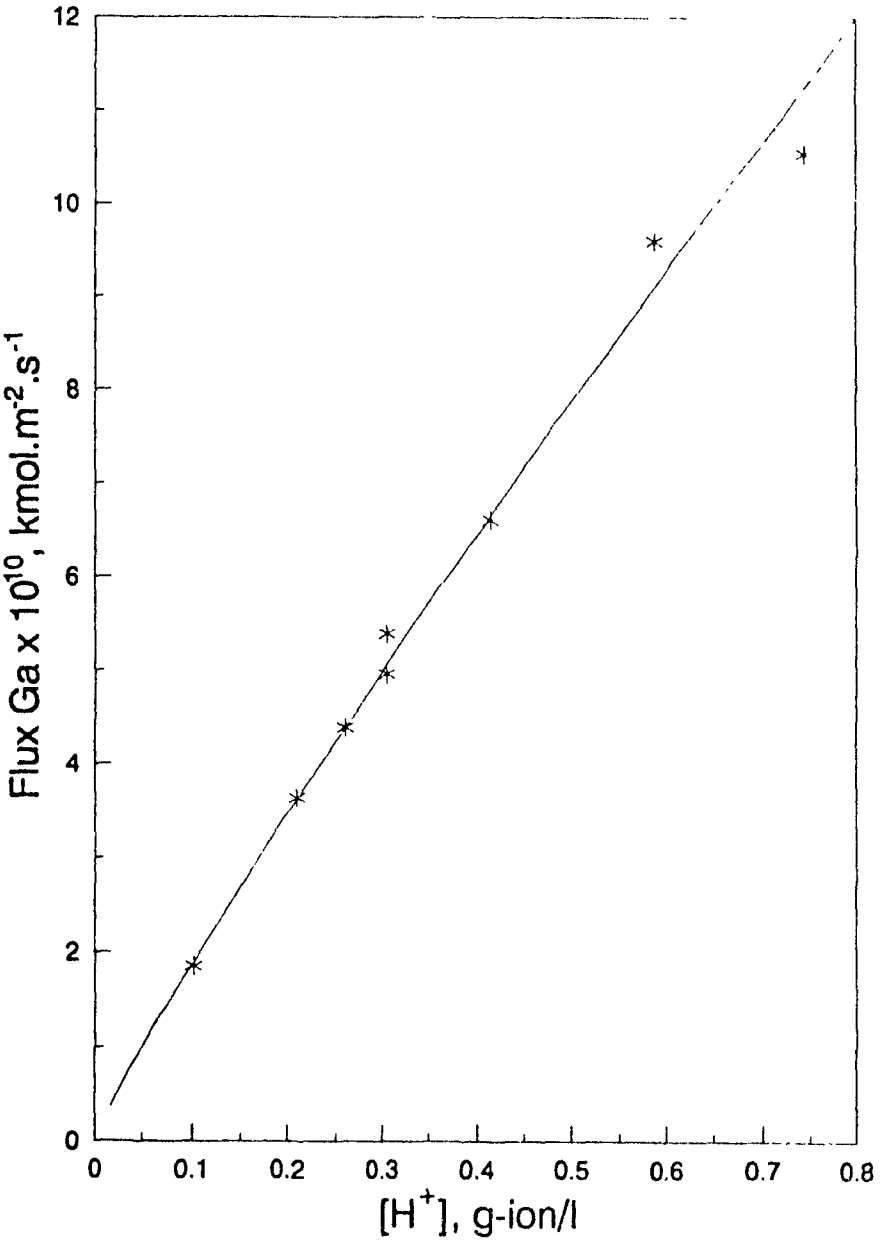

Figure 4.30: Stripping kinetics with D2EHPA. Effect of aqueous acidity. $Ga_{(org)} = 3.8 \times 10^{-3}$ g-ion/l, D2EHPA = 0.07 F, t = 20 °C.

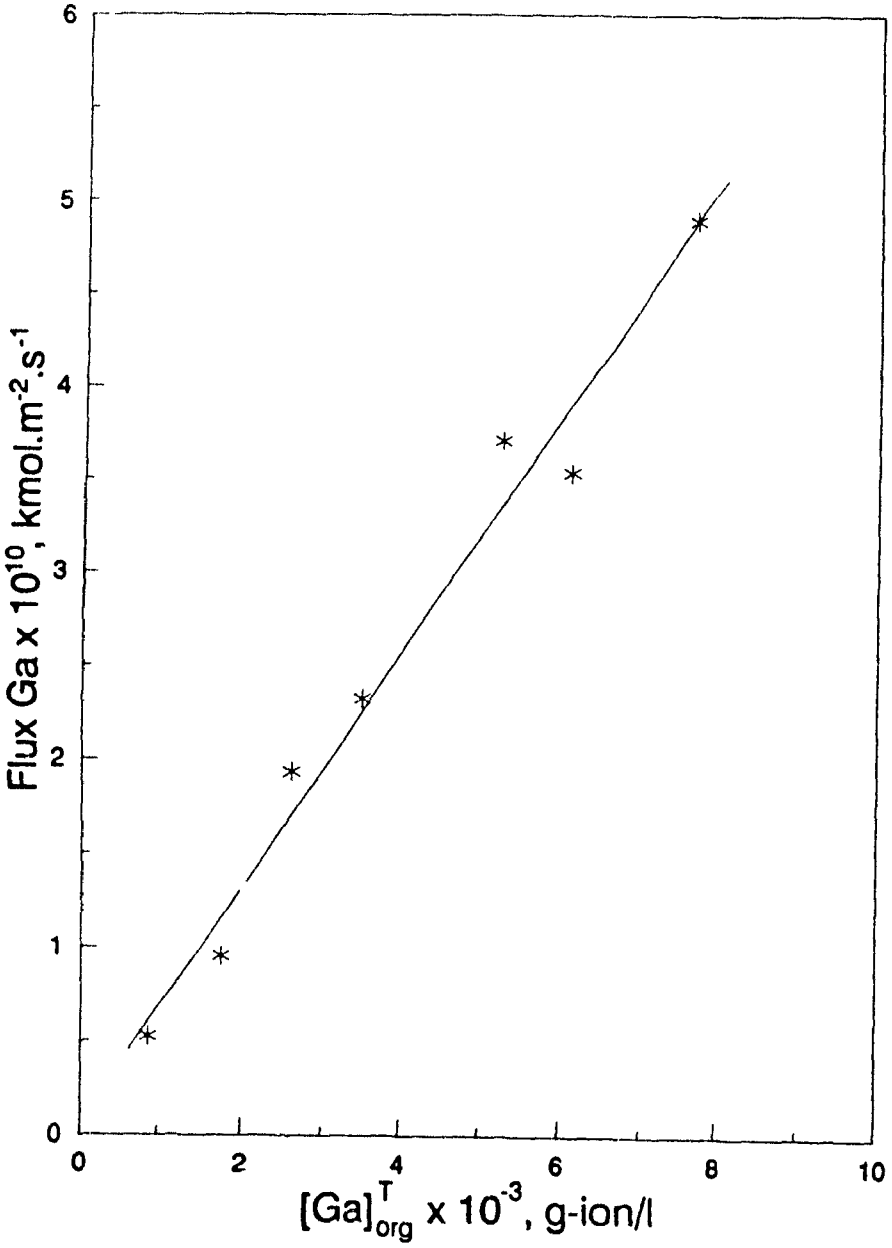

Figure 4.31: Stripping kinetics with D2EHPA. Effect of metal concentration in the organic phase. D2EHPA $\approx$ 0.18 F, $[H^+]$ = 0.50 g-ion/l, t = 20 °C.

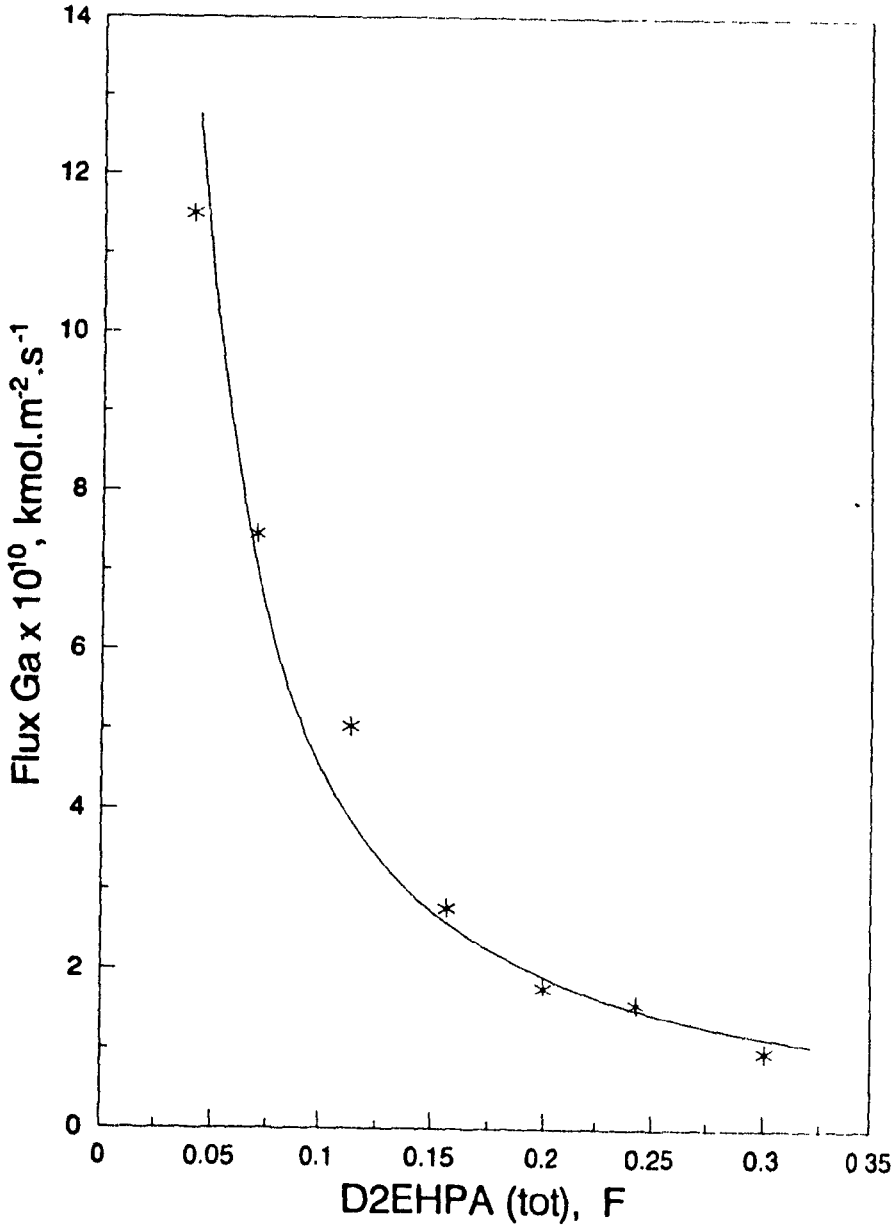

Figure 4.32: Stripping kinetics with D2EHPA Effect of D2EHPA concentration. $Ga_{(org)} = 3.8 \times 10^{-3}$ g-ion/l, $[H^+] = 0.50$ g-ion/l, t = 20 °C.

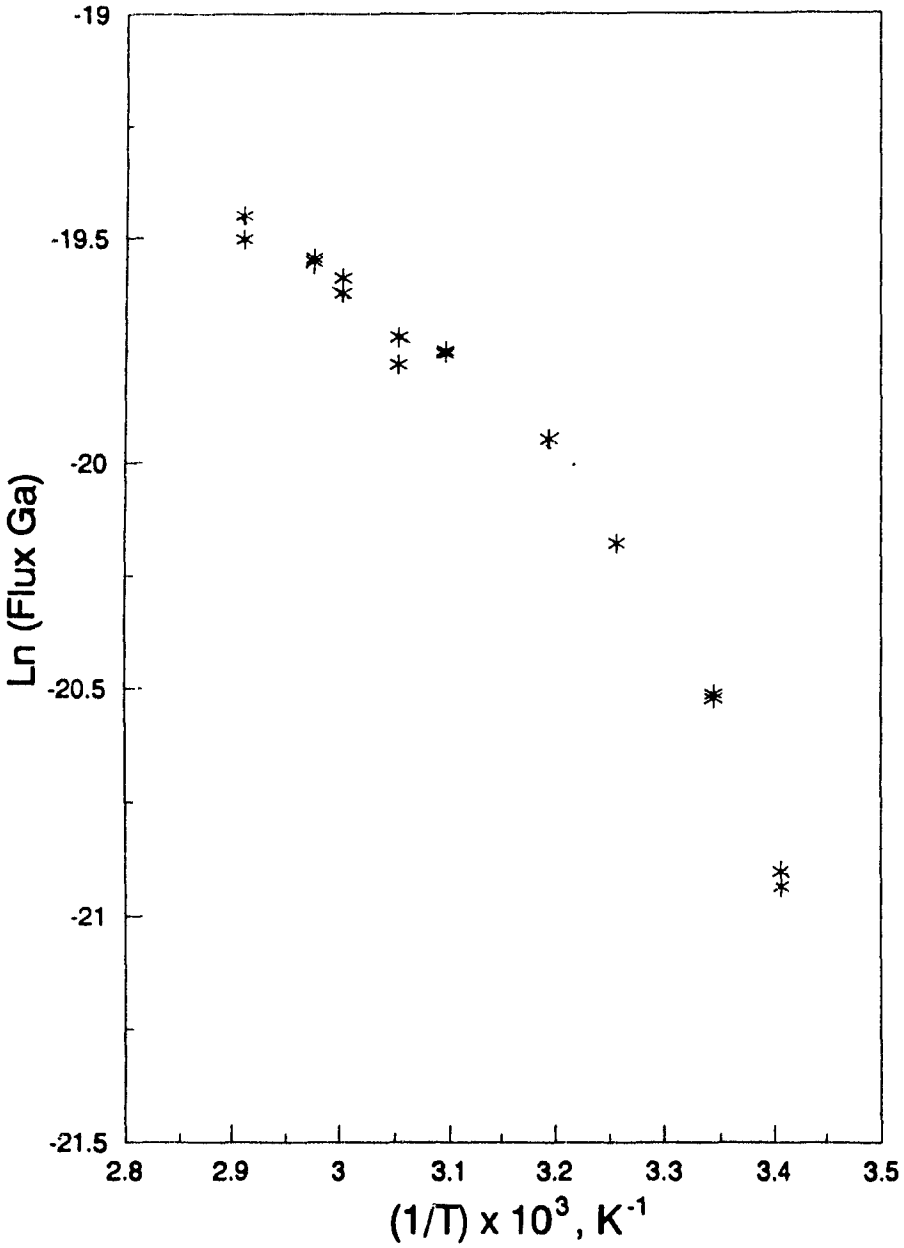

Figure 4.33: Stripping kinetics with D2EHPA. Temperature effect. $Ga_{(org)} = 3.8 \times 10^{-3}$ g-ion/l, D2EHPA = 0.11 F, $[H^+] = 0.75$ g-ion/l.

extractant notation	mole fraction mono-OPAP, x
extr. M	0.987
extr. O	0 623
extr. T	0.214

Table 4-8: Compositions of OPAP reagents used in the extraction kinetics experiments.

4.6 Extraction Kinetics of Gallium with OPAP Extractants

The kinetic experiments were carried out with three different compositions of the OPAP reagent (Table 4-8), and in the same way as described for gallium extraction with D2EHPA. The effect of the following parameters was determined:

- pH of the aqueous solution—for pH from 0.80 to 1.60
- Gallium concentration in the aqueous phase—in the range from 1.0×10^{-3} to 5.0×10^{-3} g-ion/l
- Total concentration of OPAP in the organic phase—from 0.05 to 0.25 F
- Composition of OPAP (Table 4-8)
- Temperature—from 20 °C to 65 °C

The preliminary tests showed that the extraction rate increases linearly with the interfacial area (fig. 4.34) and is independent on the volume ratio of the two phases. A slight dependence on stirring was observed (fig. 4.35). As was the case with the other kinetic experiments, the 'linearity' tests again showed similar results (fig. 4.36).

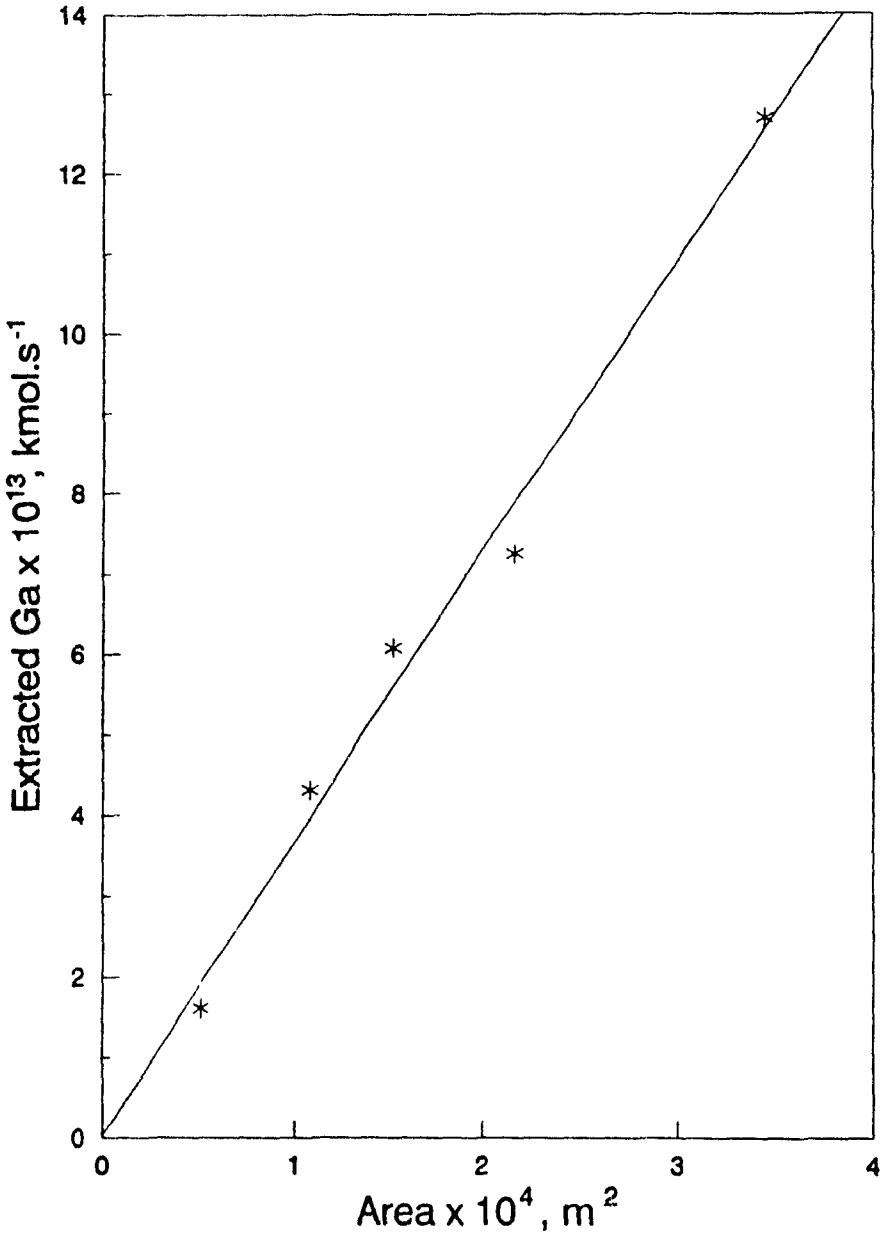

Figure 4.34: Extraction kinetics with OPAP. Effect of the interfacial area. $Ga_{(aq)}$ = 3.9×10^{-3} g-ion/l, OPAP = 0.14 F (extr. O), pH = 1.00, t = 20 °C.

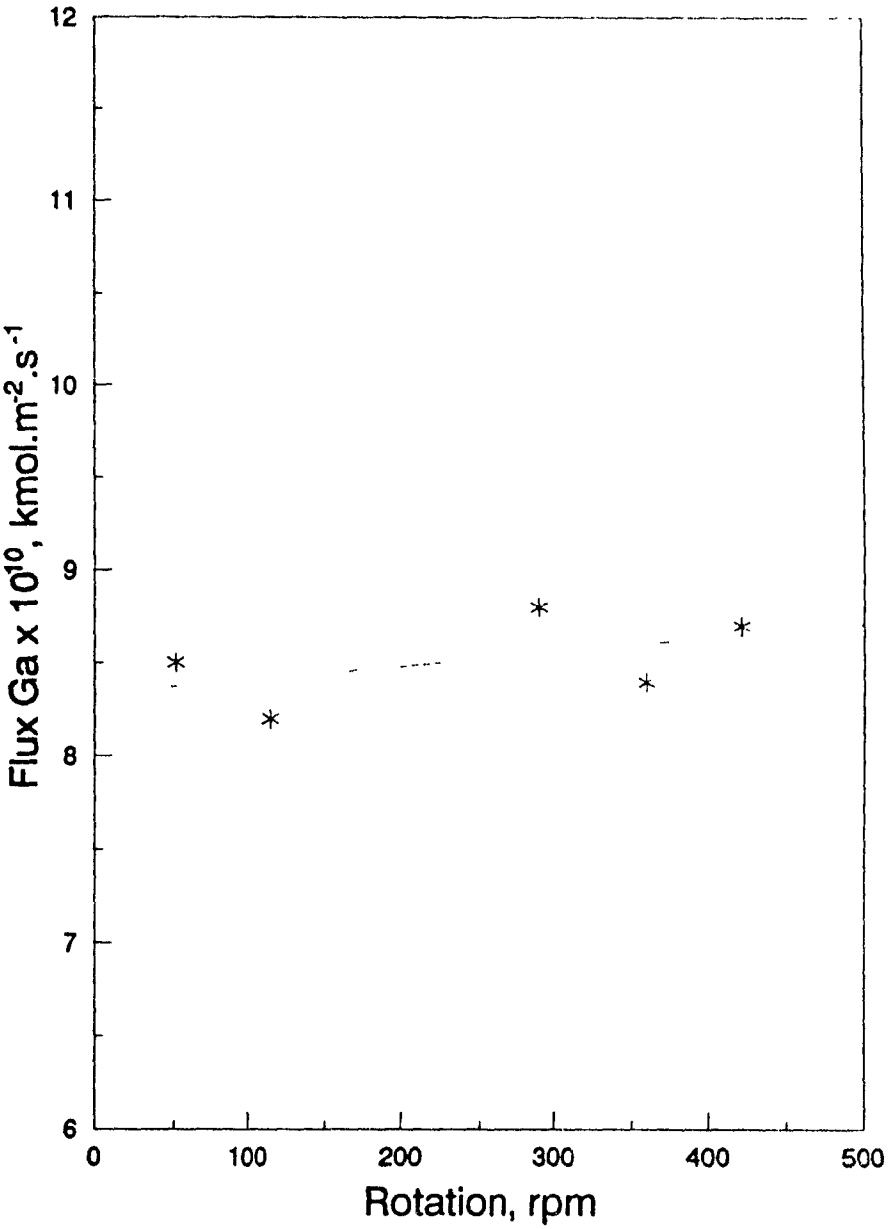

Figure 4.35: Extraction kinetics with OPAP. Effect of stirring. $Ga_{(aq)} = 3.7 \times 10^{-3}$ g-ion/l, OPAP = 0.14 F (extr. O), pH = 0.69, t = 21 °C.

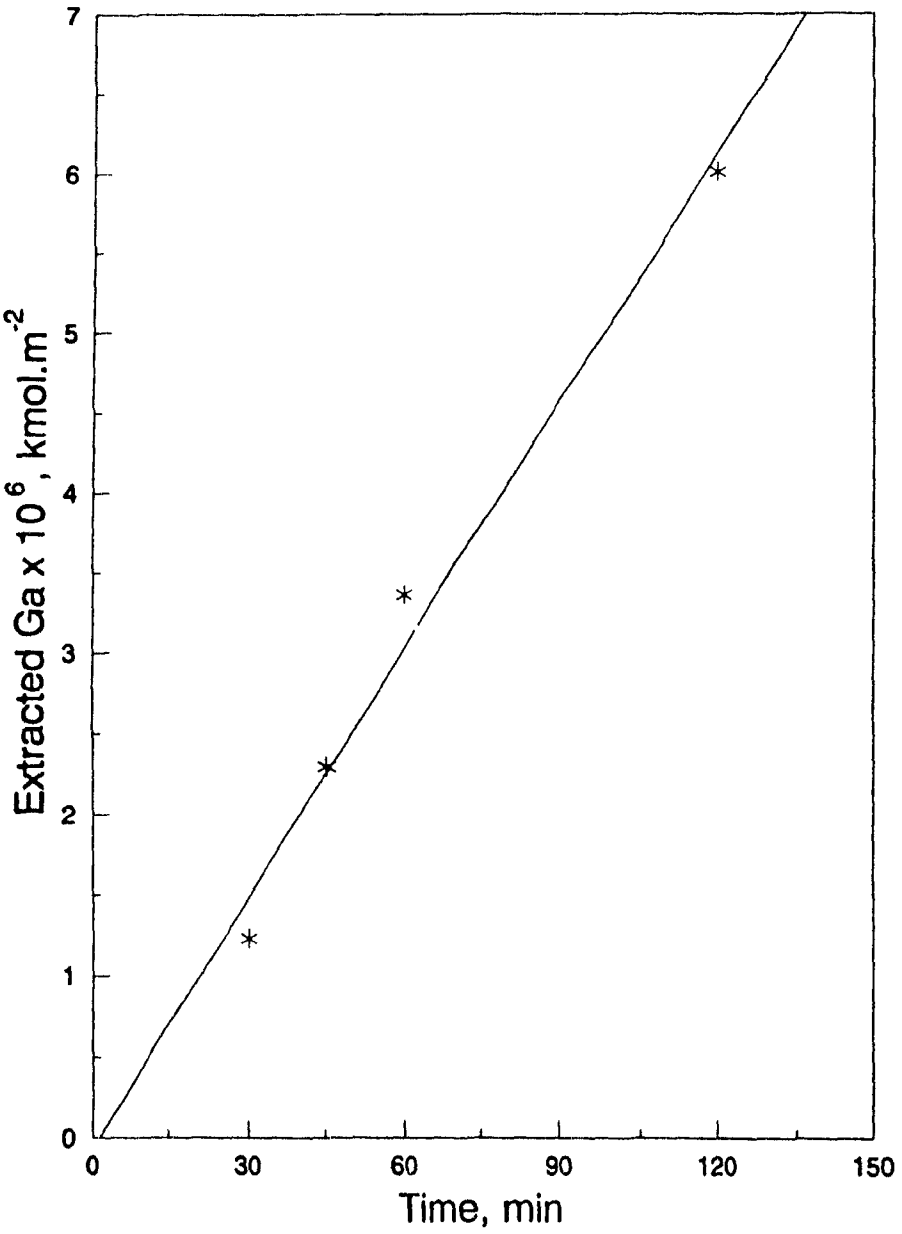

Figure 4.36: Test for constant extraction rate. $Ga_{(aq)} = 3.9 \times 10^{-3}$ g-ion/l, OPAP = 0.14 F (extr. O), pH = 1.00, t = 21 °C.

Effect of pH, metal and extractant concentrations

Results for the dependence of gallium extraction rate, with OPAP reagents, on pH, metal concentration in the aqueous phase, and the extractant concentration are presented on figures 4.37, 4.38, and 4.39, respectively. As expected, the rate increases with increasing pH, as well as the metal and extractant concentrations. Also, the results show that the rate is higher for the OPAP reagents with higher mole fraction of mono-OPAP. The observed respective dependencies appear similar to those for extraction with D2EHPA.

Effect of temperature

The results for the temperature dependence of gallium extraction rate with OPAP reagents are given on fig. 4.40. The following values of E_a were determined:

$$E_a = 51.6\text{kJ/mol}, \quad \text{for extr. M}$$

$$E_a = 57.1\text{kJ/mol}, \quad \text{for extr. O}$$

$$E_a = 58.9\text{kJ/mol}, \quad \text{for extr. T}$$

It is evident that the values are lower then those obtained for D2EHPA, and also the reagent with highest mono-OPAP content (extr. M) has the lowest apparent activation energy. This indicates that these values probably reflect mixed chemical reaction with mass-transfer control.

It should be emphasized, however, that in the case of OPAP reagents, there are several extraction reactions taking place simultaneously with the mass-transfer.

4.7 Summary

The experimental results on gallium extraction equilibria and kinetics with D2EHPA and OPAP extractants, presented in this Chapter, can be summarized as follows:

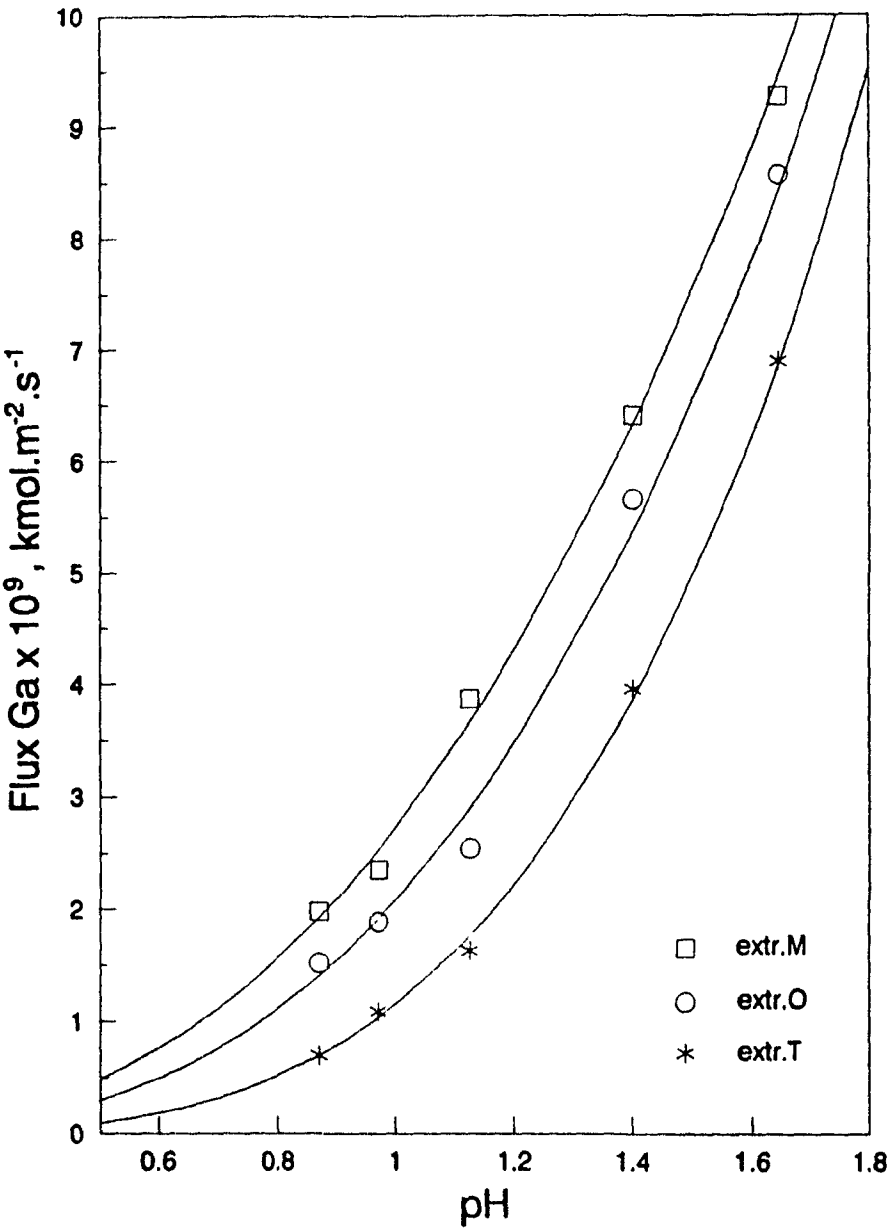

Figure 4.37: Extraction kinetics with OPAP. Effect of pH. $Ga_{(aq)} = 6.53 \times 10^{-3}$ g-ion/l, OPAP: 0.116 F (extr. M), 0.101 F (extr. O), 0.107 F (extr. T), t = 20 °C.

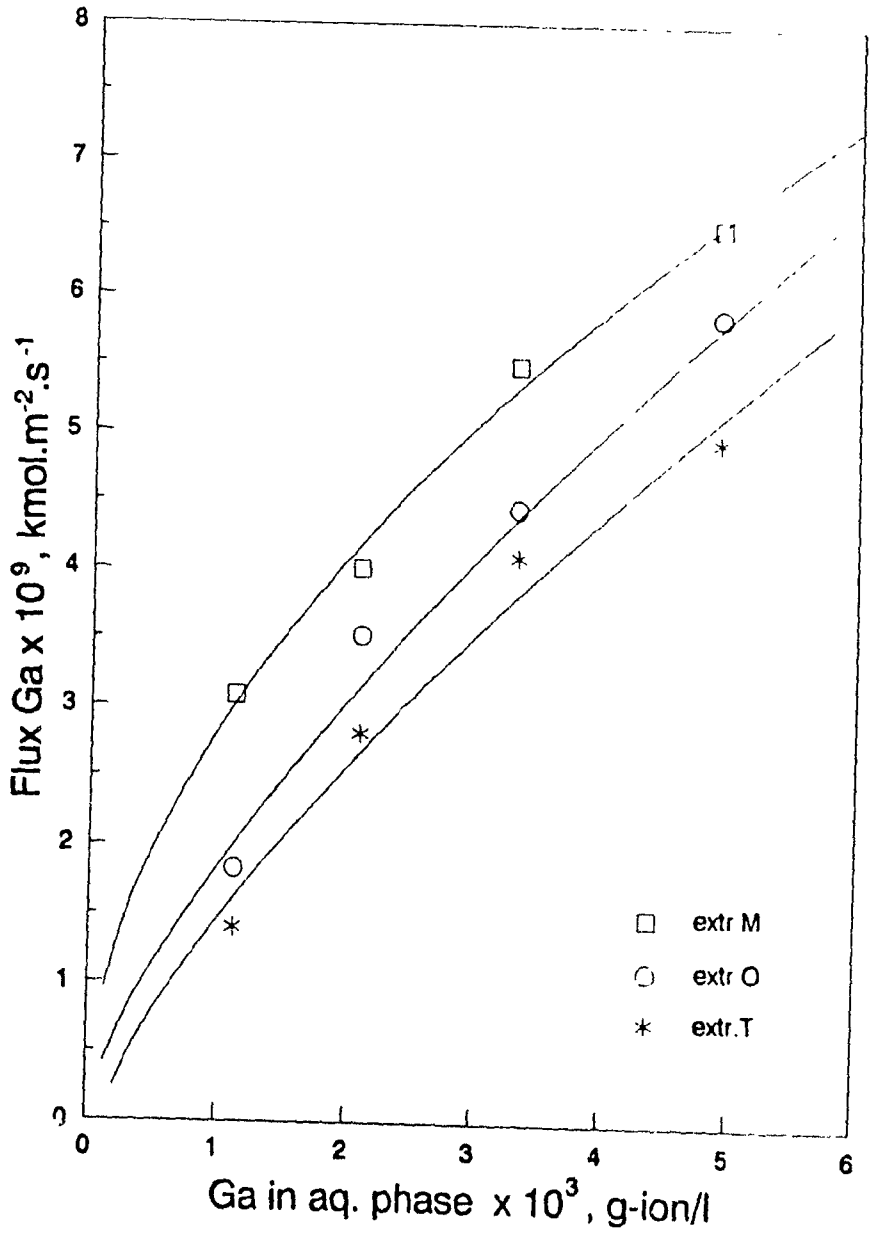

Figure 4.38: Extraction kinetics with OPAP. Effect of metal concentration in the aqueous phase. OPAP: 0.106 F (extr. M), 0.101 F (extr. O), 0.108 F (extr. T), pH = 1.41, t = 20 °C.

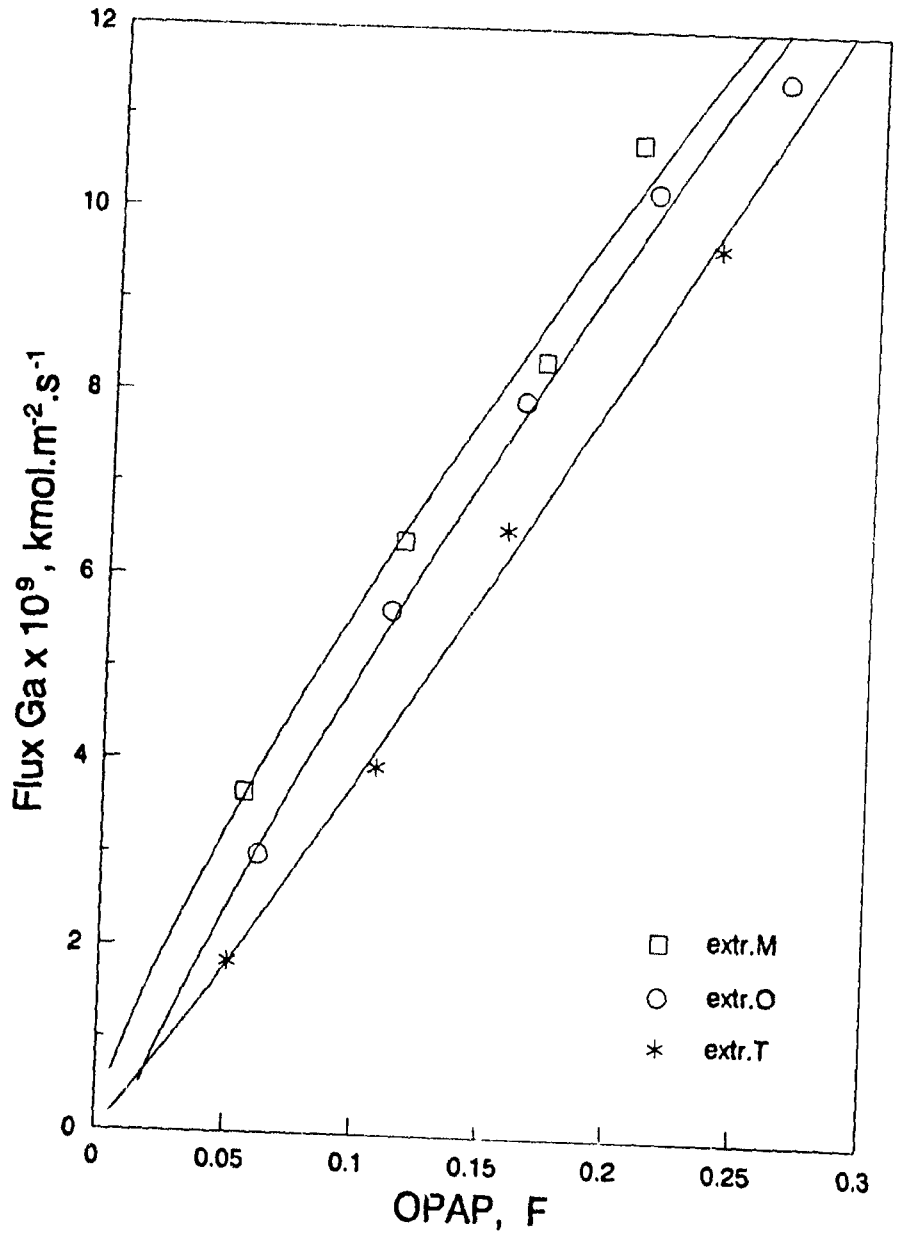

Figure 4.39: Extraction kinetics with OPAP. Effect of OPAP concentration. $Ga_{(aq)} = 6.53 \times 10^{-3}$ g-ion/l, pH = 1.41, t = 20 °C.

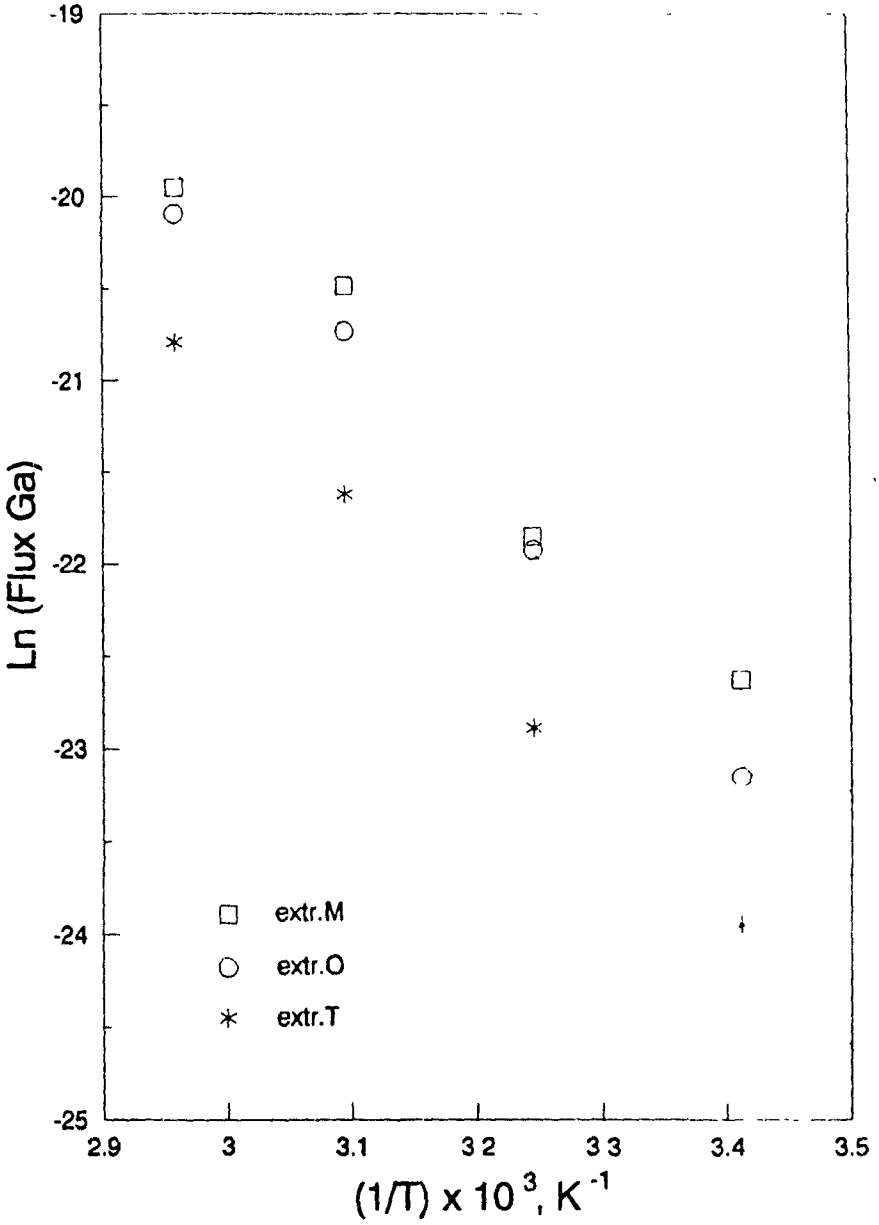

Figure 4.40: Extraction kinetics with OPAP. Temperature effect $Ga_{(aq)} = 6.53 \times 10^{-3}$ g-ion/l, OPAP: 0.106 F (extr. M), 0.101 F (extr. O), 0.108 F (extr T), pH = 0.78.

- Gallium is extracted with D2EHPA and OPAP by cation exchange for the acidity range studied at pH above 0.4–0.5. Sulphates from the aqueous solution are not extracted.

- The overall stoichiometry of the extraction reaction of gallium with D2EHPA is given by reaction 4.10 and K'_{ex} is 0.757 mol/l (for $I = 0.5$). The predominant complex is $GaR_3 \cdot HR$. The results indicate possible formation of $GaR_3 \cdot 3HR$ at low metal loadings (high excess of extractant), while, under conditions of organic saturation or when the loading capacity is reached, the molar metal-extractant ratio corresponds to the complex GaR_3.

- The extraction of gallium with OPAP is described by four simultaneous reactions, leading to the formation of four metal-extractant complexes—GaM_3, GaD_3, GaM_2D, and $GaMD_2$—with their respective equilibrium constants given in Table 4-5. Increasing the mole fraction of mono-OPAP in the mixtures of the two OPAP reagents leads to increased gallium extraction. The presence of alcohol, *n*-decanol, in the OPAP organic solution, is needed for improved phase separation. At the same time, the alcohol serves to prevent extractant dimerization and formation of solvated metal-extractant complexes.

- OPAP reagents extract gallium better and at lower acidities than D2EHPA. This is explained by their more acidic nature in comparison to D2EHPA. Furthermore, due to the higher formula weights of di-OPAP and mono-OPAP with respect to D2EHPA and M2EHPA, their aqueous solubilities are expected to be comparable to those of D2EHPA and M2EHPA, if not lower.

- The rate of gallium extraction increases with increasing pH, metal concentration in the aqueous phase, and extractant concentration. For OPAP extractants, the rate increases with increasing mole fraction of mono-OPAP. The rate is also strongly dependent on temperature. For extraction with OPAP, values for E_a from 51.6 to 58.9 kJ/mol are determined, depending on the extractant compo-

sition (fig. 4.40) for otherwise fixed conditions. In extractions with D2EHPA, the values of the apparent activation energy change significantly with the experimental conditions (fig. 4.26). This can be explained in terms of changing contributions of both chemical reaction and mass-transfer to the rate control of the process. For experimental conditions where the chemical rate is expected to be controlling, e.g., low pH and temperature, E_a of 74.6 kJ/mol is determined and is considered to be close to the true activation energy—of the chemical reaction.

- The rate of gallium stripping from loaded D2EHPA increases with increasing aqueous acidity and metal concentration in the organic phase. The rate decreases with increasing extractant concentration. For the effect of temperature, the Arrhenius plot (fig. 4.33) shows that the apparent activation energy does not remain constant within the studied temperature range, which indicates a change from chemical to diffusion controlled process. For the low temperature region, E_a is determined as 41.8 kJ/mol, and for the range of high temperatures--14.2 kJ/mol. Both values are smaller than those for the extraction rate. A more detailed discussion on the reaction mechanism, based on the kinetic data, will be presented in Chapter 6.

- The presence of sulphates in the aqueous solution has a significant effect on both gallium equilibrium distribution and extraction rate. Lower D_{Ga} values and extraction rates result when the sulphate concentration increases. This is clearly due to gallium complexation in the aqueous phase. In Chapter 5, this subject will be discussed in more detail, so enabling quantitative prediction of this effect on the extraction performance.

Chapter 5

Gallium Complexation in Sulphate Solutions

5.1 Introduction

In the previous Chapter 4, the experimental results have shown that the presence of sulphates in the aqueous solution has a profound effect on gallium equilibrium distribution, expressed by D_{Ga}, and the rate of extraction. It is therefore necessary to take into account the complexation phenomena when describing the relevant processes of gallium extraction from sulphate solutions.

Thus the purpose of the present Chapter is to develop a quantitative tool for determining the concentrations of the reacting species, which are then related to the extraction performance, from the aqueous solution parameters that can be readily found. The result must be applicable to the solution conditions encountered in hydrometallurgical practice, including sulphate concentrations and ionic strengths.

The following steps are considered in solving this problem:

- Identification of all possible existing gallium complexes for the range of conditions of interest.
- Collection of data for the mass-stability constants of the respective complexes for different ionic strengths.

These two steps are based here on available information from literature sources. It is obvious that the correctness of the collected data is crucial to the reliability and the usefulness of the final results from the speciation study.

- Determination of the relationship between mass-stability constants of the complexes and the ionic strength of the solution. This is necessary so that the species distribution can be determined for the required conditions.
- Development of the appropriate algorithm and computer program for the necessary calculations.
- Interpretation of the obtained results. The correctness is checked by comparing their predictions with the experimental data from gallium extraction.

All data on mass-stability constants of the complexes involved, at different ionic strengths, are collected for 25 °C, and accordingly the speciation diagrams and relevant discussion refer to that temperature. Although not performed in the present study, it is possible to extrapolate the data, using basic thermodynamic functions, to higher temperatures. Thus, the distribution of species at a particular temperature can be found, if needed.

5.2 Complexes and Stability Constants

In sulphate solutions, the available ligands for complex formation are OH^-, SO_4^{2-}, and HSO_4^-—from the incomplete second dissociation of sulphuric acid. Neutral water molecules may also be present as ligands in the inner sphere around the central metal cation.

The mass-stability constant (for ionic strength I) of any complex MeL_n is defined as

$$\beta_n = \frac{[MeL_n]}{[Me][L]^n} \tag{5.1}$$

These two steps are based here on available information from literature sources. It is obvious that the correctness of the collected data is crucial to the reliability and the usefulness of the final results from the speciation study.

- Determination of the relationship between mass-stability constants of the complexes and the ionic strength of the solution. This is necessary so that the species distribution can be determined for the required conditions.
- Development of the appropriate algorithm and computer program for the necessary calculations.
- Interpretation of the obtained results. The correctness is checked by comparing their predictions with the experimental data from gallium extraction.

All data on mass-stability constants of the complexes involved, at different ionic strengths, are collected for 25 °C, and accordingly the speciation diagrams and relevant discussion refer to that temperature. Although not performed in the present study, it is possible to extrapolate the data, using basic thermodynamic functions, to higher temperatures. Thus, the distribution of species at a particular temperature can be found, if needed.

5.2 Complexes and Stability Constants

In sulphate solutions, the available ligands for complex formation are OH^-, SO_4^{2-}, and HSO_4^-—from the incomplete second dissociation of sulphuric acid. Neutral water molecules may also be present as ligands in the inner sphere around the central metal cation.

The mass-stability constant (for ionic strength I) of any complex MeL_n is defined as

$$\beta_n = \frac{[MeL_n]}{[Me][L]^n} \tag{5.1}$$

according to its formation reaction:

$$Me + nL \rightleftharpoons MeL_n \tag{5.2}$$

Hydroxy complexes

Four complexes, $Ga(OH)_n^{3-n}$ where $n = 1, \ldots, 4$ are known to exist in aqueous solutions [118, 119]. In highly alkaline media, $Ga(OH)_4^-$ is predominant [118], although possible existence of $Ga(OH)_5^{2-}$ and $Ga(OH)_6^{3-}$ has also been suggested [120]. In concentrated gallium solutions (more than 0.1 g-ion/l Ga) one or more polynuclear species with an approximate formula $Ga_{26}(OH)_{65}^{13-}$ exist at pH above 3 [118]. In this work, acidic solutions with fairly low gallium concentrations (in general, below 0.01 g-ion/l Ga) are of interest, and therefore only the four mono-nuclear complexes are further considered.

The data collected for the mass-stability constants of the four hydroxy complexes for different ionic strengths are summarized in Table 5-1. It is seen that the reported values from various sources agree well for $I = 0.1$, and a significant disagreement exists at higher ionic strengths. Two opposite trends are observed as to how the constants change with the ionic strength. For the data reported in the handbook of Kotrlý and Šucha [119], β decreases with I, while for those reported by Biryuk and Nazarenko [123] and cited by Högfeldt [104], the stability constants increase with ionic strength. Such controversies are unfortunately quite common, and not only for gallium, in the literature on stability constants (e.g., refs. [124, 125, 126]). This is the reason why it is always necessary to extract, when possible, information from the original references.

The data compiled by Kotrlý and Šucha [119] appear to have been taken from the book of Baes and Mesmer [118] who have used the original data reported by Nazarenko *et al.* [122] for the three complexes, $Ga(OH)^{2+}$, $Ga(OH)_2^+$, and $Ga(OH)_3$, and at $I = 0.1$ only, to extrapolate to other ionic strengths.

It becomes clear now that the original data, reported later in various compila-

tion handbooks [104, 119, 121], were obtained in the same laboratory using the same method[1] by the same research group [122, 123]. In fact, the second study [123] extends the previous one to gallium perchlorate solutions having different ionic strengths—0.1, 0.3, 0.5, and 1.0. The results for $I = 0.1$ were found to agree well with those in the previous report [122]. Because these values for the stability constants for several ionic strengths have been obtained directly from experiment and not produced by extrapolation, they are considered relatively more accurate than those found in the other sources [118, 119], and therefore the former are selected for this work.

One disadvantage of the two studies [122, 123] is that neither takes into account the fourth gallium complex $Ga(OH)_4^-$. This is probably because the solutions employed covered the pH range up to around 5. In the work here, data for this complex are taken from Kotrlý and Šucha [119], although it is obvious that its presence in acidic solutions will be negligible.

Sulphate complexes

There are two sulphate complexes, $Ga(SO_4)^+$ and $Ga(SO_4)_2^-$ known to form [127, 128, 129]. The data have been extrapolated to, and reported for $I = 0$ by the original authors, using the extended Debye-Hückel equation:

$$\log \gamma_{\pm} = \frac{-z^2 A_D \sqrt{I}}{1 + B_D d_a \sqrt{I}} + b_e z^2 I \qquad (5.3)$$

where $\gamma_{\pm}$ is the mean activity coefficient, z^2 is the sum of squares of ionic charges, A_D and B_D are the Debye-Hückel constants, d_a is the mean distance of approach of the ions, and b_e is an empirical constant accounting for the dielectric properties and other effects of the medium near the ion.

The data are summarized in Table 5-1. The values for $Ga(SO_4)^+$ differ, as given from the three sources [127, 128, 129]. This is probably because the analytical

[1] A spectrophotometric method, using systems of competing organic ligands, e.g., Pyrocatechol Violet, Alizarin Red S, which form coloured complexes with hydroxide ions

complex	$\log \beta$	I	Reference
$Ga(SO_4)^+$	2.77	0	[127]
	2.59	0	[128]
	2.99	0	[129]
	1.55	0 5	[130]
	1.88	0.5	[132]
$Ga(SO_4)_2^-$	2.77	0	[127]
$Ga(OH)^{2+}$	11.4	0	[119, 121]
	10.9	0.1	[122]
	11.13	0.1	[123]
	11.52	0.3	[123]
	10.8	0.5	[119]
	11.7	0.5	[123]
	10.6	1.0	[119]
	12.22	1.0	[123]
$Ga(OH)_2^+$	22.1	0	[119, 121]
	21.5	0.1	[122]
	21.46	0.1	[123]
	22.23	0.3	[123]
	22.8	0.5	[123]
	20.6	1.0	[119]
	24.13	1 0	[123]
$Ga(OH)_3$	31.7	0	[119, 121]
	30.9	0.1	[122]
	30.93	0.1	[123]
	32.31	0.3	[123]
	33.36	0.5	[123]
	29.8	1.0	[119]
	35.85	1.0	[123]
$Ga(OH)_4^-$	39 4	0	[119, 121]
	34.7	1.0	[119]

Table 5-1: Mass-stability constants for gallium complexes in sulphate solutions.

methods used have been different—calorimetry [127], pressure-jump relaxation technique [128], and indirect spectrophotometry [129]. In the present work, the value of $\log\beta = 2.77$ for $Ga(SO_4)^+$ has been chosen as an approximate average of the reported constants.

Values for the mass-stability constants of the sulphate complexes for ionic strengths other than zero have been found only for $Ga(SO_4)^+$ and are given in Table 5-1. In a series of studies Shishkova [130, 131, 132] reported data for $\log\beta$ at $I = 0.5$ for this complex in various aqueous and aqueous-organic solutions, determined by ion-exchange. For the system $Ga(ClO_4)_3$–H_2O–Na_2SO_4–$HClO_4$, a value of $\log\beta = 1.55$ has been found [130], and for $Ga(ClO_4)_3$–H_2O–H_2SO_4–$HClO_4$ system—$\log\beta = 1.88$ [132]. The author claims that the difference between the two values is not significant. The absence of other comparative studies, however, makes it difficult to estimate the reliability of the reported data. Hence, the criterion for reliability, accepted in the work here, is how well the results based on these data may agree with experimental findings for the effect of sulphates on gallium extraction.

Bisulphate complexes

It is well known that in sulphate solutions bisulphate ions are also present:

$$HSO_4^- \rightleftharpoons H^+ + SO_4^{2-} \tag{5.4}$$

and the second dissociation constant, K_2, is given by

$$K_2 = \frac{[H^+][SO_4^{2-}]}{[HSO_4^-]} \tag{5.5}$$

The reaction has been well studied and the values of K_2 at different ionic strengths and temperatures determined [133]. The following equation, based on the extended Debye-Hückel equation, has been found to correlate well the obtained values of K_2 with the ionic strength and temperature [133]:

$$\log K_2 = \log K_2^0 + 4 \times 0.509 \frac{\sqrt{I}}{(1 + A_k\sqrt{I})} \tag{5.6}$$

where K_2^0 is the value at $I = 0$ ($K_2^0 = 1.03 \times 10^{-2}$ mol/kg), $A_\lambda = 0.94$ at 25 °C, and the concentrations of species in eqn (5.5) as well as I are expressed on a molal scale. Complete first dissociation of sulphuric acid is also assumed. The above equation (5.6) was used in the present work.

Once HSO_4^- ions are present in the aqueous solution, it appears probable that gallium bisulphate complexes, $Ga(HSO_4)_n^{3-n}$, may form. Such complexes, as well as mixed sulphate-bisulphate complexes, are known, for example, for Fe^{3+} [134, 135].

However, none of the above mentioned studies on gallium sulphate complexes nor others, dealing with their stability and lability (rates of ligand exchange) e.g., refs. [136, 137, 138, 139], have found evidence for existence of bisulphate gallium complexes. In fact, in some sources the following complex formation reaction has been suggested [132, 136]:

$$Ga^{3+} + HSO_4^- \rightleftharpoons GaSO_4^+ + H^+ \tag{5.7}$$

Aluminum forms similar, though more stable, sulphate complexes than gallium.[2] It has been found from NMR and molar-volume studies of aluminum sulphate complexes, that addition of hydrochloric acid to the solution results in decreasing the peak corresponding to the $Al(SO_4)^+$ complex [140, 141]. This certainly means that the complex is sulphate- and not bisulphate-based, since with increasing acidity the concentration of HSO_4^- increases.

Based on the above results and the similarities between gallium and aluminum sulphate complexation, it is assumed here that gallium bisulphate complexes do not form. It may be suggested that in very acidic sulphate solutions only, where HSO_4^- will predominate over SO_4^{2-}, bisulphate complexes could form:

$$Ga^{3+} + HSO_4^- \rightleftharpoons GaHSO_4^{2+} \tag{5.8}$$

although this contradicts reaction 5.7 and there is no experimental evidence to support it at present.

[2]The same, however, does not apply to chloride complexes, see page 12

Finally, it should be noted that the existence of such complexes as $Ga(HSO_4)_n^{3-n}$ ($n = 1,\ldots,6$) was indeed proposed and used to explain gallium and aluminum extraction data from chloride-sulphate solutions with ketones [142, 143]. Unfortunately, it was impossible to find the authors' report in the specified journal (referred to in their studies [142]), and containing the data for stability constants of the gallium complexes, supposedly determined by them.

5.3 Stability Constants and Ionic Strength

As expected, the data collected for the mass-stability constants show that they change with the ionic strength. Therefore, a relationship linking stability constants and ionic strength is needed so that they can be calculated with sufficient accuracy at a particular value of I. Such relationships are known—they reflect the change in activity coefficients with ionic strength, and often are based on the extended Debye-Hückel equation. This equation can be written for the stability constant β_n of the complex MeL_n (reaction 5.2) as

$$\log \beta_n = \log \beta_n^0 + \frac{\Delta z^2 A_D \sqrt{I}}{1 + B_D d_a \sqrt{I}} + bI \tag{5.9}$$

where z is the charge of species in

$$\Delta z^2 = z^2_{MeL_n} - z^2_{Me} - n z^2_L$$

The stability constant β_n^0 refers to $I = 0$, b is an empirical parameter, and I is the ionic strength expressed on a molar scale, i.e.,

$$I = \frac{1}{2} \sum_j c_j z_j^2 \tag{5.10}$$

where c is the molar concentration of species.

It has been proposed [144, 145] that for many complexes the value of d_a can be assumed to be constant ($d_a = 4.9$Å). Although a simplification, this assumption is justified because the uncertainties involved in determination of stability constants of

complexes in solution are much more significant than those for activity coefficients. Thus, eqn (5.9) becomes

$$\log \beta_n = \log \beta_n^0 + \frac{\Delta z^2 A_D \sqrt{I}}{1 + 1.6\sqrt{I}} + bI \qquad (5.11)$$

in which b is the parameter needed to be determined from the data for β_n at different ionic strengths. Furthermore, eqn (5.11) can be used to check compatibility of data reported by various sources for a given complex at different ionic strengths. Equation (5.11) predicts that a straight line with a slope of b should result when data are presented in coordinates

$$\log \beta_n - \frac{\Delta z^2 A_D \sqrt{I}}{1 + 1.6\sqrt{I}} \quad \text{vs} \quad I$$

Indeed, this has been the case for a number of complexes of different nature and composition [145]. The equation has also been found valid for ionic strengths up to 5.

Equation (5.11) was also adopted in this work for correlating the data for stability constants at different ionic strengths. The value of b was calculated by the least squares method for each gallium complex, except $Ga(SO_4)_2^-$, for which the stability constant only at $I = 0$ was known (Table 5-1), and hence a value of b equal to zero had to be assumed for that complex. Reasonably good correlation coefficients were obtained when the selected values (from ref. [123]) of the gallium hydroxy complexes were used.[3]

5.4 Algorithm and Program Development

The algorithm is based on the mass-balance equations for the metal, or metals, present in the solution (in this particular case—gallium) in various complex forms, for sulphates, and the charge-balance equation—the condition for electroneutrality of the solution.

[3]With the exception of the $Ga(OH)_4^-$ complex, since values for only two ionic strengths are reported (Table 5-1).

Derivation of the appropriate equations and description of the iterative procedure for determination of species distribution is given in Appendix B. Essentially, the concentration of all species in solution can be expressed in terms of the three unknowns—the concentrations of Ga^{3+}, SO_4^{2-}, and H^+—using the definition equations for stability constants of each complex as well as the equation for the second dissociation of sulphuric acid (eqn 5.5) and the dissociation constant of water, K_w.[4] Thus, a system of three nonlinear equations with three unknowns is obtained. The Newton-Raphson iterative method is selected as a computational method here because of its rapid convergence. A modified iteration formula is used, as it has been suggested [146], in order to avoid negative roots.

Also included in the program is a second iteration loop for the ionic strength. Once a solution for the system of equations is reached, the concentrations of all species are calculated and thus the ionic strength. The stability constants of species are then calculated for this value of I, and the computations are repeated—until the difference between the two consecutive values of I becomes less than a pre-specified small number (i.e., the requirement that the stability constants are calculated for the true ionic strength of the solution is fulfilled). In this work, 6–8 iterations have been necessary before this condition is satisfied.

5.5 Results and Discussion

Two cases are considered for the distribution of species in gallium sulphate solutions. The first is here called the 'case of non-specified acidity'. The system is defined as a mixed electrolyte solution of $Ga_2(SO_4)_3$ and H_2SO_4 in water, and no other substances are present. The total concentrations of gallium and sulphates are known. Next, the concentration of free sulphuric acid (in mol/l) is defined as

$$[H_2SO_4] = [SO_4]^T - 1.5[Ga]^T$$

[4] K_w also changes with ionic strength and this is taken into account by correlating available data for K_w at different I [121] using eqn (5.11)

since $1.5[Ga]^T$ is the amount of sulphates originating from $Ga_2(SO_4)_3$. It is obvious that in this case, the acidity of the solution (i.e., the concentration, or activity, of H^+) as well as the ionic strength will be determined from the distribution of species in the solution.

The second case will be called 'case of specified acidity'. The system is defined as consisting of gallium electrolyte (gallium sulphate or another salt with non-complexing anion—e.g., gallium perchlorate or nitrate), a source of sulphates (e.g., H_2SO_4 or Na_2SO_4), and indifferent electrolyte(s)[5] (e.g., nitric or perchloric acids and their sodium salts) which serves to pre-determine the acidity (pH) and the ionic strength of the solution. This case is important, because it refers to the type of solutions used in the gallium extraction experiments, described in the previous Chapter. The calculations for species distribution in this case are simpler than those outlined in Appendix B for the case of non-specified acidity. The reason is that the concentration of one of the key components, $[H^+]$, and the ionic strength are known in advance, and also the charge-balance equation becomes unnecessary.

5.5.1 Case of Non-specified Acidity

The percent distribution of gallium species is presented here as a function of the free H_2SO_4 concentration at constant total gallium concentration, $[Ga]^T$. Results for two values of $[Ga]^T$ are given on fig. 5.1 and 5.2.

The speciation diagrams clearly show that gallium is significantly complexed in aqueous sulphate solutions and the predominant species is $Ga(SO_4)^+$. At very low (and zero) acid concentrations, the first gallium hydroxy complex, $Ga(OH)^{2+}$, exists to a noticeable extent, but disappears as soon as the acidity is further increased, even slightly. This is the reason for the displayed maximum in the percentage of free Ga^{3+} in this region of low acid concentrations

[5]Here, the electrolyte is considered indifferent only if its ions do not take part in complexing reactions and, with respect to solvent extraction, they are not extracted in any form within the range under study

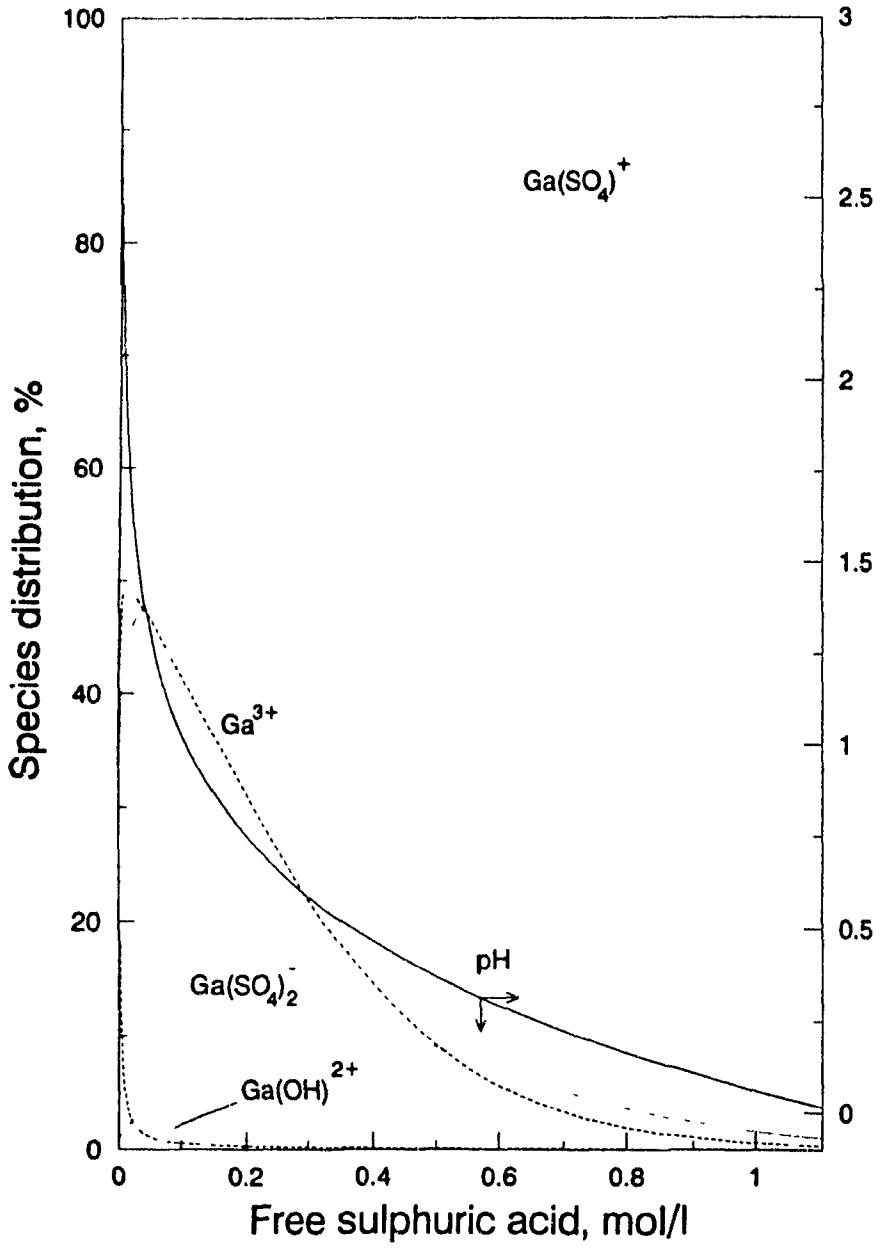

Figure 5.1: Distribution of gallium species in aqueous sulphate solutions. Case of non-specified acidity. $[Ga]^T = 0.01$ g-ion/l.

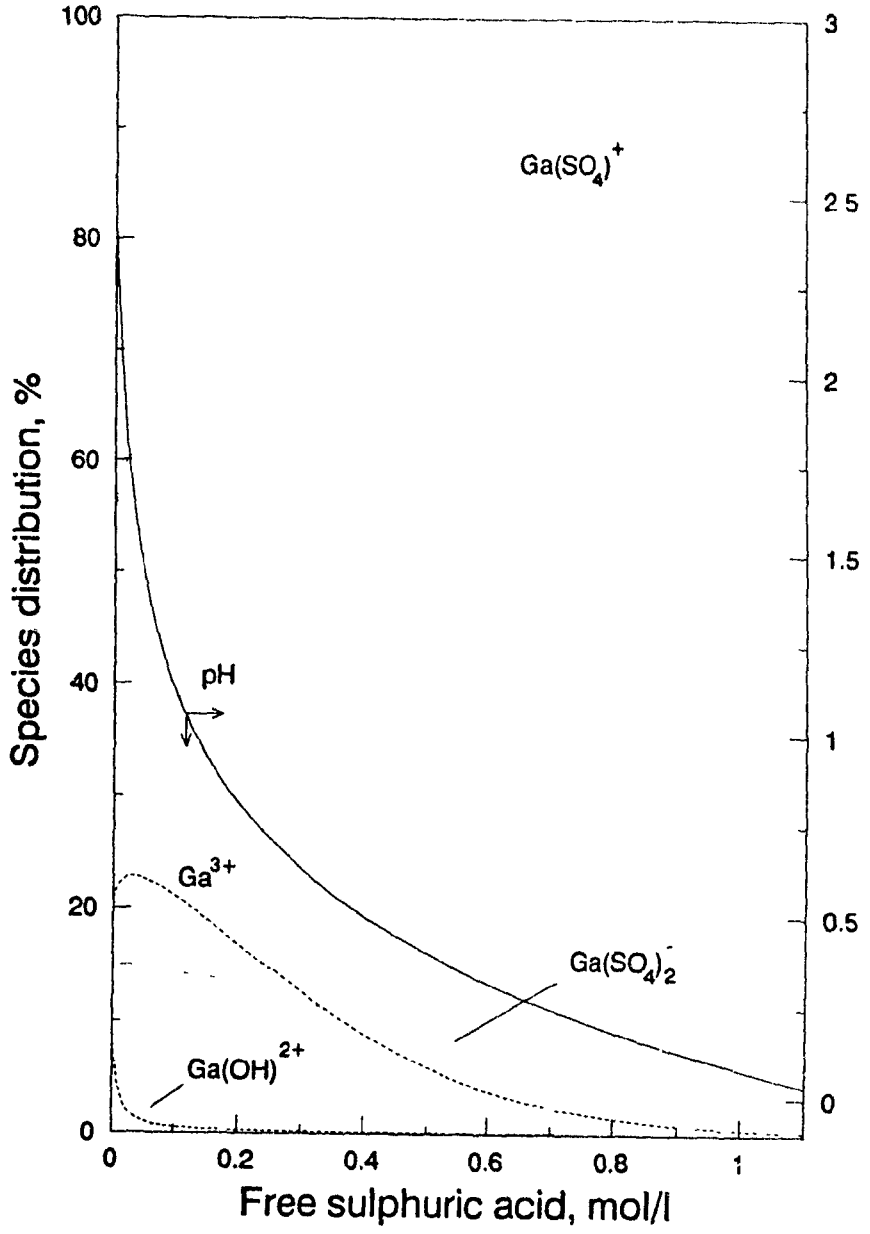

Figure 5.2: Distribution of gallium species in aqueous sulphate solutions. Case of non-specified acidity. $[Ga]^T = 0.10$ g-ion/l.

A maximum is also found in the presence of the second gallium sulphate complex, $Ga(SO_4)_2^-$. As expected, an increase in H_2SO_4 concentration leads initially to increase in the concentration of the free SO_4^{2-}. Accordingly, $[Ga(SO_4)_2^-]$ increases as well. At the same time, however, acidity also increases, thus causing gradual shift of the sulphate/bisulphate equilibrium (eqn 5.4) towards formation of bisulphate. This results in decreasing the percentage of the $Ga(SO_4)_2^-$ complex, which apparently is less stable than $Ga(SO_4)^+$. It is obvious, however, that under conditions of constant free H_2SO_4 concentration, an increase in the total concentration of sulphates by addition, for example, of Na_2SO_4, will increase the percentage of $Ga(SO_4)_2^-$.

pH and species distribution

As mentioned earlier, the resulting pH of the solution reflects, in this case, the distribution of species. Hence, the measurement of pH may provide a convenient experimental tool for at least partial verification for the predictions of the speciation diagrams.

For that reason, several mixed $Ga_2(SO_4)_3$–H_2SO_4 solutions with constant $[Ga]^T = 0.01$ g-ion/l and variable acid concentration from 0 to 0.1 mol/l H_2SO_4 were prepared and their pH values measured. The results showed that the measured values were quite close to those predicted from the speciation. For example, for 0 mol/l H_2SO_4 the predicted pH is 2.72 (fig. 5.1), while pH of 2.75 is measured; for the case of 0.1 mol/l H_2SO_4, the predicted and measured pH are 1.03 and 0.98, respectively.

Notwithstanding the observed close agreement between predicted and measured pH values, it should be emphasized that it refers to relatively low acid concentrations and ionic strengths. Hence, the agreement itself can only be interpreted as a proof that the values for the mass-stability constants of complexes involved, and therefore the distribution of species based on these values are probably correct for the particular range of ionic strengths. This, however, will not necessarily be true

for high acidities and ionic strengths. Except for the case of zero and close-to zero free H_2SO_4 concentrations, where the resulting pH is strongly dependent on $[Ga]^T$, it appears that the pH remains very much the same for the same concentration of free H_2SO_4 regardless of $[Ga]^T$. This is evident when the pH curves of figures 5.1 and 5.2 are compared. In other words, for the range of high acid concentrations, the pH reflects mostly the sulphate/bisulphate equilibrium, while the effect of then relatively low $[Ga]^T$ becomes negligible. Hence, this would lead to inconclusive results about gallium complexation if pH is measured under such conditions.

Finally, it should also be remembered that an additional uncertainty for the speciation at high ionic strengths is introduced from the necessary assumption[6] that the stability constant of $Ga(SO_4)_2^-$ complex remains the same regardless of the ionic strength.

5.5.2 Case of Specified Acidity

Here, the distribution of gallium complexes is presented as a function of pH at constant $[Ga]^T$, $[SO_4]^T$, and ionic strength. Figures 5.3–5.7 show the speciation diagrams for several differently chosen conditions.[7] The case of 0.01 mol/l $Ga_2(SO_4)_3$ dissolved in aqueous solution of indifferent electrolyte, which serves to maintain constant ionic strength of $I = 0.1$, is represented on fig. 5.3. How the distribution changes when the ionic strength is increased for the same conditions of fig. 5.3 is found by comparison with the next fig. 5.4. The two following figures 5.5 and 5.6 illustrate the changes in the distribution of complexes when $[SO_4]^T$ is increased for otherwise the same conditions of fig. 5.4. A comparison between figures 5.5 and 5.7 yields the differences in species distribution due to increased total gallium concentration.

[6] See page 119

[7] Clearly, such diagrams can be produced for any particular conditions when needed

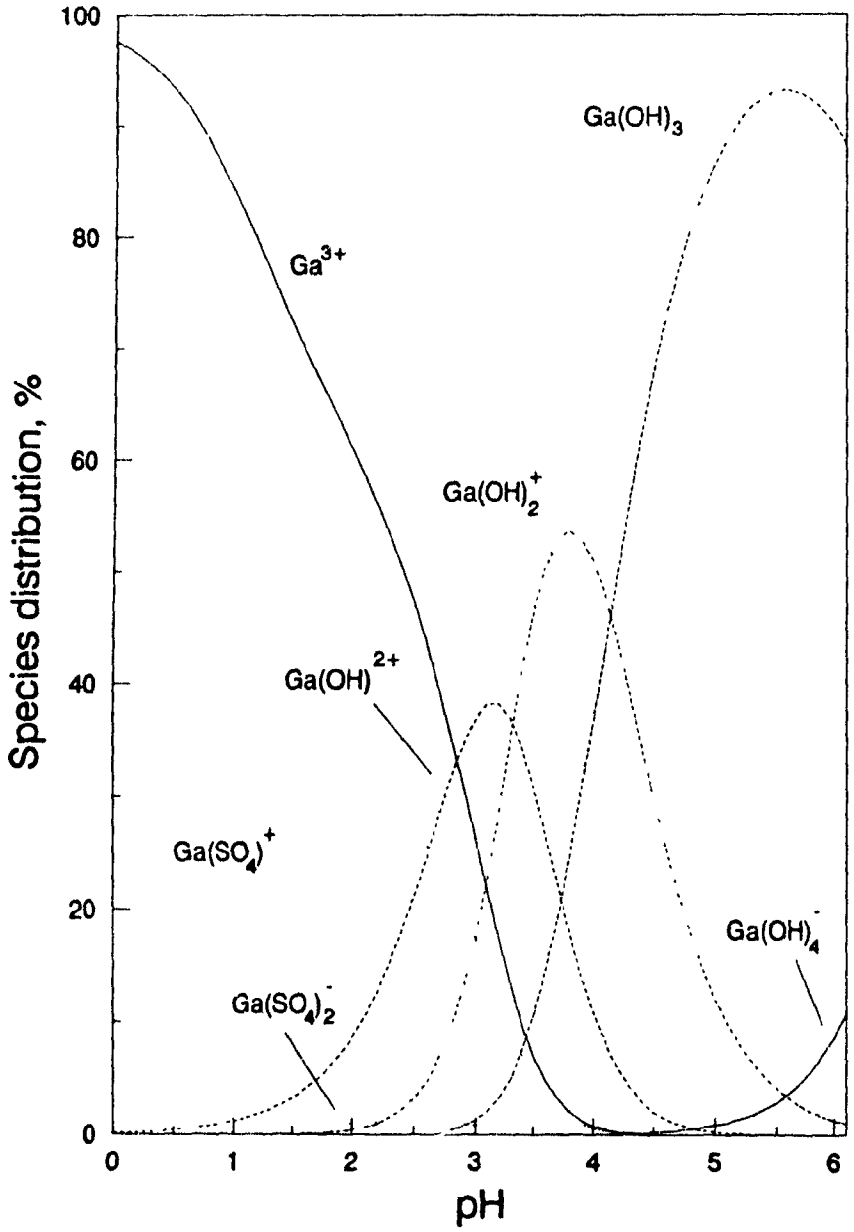

Figure 5.3: Distribution of gallium species in aqueous sulphate solutions. Case of specified acidity. $[Ga]^T = 0.01$ g-ion/l, $[SO_4]^T = 0.015$ g-ion/l, $I = 0.1$.

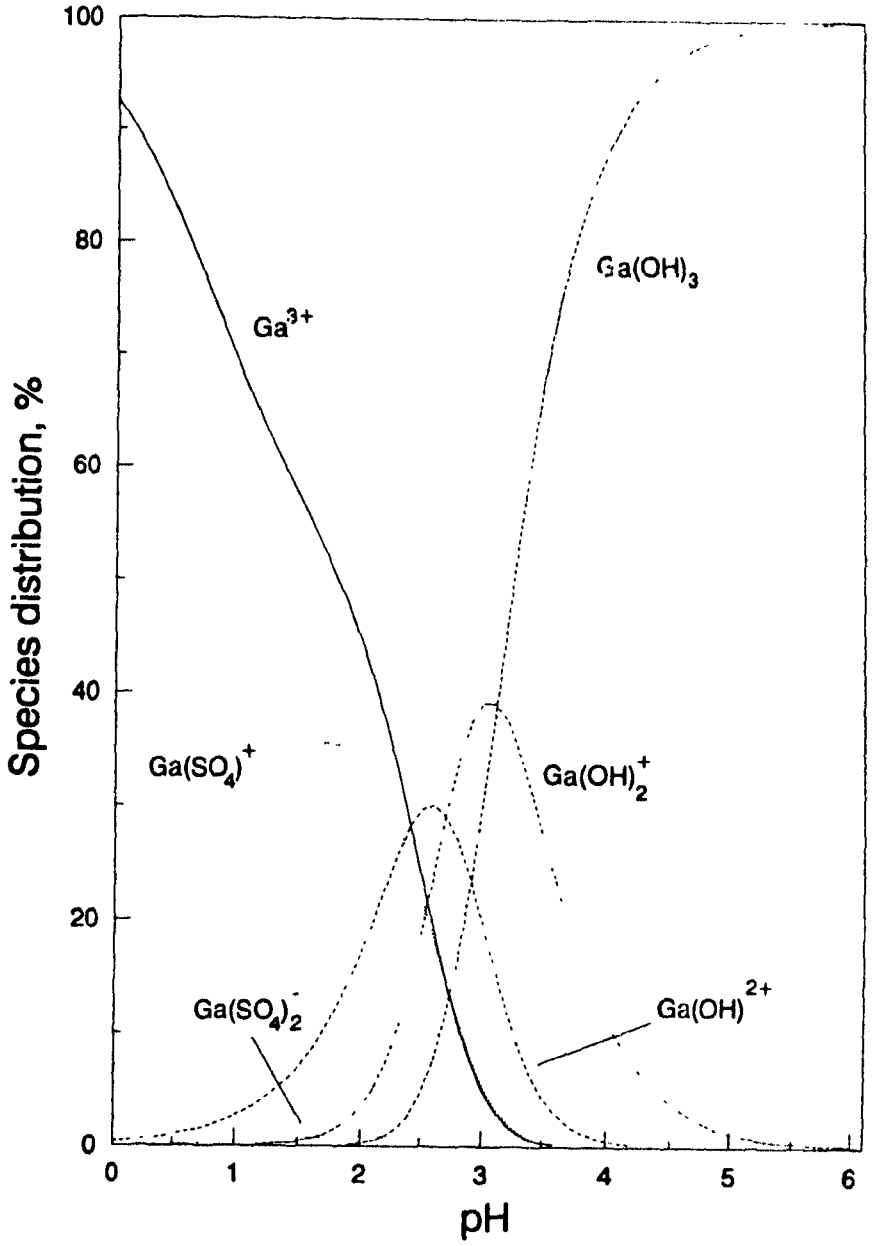

Figure 5.4: Distribution of gallium species in aqueous sulphate solutions. Case of specified acidity. $[Ga]^T = 0.01$ g-ion/l, $[SO_4]^T = 0.015$ g-ion/l, $I = 0.5$.

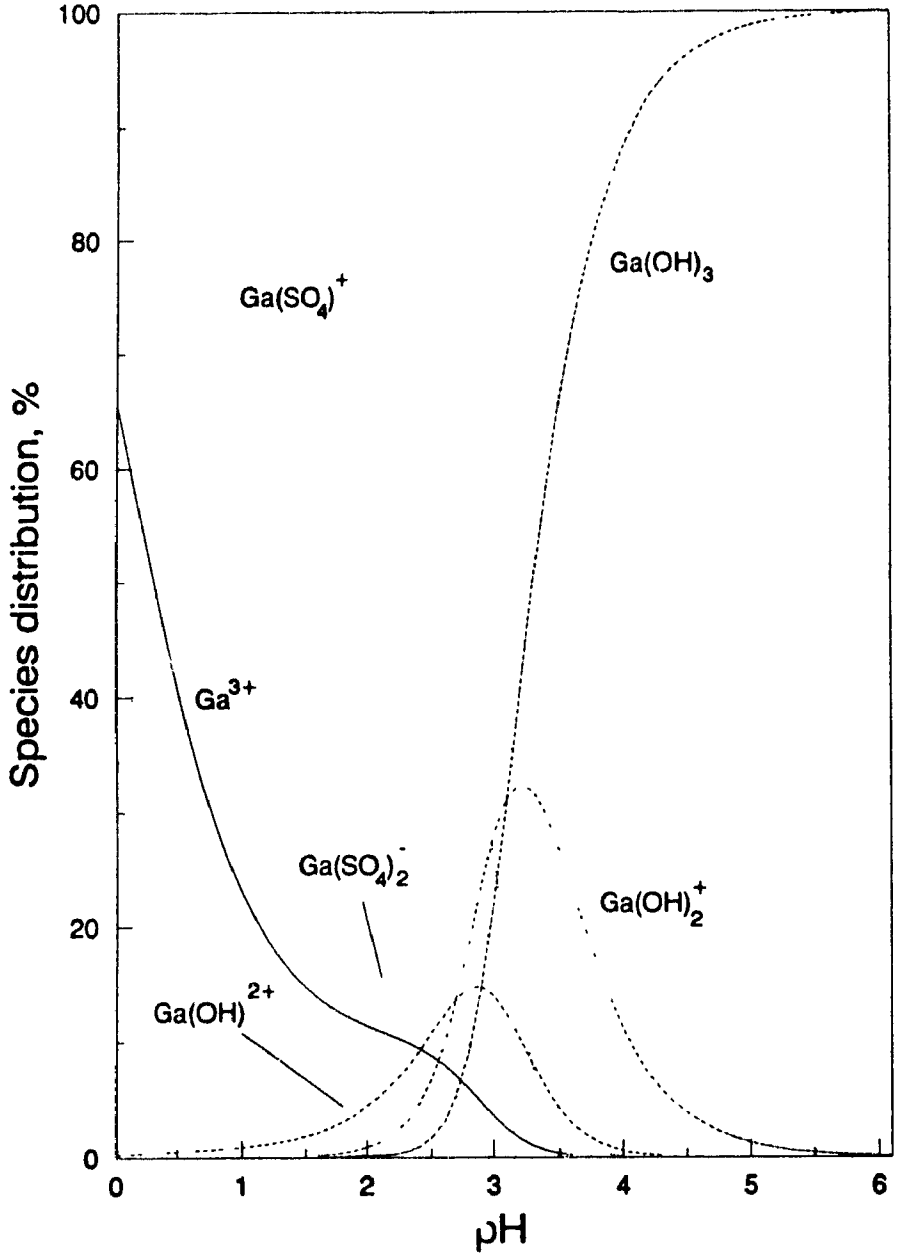

Figure 5.5: Distribution of gallium species in aqueous sulphate solutions. Case of specified acidity. $[Ga]^T = 0.01$ g-ion/l, $[SO_4]^T = 0.1$ g-ion/l, $I = 0.5$.

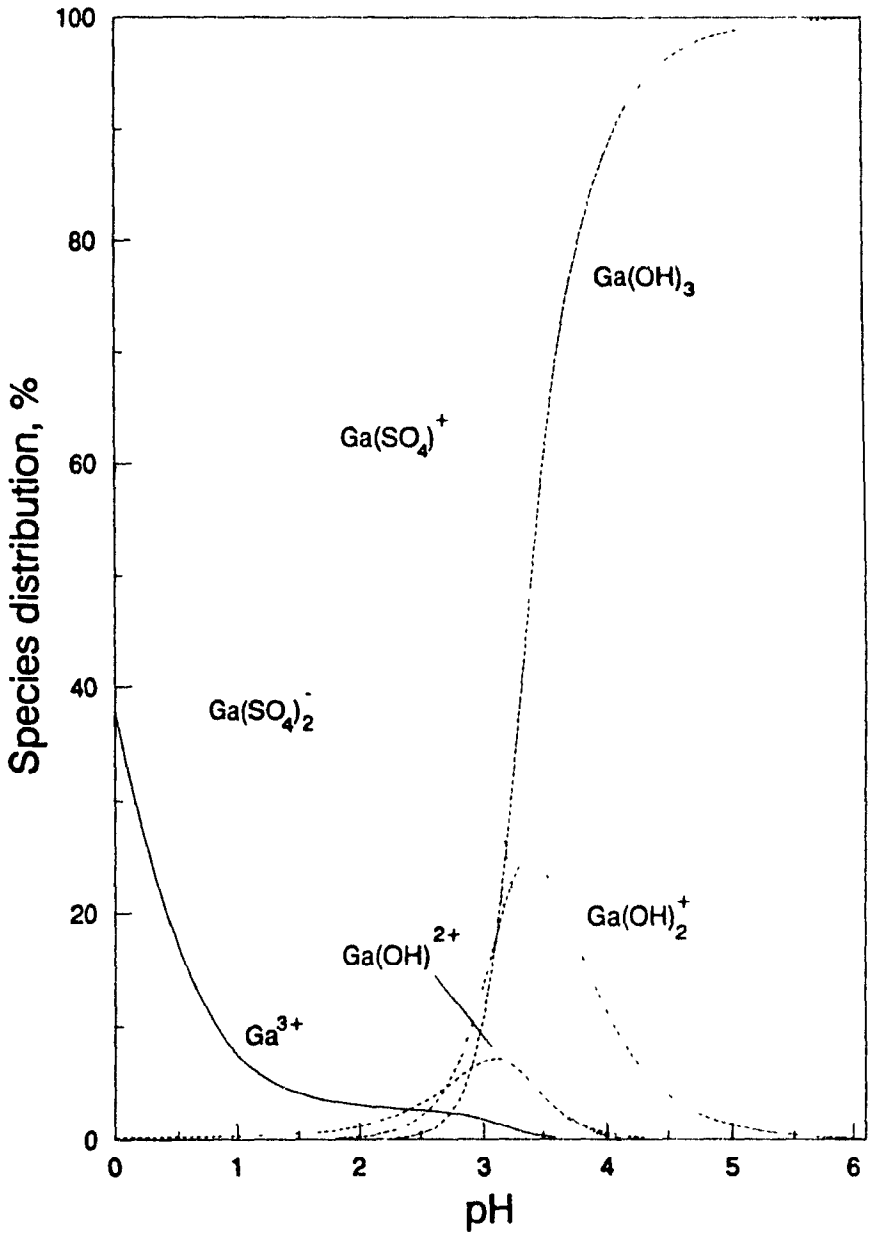

Figure 5.6: Distribution of gallium species in aqueous sulphate solutions. Case of specified acidity. $[Ga]^T = 0.01$ g-ion/l, $[SO_4]^T = 0.3$ g-ion/l, $I = 0.5$.

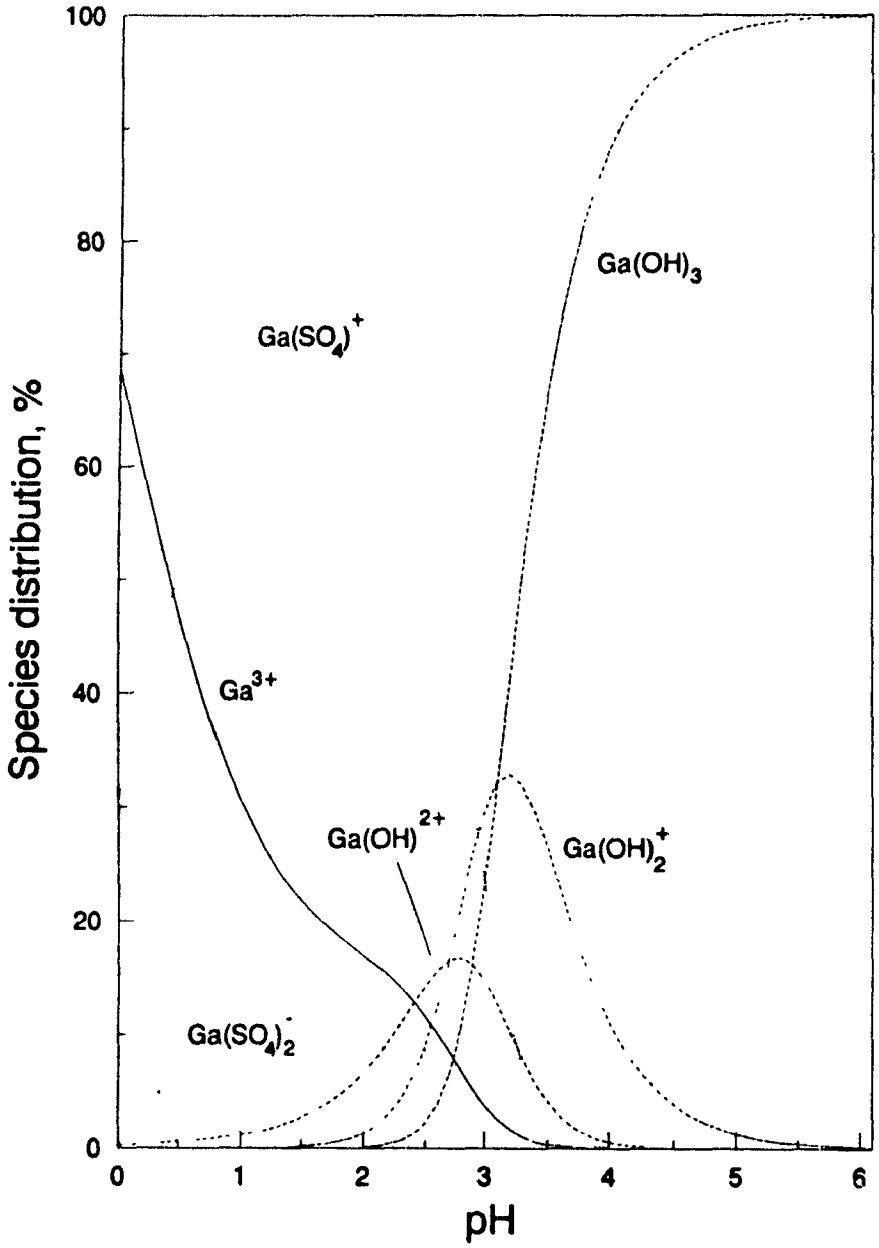

Figure 5.7: Distribution of gallium species in aqueous sulphate solutions. Case of specified acidity. $[Ga]^T = 0.05$ g-ion/l, $[SO_4]^T = 0.1$ g-ion/l, $I = 0.5$.

Distribution of hydroxy complexes

The results clearly show the common tendency of increasing percentage of the hydroxy complexes as pH increases. At the same time, the distribution changes slightly when the total gallium concentration is increased (fig. 5.7). The predominant species among the hydroxy complexes changes from the first, $Ga(OH)^{2+}$, to the fourth, $Ga(OH)_4^-$, complex with increasing pH (fig. 5.3). Thus, the results for the hydroxy complexes alone, e.g., when the sulphate complexes are either not present or excluded from consideration, are well in agreement with similarly constructed speciation diagrams available in the literature [118, 122, 123]. This, of course, is not very surprising since the mass-stability constants data for the hydroxy complexes used in this work originate from the above mentioned sources.

This agreement alone cannot be taken as proof of validity. For example, the distribution of the hydroxy complexes appears to be strongly dependent on the ionic strength of the solution. While the results for $I = 0.1$ (fig. 5.3) correctly predict the known fact [118] that at high pH the predominant complex (if not the only one among the mononuclear species) will be $Ga(OH)_4^-$, those referring to a higher ionic strength (e.g., fig. 5.4) predict its percentage considerably decreased,[8] and $Ga(OH)_3$ appears to be the predominant complex instead. The reason is in the different dependence of the respective mass-stability constants on the ionic strength (Table 5-1). Nevertheless, these predictions for the high pH range are obviously doubtful because they will not explain why gallium is soluble in such solutions.

This example serves to illustrate how uncertainties in the available data on stability constants may lead to erroneous or at least doubtful results. For the low pH range, however, which is mainly of interest in the present work, these uncertainties about $Ga(OH)_4^-$ complex will have a negligible impact.

[8]Since it is less than 1 % for the pH range of figures 5.4-5.7, the presence of $Ga(OH)_4^-$ is not shown there

Distribution of sulphate complexes

In the range of low pH, the predominant gallium complex is $Ga(SO_4)^+$. Its corresponding curve shows a maximum, the exact position of which (with respect to pH) depends on the particular solution conditions (figures 5.3–5.7). The reason for this maximum is that as acidity increases, the concentration of free SO_4^{2-}, available for complexation, decreases according to the sulphate/bisulphate equilibrium (eqn 5.4). At the other end, above a certain pH, the formation of the hydroxy complexes becomes important. Thus, according to the speciation diagrams, at pH above 3.8–4.0 the presence of the sulphate complexes will be negligible.

As expected, increase in the total sulphate concentration leads to increased percentage of both gallium sulphate complexes (figures 5.3–5.6). The presence, however, of the second complex, $Ga(SO_4)_2^-$, appears to be less significant, especially at lower pH. At high sulphate concentrations and in the pH range of 1.5–3.0, there is competitive formation of $Ga(SO_4)_2^-$, which affects considerably the percentage of $Ga(SO_4)^+$ (fig. 5.5 and fig. 5.6).

When the total gallium concentration in solution is increased (fig. 5.5 and fig. 5.7), the presence of the two sulphate complexes decreases and, accordingly, the amount of free Ga^{3+} increases. These changes, however, in the distribution of species appear to be slight.

The fact, that in the region of low pH (less than 0.5–0.6) the complexation of gallium with sulphates becomes less pronounced, will be important for its solvent extraction. The effect of sulphates on extraction will be less significant under more acidic conditions, but for the *same* total concentration of sulphates. This, of course, will be useful provided that there is a reagent which will be able to extract efficiently from such acidic solutions. On the other hand, high sulphate concentrations, and therefore the complexation, will have beneficial effect for the same acidity (activity of H^+) when stripping from the loaded extractant is considered.

Furthermore, the absence of bisulphate complexes with gallium can, in princi-

ple, facilitate metal separations by extraction from this type of solution. One example, where such potential may exist, are mixed solutions with iron(III), which is known to form such complexes [134, 135].

5.5.3 Sulphate Complexation and Gallium Extraction

With the program developed for calculation of species distribution, it is now possible to check how its predictions may compare with the obtained results for the effect of sulphate concentration on both the equilibrium distribution of gallium (Section 4.2.4, page 46) and the rate of extraction (Section 4.5.1, page 84).

Interpretation of extraction equilibrium results

As discussed in Chapter 4, Section 4.2.4, the presence of sulphates has a negative effect on D_{Ga} (fig. 4.4). This effect can be incorporated in the expression (eqn 4.17) for $\log D_{Ga}$ as a function of free extractant concentration and pH at equilibrium:

$$\log D_{Ga} = \log K'_{ex} + 2\log[(HR)_2] + 3pH - \log \frac{[Ga]^T_{aq}}{[Ga^{3+}]} \qquad (5.12)$$

or written as (eqn 4.18):

$$\log D_{Ga} = \log D_{Ga_0} - \log \frac{[Ga]^T_{aq}}{[Ga^{3+}]} \qquad (5.13)$$

Essential here, when complexation is considered, is the logarithmic term, representing the ratio of the total metal concentration to the concentration of reacting species, at equilibrium. This term has to be determined, which is now possible using the speciation diagrams.

In a typical extraction equilibrium experiment, the metal concentration (total) in the raffinate as well as the pH can be determined. Also known is the total concentration of sulphates. The ionic strength of the solution is assumed to be the same as that of the initial solution. This is justified because of the relatively small amounts of metal initially present, and extracted, with respect to the concentration of the indifferent electrolyte.

With this information available, the term $\log\left([Ga]^T_{aq}/[Ga^{3+}]\right)$ can be calculated after the distribution of species for the particular conditions of each experiment is found. Then, D_{Ga_0}, the hypothetical distribution coefficient of gallium which should be obtained if there is no complexation, can be calculated from eqn (5.13), using the experimentally determined values of D_{Ga}.

It is evident, that if the distribution of complexes has been correctly determined, then the calculated values of D_{Ga_0} from eqn (5.13) should coincide with those values of D_{Ga} found for the same conditions, but in absence of complexing sulphate ions.

For the extraction equilibrium experiments of fig. 4.4, in the presence of sulphates, the values of D_{Ga_0} have been calculated and are given on fig. 5.8. Also shown, for comparison, are the same data (D_{Ga}) from fig. 4.4, for the experiments in the absence of sulphates.

The results show that there is a reasonably good agreement between the calculated D_{Ga_0} and experimental D_{Ga} values. Also, the slope of the lines $\log D_{Ga_0}$ *vs* pH is now very close to the expected value of 3, while for the original data in the presence of sulphates the slopes are noticeably less than 3 (Section 4.2.4).

Analysis of the complexation results shows that in $\log D$ *vs* pH coordinates the slope changes from 3 because of the $\log\left([Ga]^T_{aq}/[Ga^{3+}]\right)$ term, which is pH dependent. With increasing pH this term also increases for the pH range of the experiments (0.4–2.0). This reflects the observation, discussed earlier, that for the range of low pH the complexation becomes less significant as pH decreases.

Hence, in the expression for $\log D_{Ga}$ (eqn 5.12) there will be one term that changes with pH.[9] It is obvious, therefore, that just plotting $\log D_{Ga}$ *vs* pH, when extraction is affected by complexation in the aqueous phase, will not yield the correct value for the stoichiometry of the reaction with respect to H^+. Furthermore, the term

[9] Another term in the equation that may indirectly change with pH is the concentration of the free extractant

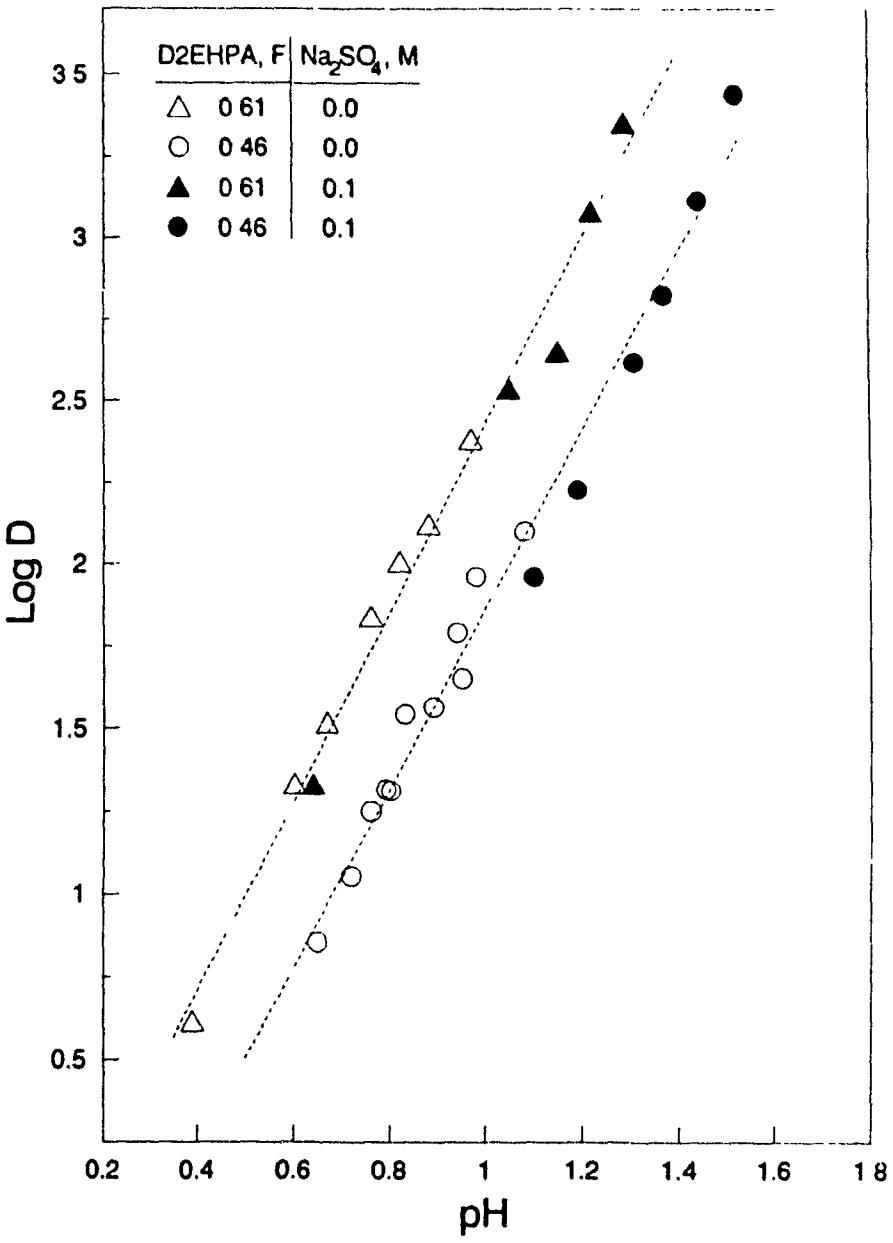

Figure 5.8: Comparison between D_{Ga} and calculated D_{Ga_0} values. Data of fig. 4.4.

$\log\left([Ga]^T_{aq}/[Ga^{3+}]\right)$ changes gradually with pH and this is probably the reason why, despite complexation, the experimental data are still well correlated by a straight line in $\log D$ *vs* pH coordinates. The resulting slope, however, will be less than 3 because of the increasingly negative impact of complexation on $\log D_{Ga}$ as pH increases.

Extraction kinetics data

The experiments have shown that the rate of gallium extraction decreases with increase in the total sulphate concentration in the aqueous phase (Section 4.5.1, page 84).

From the parameters of the aqueous solutions used in the experiments for the effect of sulphates (fig. 4.25), it is possible to calculate the respective concentrations of free Ga^{3+} using the speciation program. The results are given on fig. 5.9, where the data for the rate of gallium extraction are the same as those on fig. 4.25 but plotted *vs* the calculated values of $[Ga^{3+}]$.

The results, obtained in this way for the dependence of gallium rate on Ga^{3+} concentration in the aqueous phase, seem to be similar to those found in absence of sulphates (fig. 4.23). In other words, the kinetic data for the effect of sulphates, after the complexation has been taken into account, appear to become very close to those for the effect of metal concentration for otherwise the same conditions. This allowed, in the subsequent modelling work (Chapter 6), sulphate complexation to be treated as a special case when considering the effect of metal concentration in the aqueous phase on the rate of gallium extraction.

It should be noted, however, that the above treatment to account for sulphates complexation and the effect on extraction rate refers only to the *bulk* properties of the aqueous solution, i.e., away from the aqueous/organic interface and the aqueous diffusion layer. It is obvious that the distribution of species close to the interface will depend on the local properties there—pH, metal, and sulphate concentrations—which will be different from the respective bulk values Therefore, in the determi-

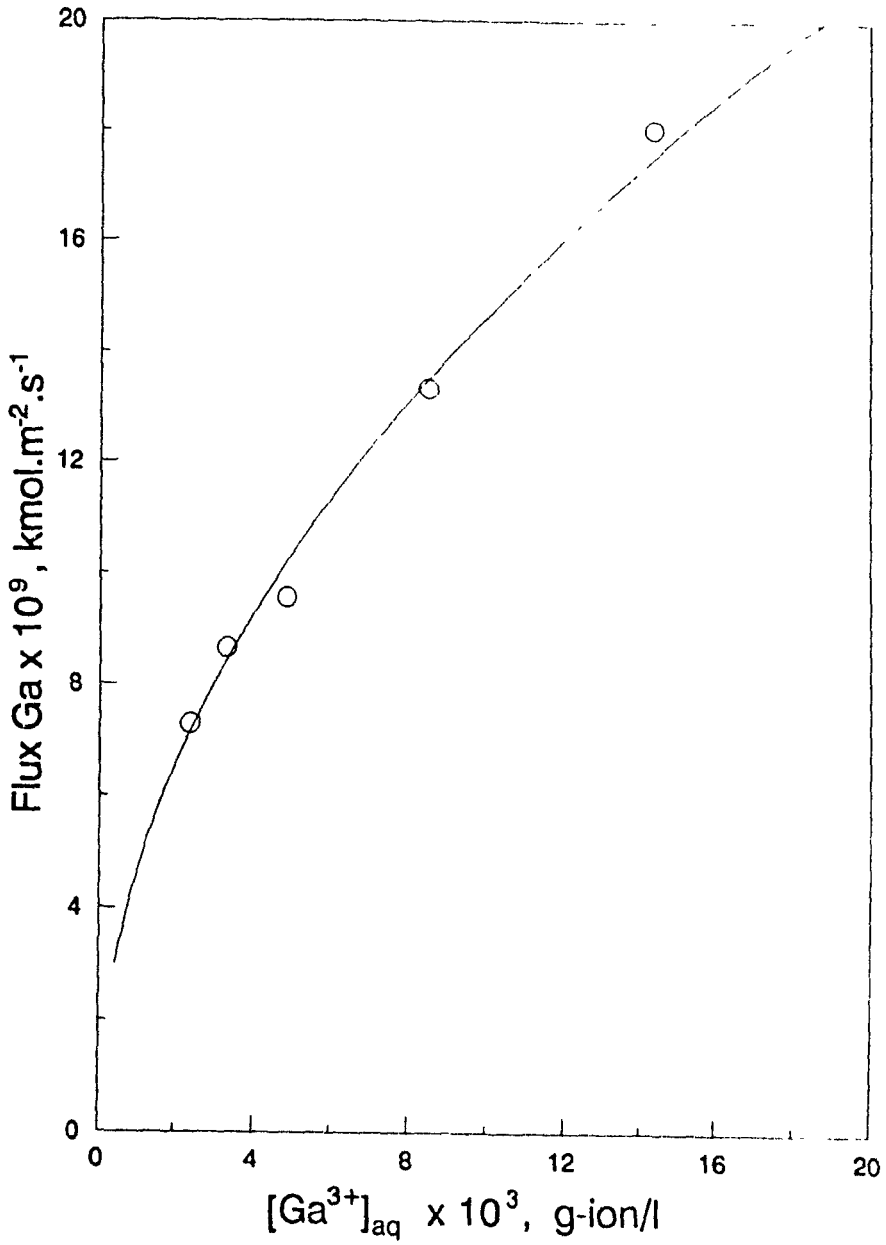

Figure 5.9: Gallium extraction kinetics with D2EHPA. Data of fig. 4.25.

nation of concentration profiles for the reacting species (Chapter 6), the additional effect of complexation in the region close to the interface should also be considered. This, however, has not been done in the present work mostly because additional assumptions will have to be made,[10] which will seriously undermine the anticipated improvement. Also, the fact that the calculated data from the experiments for the sulphates effect are in relatively good agreement with results for the effect of gallium ***bulk*** concentration in the aqueous phase implies that further improvements by accounting for complexation in the aqueous diffusion layer will probably not yield significantly different results.

5.6 Summary

In this Chapter, the problems associated with gallium complexation in aqueous sulphate solutions and its effects on extraction have been discussed. Using the available literature data on mass-stability constants of gallium species present in solution, a program for calculation of species distribution has been developed Two cases have been considered:

- Case of non-specified acidity. The system is $Ga_2(SO_4)_3$-H_2SO_4-H_2O, the total concentrations of metal and sulphate are known, and the distribution of species determines the acidity (pH) and the ionic strength of the solution.
- Case of specified acidity This is a particular and simpler case of the previous one because both pH and the ionic strength are predetermined from indifferent electrolyte(s) present in the solution. This case corresponds to the type of gallium aqueous solutions used in the extraction experiments

The results for the distribution of species as a function of free H_2SO_4 concentration (fig 5.1 and fig. 5.2) or pH (figures 5.3-5.7) have shown that gallium is

[10] For example, one problem will be that $[Ga]^{I}_{aq}$, $[SO_4]^{I}_{aq}$ are no longer constants but functions of distance from the interface, and dependent on the concentration profiles of all gallium- and sulphate-containing species

significantly complexed in sulphate solutions.

From the available literature on gallium complexes, it has been concluded that gallium does not form bisulphate complexes [11] The absence of formation of these species leads to a lower percentage of complexed gallium when pH is low and decreases. Such absence may be potentially useful when metal separations from this type of solution are considered

For the case of non-specified acidity, the obtained results from species distribution calculations were verified by comparing experimentally measured and calculated pH values for prepared gallium sulphate-sulphuric acid solutions Both values were found to agree quite well. The predictions of species distribution program were used in interpreting the experimental results for the effect of sulphates on D_{Ga} and the rate of extraction. When this effect is taken into account according to the calculated species concentrations, a reasonably good agreement is found with the results obtained under the same conditions but in absence of sulphates This means that by using the results for distribution of complexes, it will be possible to predict the extraction performance under particular conditions—acidity, total sulphate concentration, etc.

Hence, some of the important advantages (and limitations) of considering metal complexation in solution are.

- Prediction with some degree of accuracy of extraction behaviour – how (and presumably—how much) the concentration of the complexing ligand will affect metal loading and extraction kinetics
- More information can be obtained about the reacting species It is possible, using the information from species distribution, to verify a hypothesis that a certain species is the one that reacts, by correlating the obtained experimental data with properties particular to that species

[11] The same appears to apply to aluminum and indium as well [119, 121, 140, 141]

- The principles and the algorithm on which the calculation of species distribution is based remain the same, regardless of whether one or more metals are present in solution At the same time, from the respective speciation diagrams, conditions for improved metal separation can be determined.

- The construction of species distribution diagrams can be extended to higher temperatures using available thermodynamic data. This is of particular importance in leaching systems.

- Among the limitations in determination of complexes distribution, probably the most significant when it occurs, is the lack of reliable data for the mass-stability constants. Controversy is more of a rule than an exception. This requires careful examination of the originally reported data, cross-checking, and eventually—comparison with what is experimentally observed.

Chapter 6

Reaction Kinetics and Mechanism of Gallium Extraction

6.1 Introduction

In this Chapter, the experimental results on gallium kinetics, presented in Chapter 4, will be used in elucidating the reaction mechanism as a series of elementary steps. The purpose is to describe them through a mathematical model based on physico chemical properties of the extraction system, which would enable a better understanding and prediction of extraction behaviour, while on the other hand, provide a basis for comparison with reported data on extraction of other metals in similar systems.

First, relevant existing models will be briefly outlined where the distinction will be made with respect to the locus of the chemical reaction. Secondly, the model of mass-transfer with chemical reaction (MTWCR) found to describe well the extraction data, will be presented with an emphasis on its further developments believed to be appropriate in this work. Then, model predictions will be tested by the comparison with the experimental data from gallium-D2EHPA system.

The implications of the important model parameters for metal extraction and separation will then be discussed, and specifically the role of the rate constant of ligand exchange will finally be illustrated with the example of gallium/aluminum

separation based on different rates.

6.2 Extraction Models and Locus of the Chemical Reaction

A starting point in modelling the process of metal extraction is the determination of the site of the chemical reaction. When the two immiscible liquids—the metal-containing aqueous phase and the organic extractant solution—are brought into contact, there are, in general, three options for where the reaction may occur: in the organic phase, at the interface, or in the aqueous phase. The first option is viewed as impossible since the reacting metal species from the aqueous solution are insoluble as such in the organic phase.

Thus, the two alternative options are evaluated when considering the mechanism of metal extraction. However, the selected site—at the interface or in the aqueous phase—and the reasoning behind its choice is often a subject of controversy among different research groups. The main arguments favouring the interfacial chemical reaction option are [149, 150]:

- Very low aqueous solubility of most extractants which, of course, is a prerequisite for successful commercial application.
- Clearly displayed interfacial activity by a large number of extractants including various chelating reagents, sulphonic, carboxylic, organophosphorus acid extractants.

On the other hand, reactions in the aqueous phase (extractant dissolving, even in minute amounts, in the aqueous solution and reacting with metal therein) have been proposed and used to explain extraction results in several systems. Hence, for the same extraction system, contradictory mechanisms are often proposed. One example is copper extraction with hydroxyoximes, where formation of the metal-extractant

complex is said to occur in the aqueous phase [151, 152, 153], while other studies [154, 155, 156] point towards interfacial chemical reaction

Undoubtedly, the properties of the aqueous organic interface play a significant role in metal extraction, a fact recognized also by researchers holding the view of predominant aqueous phase reaction [157]. Therefore, chemical reactions at the interface cannot be excluded from consideration On the other hand, many extractants do possess limited aqueous solubility. Thus, the possibility for the reaction to proceed in the aqueous phase should not be ruled out either. In this respect, the general concept of a chemical reaction at the interface that may also extend into the aqueous diffusion layer, adjacent to the interface, depending on the properties of the particular extraction system [158], seems to be more accommodating and realistic than concepts restricted to either interfacial or aqueous phase chemical reaction.

6.2.1 Interfacial Properties of Extractants

There have been a number of studies devoted to the interfacial activity and other properties of the aqueous-organic interface (for example, adsorption/desorption phenomena, interfacial viscosity, etc.) of commercially used extractants, such as hydroxyoximes (e.g., refs. [159]–[163]) and organophosphorus acids [164, 165, 166] Among the interfacial properties, the interfacial tension appears to have been studied the most because of relative ease of measurement [167, 168].

It is well known that these reagents are surface active due to their amphipathic nature—i.e., having in their molecules both hydrophobic non-polar hydrocarbon groups and a hydrophillic polar functional group which takes part in the cation-exchange extraction reaction Such molecules tend to adsorb at the interface with their hydrophobic group oriented towards the bulk organic phase, and the hydrophillic group to the aqueous phase Thus, even at very low concentrations, molecules of the extractant saturate the interface, forming an adsorbed monolayer. This is evident from the dependence of the interfacial tension, σ_j, on reagent concen-

tration, C_j [150]. In coordinates σ_j *vs* $\ln C_j$, an inverse S-shaped curve is generally displayed with three distinct regions determined by two specific values of $\ln C_j$. The first one corresponds to C_j^{MIN}--the minimum bulk phase concentration required for an ordered monolayer of extractant molecules to start forming at the interface, and the second (and higher) one—to the critical micelle concentration C_j^{CMC}, when complete saturation of the interface is achieved, and above which spontaneous aggregation of extractant molecules and micelle formation[1] starts For the intermediate range of concentrations $C_j^{MIN} < C_j < C_j^{CMC}$ the interfacial tension decreases linearly with $\ln C_j$ and can be described by Gibbs' adsorption isotherm [170]·

$$\Gamma_j = -\frac{1}{RT}\left(\frac{\partial \sigma_j}{\partial \ln C_j}\right)_T$$

where Γ_j is the surface excess (in number of moles per area) of the solute j, the extractant in this case, R is the gas constant, and T is the absolute temperature. This equation is the basis for experimental determination of C_j^{MIN} as well as the area per molecule of extractant at the saturated interface.[2]

The value of C_j^{MIN} is often used as a measure for interfacial activity of the extractant—the smaller C_j^{MIN} is the stronger is the tendency for molecules to adsorb at the interface, i e., the more surface active the reagent is The values of C_j^{CMC} are usually from one to two orders of magnitude higher [150].

For hydroxyoximes C_j^{MIN} is in the order of 10^{-2} in aromatic diluents (toluene) and 10^{-4} mol/l in aliphatic diluents (hexane) [150]. In general, the values of C_j^{MIN} for organophosphorus acids are lower—for example, a value of C^{MIN} in the order of 10^{-6} has been determined for di-hexoxy ethyl phosphoric acid in dodecane [164]. For D2EHPA in dodecane $\log C^{MIN}$ varies from -2.1 (in contact with 0.001 M HNO_3 aqueous phase) to -3.6 (for 1 M HNO_3 solution) [164, 169, 171].

[1]These are often called reversed micelles [169] since the hydrophilic groups orient themselves towards the interior (and interact through hydrogen bonding) while the hydrophobic ones point to the outer surface of the aggregate

[2]Once Γ_j is determined experimentally, the area is calculated as $(N_a\Gamma_j)^{-1}$, where N_a is the Avogadro number

The interfacial activity depends on extractants' structure and reactivity as well as the solvating ability of the diluent. Stronger solute-solvent interactions lead to higher C_j^{MIN} values. The interfacial activity increases in the order of increasing acidity of the extractant: sulphonic acid > phosphoric acid > hydroxyoxime [150]. This has also been observed within the same class of reagents. Such an example is the series of di-alkyl phosphoric acids (i.e., with similar spacial environment around the hydrophillic group) where a very good linear correlation between $\log C_j^{MIN}$ and pK_a has been found [164]. On the other hand, interfacial activity increases in the order phosphoric < phosphonic < phosphinic extractants, despite decreasing acidity at the same time. This has been explained by the increasing influence, from phosphoric to phosphinic, of steric hindrance around the central phosphorus atom, and particularly the oxygen atoms, due to orderly replacement of C-O-P with C-P bonds. This inhibits extractant aggregation through hydrogen bonding [164]. Furthermore, extractant monomers are expected to be more surface active than dimers and other polymeric aggregates of higher order since their outer surface is hydrophobic (see footnote 1). Hence, factors contributing to prevent extractant polymerization are likely to cause increased interfacial activity [150].

Extraction models based on interfacial reaction

The models assuming extraction reaction occurring at the interface consider the overall process as a sequence of the following steps [155, 163, 166, 172]:

- Diffusion of reactants to the interface. Concentration gradient may exist in the diffusion layer adjacent to the interface.
- Adsorption of extractant molecules at the interface. For the species on the aqueous side of the interface, metal cations are not considered surface active, but adsorption of H^+ is thought to be important – to the extent that it supposedly hinders diffusion of reaction products and thus retards extraction [166]. An alternative explanation of this retardation effect, however, may well have its

origin in the adsorption of extractant molecules with their polar OH-groups oriented to the aqueous phase, and subsequent acid dissociation which will raise $[H^+]$ in the region [164].

- One or more chemical reactions at interface to yield the final (and electroneutral) metal-extractant complex.

- Desorption of the complex and diffusion to the bulk organic phase.

In order to describe the adsorption/desorption phenomena of surface active species, most models [155, 173, 174] assume that they obey the Langmuir adsorption isotherm [177]:

$$\theta_j = \frac{K^* C_j}{1 + K^* C_j}$$

where C_j is the concentration of species j, and θ_j is defined as

$$\theta_j = \frac{\text{number of occupied adsorption sites by } j}{\text{total number of available sites}}$$

The rate of adsorption of j-species is proportional to C_j and the fraction of non-occupied sites $(1 - \theta_j)$, and the rate of desorption—to the fraction of occupied sites θ_j, accordingly. At equilibrium the two rates are equal, and thus the expression for Langmuir isotherm[3] is obtained with the ratio of the two respective rate constants equal to K^*—the equilibrium constant of the adsorption/desorption process for species j. Furthermore, from the definitions of θ_j and Γ_j it follows that

$$\theta_j = \frac{\Gamma_j}{\Gamma_j^\infty}$$

where Γ_j^∞ is the surface excess at saturation of the interface. It is clear that for most extractants θ_j will become unity even at very low concentrations.

[3]The derivation assumes equal probability of site occupancy, not affected by whether or not other sites have already been occupied. Other isotherms, e.g., Freundlich's, Temkin's, etc., can also be used [161, 162, 163]

Extractant species at interface

An important aspect of reaction kinetics concerns the forms in which the extractant may exist and their distribution at the interface. This question is of particular importance to organophosphorus acid reagents, known to exist predominantly as dimers in the bulk organic phase, especially when the diluent is non-polar. With respect to hydroxyoximes, dimerization has little effect on interfacial activity and extraction kinetics, as expected [162].

When dimers, $(HR)_2$, are the predominant form of the extractant, a number of researchers include in the extraction model (e.g., copper [175], zinc [178, 179], yttrium [180] extraction studies) adsorption of dimer molecules at the interface, followed by acid dissociation of the dimer, and reaction with metal cations:

$$(HR)_{2\ (org)} \rightleftharpoons (HR)_{2\ (ads)} \tag{6.1}$$

$$(HR)_{2\ (ads)} \rightleftharpoons H^+ + HR_2^- \tag{6.2}$$

$$Me^{n+} + HR_2^- \rightleftharpoons MeR_2^{(n-2)+} + H^+ \tag{6.3}$$

Similar reactions to those above for $(HR)_2$ have also been considered in extraction models based on chemical reaction at interface, and extending into the aqueous diffusion layer [87, 181].

However, the notion of extractant dimers existing at the interface, and even distributing to the aqueous phase with subsequent dissociation and creation of the acid anion HR_2^-, should be viewed as quite unlikely.

Firstly, the interfacial activity of the dimer is much less than that of the monomer because the hydrophilic groups are already engaged through hydrogen bonding in the dimer structure [150, 164]. Therefore, it is reasonable to expect that it will be the monomer species that are predominantly adsorbed at the interface. This, however, does not necessarily exclude possible transport of dimers through the diffusion layer on the organic side of the interface.

Secondly, even if interfacial properties are neglected, the existence of extractant dimers in the interfacial region is highly improbable due to the presence of the polar solvent there—water. If alkyl alcohols can cause monomerization [94, 95], this will be more so when water is present. Thus, it is expected that dimers' hydrogen bonds will be destroyed for preferential bonding with water molecules, an argument suggested recently by other researchers [182, 183, 184] too.

Thirdly, the idea of a dimer molecule undergoing acid dissociation (eqn 6.2) in aqueous medium, i.e., with breakage of the O–H bond in the hydroxyl group, while, at the same time, the much weaker hydrogen bond keeping together the two extractant molecules is left intact, is indeed doubtful.

Therefore, the reacting extractant species, regardless of where the locus of the reaction is—at the interface or in the aqueous diffusion layer (or phase)—is considered to be the monomer and/or the organic anion, R^-, produced from the acid dissociation of HR. This follows despite the fact that the dimer, $(HR)_2$, may be the predominant species in the bulk organic phase.

6.2.2 Mass-transfer *vs* Chemical Reaction Control

Clearly, the rate of the overall extraction process can be limited by the diffusion of reactants and products to and from the reaction zone (regime of mass-transfer control) or by the chemical reaction itself (regime of reaction control), or by both (mixed control kinetics).

The common and easiest (as a concept) criterion to distinguish between the two regimes is by the rate dependency on stirring of the two liquid phases [167]. As the rate of stirring increases, so do the mass-transfer coefficients due to decreasing thickness of the diffusion layers at the interface. Usually a 'plateau' region can be found, in rate *vs* stirring coordinates, where the rate of extraction becomes independent of the rate of stirring. Such independence is often considered as a proof that the diffusional resistances are eliminated and the process is solely controlled by the

chemical reaction alone. This, however, may not always be the case. It is possible that further increase in stirring simply does not decrease any more the thickness of the diffusion layer (therefore increasing the mass-transfer coefficients), thus simulating a chemical kinetic regime [167]. Furthermore, it has been shown [185, 186] that such a pseudo-kinetic regime in a plateau region can be a consequence of simultaneous mixed kinetic and mass-transfer control. For these reasons, it is appropriate, in the mathematical description of the process, to include simultaneously the equations describing the diffusion and the chemical kinetics [167]. Such approach is followed in this work too.

Another criterion that may give information on the controlling regime is the value of the apparent activation energy, E_a, of the process [167]. This is based on the generally much lesser dependence of diffusion coefficients on temperature than rate constants. However, in much the same way as for the criterion related to stirring, where a 'plateau' region is a necessary but not a sufficient condition for a kinetic regime, a low value of E_a does not necessarily indicate purely diffusional control because often chemical reactions in solvent extraction have values of E_a similar to diffusional processes [167].

Therefore, in order to evaluate the controlling regime, more than a single criterion must be considered together with the solution chemistry of the extraction system. The interfacial properties and aqueous solubility of the extractant, as well as the ligand exchange phenomena specific to the hydrated metal species are of particular relevance. These will also affect to a significant degree the site of the chemical reaction.

6.2.3 Criteria for Determination of Reaction Site

In general, the site of the chemical reaction will depend not only on the interfacial properties of the extractant (in a particular organic solution) but also on its aqueous solubility as well as the chemistry of the aqueous metal complexes [163, 187, 188, 189].

Thus, it seems more relevant to discuss the reaction site in terms of relative contributions of *both* interfacial and aqueous diffusion layer reactions, instead of considering one and neglecting the other. In other words, such a view corresponds to the idea of reaction at the interface extending also into the adjacent aqueous diffusion layer.

A relationship between aqueous solubility of the extractant and the contribution of reaction in the aqueous diffusion layer has been observed in several studies. For example, while the extraction reaction of copper with 2 hydroxy 5-dodecyl benzaldehyde has been found to occur mainly at the interface, the same reaction with 2-hydroxy 5-ethyl benzaldehyde proceeds exclusively in the aqueous phase [163]. The latter extractant has higher aqueous solubility than the former, and an ethyl group in place of the dodecyl group. Similarly, copper reaction with benzoylacetone, another chelating extractant with relatively large solubility in water, has been found [187] to proceed mainly in the aqueous phase, although the interfacial reaction also plays a significant role.

The partition coefficient of an extractant, HR, defined as

$$P_{\mathrm{HR}} = \frac{\overline{C}_{\mathrm{HR}}}{C_{\mathrm{HR}}} \tag{6.4}$$

or its distribution coefficient

$$D_{\mathrm{HR}} = \frac{\overline{C}_{\mathrm{HR}}}{C_{\mathrm{HR}} + C_{\mathrm{R}^-}} \tag{6.5}$$

give information about extractant solubility in water (overbar denotes concentrations in the organic phase). In general, most of the commercial chelating reagents are less soluble than the organophosphorus acid extractants as well as much less acidic. For example, the partition coefficient of Kelex 100 is 3.31×10^5 and its K_a is 4×10^{-11} mol/l [79], and for 2-hydroxy 5-nonyl acetophenone oxime (the *anti*-isomer) these values are 7.4×10^3 and 2×10^{-11} mol/l [155], respectively. For benzoylacetone, an extractant with larger aqueous solubility, P_{HR} is 1087 and K_a is 5.3×10^{-9} (enol form) and 2.3×10^{-9} mol/l (keto form) [187]. The respective values for D2EHPA are given

diluent	K_a mol/l	P_{HR} —	K_d l/mol	Reference
n-heptane	3.1×10^{-2}	1600	3.13×10^1	[190]
n-heptane	1.26×10^{-2}	410	6.60×10^1	[182]
kerosene	5.1×10^{-2}	3100	2.75×10^4	[191]
kerosene		800	1.26×10^4	refs. [22] and [27] in [192]

Table 6-1: Physico-chemical properties of D2EHPA.

in Table 6-1. There, K_d denotes the dimerization constant defined as

$$K_d = \frac{\overline{C}_{(HR)_2}}{\overline{C}^2_{HR}} \tag{6.6}$$

Despite the apparent disagreement between constants for D2EHPA reported by the various researchers, which may probably be due in part not only to different analytical methods employed but also to assumptions which may not be correct (for example, distribution of D2EHPA dimers to the aqueous phase is assumed in ref. [191]), the data in Table 6-1 clearly show the much more acidic nature of D2EHPA in comparison with the above cited chelating reagents. On the average, the partition coefficient of D2EHPA is in the same order of magnitude as the coefficient for benzoylacetone, one reagent with a relatively higher solubility among the chelating extractants. Of course, this is not to imply that D2EHPA has high solubility in water, but to emphasize that under similar conditions the role of the extraction reaction in the aqueous diffusion layer will be larger for D2EHPA than for a less soluble (and much less acidic) chelating extractant [4]

Whether the chemical reaction (when it is rate-limiting) occurs in the interfacial region or in the bulk aqueous phase can be determined by carrying out experiments with different aqueous volumes at constant interfacial area and all other conditions constant [167, 189]. Obviously, if the reaction is in the bulk aqueous solution then the overall rate will be proportional to the aqueous volume and in-

[4]On the other hand, D2EHPA, as an alkyl phosphoric extractant, will be more interfacially active than chelating reagents. This means lower C^{MIN} values for D2EHPA but not necessarily much different adsorption/desorption kinetics

dependent of the interfacial area. In contrast, if the chemical reaction occurs at the interface, then the rate of extraction will be linearly dependent on the interfacial area, and accordingly—independent of the aqueous phase volume. The problem is that the same dependencies will also be observed if the reaction is in the aqueous diffusion layer adjacent to the interface [187, 193, 194]. In order to resolve this problem, several approaches have been proposed [167, 189, 194, 195] and will be outlined below.

Rate and extractant concentration

This proposed criterion is based on the theoretically different dependence of rate on extractant concentration when the concentration becomes higher than C^{CMC} [167, 194]. If the reaction is solely interfacial, then the extraction rate should remain constant beyond C^{CMC}, since further increase in extractant concentration will lead only to micelle formation while the interfacial concentration will be unchanged—and so will be the extraction rate, for otherwise the same conditions. On the other hand, if the reaction extends also into the aqueous diffusion layer, then the rate will continue to increase for concentrations higher than C^{CMC} because of the contribution from the aqueous layer reaction [167]. The resulting curves for the two cases, in coordinates rate *vs* extractant concentration in organic phase, are shown schematically on fig. 6.1, taken from ref. [167].

Extraction rate constants and rate constants of water ligand exchange

Another possibility for distinguishing between the roles of interfacial and aqueous diffusion layer reaction is by comparing the experimentally obtained rate constants for several metals with their known rate constants of water ligand exchange [189].

The exchange reaction of a water ligand in a hydrated metal complex can be schematically represented as

$$[Me(H_2O)_l]^{n+} + H_2O^* \overset{k_w}{\rightleftharpoons} [Me(H_2O)_{l-1}H_2O^*]^{n+} + H_2O \qquad (6.7)$$

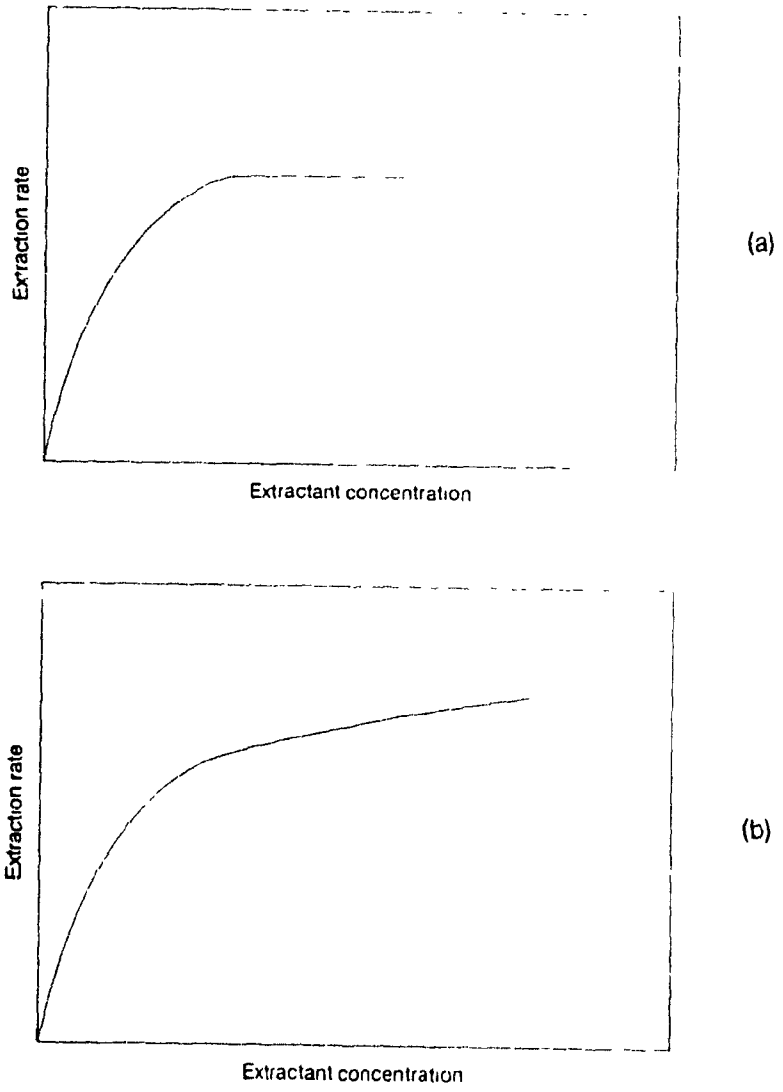

Figure 6.1: Extraction rate *vs* extractant concentration in bulk organic phase. (a) Interfacial reaction; (b) Aqueous and interfacial reaction.

and its rate constant denoted as k_w.[5] It is known [9] that for homogeneous reactions k_w depends mostly on the nature of the central metal cation Me^{n+} and not so much on the kind of the particular ligand. Small and highly charged cations form the most inert complexes. Data for water ligand exchange rate constants are available for a large number of metal cations [9, 196]

In extraction kinetics, the formation of a metal-extractant complex, which eventually distributes to the organic phase, is conceived as proceeding through a series of elementary ligand exchange steps—water ligands replaced by organic ligands, with one of them (in many cases it is the first substitution) being rate controlling. Therefore, if reaction in the aqueous diffusion layer predominates (which is also a homogeneous reaction) then the differences observed for experimentally determined extraction rate constants for several metals should be approximately of the same order of magnitude as the differences between their rate constants of water ligand exchange. On the other hand, if the interfacial reaction is the predominant one, then such an analogy should not exist, and the extraction rate constants should even be similar. The reason is that at the interface, a viscous layer of structured water exists, and in such an environment it is expected [189] that the rates of ligand exchange are not any more cation-dependent.

Verification of this hypothesis has been attempted with the example of cobalt, nickel, and zinc extraction kinetics with D2EHPA in dodecane [189]. The reported values for the extraction rate constants obtained for the three metals are indeed similar, in contrast with their known water ligand exchange rate constants. Thus, the results appear to support the idea of cation-independent exchange at the interface. At the same time, however, these findings seem to contradict other extraction kinetics results, obtained for the same metals and extractant (but with heptane as a diluent) where considerable differences in extraction rates for the three metals are reported [89, 181] Probably, more experimentation will be needed in order to obtain conclusive

[5]Reaction 6.7 represents the overall ligand exchange process However, k_w refers to a first (or pseudo-first) order elementary reaction and has dimensions of s^{-1}

evidence for this hypothesis and subsequently to use it as a criterion for determination of the reaction site.

Different ratios of (C_{Me}/C_{HR}) at $(C_{Me}C_{HR}) = const$

Mathematical analysis of models developed on the basis of interfacial chemical reaction [154] or reaction extending into the aqueous diffusion layer [158] (MTWCR model) have shown that for a fairly large interval of experimental conditions they both may well describe the obtained results [195]

At the same time, however, this analysis has shown that the two models will behave differently if the product of metal and extractant concentrations, $\prod = (C_{Me}C_{HR})$, is kept constant but their ratio (C_{Me}/C_{HR}) is varied. The interfacial model predicts constant rate as long as $\prod$ remains constant. In the MTWCR model, on the other hand, different rates are obtained when the concentration ratio is changed even when $\prod$ is set constant. Therefore, these differences in predictions give a relatively simple way to select or verify an extraction model.

In the present work, based on the obtained results for gallium extraction kinetics and using the criteria to determine the reaction site outlined above, as well as the considerations related to metal and extractant solution chemistry, it has been concluded that the MTWCR model, originally developed by Hughes and Rod [197, 158] and applied for the case of copper extraction with chelating reagents [198], can be used for describing gallium extraction in the presently studied system. In the following section, the physical grounds of the model will be presented, along with some further developments considered necessary when organophosphorus acid extractants are employed. The detailed mathematical derivations are given in Appendix C.

6.3 Mass-transfer with Chemical Reaction Model

6.3.1 Basic Concepts and Assumptions

The model is based on the two-film theory of mass-transfer [199] Here, it is assumed that close to the liquid-liquid interface there is a stagnant film of thickness δ on both sides. It is through this film that the transport process takes place by molecular diffusion due to existing concentration gradients there, while the conditions in the bulk of each phase are considered to be constant The effect of changing the hydrodynamic conditions is reflected in changes of the thickness δ Thus, the theory predicts that under the same hydrodynamic conditions, the physical mass-transfer coefficient (i.e., in absence of chemical reaction) for j-species, κ_j^0, should be proportional to the molecular diffusivity $\mathcal{D}_j$, according to its definition as

$$\kappa_j^0 = \frac{\mathcal{D}_j}{\delta} \tag{6.8}$$

However, this contradicts experimental evidence showing that $\kappa_j^0 \propto \sqrt{\mathcal{D}_j}$, and in some liquid-liquid systems, κ_j^0 is proportional to the 2/3 power of $\mathcal{D}_j$ [200] Other theories (e.g., penetration and surface renewal models of Higbie and Danckwerts) predict correctly the dependence of κ_j^0 on $\mathcal{D}_j$ Nevertheless, the simplicity of the film theory, which makes it possible to obtain exact mathematical solutions for a number of problems only within its framework, together with its ability to describe well the effects of chemical reaction on mass-transfer, make the film theory a useful and powerful tool, despite the fact that it is clearly an inappropriate method to calculate physical mass transfer coefficients. In fact, all three theories—the film theory, the penetration and the surface renewal theories—predict with minor differences [199, 201] the ratio (κ_j/κ_j^0), where κ_j is the mass-transfer coefficient when a chemical reaction takes place, as a function of $\mathcal{D}_j$ and the reaction rate constant. When a chemical reaction between components from the two liquid phases takes place, the rate of their mass-transfer is enhanced because they are consumed in the course of the reaction and therefore the concentration gradients are maintained high Thus, κ_j

will be greater than κ_j^0.

The concentration profiles of species involved in the extraction reaction, in the vicinity of the interface, are presented schematically on fig 6.2, according to the two-film theory, on which the MTWCR model is based. Also shown is the profile for the dissociated organic anion, R^-, for the a[illegible]le. Its presence, of course, will depend on the acid dissociation constant, K_a and the solubility of the extractant as well as the chemical reaction rate relative to the rate of mass-transfer. In the special case, when $P_{HR} \to \infty$ and also $P_{MeR_3} \to \infty$, their concentrations in the aqueous phase are zero [158].

The differential equations, describing the simultaneous mass transfer with chemical reaction in a liquid phase can be written, in a general form for any reacting species j as [200]:

$$\mathcal{D}_j \Delta_2 C_j = \vec{u} \cdot \nabla C_j + \frac{\partial C_j}{\partial t} + r \tag{6.9}$$

where $\mathcal{D}_j \Delta_2 C_j$ is the molecular transport term, which is due to convection (the $\vec{u}\nabla C_j$ term, where $\vec{u}$ is the velocity vector), accumulation ($\partial C_j/\partial t$), and the production (or consumption) of j due to the chemical reaction with rate r [6]

The film theory assumes that the process is at steady-state, hence there is no accumulation and therefore $(\partial C_j/\partial t) = 0$. Also, it assumes that $\vec{u} = 0$, i.e., there is no convective transport of species (the diffusion layer is considered as stagnant). Another simplification is that the interface is considered to be plane--this results from the assumption that the radii of interfacial curvatures are much greater that the diffusion layer thickness.

Thus, the general equation (6.9) is simplified and becomes, when written in the direction of the transport—along the x-axis, perpendicular to the interfacial plane:

$$\mathcal{D}_j \frac{d^2 C_j}{dx^2} = r \tag{6.10}$$

Equation (6.10) forms the basis of the MTWCR model--it provides the relationship

[6] Equation (6.9) is in fact the mass-balance of species j in the elementary volume $dV = dx\,dy\,dz$

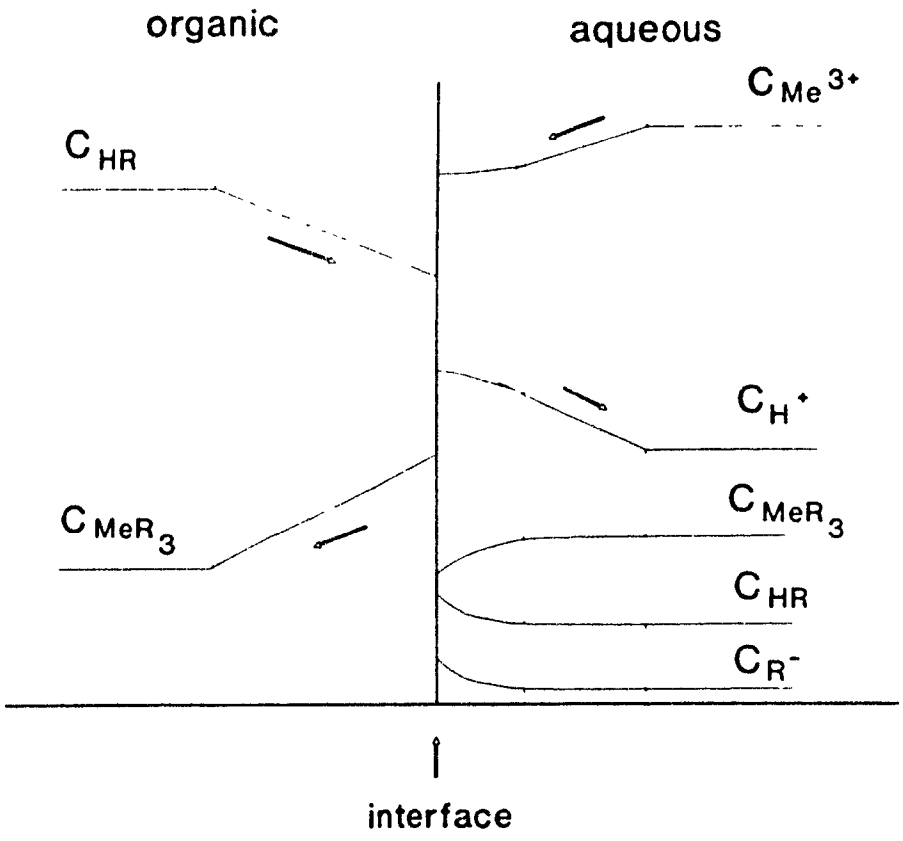

Figure 6.2: Schematic representation of concentration profiles, near the interface, of reactants and products, according to the film theory.

between the mass transport of species and the simultaneously proceeding chemical reaction.

6.3.2 Gallium Extraction: Reaction Scheme

The form of the expression for r depends on which is the controlling step in the series of elementary chemical reactions. The overall extraction reaction of gallium with D2EHPA (eqn 4.10, page 41):

$$Ga^{3+} + 2(HR)_{2\ (org)} \rightleftharpoons GaR_3 \cdot HR_{\ (org)} + 3H^+ \qquad (6.11)$$

can be presented as a sequence of the following elementary steps, involving partitioning of the extractant and its dissociation:

$$(HR)_{2\ (org)} \rightleftharpoons 2HR_{(org)} \qquad \text{Step 1}$$

$$HR_{(org)} \rightleftharpoons HR \qquad \text{Step 2}$$

$$HR \rightleftharpoons H^+ + R^- \qquad \text{Step 3}$$

and then sequential formation of the gallium-extractant complex:

$$Ga^{3+} + R^- \rightleftharpoons GaR^{2+} \qquad \text{Step 4}$$

$$GaR^{2+} + R^- \rightleftharpoons GaR_2^+ \qquad \text{Step 5}$$

$$GaR_2^+ + R^- \rightleftharpoons GaR_3 \qquad \text{Step 6}$$

The complex GaR_3, formed in step 6, may react further with a HR molecule, with the product, $GaR_3 \cdot HR$, subsequently distributing to the organic phase:

$$GaR_3 + HR \rightleftharpoons GaR_3 \cdot HR \qquad \text{Step 7a}$$

$$GaR_3 \cdot HR \rightleftharpoons GaR_3 \cdot HR_{(org)} \qquad \text{Step 8a}$$

or, GaR_3 may first distribute to the organic phase and there $GaR_3 \cdot HR$ can be formed through solvation reactions like the one shown in step 8b:

$$GaR_3 \rightleftharpoons GaR_{3\ (org)} \qquad \text{Step 7b}$$

$$2GaR_{3\ (org)} + (HR)_{2\ (org)} \rightleftharpoons 2GaR_3\ \ HR_{(org)} \qquad \text{Step 8b}$$

Considering the fact, however, that the exact stoichiometry of the metal-extractant complex, or complexes, depends on and changes with the extent of metal loading,[7] it is more likely that $GaR_3 \cdot HR$ complex will be formed by solvation reactions in the organic phase (step 8b) rather than in the aqueous phase (step 7a). Thus, the reaction route from step 1 to step 6, and then steps 7b and 8b, is assumed here to represent the extraction reaction of gallium with D2EHPA, existing mostly as dimers in the organic phase.

6.3.3 Development of the Model

Assumptions

The following assumptions are considered in the model development [197]:

- Any reactions in either bulk phase are sufficiently fast so that the bulk concentrations of all species are in equilibrium
- The net flux of the extractant in all its forms is zero.
- The concentrations of the intermediate complexes, GaR^{2+} and GaR_2^+, and their fluxes in the diffusion layer, are negligibly low in comparison to those of the other species.

The first assumption essentially limits the rate-determining reaction zone to the interface and the diffusion layer, thus allowing use of an equilibrium constant when referring to bulk concentrations. The experimental results (Table 4-7), showing independence of extraction rate on aqueous phase volume at constant interfacial area, justify this assumption.

The second assumption follows the mass-balance requirements for the extractant, under steady-state conditions ($\partial C_j/\partial t = 0$) and therefore absence of extractant

[7] See page 45

accumulation.[8] It allows formulation then of the appropriate mass-balance flux equations.

The third assumption is reasonable because it refers to reaction intermediates, and will be even more so if the rate-limiting step is the first organic ligand addition (step 4). If step 5 or step 6 are rate-determining, then higher concentrations of GaR^{2+} or GaR_2^+, resp., may be anticipated. Even in such case, however, they are expected to be negligibly lower, and then respective fluxes too, in comparison to the other species. In the development of the original model [197] this third assumption refers also to the dissociated organic anion R^-. As discussed earlier, while in the case of a chelating reagent such assumption is reasonable, in the case of an acid organophosphorus extractant like D2EHPA, it is considered inappropriate.

It is also assumed that the partition coefficient of GaR_3, P_{GaR_3}, is equal to P_{HR}. With respect to gallium sulphate complexation in the aqueous phase, the assumption is that it affects the bulk concentrations of species only. In other words, the additional effect of possibly changing sulphate concentration in the diffusion layer on distribution of species there is neglected.

Equations of elementary steps

As discussed in Chapter 4, the rate of extraction is expressed by the molar flux of the product through the interface (moles gallium extracted per area per time). Based on the second assumption and the reaction scheme described above (steps 1–8b), it follows that

$$J_{i_{HR}} = -3J_{i_{GaR_3}} \tag{6.12}$$

where $J_{i_{HR}}$ is the flux of extractant through the interface and $J_{i_{GaR_3}}$ is the flux of the product, in the opposite direction. The number coefficient before $J_{i_{GaR_3}}$ follows from the stoichiometry. The values of $J_{i_{GaR_3}}$ are experimentally determined and

[8] The unsteady conditions of initial accumulation of extractant at interface by adsorption are neglected—as mentioned earlier, the film theory assumes that the system is at steady-state.

numerically equal to the amount of metal transferred from one phase to the other per unit area and time (in kmol $m^{-2}.s^{-1}$), as explained in Chapter 3.

The equilibria of steps 1, 2, and 3, are described respectively by the extractant's dimerization constant K_d, partition coefficient P_{HR}, and acid dissociation constant K_a. The equilibrium constants of the subsequent three ligand-addition steps are defined accordingly as:

$$K_I = \frac{C_{GaR^{2+}}}{C_{Ga^{3+}} C_{R^-}} \tag{6.13}$$

$$K_{II} = \frac{C_{GaR_2^+}}{C_{GaR^{2+}} C_{R^-}} \tag{6.14}$$

$$K_{III} = \frac{C_{GaR_3}}{C_{GaR_2^+} C_{R^-}} \tag{6.15}$$

The distribution of the product, GaR_3, to the organic phase (step 7b) is described by its partition coefficient P_{GaR_3}, and finally, for step 8b an equilibrium constant is defined as:

$$K_G = \frac{\overline{C}^2_{GaR_3\,HR}}{\overline{C}^2_{GaR_3} \overline{C}_{(HR)_2}} \tag{6.16}$$

which is in accordance with the assumption of established equilibrium in the bulk of each phase. Similarly, for the aqueous bulk phase, the concentrations of reactants and products are inter-related and this can be expressed by an equilibrium constant K_{eq}, defined as:

$$K_{eq} = \frac{C_{GaR_3} C^3_{H^+}}{C_{Ga^{3+}} C^3_{HR}} \tag{6.17}$$

From the definition equations for K_I, K_{II}, K_{III}, and K_{eq}, it follows that

$$K_{eq} = K_I K_{II} K_{III} K_a^3 \tag{6.18}$$

Furthermore, the equilibrium constant of the overall extraction reaction 6.11, K'_{ex}, is related to K_G by

$$K_G = \frac{K_d^3 K'^2_{ex}}{K'^2} \tag{6.19}$$

where K' is defined as

$$K' = \frac{\overline{C}_{GaR_3} C^3_{H+}}{C_{Ga^{3+}} \overline{C}^3_{HR}} \tag{6.20}$$

and is also equal to

$$K' = \frac{P_{GaR_3}}{P^3_{HR}} K_{eq} \tag{6.21}$$

It should be emphasized that these relationships are valid only under equilibrium conditions.

Rate equations

As mentioned earlier, the form of the expression for the reaction rate r in eqn (6.10) depends on which of the elementary steps is the rate-limiting one (RLS). Evidently, different relationships will result based on a different initial choice of RLS. Thus, the comparison of the model predictions, following from a certain choice, with the experimental findings can serve as a criterion to determine the RLS.

The concept of an elementary step being the slowest one also implies that all others are at equilibrium—in other words, a change in the concentration of reactants and products, due to the RLS, results in a much faster adjustment of the equilibria for the steps before and after the RLS, respectively. Thus, it can be assumed that the equilibria of all steps except the RLS are continuously maintained.

The possibility for any of the steps 1, 2, or 3, to be the rate-limiting one is readily rejected on the grounds that if this were the case then the extraction rate should not be dependent on metal concentration [9].

One of the organic ligand addition steps is usually rate-limiting, and in most solvent extraction systems the RLS is the first ligand addition (step 4 in the reaction scheme here). This has been considered to be due to significant structural changes associated with the addition of this first organic ligand to the hydrated metal cation [50].

[9] Clearly, species taking part only in elementary reactions which are *after* the RLS, cannot affect its rate (or more precisely—its rate in a forward direction).

In this work also, the first ligand addition (step 4) is found to be the RLS, as it will be discussed further.

If step 4 is rate-limiting then the reaction rate will be given by

$$r = k_f C_{Ga^{3+}} C_{R-} - k_b C_{GaR^{2+}} \tag{6.22}$$

where k_f and k_b are the rate constants of the forward and backward reaction, respectively. By definition, the equilibrium constant equals the ratio of the two rate constants:

$$K_1 = \frac{k_f}{k_b} \tag{6.23}$$

and therefore, after substituting for C_{R-} in eqn (6.22) from the expression for K_a, it follows that

$$r = k_f \left(\frac{C_{Ga^{3+}} C_{HR}}{C_{H+}} K_a - \frac{1}{K_1} C_{GaR^{2+}} \right) \tag{6.24}$$

From this equation, when $C_{GaR^{2+}}$ is substituted with C_{GaR_3} using eqns (6.14) and (6.15), then applying eqn (6.18), and after final rearrangement, the following expression for r is obtained—for the case when step 4 is rate-limiting:

$$r = k_f K_a \frac{C_{HR}}{C_{H+}} \left(C_{Ga^{3+}} - \frac{1}{K_{eq}} \frac{C_{GaR_3} C_{H+}^3}{C_{HR}^3} \right) \tag{6.25}$$

Obviously, it reduces to

$$r = k_f K_a \frac{C_{HR} C_{Ga^{3+}}}{C_{H+}} \tag{6.26}$$

if the backward reaction is neglected, which, in principle, is possible in case of initial extraction rates. It should be emphasized, however, that even under such conditions the reverse reaction may have an effect on the overall rate due to the presence of the metal-extractant complex in the reaction zone even though its organic bulk concentration is virtually zero [186, 198]

The appropriate rate expressions, analogous to eqn (6.25), for the cases when step 5 and step 6 are rate-limiting, can be similarly derived:

$$r = k_f K_1 K_a^2 \frac{C_{HR}^2}{C_{H+}^2} \left(C_{Ga^{3+}} - \frac{1}{K_{eq}} \frac{C_{GaR_3} C_{H+}^3}{C_{HR}^3} \right) \tag{6.27}$$

when the second ligand addition is the RLS (step 5), and

$$r = k_f \frac{K_{eq}}{K_{III}} \frac{C_{HR}^3}{C_{H+}^3} \left(C_{Ga^{3+}} - \frac{1}{K_{eq}} \frac{C_{GaR_3} C_{H+}^3}{C_{HR}^3} \right) \tag{6.28}$$

when step 6, the third organic ligand addition, is rate-limiting.[10] The above rate expressions clearly show that r will be differently dependent on C_{HR} and C_{H+} for a different ligand addition step being rate-limiting

Thus, combining the rate expression derived for the case of step 4 being the RLS, and eqn (6.10), written for HR, the following equation results:

$$\mathcal{D}_{HR} \frac{d^2 C_{HR}}{dx^2} = k_f K_a \frac{C_{HR}}{C_{H+}} \left(C_{Ga^{3+}} - \frac{1}{K_{eq}} \frac{C_{GaR_3} C_{H+}^3}{C_{HR}^3} \right) \tag{6.29}$$

Differential flux equations and boundary conditions

In the aqueous diffusion layer (for x from 0 to δ) there is transport of reactant and products of the extraction reaction. Their fluxes in the layer can be described by the following differential equations:

$$\mathcal{D}_{H+} \frac{dC_{H+}}{dx} + 3\mathcal{D}_{Ga^{3+}} \frac{dC_{Ga^{3+}}}{dx} = 0 \tag{6.30}$$

$$\mathcal{D}_{HR} \frac{dC_{HR}}{dx} + \mathcal{D}_{R^-} \frac{dC_{R^-}}{dx} + 3\mathcal{D}_{GaR_3} \frac{dC_{GaR_3}}{dx} = 0 \tag{6.31}$$

$$\mathcal{D}_{HR} \frac{dC_{HR}}{dx} + \mathcal{D}_{R^-} \frac{dC_{R^-}}{dx} - 3\mathcal{D}_{Ga^{3+}} \frac{dC_{Ga^{3+}}}{dx} = -J_{_{HR}} = 3J_{_{GaR_3}} \tag{6.32}$$

where $\mathcal{D}_j$ is the diffusion coefficient of j-species in aqueous medium

The above equations (6.30), (6.31), and (6.32), express the mass-balance requirements for the components involved, and are based upon the assumptions of the film theory for steady-state conditions in the diffusion layer resulting in the absence of species accumulation.

[10] The rate constant k_f in eqns (6.27) and (6.28) refers to the respective RLS, the same notation being used here only for simplicity

Equation (6.30) reflects the fact that for every g-ion of metal diffusing to the interface, three g-ions of protons, produced as a result of the reaction, diffuse in the opposite direction.

It should also be remembered here that the term 'metal concentration' implies the concentration of the free (or, more precisely, the hydrated) metal cations. While the effects of sulphate complexation are already taken into account with respect to the bulk values through the speciation program, additional changes in concentration profiles of H^+ and Ga^{3+} due to changing species distribution within the aqueous diffusion layer are neglected, as discussed in Chapter 5 (page 138).

Equation (6.31) follows the assumption that the net flux of the extractant in all its forms is zero. In this eqn (6.31) as well as in eqn (6.32) the term

$$\mathcal{D}_{R^-}\frac{dC_{R^-}}{dx}$$

which describes the flux of the dissociated organic anion, can be neglected when the extractant is a very weak acid, as it is in the case of most chelating reagents [197]. Equation (6.32) expresses the fact that the difference between the fluxes of extractant (in dissociated and non-dissociated form) and metal is due to, and equal to the flux of extractant $J_{t_{HR}}$ through the interface. The latter is related to $J_{t_{GaR_3}}$ in accordance with eqn (6.12).

The differential equations (6.29)-(6.32) are valid within the aqueous diffusion layer, and the following boundary conditions apply—at $x = 0$:

$$\begin{aligned} C_{HR} &= C_{t_{HR}} \\ C_{R^-} &= C_{t_{R^-}} \\ C_{GaR_3} &= C_{t_{GaR_3}} \\ \left(\frac{dC_{Ga^{3+}}}{dx}\right) &= 0 \\ \left(\frac{dC_{H^+}}{dx}\right) &= 0 \end{aligned} \qquad (6.33)$$

where the last two result from the condition of zero transport through the interface due to insolubility in the organic phase. At $x = \delta$:

$$\begin{aligned} C_{\mathrm{HR}} &= C_{0_{\mathrm{HR}}} \\ C_{\mathrm{R}^-} &= C_{0_{\mathrm{R}^-}} \\ C_{\mathrm{GaR_3}} &= C_{0_{\mathrm{GaR_3}}} \\ C_{\mathrm{Ga^{3+}}} &= C_{0_{\mathrm{Ga^{3+}}}} \\ C_{\mathrm{H^+}} &= C_{0_{\mathrm{H^+}}} \\ \left(\frac{dC_{\mathrm{HR}}}{dx}\right) &= 0 \\ \left(\frac{dC_{\mathrm{GaR_3}}}{dx}\right) &= 0 \end{aligned} \tag{6.34}$$

where the subscripts i and o denote interfacial and bulk values, respectively. Also, in the bulk aqueous phase, it follows from eqn (6.17) that

$$K_{\mathrm{eq}} = \frac{C_{0_{\mathrm{GaR_3}}} C_{0_{\mathrm{H^+}}}^3}{C_{0_{\mathrm{Ga^{3+}}}} C_{0_{\mathrm{HR}}}^3} \tag{6.35}$$

The system of differential equations (6.29)-(6.32), subject to the boundary conditions (6.33) and (6.34), provides the basis of the MTWCR model. The derivation of the appropriate expressions to calculate $C_{i_{\mathrm{Ga^{3+}}}}$ and $C_{i_{\mathrm{H^+}}}$ as well as $C_{0_{\mathrm{HR}}}$ is given in Appendix C. In order to do so, however, knowledge of the respective diffusion coefficients is also required.

Diffusion coefficients of species

The Wilke-Chang relationship is usually employed for estimation of diffusion coefficients of non-electrolytes in liquids [202]:

$$\frac{\mathcal{D}_j \mu}{T} = \frac{7.4 \times 10^{-12} \sqrt{sM}}{V_{\mathrm{B}_j}^{0.6}} \tag{6.36}$$

where $\mathcal{D}_j$ and V_{B_j} are the diffusion coefficient (in $\mathrm{m^2/s}$) and the molar volume at boiling point of the solute j, resp., while μ, M, and s are the viscosity (in cP),

molecular weight, and association factor of the solvent, resp., and T is the temperature in Kelvin.

Direct use here of eqn (6.36) for estimation of $\mathcal{D}_j$ for extractant-containing species in the aqueous and in the organic solution is impossible, firstly because kerosene is not a single component diluent, and secondly, because the data necessary to calculate V_{B_j} are not available for gallium, and thus for its species with the extractant.

On the other hand, diffusion coefficients of D2EHPA, and also of its zinc complexes, in n-heptane have been estimated [89] using the Wilke-Chang relationship. For zinc, in particular, this is possible since data are available [202]. However, the lack of needed information for cobalt and nickel—the other two metals in that study [89]—has apparently forced the authors to use for them the data for zinc.

Taking into account that in comparison to n-heptane kerosene has higher viscosity but also higher, on an average, molecular weight[11], and assuming the same solvent association factor, it is reasonable to expect that the diffusion coefficients of species in kerosene will be approximately equal to those in n-heptane.

Thus, for D2EHPA, the diffusion coefficients for the monomer and the dimer are taken as equal to those in n-heptane, and for its gallium complexes in kerosene approximate values are assigned. These values, along with the diffusion coefficients of species in the aqueous solution, are given in Table 6-2. Although most of them are just approximate, subsequent tests of the model have shown that the predicted flux values are insensitive to variations in these diffusion coefficients, which is even more so whenever the ratio of the coefficients appears instead in the respective formulas.[12] This seems to be also a feature of the original MTWCR model [158]

[11]Since kerosene is a mixture of C_{10}–C_{16} hydrocarbons, its average molecular weight is often assumed to be close to that of dodecane.

[12]This is the case with all of the expressions, presented in Appendix C, for calculation of species concentrations

species	org phase	aq. phase	Reference
	$\mathcal{D} \times 10^9$ m^2/s		
HR	1.52	0.42	[89]
$(HR)_2$	1.003	—	[89]
R^-	—	0 82	†
GaR_3	0.70	0.19	†
$GaR_3 \cdot HR$	0.60	—	†
H^+	—	5.85	[202]
Ga^{3+}	—	1.00	†

Table 6-2: Diffusion coefficients of species. †Estimated approximate values.

Approximate solution for two limiting reaction regimes

In general, an exact analytical solution of the system involving the differential equations (6.29)-(6.32), with the boundary conditions (6.33) and (6.34), is not possible due to mathematical complexity. An approximate solution can be found assuming that one of the two limiting cases holds [197, 200]:

- reversible pseudo-first order reaction
- instantaneous reversible reaction

Clearly, the approximate solution would become exact for the respective limiting case. The regime of reversible pseudo-first order reaction implies that the metal and proton concentrations are high enough so that their bulk and interfacial values are approximately equal:

$$C_{0_{Ga^{3+}}} \approx C_{i_{Ga^{3+}}}$$

$$C_{0_{H^+}} \approx C_{i_{H^+}} \tag{6.37}$$

On the other hand, in the case of instantaneous reaction the two reacting species (metal and extractant) cannot coexist together and their concentrations at the reaction plane are zero [200]. Furthermore, in the transitional regime between these

two limiting cases $C_{Ga^{3+}}$ and C_{H^+} can be assumed to be constant, and equal to their interfacial values, in the region close to the interface [200] because

$$\left(\frac{dC_{Ga^{3+}}}{dx}\right)_{x=0} = 0 \qquad \text{and} \qquad \left(\frac{dC_{H^+}}{dx}\right)_{x=0} = 0$$

with these relationships being part of the boundary conditions (eqn 6.33).

Thus, in the case of reversible pseudo-first order reaction eqn (6.29) becomes

$$\mathcal{D}_{HR}\frac{d^2C_{HR}}{dx^2} = k_f K_a \frac{C_{HR}}{C_{t_{H^+}}}\left(C_{t_{Ga^{3+}}} - \frac{1}{K_{eq}}\frac{C_{GaR_3}C^3_{t_{H^+}}}{C^3_{HR}}\right) \tag{6.38}$$

and in the case of instantaneous reaction

$$\mathcal{D}_{HR}\frac{d^2C_{HR}}{dx^2} = k_f K_a \frac{C_{HR}}{C_{t_{H^+}}}\left(C_{t_{Ga^{3+}}} - \frac{1}{K_{eq}}\frac{C_{t_{GaR_3}}C^3_{t_{H^+}}}{C^3_{t_{HR}}}\right) \tag{6.39}$$

as shown in the original model [197]. If the backward reaction (i.e., the stripping of metal) is neglected, then eqns (6.38) and (6.39) become identical:

$$\mathcal{D}_{HR}\frac{d^2C_{HR}}{dx^2} = k_f K_a \frac{C_{t_{Ga^{3+}}}}{C_{t_{H^+}}}C_{HR} \tag{6.40}$$

The integration of these equations and the resulting expressions for $J_{t_{HR}}$ are given in Appendix C. In the case when initial extraction rates are considered, described by eqn (6.40), the result then for $J_{t_{HR}}$ (eqn C.57) is:

$$J_{t_{HR}} = \sqrt{\frac{\left(\mathcal{D}_{HR} + \frac{\mathcal{D}_R K_a}{C_{t_{H^+}}}\right)^2}{\mathcal{D}_{HR}P^2_{HR}} k_f K_a \frac{C_{t_{Ga^{3+}}}}{C_{t_{H^+}}}\left(\overline{C}^2_{t_{HR}} - P^2_{HR}C^2_{0_{HR}}\right)} \tag{6.41}$$

which, in the case of weakly acidic extractant, i.e., when $K_a \to 0$, will become

$$J_{t_{HR}} = \sqrt{\frac{\mathcal{D}_{HR}}{P^2_{HR}} k_f K_a \frac{C_{t_{Ga^{3+}}}}{C_{t_{H^+}}}\left(\overline{C}^2_{t_{HR}} - P^2_{HR}C^2_{0_{HR}}\right)} \tag{6.42}$$

The corresponding expressions, when steps 5 or 6 are rate-limiting, are given by eqns (C.60) and (C.61), respectively.

Computational procedure

The system of respective equations for reactants and products concentrations (equations C.7, C.11, C.15, C.31, and C.33), together with the appropriate equation for $J_{i_{HR}}$, selected for a particular rate-limiting step and reaction regime assumed, has to be solved simultaneously for $J_{i_{HR}}$.

The fitting parameters in the model are the rate constant k_f of the slowest step, K' (or K_{eq}), and the mass-transfer coefficients of Ga^{3+} and H^+ in the aqueous phase and those of species in the organic phase. The rate constant k_f is incorporated in the parameter Θ defined as

$$\Theta = \frac{k_f}{\mathcal{D}_{HR} P_{HR}^2} \tag{6.43}$$

and the mass-transfer coefficients of species in the organic phase are expressed by the following relationships involving only $\overline{\kappa}_{HR}$:

$$\begin{aligned} \overline{\kappa}_{GaR_3} &= 0.60\overline{\kappa}_{HR} \\ \overline{\kappa}_{GaR_3 \cdot HR} &= 0.54\overline{\kappa}_{HR} \\ \overline{\kappa}_{(HR)_2} &= 0.76\overline{\kappa}_{HR} \end{aligned} \tag{6.44}$$

which are derived based on their diffusion coefficients (Table 6-2) and the approximate (2/3)-order dependence for the respective mass-transfer coefficients in liquid-liquid systems [200].

The computational procedure involves an iterative non-linear least squares method for estimation of the fitting parameters with an internal iterative loop, based on the secant method, for solving the system of the above mentioned equations with respect to $J_{i_{HR}}$ for the current set of parameters' estimates. It should be noted, however, that considerable sensitivity to initial estimates thus causing rapid divergence of the procedure was experienced. Therefore, it was necessary to find first, by trial and error, a sufficiently close set of initial estimates, which would assure convergence of the solution thereafter.

6.4 Interpretation of Experimental Kinetics Results

6.4.1 Extraction Rates and Model Predictions

As discussed in Chapter 4, the preliminary approximate analysis of gallium extraction kinetics data has led to the empirical equation (4.58)

$$\text{Flux Ga}\left(\frac{\text{kmol}}{\text{m}^2.\text{s}}\right) = 1.82 \times 10^{-9}\,[\text{Ga}^{3+}]_0^{0.71}\,[(\overline{\text{HR}})_2]_{0\,(\text{org})}^{0.60}\,[\text{H}^+]_0^{-1.53} \qquad (6.45)$$

This was found to describe well the data but mostly under conditions of low extraction rates.

Rate-limiting step

Comparison between the above eqn (6.45), with its empirical power coefficients, and the flux equation, for step 4 being rate-limiting, in the simplified form (6.42)--when the backward reaction and the diffusion of R^- are neglected--suggests that the latter may be relevant for describing the extraction kinetics results. Assuming, for example, that bulk and interfacial concentrations are equal and diffusional resistances are minimal, eqn (6.42) then predicts a half-order dependence on metal concentration, a first-order on extractant monomer (which virtually means a half-order on dimer) organic phase concentration, and an inverse half-order with respect to H^+ concentration. Clearly, except for the dependence on acidity, eqn (6.42) would yield power orders quite close to those in the empirical equation (6.45).

Furthermore, this preliminary analysis ruled out the possibility for step 5 or step 6 in the reaction scheme to be rate-limiting. While the respective flux equations (C.60) or (C.61) predict the same dependence on Ga^{3+} and eqn (C.61) gives an inverse one-and-a-half order on H^+, both predict a too strong dependence on extractant concentration. Thus, a more detailed analysis, taking into account the reverse reaction and possible diffusional resistances, has further shown that it is impossible

to find a set of model parameters' estimates with physically reasonable values, assuming step 5 or step 6 as rate-limiting, that would well describe all data on gallium extraction kinetics with D2EHPA.

Therefore, based on the above considerations, it is concluded that step 4, namely the first organic ligand addition, is the slowest step in the series of elementary chemical reactions.

Extractant dissociation and rate dependence on acidity

As mentioned above, the anticipated major disagreement between the flux eqn (6.42) and the empirical eqn (6.45) is for the dependence on acidity. Even when the full-form flux equation for either limiting regime—eqns (C.48) or (C.56)—is employed, the predicted gallium extraction rate dependence on acidity differs significantly from the one experimentally observed, as shown on fig. 6.3.

Various options have been considered in order to explain the disagreement. The only one, however, thought to be physically plausible and therefore offered here, is that diffusion of the dissociated organic anion R^- cannot be neglected and must be included in the relevant model equations when the extractant is a relatively strong acid. D2EHPA, as well as the two OPAP reagents, used in this study, are such extractants.

One other option, which has been considered possible is that the reacting species is not Ga^{3+}, but another gallium-containing complex. As the results from species distribution (Chapter 5) has shown, there are several cationic species existing in the pH range of interest. The sulphate containing $GaSO_4^+$ complex is certainly not the reacting species—firstly, because sulphates are not extracted (see page 39), and secondly because the extraction rate as well as D_{Ga} should then increase with increasing the sulphate concentration. Thus, among the hydroxy complexes, the most probable one is $Ga(OH)^{2+}$ (e.g., see fig. 5.4). Using the speciation program and the needed parameters from the conditions of the kinetic experiments, the relevant

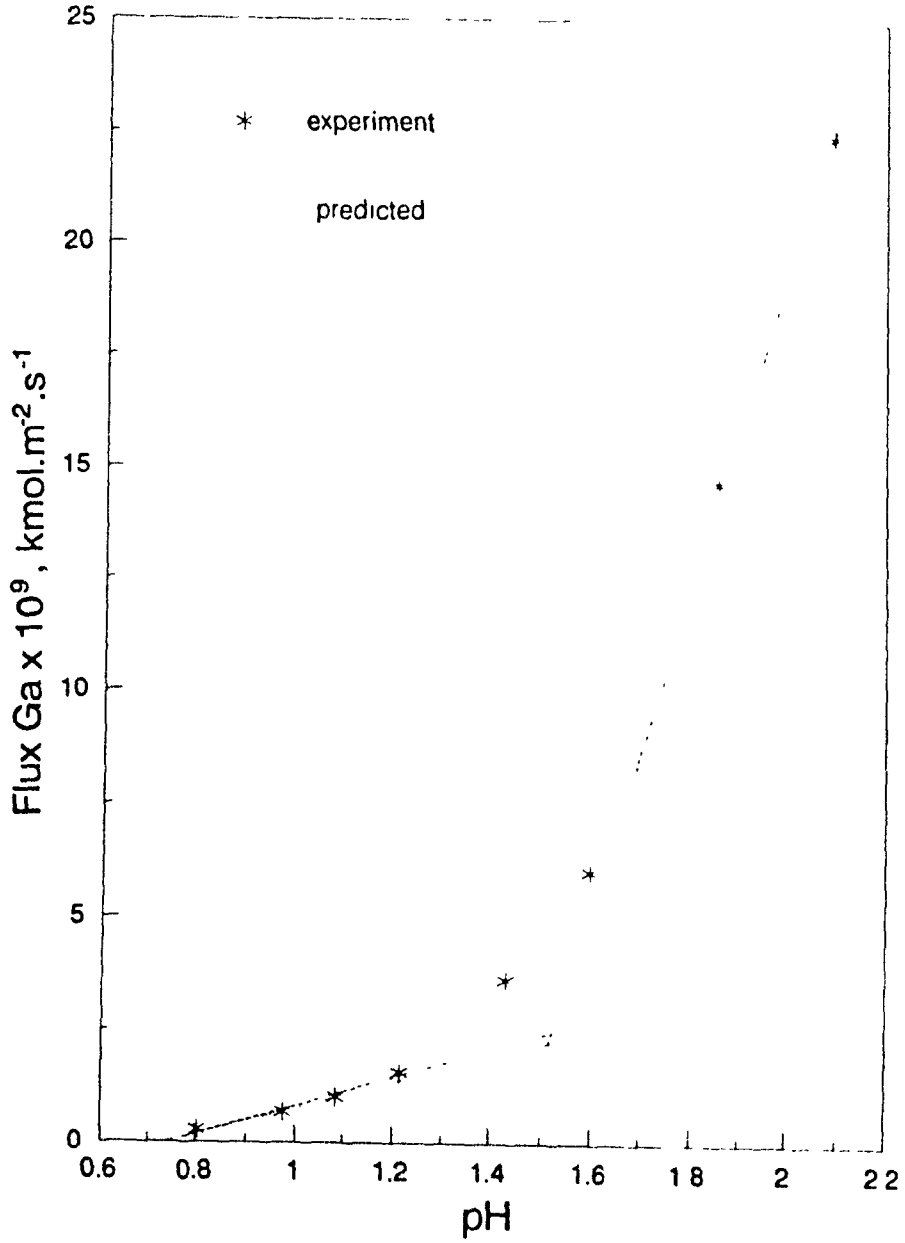

Figure 6.3: Comparison between model predictions based on eqns (C 48) or (C.56) and experimental data. Data and conditions are those of fig 4 22

concentrations of $Ga(OH)^{2+}$ were calculated and then tried for explaining the above disagreement. This was, however, unsuccessful. Under the acidic conditions of experiments the increase in $Ga(OH)^{2+}$ is very small and cannot explain the experimentally found rate dependence on pH (fig. 4.22).

The range of low pH, which is important for gallium extraction and studied here, coincides with the region where the contribution of R^- to the extractant's distribution coefficient (defined by eqn 6.5) becomes significant. Indeed, from eqn (6.5) it follows that:

$$D_{HR} = \frac{\overline{C}_{HR}}{C_{HR}\left(1 + \frac{K_a}{C_{H^+}}\right)} \tag{6.46}$$

It is clear that eqn (6.46) would yield a different dependence of D_{HR} on acidity as the latter changes. Thus, it can be approximated by two asymptotes. At low pH D_{HR} will be independent of C_{H^+} while at high pH D_{HR} will decrease linearly with decreasing acidity. The intersection point of the two asymptotes obviously depends on the value of K_a, and this is the idea behind some of the methods for its determination [190, 191]. Figure 4.6, which refers to aqueous solubility of OPAP, can serve as an example for the shape of the curve resulting from eqn (6.46).

Furthermore it is readily seen that the form of the observed dependence of gallium extraction rate on pH in the case of D2EHPA (fig. 4.22), as well as OPAP extractants (fig. 4.37), closely resembles the one of fig. 4.6 and those related to D2EHPA [190]. It is unlikely this is a mere coincidence. In addition, if the two asymptotes are drawn for the curve on fig. 4.22, they will intercept at approximately pH of 1.5, as illustrated (the dashed lines) on fig. 6.3, which is well within the range of reported values of K_a for D2EHPA (Table 6-1). Such a direct comparison for the case of OPAP extractants is not readily possible because of the mixed system and absence of data for the respective K_a values in the literature, but it is nevertheless clear that the same argument will be valid for them too.

These apparent similarities are considered here as supporting evidence that an extraction reaction, taking place in the aqueous diffusion layer, plays a significant

Parameter	Estimated value
Θ	5.11×10^{9} m^2/s^2
K'	1.0×10^{4}
$\kappa_{Ga^{3+}}$	1.1×10^{-5} m/s
κ_{H^+}	3.8×10^{-5} m/s
$\bar{\kappa}_{HR}$	2.5×10^{-5} m/s
$\bar{\kappa}_{GaR_3}$	1.4×10^{-5} m/s

Table 6-3: Estimated model parameters

role in the overall extraction mechanism. In addition, such similarities clearly suggest that the flux of R^- cannot be neglected and has to be also taken into account in the model.

Model parameters and predictions

Thus, based on eqn (C.47) for $J_{i_{HR}}$ and the respective equations for species concentrations, the model parameters that give the best fit to the experimental data, have been estimated and are summarized in Table 6-3. The model predictions, as compared with the experimental results, are presented on figures 6.4, 6.5, and 6.6.

Virtually the same predictions are obtained if eqn (C.55), which is based on reversible pseudo-first order limiting regime, is used instead for $J_{i_{HR}}$. This is not surprising since the experimental conditions are such that the effects of the reverse reaction on $J_{i_{HR}}$ are very small, i.e., conditions of initial rates. In such case the expression for $J_{i_{HR}}$ is the same for both limiting regimes (eqn C.57).

It is evident from figs. 6.4-6.6 that the model describes well the experimental data for gallium extraction kinetics with D2EHPA. The same also applies for the effect of sulphate complexation, as shown on fig. 6.7 following the discussion of fig. 5.9 and plotted in the same coordinates.

Although it is clearly necessary for the model to be able to describe the already available data (on which basis it has been built, and fitting parameters estimated), this alone is not enough for considering it as correct (with respect to the assumed

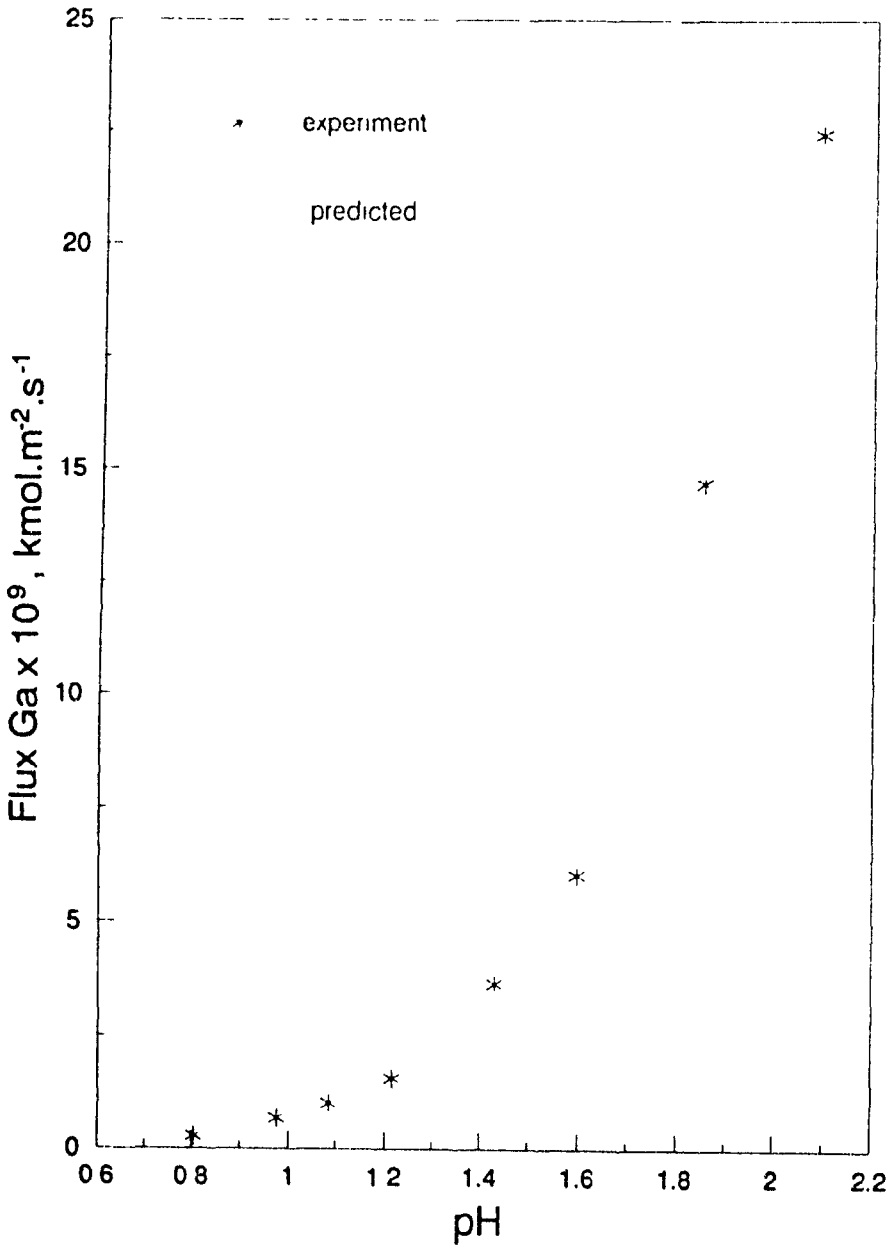

Figure 6.4: Effect of pH. Comparison between model predictions (parameters of Table 6-3) and the experimental results. Data and conditions are those of fig. 4.22.

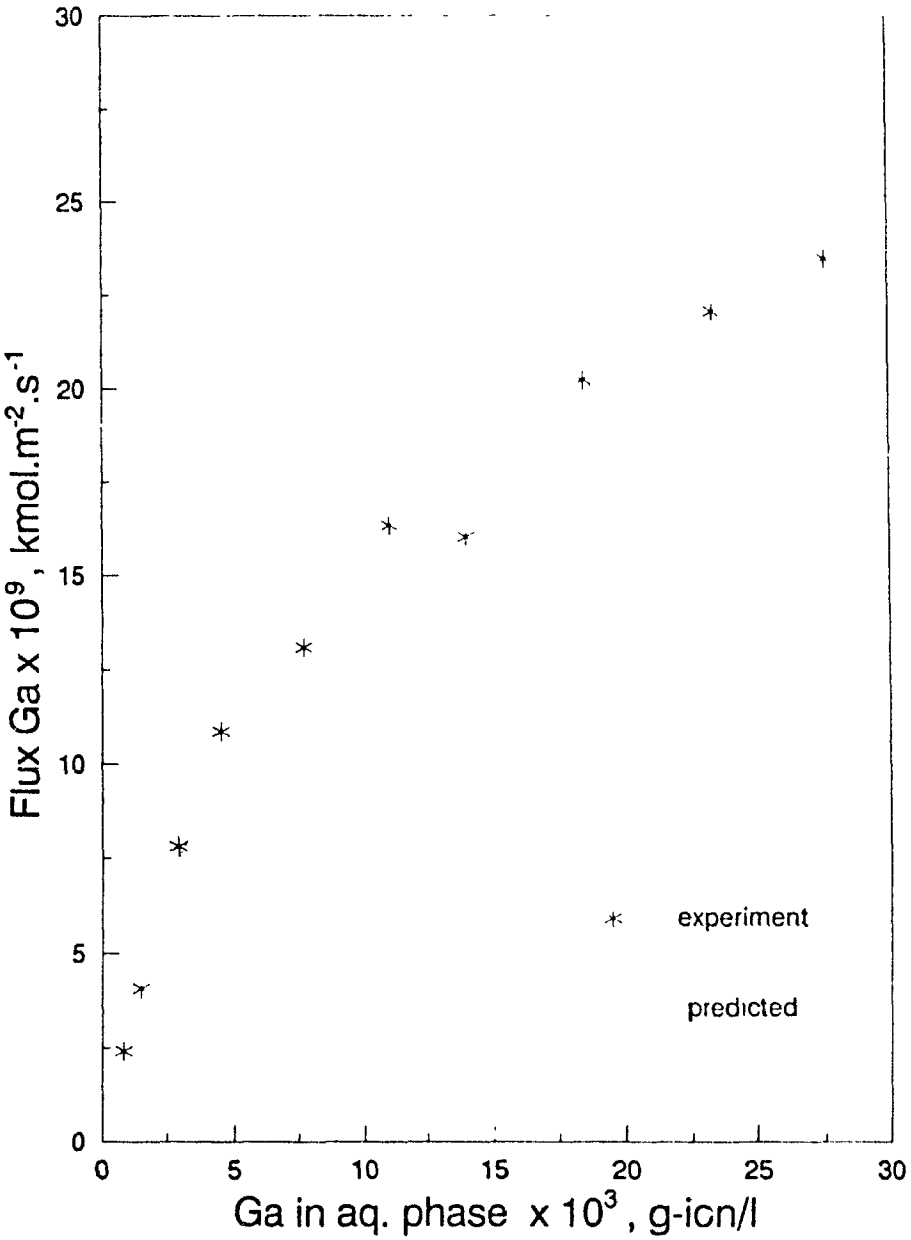

Figure 6.5: Effect of metal concentration. Comparison between model predictions (parameters of Table 6-3) and the experimental results. Data and conditions are those of fig. 4.23.

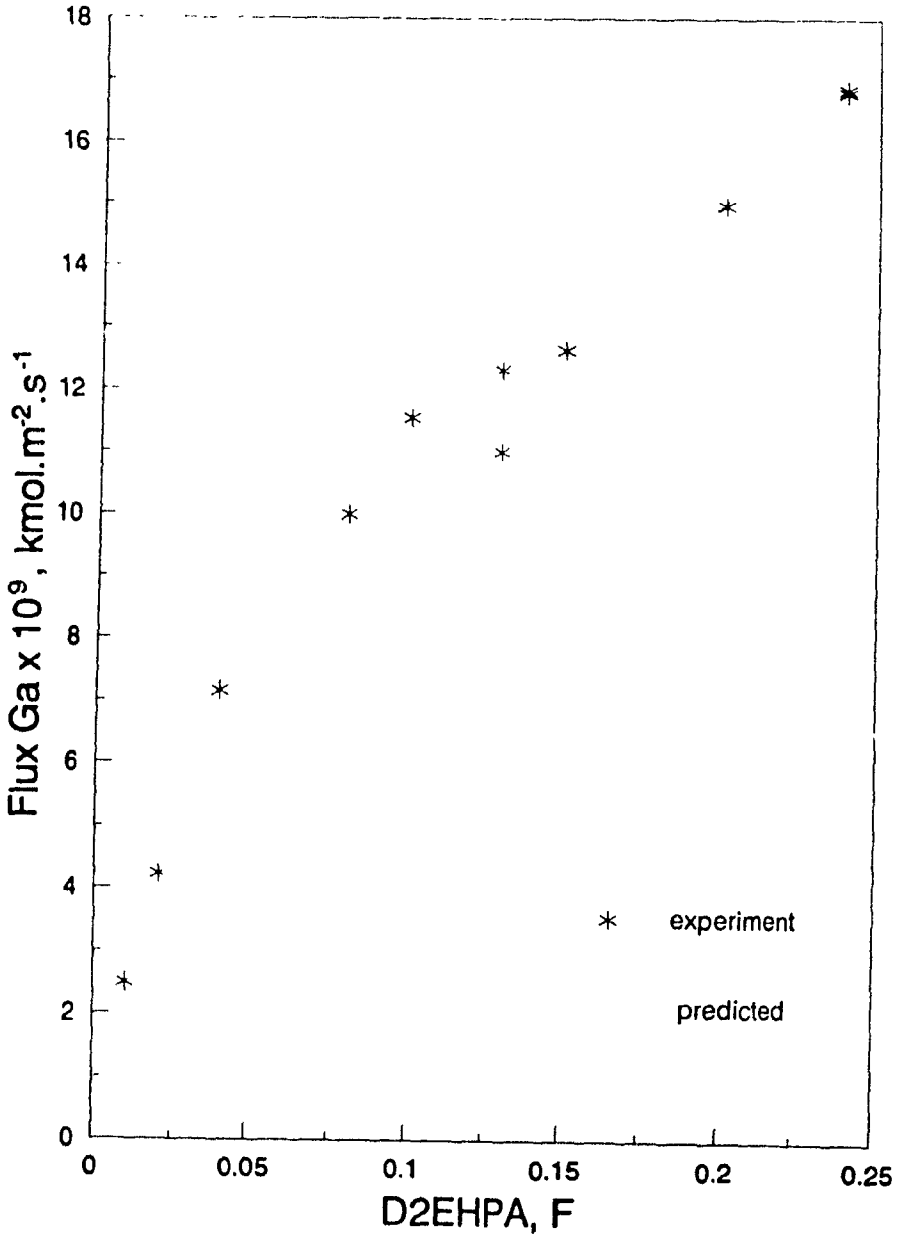

Figure 6.6: Effect of D2EHPA concentration. Comparison between model predictions (parameters of Table 6-3) and the experimental results. Data and conditions are those of fig. 4.24.

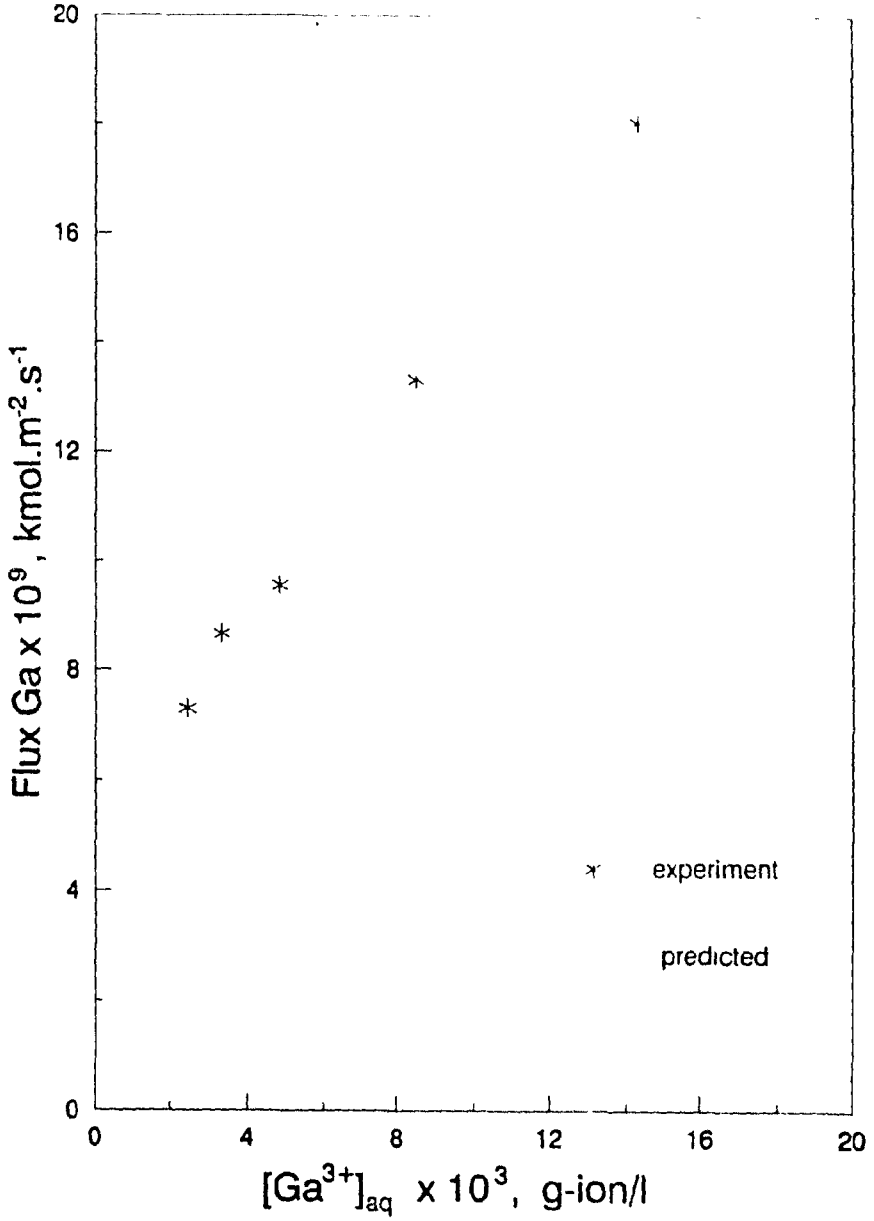

Figure 6.7: Effect of sulphate complexation. Comparison between model predictions (parameters of Table 6-3) and the experimental results. Data for the free Ga^{3+} concentration from fig. 5.9; experimental flux values and conditions are those of fig. 4.25.

mechanism) and for having confidence in its predictions, particularly *outside* the range of the currently investigated experimental conditions.

For these reasons, first the physical significance of the model parameters will be discussed, then its predictions under stripping, i.e., quite different from initial extraction rates, conditions will be verified, and finally model behaviour at near-equilibrium conditions will be tested

The most sensitive parameters of the MTWCR model [158] are Θ, because it includes the rate constant k_f, and the mass-transfer coefficients, which are dependent on the particular hydrodynamic conditions of the experimental set-up. With the estimated value of Θ (Table 6-3) and selecting $P_{HR} = 1600$ from Table 6-1 k_f is calculated from eqn (6.43):

$$k_f = 5.5 \times 10^6 \quad m^3.kmol^{-1}.s^{-1} \tag{6.47}$$

This value of k_f appears to be reasonable when compared with those reported [181] for other metal-D2EHPA systems using the same RDC technique, as shown in Table 6-4. It should be noted, however, that the data for k_f in Table 6-4 for all systems, except vanadium-D2EHPA, have been obtained using a model which assumes that D2EHPA exists and reacts solely as dimer [181]. On the other hand, a different value for the Co^{2+}-D2EHPA system—7.9×10^6—has been reported[13] by Dreisinger and Cooper in their studies [89], using the RDC method and the MTWCR model developed by Hughes and Rod [158] Still, it is clear from Table 6-4 that the values of k_f generally obey the tendency of decreasing in the order $Cu^{2+} > Zn^{2+} > Co^{2+} > Ni^{2+}$ which is explained primarily with the fact that it is in the same order that their respective water ligand exchange rate-constants k_w also decrease [9, 196]. Indeed, this can be seen from the expression for J_{HR} given by eqn (C.47). According to eqn (C.47), as long as the extractant is the same, the differences in J_{HR} found for different metals, obeying the same extraction mechanism, will be due exclusively to their different

[13]The units, s^{-1}, given for this value in ref [89], are apparently mistaken since k_f is a second-order rate constant

System	k_f $m^3\ kmol^{-1}.s^{-1}$	k_w s^{-1}
Cu^{2+}-SO_4^{2-}/D2EHPA-heptane	2.46×10^5	$\sim 4 \times 10^8$
Zn^{2+}-SO_4^{2-}/D2EHPA-heptane	2.47×10^9	$\sim 4 \times 10^7$
Co^{2+}-SO_4^{2-}/D2EHPA-heptane	1.05×10^8	$\sim 3 \times 10^5$
Ni^{2+}-SO_4^{2-}/D2EHPA-heptane	6.53×10^6	$\sim 1 \times 10^4$
VO^{2+}-SO_4^{2-}/D2EHPA-hexane	2.21×10^9	$\sim 10^7$

Table 6-4: Comparative data for k_f, taken from ref. [181] Data for k_w are from refs. [9, 196], except for vanadium [181].

values of k_f. On the other hand, k_f refers to a ligand exchange reaction which will undoubtedly involve removal of water ligands from the hydrated metal cation and therefore will be directly related to k_w. The two constants, however, cannot be compared numerically because of their different units of measurement.

For Ga^{3+}, k_w has been found to be $1.82 \times 10^3\ s^{-1}$ [137]. Therefore, from the comparison of this value with those for the other metals listed in Table 6-4, the rate constant k_f for the extraction reaction of gallium with D2EHPA should be expected to be similar to the one for nickel, for example, but less than the values of k_f for the other metals. This, indeed, is observed Although the difference, on the other hand, between the value of k_f obtained here for gallium and the value for cobalt reported by Dreisinger and Cooper [89], is rather small, considering their water ligand exchange rate-constants, still the extraction reaction rate constant k_f for gallium is regarded as reasonably correct given the number of assumptions and approximations that have been unavoidably required in the model development.

The aqueous- and organic-side mass-transfer coefficients (κ and $\overline{\kappa}$, resp.), determined as fitting parameters, differ significantly in the various studies employing the RDC technique and using the Hughes and Rod's model for data interpretation. For example, for the first four extraction systems summarized in Table 6-4 the values of κ are approximately about 7×10^{-5} m/s, and 1.5×10^{-5} m/s for $\overline{\kappa}$, while for

the vanadium D2EHPA system they are 4×10^{-6} m/s and 7.4×10^{-6} m/s, respectively [181]. For the zinc-D2EHPA system, the aqueous-side mass-transfer coefficient for Zn^{2+} has been found [89] to be approximately 2×10^{-5} m/s, and $\overline{\kappa}$ for D2EHPA dimers -4.2×10^{-6} m/s. Furthermore, by applying the MTWCR model to the original data of Albery and Fisk [83] on copper extraction kinetics studied by the RDC technique, Hughes and Rod have determined [158] κ and $\overline{\kappa}$ to be 2.2×10^{-5} m/s and 1.0×10^{-5} m/s, resp., noting, at the same time, that they appear relatively small and explaining this with possible resistances through the membrane.

Hence, from this review of available data on mass-transfer coefficients previously determined in studies with the RDC technique, it is seen that the values found in this work (Table 6-3) are reasonably within their range. Although this alone cannot be taken as a proof for correctness, it nevertheless gives a certain degree of confidence in the obtained data. Still, it should be remembered that, as fitting parameters, the mass-transfer coefficients in the MTWCR models may implicitly include other, unaccounted for, phenomena and processes.

Such an example is the mass-transfer coefficient for D2EHPA monomer, $\overline{\kappa}_{HR}$, for which a relatively high value has been determined here. First of all, $\overline{\kappa}_{HR}$ includes possible effects of diffusion through the organic-impregnated porous membrane. Obviously, this diffusion, and not only of HR but also of $(HR)_2$ and the metal-extractant complexes, is part of the overall transport process. In this respect, the logical question to ask is whether diffusion through the membrane may in fact be the rate-limiting step. Dreisinger *et al.* [88] have shown that in such case the resulting flux $J_{t_{HR}}$ would still be about one order of magnitude higher than what is experimentally found, i.e., this diffusion cannot be the limiting step.

Furthermore, if diffusion through the membrane limits in some way the transport, then the membrane would be part of the organic diffusion layer [85, 87, 88]. The thickness of the membrane,[14] δ_m, is approximately 2×10^{-4} m [89] and therefore,

[14]Defined as the actual thickness divided by the porosity of the membrane

assuming that it represents the organic diffusion layer and $\overline{D}_{HR}$ remains the same inside, this yields for $\overline{\kappa}_{HR}$:

$$\overline{\kappa}'_{HR} = \frac{\overline{D}_{HR}}{\delta_m} = 0.76 \times 10^{-5} \text{ m/s}$$

using the value for $\overline{D}_{HR}$ from Table 6-2. Clearly, $\overline{\kappa}'_{HR}$ is smaller than $\overline{\kappa}_{HR}$, which means that the actual thickness of the diffusion layer is less than δ_m and therefore the membrane diffusional resistance can be regarded as negligible.

Another important aspect to consider, with respect to the value of $\overline{\kappa}_{HR}$, is how well the model describes the phenomena affecting the extractant's monomeric and dimeric molecules, and their concentrations in the diffusion layer and at the interface. As mentioned earlier, the film theory, and therefore the model too, defines the interface as a plain boundary where the molecules of the two solvents (and of the solutes therein) meet each other, and physical equilibrium of extractant and metal-extractant species exists, following the respective partitioning coefficients. The interfacial concentrations, $\overline{C}_i$, however, are regarded only as resulting from diffusion through the organic layer and, of course, the chemical reaction.

In the present model here, efforts have been made to describe what really happens as fully as possible by including also the transport of dimer molecules. As mentioned in Appendix C, section C.3, a concentration gradient for $(HR)_2$ in the organic layer is thought to exist—firstly, because due to transfer of HR to the aqueous side, the dimers concentration will drop, following the monomer-dimer equilibrium, and secondly because once in contact with water molecules at the interface de-dimerization will be expected to take place. What is the extent of this second phenomenon and how it can quantitatively be described is presently not known. Therefore, the model developed here takes into account the simultaneous diffusion of dimers to the interface, but only assumes that monomer-dimer equilibrium exists there, defined by the value of K_d.

Thus, it is clear that the actual interfacial concentration of HR will probably be higher than what the model can 'understand'. Furthermore, despite its recognized

significance, the effect of extractant's interfacial activity on $\overline{C}_{HR}$ is not taken into account by the MTWCR model. At the same time, although the dimer itself is considered to be much less interfacially active than the monomer, its contribution to the value of $\overline{C}_{HR}$ through de-dimerization will still be important since the extractant exist virtually as dimer (except, presumably, at the interface).

Following these considerations, it is obvious that the only way the model can accommodate such possibly higher $\overline{C}_{HR}$ values is by attributing them to a diffusional resistance lower than what it really is. In other words, this means that the resulting value for $\overline{\kappa}_{HR}$, as a fitting parameter, will probably be higher than the actual one. These arguments may provide an explanation for the seemingly higher value of $\overline{\kappa}_{HR}$, estimated here (Table 6-3).

The other fitting parameter in the model is K'. In general, K' reflects the equilibria in the bulk phases [158, 197]. It is related to K_{eq} (equilibrium in the bulk aqueous phase) by eqn (6.21), and also to K_G (equilibrium in the bulk organic phase) and K'_{ex} by eqn (6.19). Of all these constants, only K'_{ex} is known from experiment (see page 41). Also, it is assumed that $P_{GaR_3} = P_{HR}$ and this introduces an additional uncertainty if K_{eq} is to be calculated from K' by eqn (6.21) or *vice versa*.

Using the estimated value for K' from Table 6-3 and $P_{HR} = P_{GaR_3} = 1600$ from Table 6-1, the result for K_{eq} is

$$K_{eq} = \frac{P_{HR}^3}{P_{GaR_3}} K' = 2.56 \times 10^{10}$$

If true, this high value of K_{eq} means that in the bulk aqueous phase the equilibrium (eqn 6.17) is shifted considerably to the side of the product, GaR_3, which certainly is not unreasonable to expect. Similarly, for K_G the following value is calculated using eqn (6.19) and selecting $K_d = 3.13 \times 10^4$ l/mol from Table 6-1:

$$K_G = 1.77 \times 10^5 \text{ l/mol}$$

Again, this resulting value of K_G may be viewed as an indication that the equilibrium of step 8b is shifted to the solvated complex $GaR_3 \cdot HR$, and only at high loadings

(when the concentration of $(HR)_2$ is low) will GaR_3 complex become predominant, as discussed in Chapter 4 (page 45). It should be emphasized, however, that step 8b and the equilibrium constant K_G, that describes it, is just a representative example of one or more solvation reactions in the organic phase, that may occur and lead to the formation of $GaR_3 \cdot HR$ and/or other metal-extractant complexes there. In other words, step 8b should be regarded not as an elementary step (it certainly isn't) but as a possible net result of several other solvation reaction elementary steps

Several proposed criteria have been earlier discussed as ways to distinguish between the interface and the adjacent aqueous diffusion layer as reaction locus (see pages 153–155). It is now appropriate to verify how they can be applied to the experimental results and the model predictions, and what conclusions can be reached.

From the first criterion, which is based on differently resulting dependence of rate on extractant concentration (fig. 6.1), and comparing with the relevant experimental data (figures 4.24 or 6.6), it can be seen that here, in the case of gallium extraction with D2EHPA, the reaction in the diffusion layer is indeed significant. It is evident from fig. 6.6 that even at high extractant concentrations the rate continues to increase, contrary to what should be expected if the reaction is occurring only at the interface (fig. 6.1a).

According to the second criterion, the rate constants k_f for reactions proceeding exclusively at the interface, when compared for several metals, should not be related to the respective rate constants of water ligand exchange. However, as already discussed above, the comparison between the values of k_f and k_w for gallium and the respective values for other metal-D2EHPA systems (Table 6-4) clearly shows that the order for the rate constants of water ligand exchange is closely followed by the order of the respective extraction reaction rate constants. This certainly indicates that reactions in the aqueous diffusion layer predominate.

The third criterion compares whether or not the extraction rate remains the same if the product $\prod = (C_{Me}C_{HR})$, is kept constant but the ratio (C_{Me}/C_{HR}) is

(when the concentration of $(HR)_2$ is low) will GaR_3 complex become predominant, as discussed in Chapter 4 (page 45) It should be emphasized, however, that step 8b and the equilibrium constant K_G, that describes it, is just a representative example of one or more solvation reactions in the organic phase, that may occur and lead to the formation of $GaR_3 \cdot HR$ and/or other metal-extractant complexes there. In other words, step 8b should be regarded not as an elementary step (it certainly isn't) but as a possible net result of several other solvation reaction elementary steps.

Several proposed criteria have been earlier discussed as ways to distinguish between the interface and the adjacent aqueous diffusion layer as reaction locus (see pages 153-155). It is now appropriate to verify how they can be applied to the experimental results and the model predictions, and what conclusions can be reached.

From the first criterion, which is based on differently resulting dependence of rate on extractant concentration (fig. 6.1), and comparing with the relevant experimental data (figures 4.24 or 6.6), it can be seen that here, in the case of gallium extraction with D2EHPA, the reaction in the diffusion layer is indeed significant. It is evident from fig. 6.6 that even at high extractant concentrations the rate continues to increase, contrary to what should be expected if the reaction is occurring only at the interface (fig. 6.1a).

According to the second criterion, the rate constants k_f for reactions proceeding exclusively at the interface, when compared for several metals, should not be related to the respective rate constants of water ligand exchange. However, as already discussed above, the comparison between the values of k_f and k_w for gallium and the respective values for other metal D2EHPA systems (Table 6-4) clearly shows that the order for the rate constants of water ligand exchange is closely followed by the order of the respective extraction reaction rate constants. This certainly indicates that reactions in the aqueous diffusion layer predominate.

The third criterion compares whether or not the extraction rate remains the same if the product $\prod = (C_{Me}C_{HR})$, is kept constant but the ratio (C_{Me}/C_{HR}) is

varied. If the reaction is predominantly in the aqueous diffusion layer then the rate should not be the same. The result from applying this criterion to the experimental data cannot be seen by simply comparing, for example, fig. 6.5 and fig. 6.6 (although both refer to practically the same pH), because C_{HR} need to be found first from eqn (C.15) or (C.20). The application can be illustrated with the following examples: let us select an experimental point from fig. 6.5, for example - the one at $C_{0_{Ga^{3+}}} = 4.5 \times 10^{-3}$ g-ion/l for which the flux is 10.9×10^{-9} kmol m^{-2} s^{-1}; after calculation of C_{HR} and then $\prod$ for the current conditions, the value obtained for $\prod$ can next be used to find for what total D2EHPA concentration, under the conditions of fig. 6.6, the same value of $\prod$ would be found, the answer yields 0.01 F, and this would result, making the conclusion from fig. 6.6, in having flux of 3.1×10^{-9} kmol.m^{-2}.s^{-1}, which is more than three times smaller than the first flux value; similarly, for the next experimental point on fig. 6.5, at $C_{0_{Ga^{3+}}} = 7.7 \times 10^{-3}$ g-ion/l for which the flux is 13.1×10^{-9} kmol.m^{-2}.s^{-1}, the same value of $\prod$ will be obtained for the point at 0.06 F D2EHPA on fig. 6.6, to which a value of 8.5×10^{-9} kmol.m^{-2} s^{-1} for the flux corresponds.

These examples show that the rate of gallium extraction does not remain constant if $\prod$ is the same. In other words, this is another indication which implies a predominant role for reaction occurring in the aqueous diffusion layer.

Finally, it should be noted that from the viewpoint of gallium solution chemistry and ligand exchange kinetics, it is reasonable to expect extraction under chemical kinetic control, similar to that observed for other tri-valent metals [50, 167] with relatively low values of k_w like Fe^{3+}, Cr^{3+}, Al^{3+}, In^{3+}, etc. As a consequence of the resulting generally lower extraction rates, a shift of the reaction zone to the aqueous side of the interface (and in extreme cases—even further—to the bulk aqueous phase) will clearly be more favourable.

In the next section the predictions of the model with the estimated parameters (Table 6-4), which have been based on extraction kinetics data, will be compared with

the results then obtained from the experiments on gallium stripping rate from loaded D2EHPA.

6.4.2 Model Verification: Stripping Conditions

Here, for the conditions of stripping, the modelling equations, for $J_{i_{HR}}$ and species concentrations, as well as the computational algorithm and program, remain the same as for the case of extraction.

Minor changes in the form of the equation (C.15) for $C_{0_{HR}}$ are necessary, as discussed in Appendix C (see page 239), following the condition of $C_{0_{Ga^{3+}}} = 0$ in the bulk aqueous phase. However, subsequent comparative testing of the two equations, (C.15) and its modified form (C.20), have shown that they give nearly identical results for $C_{0_{HR}}$.

Also, in the case of stripping, a more precise account for the distribution of species in the bulk organic phase is required. As mentioned earlier, these species are considered to be: HR, $(HR)_2$, GaR_3, and $GaR_3 \cdot HR$. Under conditions of negligible metal loading, the bulk concentrations $\overline{C}_{0_{HR}}$ and $\overline{C}_{0_{(HR)_2}}$ can be found simply from the total extractant concentration and using the equation for K_d (eqn 6.6). However, when metal loading is significant, as it is in the case of stripping, all four species have to be taken into account, with their respective equilibria, described by the equations for K_d and K_G. The relevant equations are given in Appendix C, and for K_G, the value found from the estimated K' parameter, is used.

It is evident that mathematically the difference between extraction and stripping, with respect to the interfacial flux $J_{i_{HR}}$ is only in its sign, and this reflects the physical change in direction. Once a positive sign for $J_{i_{HR}}$ is chosen to denote transfer of HR through the interface from organic to aqueous phase, then the flux in opposite direction, which is the result of metal being stripped from the organic, has to have a negative sign in the equations linking bulk and interfacial concentrations of species. This physically means that the concentration profiles, as schematically

shown on fig. 6.2 for the case of metal extraction, will be reversed, i.e., $C'_{i_{Ga^{3+}}}$ will be greater than $C_{0_{Ga^{3+}}}$, etc. Hence, when considering the rate of gallium stripping, the respective values for $J_{i_{HR}}$ are introduced with a negative sign in the calculations of concentration profiles.

The model predictions for the same conditions of the experimental data, previously presented on figs. 4.30-4.32, are compared with them and displayed on figs. 6.8-6.10, respectively.

Figures 6.8-6.10 show that the model predictions match closely the experimental results. It should be remembered that except for the additional developments described above, relevant to stripping kinetics,[15] the model equations and estimated parameters remain otherwise the same as for extraction.

Also, no additional fitting of the model to the data from stripping experiments has been performed, although, if undertaken, it is possible that a better set of estimates might have been obtained, as comparisons from figures 6.8-6.10 would suggest. This, however, has not been done, because the primary purpose of carrying out the stripping kinetics experiments has been to test the developed model under considerably different conditions. In this sense, the demonstrated ability of the model to give reasonably adequate predictions for these conditions too is regarded as an indication of its validity.

Finally, it should be noted that attempts to use in the model the other equation for $J_{i_{HR}}$ (eqn C.55), derived for the case of reversible pseudo-first order limiting regime, and to apply it to the stripping kinetics data, with the same already estimated parameters, were unsuccessful. While for the extraction kinetics results, both models have yielded almost the same predictions, attributed to the very small contribution of the reverse reaction for these conditions, predictions in the case of stripping rates are substantially different. Furthermore, it appeared impossible to find a set of parameters' estimates when eqn (C.55) is used, with which the model would give a

[15]The most significant is the calculation of species distribution in the organic phase, but it is based on known (K_d) or already estimated (K_G) parameters.

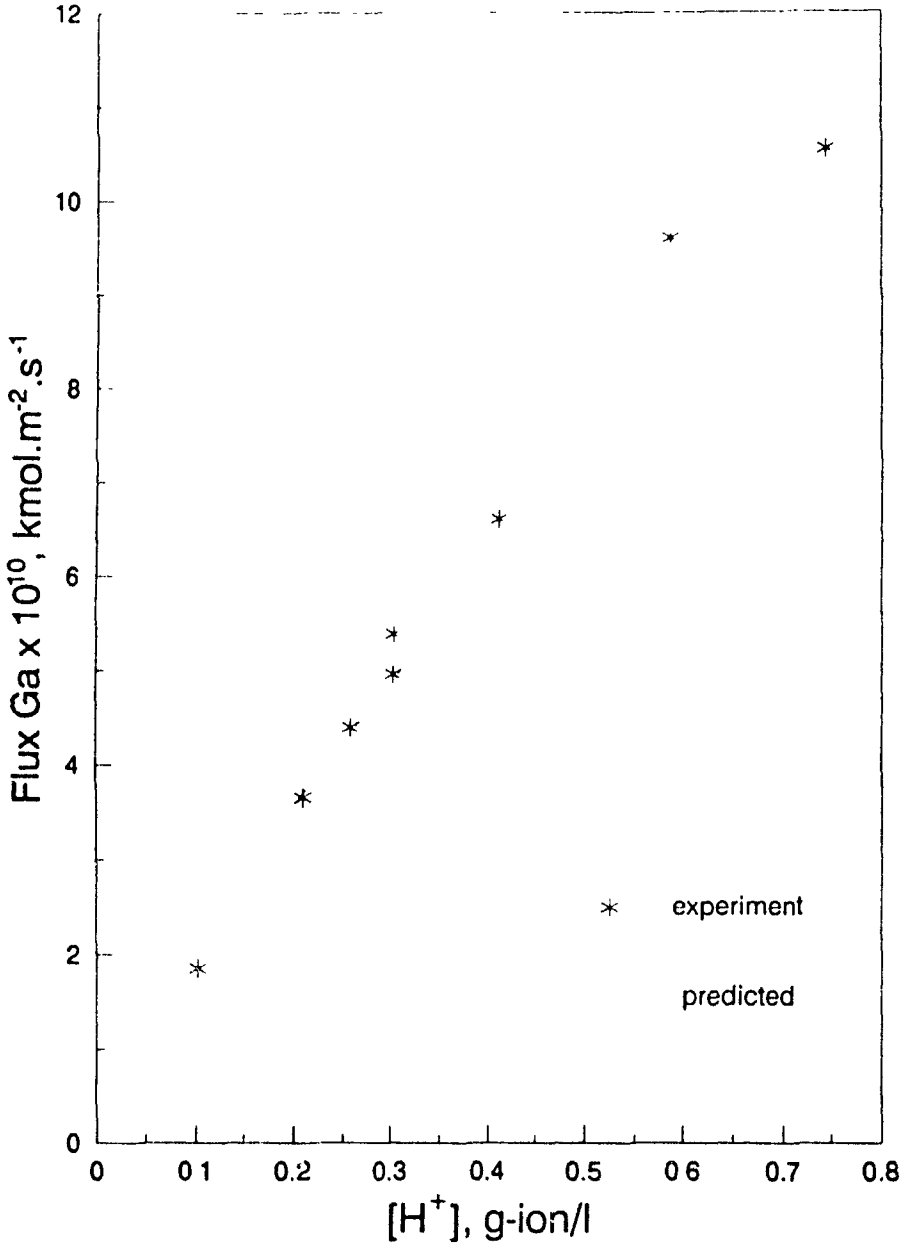

Figure 6.8: Effect of aqueous acidity. Comparison between model predictions (with the parameters from Table 6-3) and the experimental results. Data and conditions are those of fig 4.30

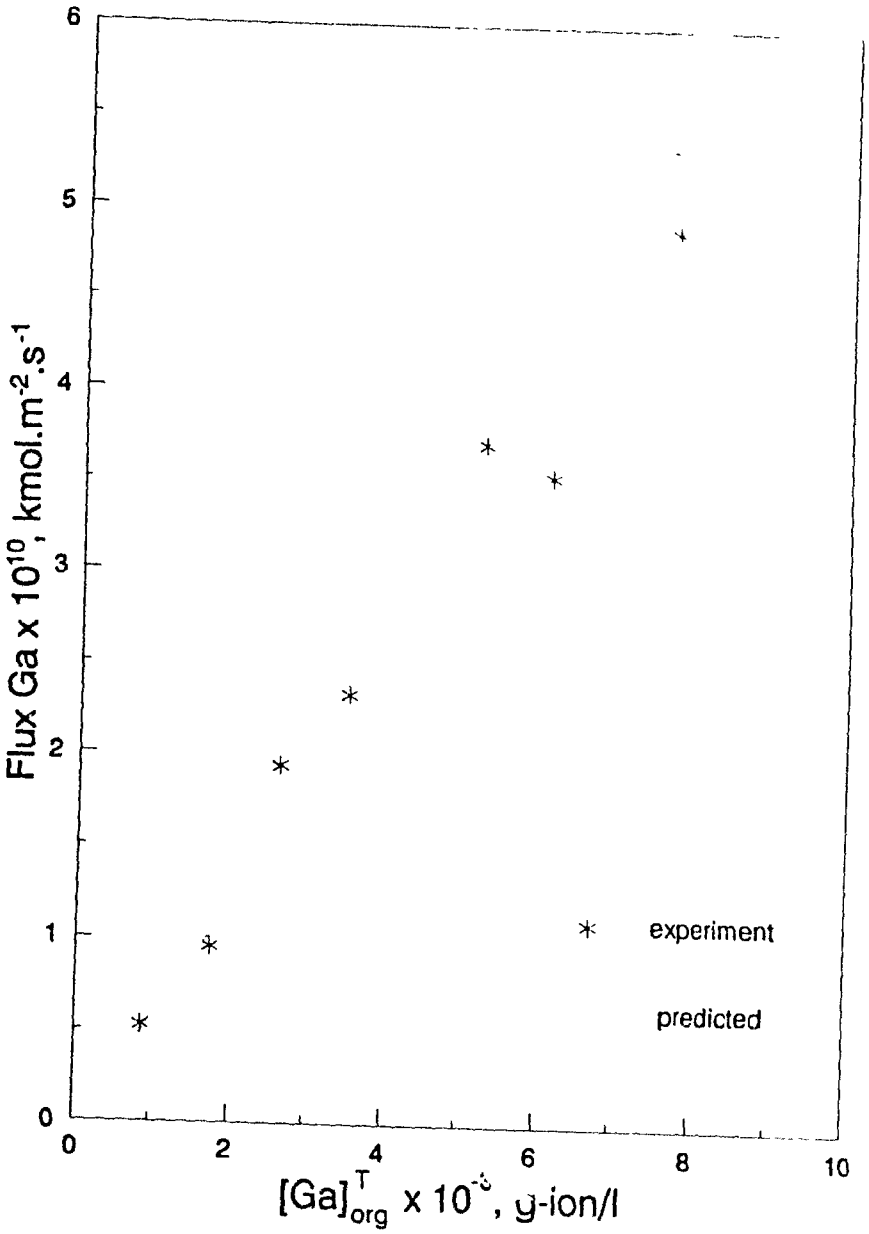

Figure 6.9: Effect of metal concentration in the organic phase. Comparison between model predictions (with the parameters from Table 6-3) and the experimental results. Data and conditions are those of fig. 4.31.

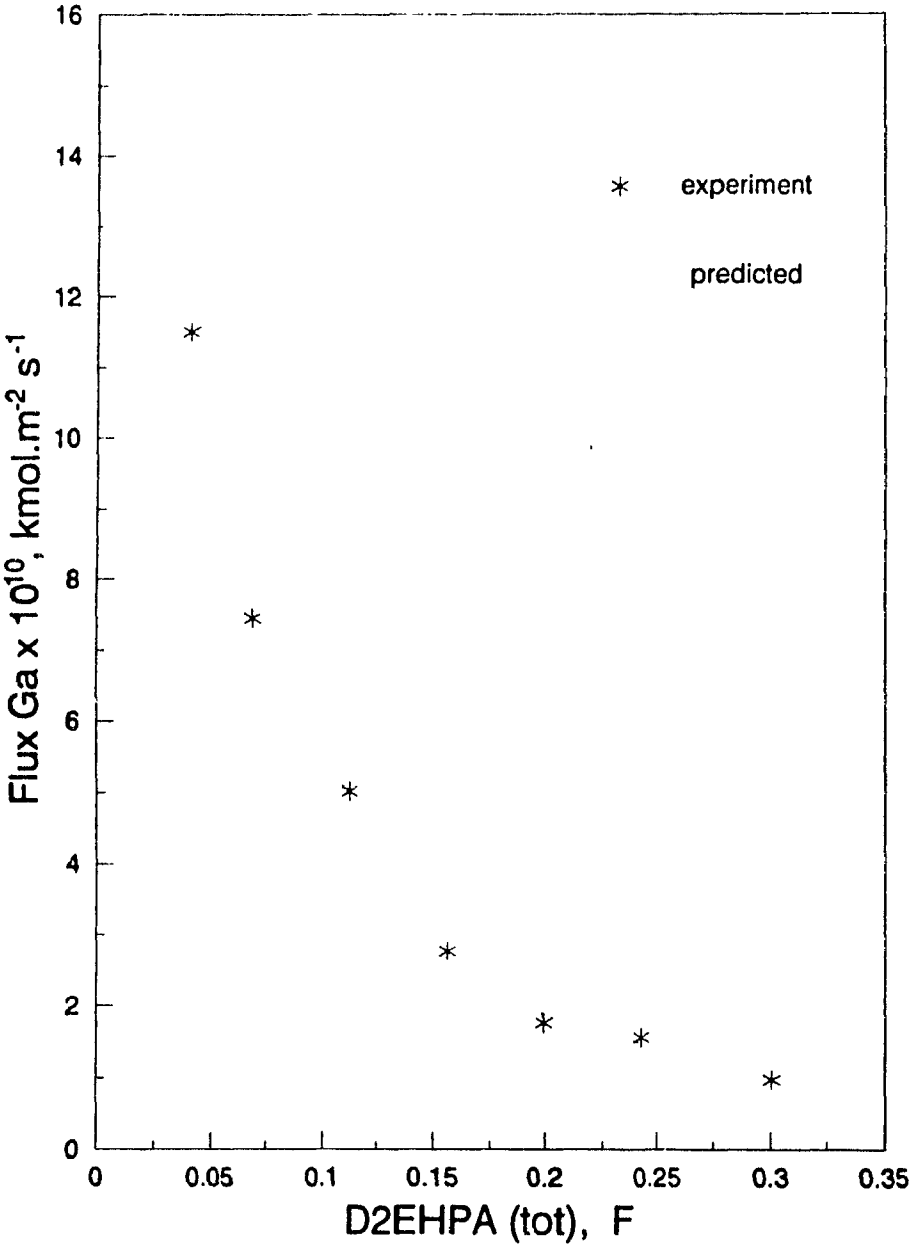

Figure 6.10: Effect of D2EHPA concentration. Comparison between model predictions (with the parameters from Table 6-3) and the experimental results. Data and conditions are those of fig. 4.32.

reasonably good description of the experimental results.

6.4.3 Model Verification: Near-Equilibrium Conditions

So far, the model has been found to closely describe the transfer kinetics of gallium under non-equilibrium conditions deliberately favouring either extraction (figs. 6.4 - 6.6) or stripping (figs 6.8–6 10). It is obvious that these two different conditions characterize the two end- (or start-) points, so to speak, of the reversible gallium extraction reaction.

Hence, a major consideration is the behaviour of the model for the intermediate conditions—between these two extreme points, which will obviously include those close to equilibrium. Therefore, going a step further, an important question is: can the model predict under what conditions equilibrium will be established in the system?

Needless to say, the ability of various models, proposed in the literature for describing solvent extraction systems, to predict with sufficient accuracy the behaviour of the system under near-equilibrium conditions is considered to be of crucial importance for a model's real usefulness and applicability.

According to Hughes and Rod, one significant advantage of their MTWCR model [158, 186, 197, 198], is that it is particularly useful in describing rates near equilibrium. Indeed, it has been shown [198] that the model predicts well the pace of copper loading with time into hydroxyoxime reagents during extraction kinetics experiments in a cell with vibrational mixing. It appears, however, that in the later kinetic studies on the various solvent extractant systems which had used the RDC technique and/or the MTWCR model for data interpretation, the rates under stripping as well as near-equilibrium conditions, and accordingly the model behaviour for such conditions, had not been considered The only exception, when the model has been applied to experimental data obtained for a system where metal is transferred from loaded organic to aqueous phase, seems to be the special case of exchange of

pre-loaded copper in D2EHPA with zinc from aqueous solution [203], the experiments being carried out in the same type of vibrational cell.

As mentioned in the previous section, the distinction between extraction and stripping rates is expressed mathematically with the different sign for $J_{i_{HR}}$ in the equations for concentrations of species, which follows the physical condition of reversed concentration profiles Hence, in case of stripping $C_{i_{HR}}$ will be lower than $C_{0_{HR}}$ and therefore the term

$$\left(\overline{C}^2_{i_{HR}} - P^2_{HR} C^2_{0_{HR}}\right)$$

in eqn (C.47) will be negative. Also, the other term in eqn (C.47):

$$\left(1 - \frac{1}{K'} \frac{\overline{C}_{i_{GaR_3}} C^3_{i_{H+}}}{C_{i_{Ga^{3+}}} \overline{C}^3_{i_{HR}}}\right)$$

which reflects the effect of the backward (stripping) reaction, will be negative too, provided that $C_{i_{Ga^{3+}}}$ is calculated correctly and therefore has a non-negative value. Obviously, in the case of extraction, both these terms are positive. This means that regardless of whether extraction or stripping is actually taking place, the calculated value for $J_{i_{HR}}$ from eqn (C.47) will always be positive, or zero—at equilibrium.

It is therefore clear, that judging only from the value of $J_{i_{HR}}$, calculated for certain conditions, is not sufficient to decide which way the reaction is going, especially when no other information is available *a priori*. Thus, the decision has to be based upon the signs of the two terms given above. In the present work, this has been the criterion used in the computing program.

Now it is possible to perform simulated runs and follow the values of $J_{i_{HR}}$ that the model will calculate under specified conditions Figure 6.11 shows the results from a series of such runs. The total extractant concentration is the same for all curves and each curve represents results for a certain constant acidity (or pH) of the aqueous phase. The total *amount* of metal in the system is also the same for all curves; what differs is the percentage $\mathcal{P}$ of this amount, assumed to have been gradually transferred to the organic phase The calculated flux values are plotted

as a function of this percentage. For any given curve, this is equivalent to having a series of experiments carried out at identical conditions, except that for every one of them the metal concentrations in the two phases are changed.[16]

In this way of presentation, each curve shows how the rate of transfer changes as the reaction progresses in the direction of achieving equilibrium. In other words, if the experiment is started at a given pH, which will be maintained constant, with all gallium being initially in the aqueous phase, i.e., at $\mathcal{P} = 0$ %, then from the corresponding curve on fig. 6.11 for that particular pH, it can be seen how the rate of extraction will gradually decrease as more and more metal is extracted. Obviously, at a certain point this rate will become equal to zero, and this is the point, predicted by the model, which will correspond to equilibrium being established in the system. Of course, the same point will be achieved if the experiment has been started under the same conditions but with all the metal being pre-loaded in the organic phase ($\mathcal{P} = 100$ %), or, more precisely, if the initial value of $\mathcal{P}$ has been higher than the particular one at equilibrium.

It is evident that the results on fig. 6.11 are consistent with the general experimental observations that the extraction rate increases with pH, while the rate of stripping decreases. Similar graphs may be generated for other values of total metal and extractant concentrations. Figure 6.12 illustrates one such example. The way it is constructed is the same as for fig. 6.11, except that here each curve refers to a particular value of total extractant concentration, while pH remains the same for all of them. Again, it is seen that the rates of extraction increase with extractant concentration, while the stripping rates decrease, as experimentally observed.

For each curve, the point of zero rate determines the equilibrium conditions of the system. The ratio of the total metal concentrations in the two phases under such conditions will represent, by definition, the distribution coefficient, D_{Ga}. Figures 6.11

[16] If T is the total amount of gallium in g-ions, V_{aq} and V_{org} -- the two volumes, C_{aq} and C_{org} - the total metal concentrations, resp., then $T = C_{aq}V_{aq} + C_{org}V_{org}$. When $\mathcal{P}$ percents of T are in the organic phase, this means $C_{org}V_{org} = (0.01\mathcal{P})T$ and $C_{aq}V_{aq} = (1 - 0.01\mathcal{P})T$

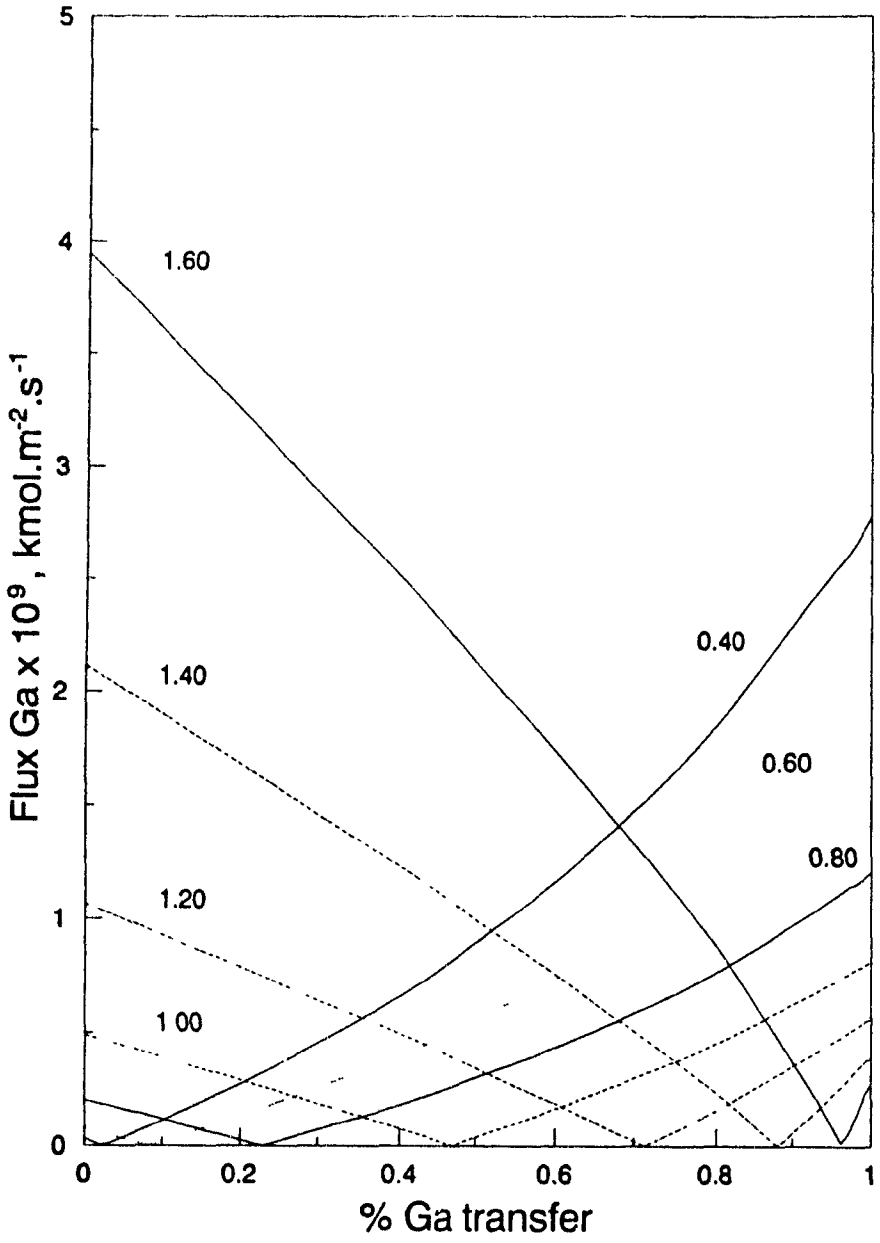

Figure 6.11: Model predictions: Changes in transfer rates of gallium as the reaction progresses. Conditions: 0.2 F D2EHPA, V_{aq} = 250 ml; V_{org} = 50 ml; total amount of gallium in the system: the equivalent of 250 ml 0.005 g-ion/l gallium solution. Numbers on lines represent the pH values.

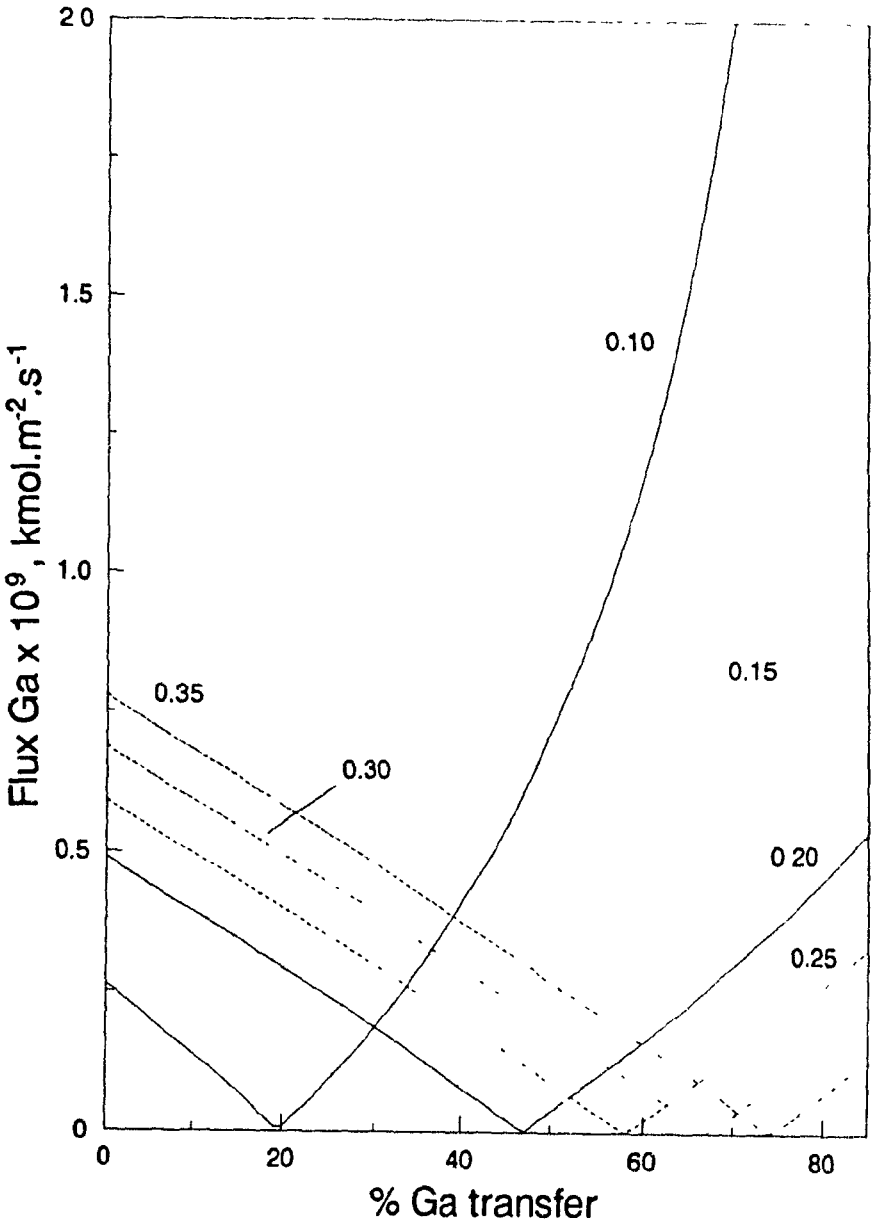

Figure 6.12: Model predictions: Changes in transfer rates of gallium as the reaction progresses. Conditions: pH=1.0; V_{aq} = 250 ml; V_{org} = 50 ml; total amount of gallium in the system: the equivalent of 250 ml 0.005 g-ion/l gallium solution. Numbers on lines represent concentrations of D2EHPA.

and 6.12 show that these points shift to higher values of $\mathcal{P}$ as pH and extractant concentration increase. At the same time it is obvious that higher values of $\mathcal{P}$ would also mean higher values of D_{Ga}. Thus, it is seen that the results on figs. 6.11 and 6.12 are also consistent with the observations that D_{Ga} increases with pH and extractant concentration. It becomes clear therefore that each figure represents and links together, in a comprehensive way, the kinetic and equilibrium properties of the extraction system.

Of course, it should be remembered that the results in figs. 6.11 and 6.12 are the model's predictions. They have been experimentally verified, as discussed in the previous sections, for the regions of initial extraction and initial stripping rates. In order to determine whether the predictions are correct for near-equilibrium conditions, what can be done is to run simulation tests, like those for figs 6.11 and 6.12, with the known parameters—initial total metal and extractant concentrations, and equilibrium pH—of the experiments on gallium extraction with D2EHPA (fig. 4.2). Once determined, the respective points of zero rate will yield the model's predictions for the equilibrium state, and therefore a value of D_{Ga} will be calculated. This value can then be readily compared with the experimental data from fig. 4.2

The results from these tests of the model are shown on fig. 6.13 along with the data reported on fig. 4.2. It appears that there is a satisfactory agreement between experimental and predicted values.

In principle, the important parameter with respect to near-equilibrium conditions in the main model equation (C.47) is K', as discussed earlier. There it replaces the equilibrium constant K_{eq}, which is totally unknown, from eqn (6.21). However, K'_{ex}, the experimentally determined equilibrium constant of the overall reaction 4.10, is not included in eqn (C.47); it is only used to find K_G from eqn (6.19) when K' is estimated. Therefore, it is only through K_G that experimentally obtained information, pertinent to the state of equilibrium, is included in the model (apart from reaction stoichiometry, of course). Hence, the value of K'_{ex} will have little effect on

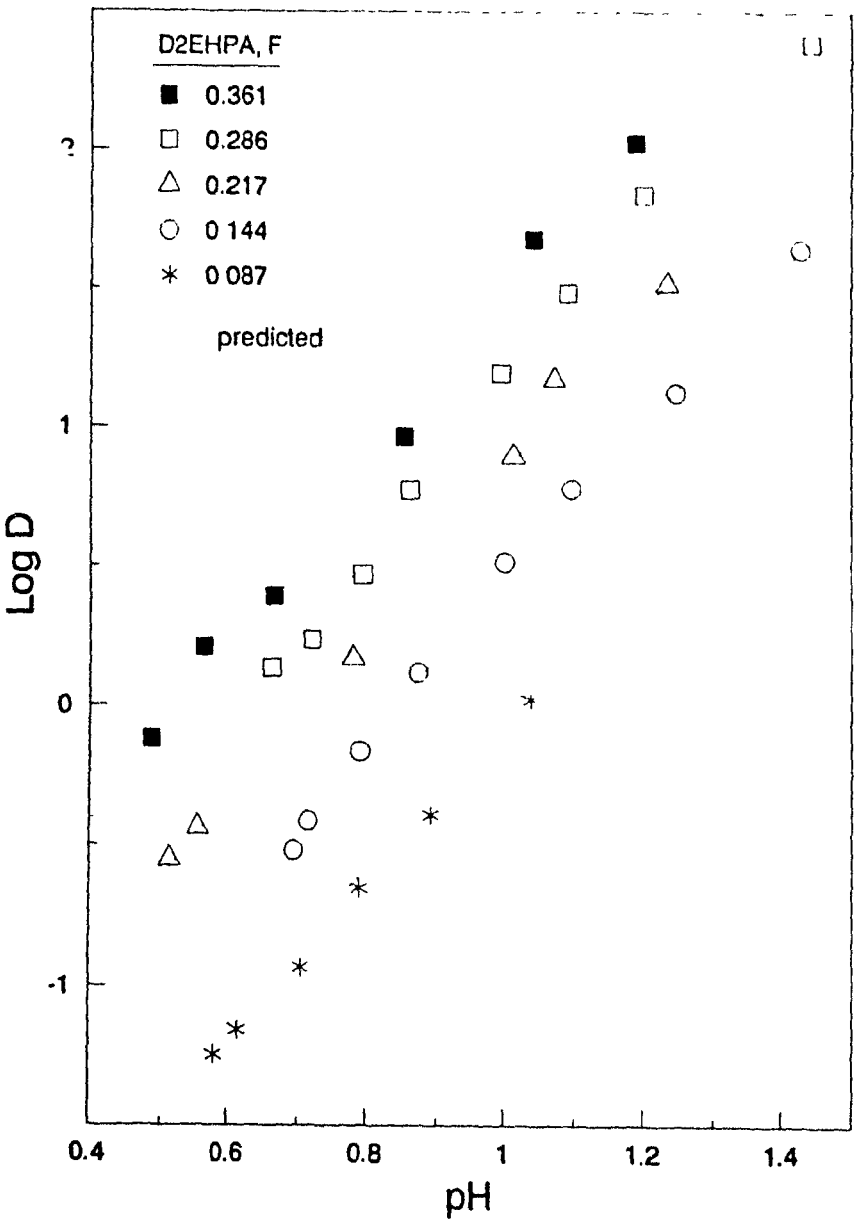

Figure 6.13: Model predictions of extraction equilibrium. Experimental data and conditions are those of fig. 4.2.

the estimated model parameters. On the other hand, although K' has a precise physical meaning, it mathematically is just a fitting parameter. While for the other fitting parameters in the model, certain conclusions about their values and whether they are reasonable can be made, following comparisons with relevant data obtained elsewhere, similar criteria with respect to K' are rather difficult to apply.

In this sense, the ability of the model to predict reasonably well the conditions for equilibrium in the system is considered as another good indication for its validity. Of course, viewed from another perspective, this also means that the experimental data—with respect to extraction equilibria and rates of extraction and stripping—obtained for the gallium-D2EHPA system for different conditions and with different techniques, are inherently self-consistent, as indeed they should be.

6.5 Reaction Model and Mechanism: Equilibrium and Kinetic Aspects of Metal Separation

6.5.1 Comparison between Gallium-D2EHPA and Gallium-OPAP Systems

Application of the model to the data from gallium extraction kinetics with the OPAP reagents has not been undertaken. The reason is that the system is much too complicated for the sparsely available information on physico-chemical parameters. According to the conclusions of the equilibrium analysis of the system (section 4.3), there are four simultaneously proceeding extraction reactions involving the two extractants—mono- and di-OPAP, which lead to the formation of four metal-extractant complexes. Hence, the model will inevitably be more complicated, although this is not expected to be a significant problem. The real difficulties are anticipated to come from the lack of available data, for example, on acid dissociation constants of the extractants, their partition coefficients as well as those of the complexes, and the diffusion coefficients of the numerous species involved which are also unknown. In any case, of course, some of these parameters would have to be approximately estimated, as was necessary for

the gallium-D2EHPA system. The difference is that when the OPAP reagents are involved, the number of these unavoidable approximations would be excessively large, and is therefore considered unacceptable

Although these problems make a precise description of the system difficult, it is in many ways similar to the gallium-D2EHPA system. For example, the same arguments about acidity of the extractants and the role of the dissociated organic anions will still be valid. Mono-OPAP is a stronger acid than di-OPAP, and both are considered to be stronger than D2EHPA This is reflected in the results from extraction kinetics with these reagents and can be seen by comparing them Figure 4.37 shows that the characteristic Flux *vs* pH curve shifts to lower pH and higher flux values as the mole fraction of mono-OPAP in the extractant increases This also means that the hypothetical 'resultant' pK_a value for the mixed system also changes to lower values.

The comparisons between the kinetic results obtained for gallium extraction with D2EHPA and with the OPAP reagents suggest that the extraction mechanism remains probably the same, with the addition of the first organic ligand to the metal cation being the rate-limiting step in the reaction scheme

When compared with gallium-D2EHPA extraction kinetics results for the same conditions, it is clear that the rates obtained with the OPAP reagents are higher. This can be seen from fig. 6.14 where the respective experimental data from extraction with OPAP reagents, taken from fig. 4.37, are given together with the model's predicted flux values for gallium-D2EHPA, calculated for the same conditions and 0.11 F D2EHPA.

At the same time, however, fig 6.14 shows that the differences between flux values for D2EHPA and extractant T (see Table 4-8, page 100, for compositions and notation) are slightly less than those between extractants T and M Furthermore, it can be expected, based on the results for extractants M, O, and T, that the corresponding curve for di-OPAP extractant alone would be very close to the one for

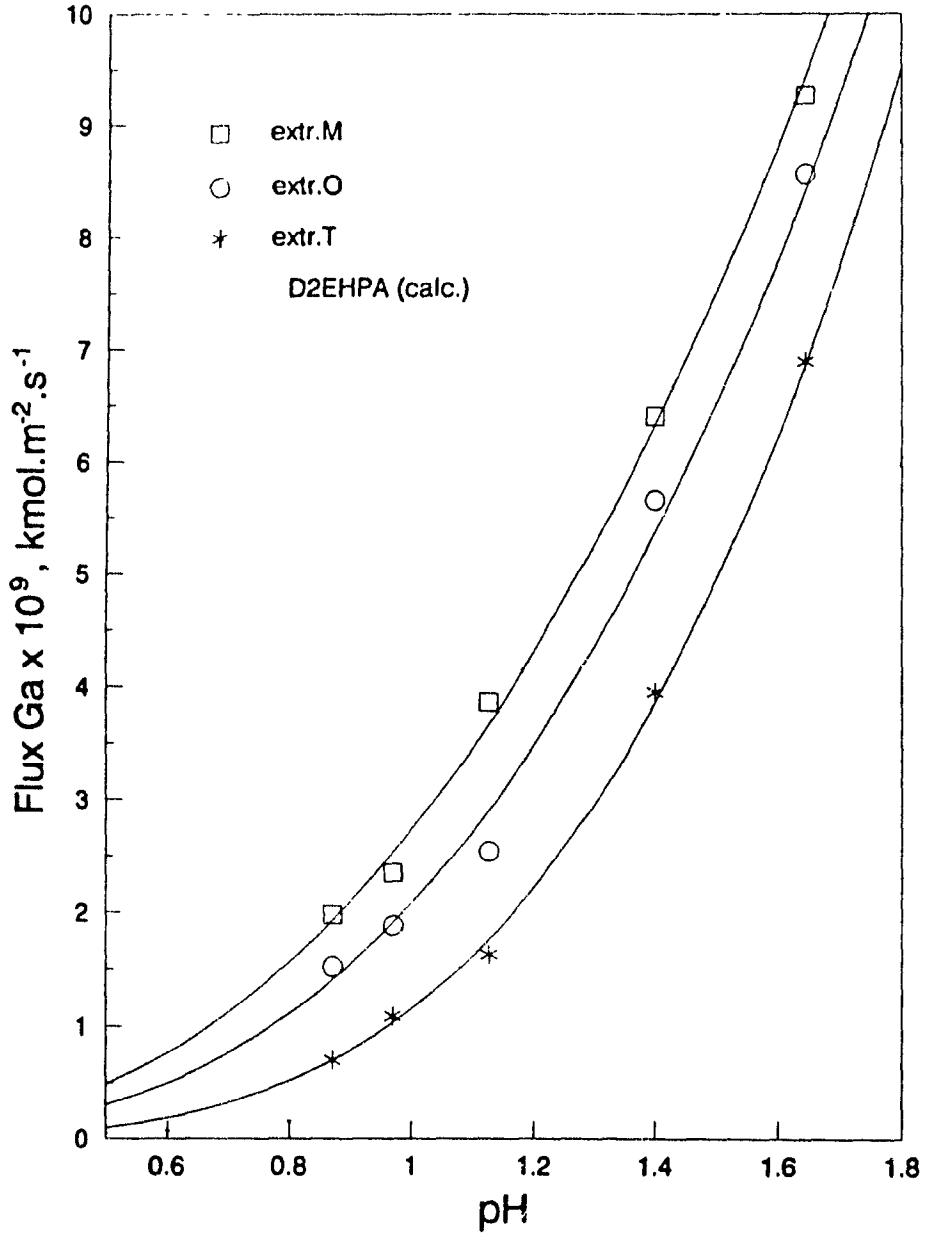

Figure 6.14: Comparison between extraction rates of gallium with D2EHPA and OPAP reagents. Values for D2EHPA are calculated for the same conditions of fig. 4.37 and 0.11 F D2EHPA. Values and conditions for OPAP are those of fig. 4.37.

D2EHPA. In other words, the extraction rates of gallium with D2EHPA and di-OPAP will be similar. Although the comparative example is given for Flux *vs* pH curves (fig. 6.14), the same also applies to the other experimental results.

This conclusion is in contrast to those with respect to gallium extraction equilibria. There, significant differences are found between the corresponding $\log D_{Ga}$ values. The same applies not only for D2EHPA *vs* di-OPAP comparisons, but also between OPAP extractants with varying compositions.

Based on the developed model, the observed differences between the extraction rates with D2EHPA and the OPAP reagents may be explained, in principle, mostly with the expected higher values of K_a for mono- and di OPAP than for D2EHPA. The lack of reliable data makes it impossible to analyze this aspect more precisely. Nevertheless, it is highly probable that these differences in extractant's acidity, possibly in combination with other factors, such as different partition coefficients, presence of alcohol causing monomerization, etc , are solely responsible for the observed different extraction rates.

The implication of this conclusion is that the chemical reaction rate constant, k_f, is probably the same, or almost the same, for gallium-D2EHPA and gallium-OPAP systems, despite the fact that the extractants are different. Given the generally predictable effects of extractant's acidity and partition coefficient on the rate, following the formulated model equations, together with the values for OPAP reagents, relative to those for D2EHPA, it is highly unlikely that the different rates can be due, in addition, to significantly different rate constants.

In principle, this should be anticipated from the well known arguments about the rate constants of ligand exchange and their dependence primarily (in homogeneous kinetics) on the nature of the cation, and to a much lesser extent on the nature of the ligand. What is significant, though, is that the conclusion here is based on specific experimental evidence regarding D2EHPA and OPAP reagents, which are important extractants for gallium.

The conclusion about the almost equal rate constants also implies that in extractions with the mixed OPAP reagents, the respective dissociated organic anions, from mono- and di-OPAP, are kinetically the same. This means that from the viewpoint of the metal cation species there will not be a particular *kinetic* preference for either mono- or di-OPAP anions In that sense, when suggesting that in the mechanism of gallium extraction with OPAP reagents, the rate-limiting step is probably the first organic ligand addition, it does not really matter whether this is the ligand from mono- or di-OPAP.

What matters, of course, is how stable the finally formed metal-extractant complex is. This, however, is a thermodynamic property and is therefore related to the equilibrium state of the system, described here by the respective extraction equilibrium constants. It is there that the differences between mono- and di-OPAP, and also D2EHPA, will be mostly manifested, following not only different acidities, but also different spacial intra-molecular environment leading to effects of certain steric hindrance, or preference for the metal.

Following this discussion it becomes evident that while the observed distribution coefficients for gallium are considerably different depending on whether D2EHPA or OPAP is the extractant, and within the OPAP reagents—on what is the mole fraction of mono-OPAP, the respective rates of extraction are similar, although the order of precedence remains the same. In other words, while the equilibrium amount of metal that can be loaded depends significantly on the particular extractant, the *rate* at which this happens is much less dependent.

This has been attributed to nearly the same extraction rate constants, which in turn is explained with the rates of ligand exchange being almost independent of the nature of the particular ligand. The reasons for this are found in the mechanism of ligand substitution reactions.

The two extreme mechanisms in which the ligand X, present in metal's coordination sphere, can be exchanged with the incoming ligand Y, represented by the

following schematic reaction

$$[MeXA_5] + Y \rightleftharpoons [MeYA_5] + X \tag{6.48}$$

are the S_N1 dissociative mechanism:

$$[MeXA_5] \xrightarrow{-X} [MeA_5]^* \xrightarrow{+Y} [MeYA_5] \tag{6.49}$$

where the slow step is the removal of ligand X from the coordination sphere thus forming the intermediate activated complex $[MeA_5]^*$, and the S_N2 associative mechanism:

$$[MeXA_5] \xrightarrow{+Y} [MeXYA_5]^* \xrightarrow{-X} [MeYA_5] \tag{6.50}$$

where the attachment of the new ligand Y to $[MeXA_5]$ is the slow step [204]. Both mechanisms include one bond making and one bond breaking step; bond making is rate-limiting for S_N2 and bond-breaking—for S_N1 mechanism.

One criterion to distinguish between the two mechanisms is from the experimentally determined entropy of activation, $\Delta S^{\ddagger}$. For the S_N1 mechanism $\Delta S^{\ddagger}$ is positive (the expulsion of X leads to increased disorder in the system), and $\Delta S^{\ddagger}$ is negative for S_N2 mechanism (increasing order). Another criterion, which has later been made available by introduction of high-pressure NMR, is the change in activation volume $\Delta V^{\ddagger}$. Clearly, $\Delta V^{\ddagger}$ will be positive for a dissociative mechanism, and will have a negative value for an associative mechanism [205].

Most ligand exchange reactions, however, are intermediate in character—because bond making and bond breaking occur simultaneously. Those reactions where bond breaking is predominantly rate-determining are described as proceeding by an interchange dissociative mechanism (I_d), which is therefore close to the S_N1 mechanism. Accordingly, when bond making is predominantly rate-determining, the mechanism is described as interchange associative mechanism (I_a), close to the S_N2 mechanism. The same arguments about $\Delta S^{\ddagger}$ and $\Delta V^{\ddagger}$ will also be valid for I_d and I_a mechanisms.

It is clear that if a reaction proceeds through a dissociative mechanism, then its rate (and the rate constant) will be independent of the nature of the incoming ligand—because it is in no way related to the rate-limiting step, as reaction scheme 6.49 illustrates. However, it will be just the opposite if an associative mechanism is predominant.

A large number of water exchange (reaction 6.7) or water substitution by an incoming ligand reactions have been found to occur by an I_d mechanism [204]. This explains why the rates of these reactions are almost ligand-independent, as discussed earlier.

There is some controversy about the exchange mechanism for gallium. Fiat and Connick [137] have studied the water exchange reaction for gallium (and also aluminum) by Oxygen-17 NMR and have determined a negative entropy change value:[17] $\Delta S^{\ddagger} = -92$ J.mol^{-1}.K^{-1}, as well as the value of k_w: 1.82×10^3 s^{-1}. Thus, they have concluded that the ligand exchange reactions for gallium follow the associative S_N2 mechanism. Similar conclusions have been later reached [206], based on proton NMR studies of ligand exchange reactions in methanol and ethanol solutions, because negative $\Delta S^{\ddagger}$ values have been determined again. These findings would imply ligand-dependent exchange rates.

However, a more recent study by Hugi-Cleary *et al.* [205] which has also included pressure-jump experiments using Oxygen-17 NMR to determine $\Delta V^{\ddagger}$, has found that $\Delta S^{\ddagger}$ and $\Delta V^{\ddagger}$ are both positive: $\Delta S^{\ddagger} = +30$ J.mol^{-1}.K^{-1}, $\Delta V^{\ddagger} = +5$ cm^3.mol^{-1}. For the rate constant of water ligand exchange, k_w, the value found is 4.03×10^2 s^{-1}. If correct, these results would mean a dissociative, and therefore ligand-independent, exchange mechanism.

It is possible that these latest findings are closer to the real mechanism, not only because their conclusions are based on additionally determined experimental parameters, but also due to the fact that the authors have taken into account effects of

[17] All values refer to 25 °C

side reactions (contributions from hydrolysed species [205]) that have been apparently neglected before.

These studies [137, 205, 206] have also dealt with the ligand exchange reaction for aluminum. In the case of aluminum, they all agree about a predominantly dissociative mechanism of ligand exchange. The value of k_w for Al^{3+} has been determined to be 0.17 s^{-1} by Fiat and Connick [137] and 1.29 s^{-1} by Hugi-Cleary *et al* [205]

This difference of 2-3 orders of magnitude between the values of k_w for Ga^{3+} and Al^{3+} can be explained with their different ionic radii:[18] 0.62 Å for Ga^{3+} and 0.51 Å for Al^{3+} [9]. Nevertheless, the two metals are chemically very similar, which makes their separation difficult. It is obvious, therefore, that the difference in their ligand exchange rate constants may provide basis for separation

6.5.2 Separation Based on Different Exchange Rates: Case of Gallium and Aluminum

In order to illustrate such a possibility, several series of experiments have been carried out to determine the pace of simultaneous gallium and aluminum loading and stripping in and from kerosene solutions of D2EHPA under different conditions as well as tests for aluminum and gallium equilibrium distribution [19]

From the comparison between the distribution coefficients for gallium and aluminum, obtained under the same conditions (fig 6.15), it is clear that their values are close—approximately 0.3 log D units difference—and therefore no significant separation can be achieved if extraction is carried out to equilibrium. Such a difference between D_{Ga} and D_{Al} means that a separation factor, $S_F = (D_{Ga}/D_{Al})$, of approximately 2 will be obtained. It also means that the respective equilibrium constants will have close values too.

[18]The rate constant k_w decreases as the charge of the central metal cation increases and its size decreases [204].

[19]Complete results, under the title 'Gallium/Aluminum Separation from Sulfate Solutions by Solvent Extraction Using D2EHPA', were presented at ISEC'90, July 16-21, 1990, Kyoto The proceedings are presently still in press

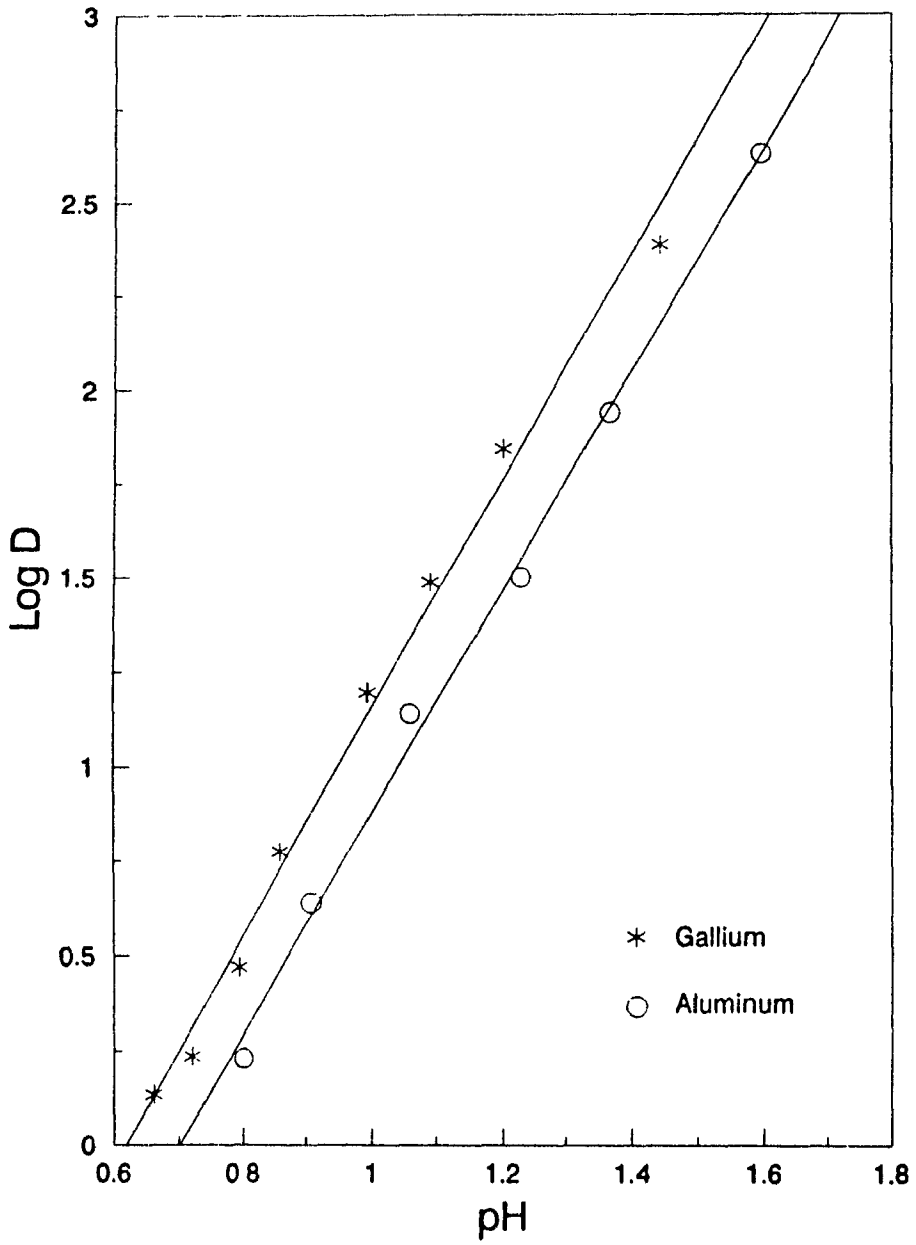

Figure 6.15: Gallium and aluminum extraction equilibrium with 10 vol% D2EHPA in kerosene. Ga_{init} = 0.006 g-ion/l, Al_{init} = 0.006 g-ion/l.

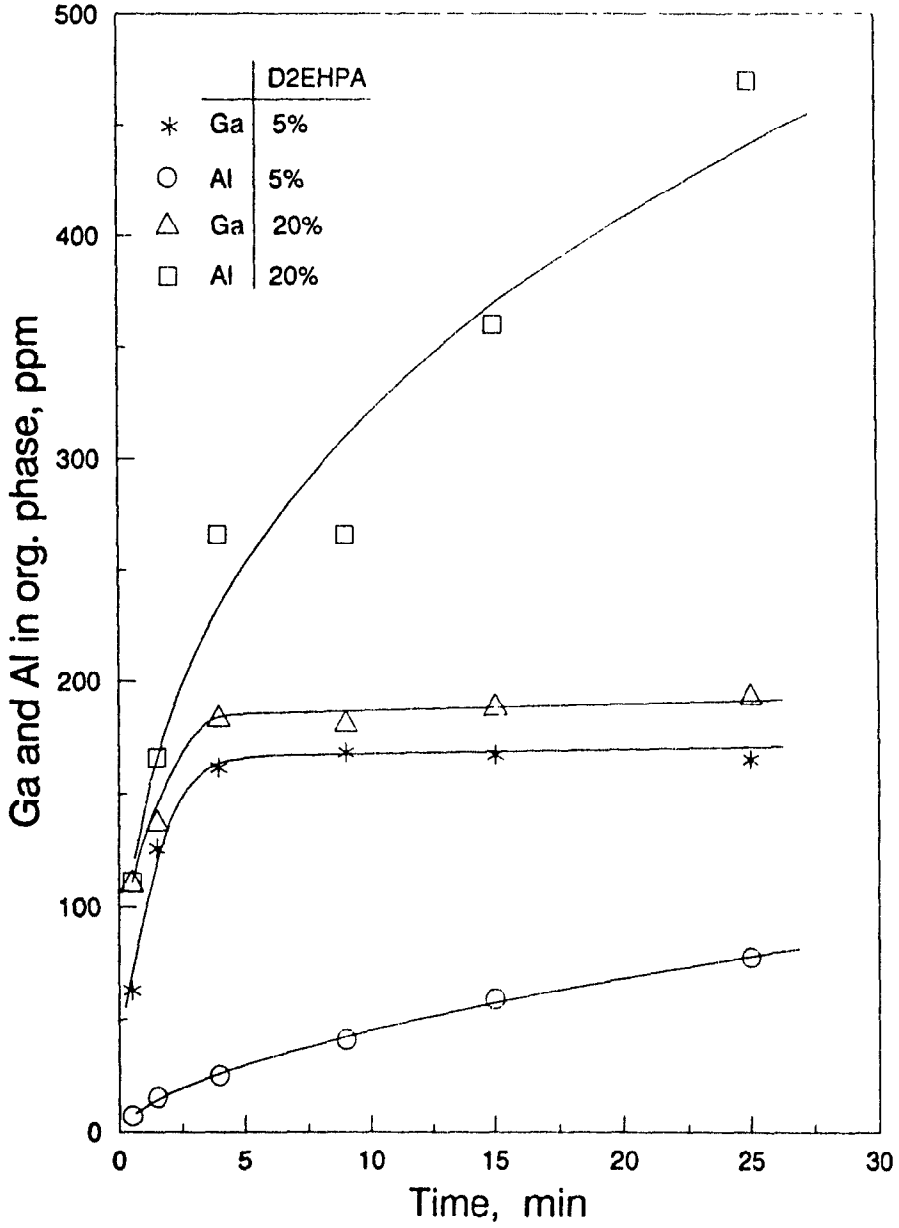

Figure 6.16: Extraction rates of gallium and aluminum. $Ga_{init} = 3.01 \times 10^{-3}$ g-ion/l, $Al_{init} = 6.86 \times 10^{-2}$ g-ion/l, pH=1.50, $[SO_4]^T = 0.1$ g-ion/l.

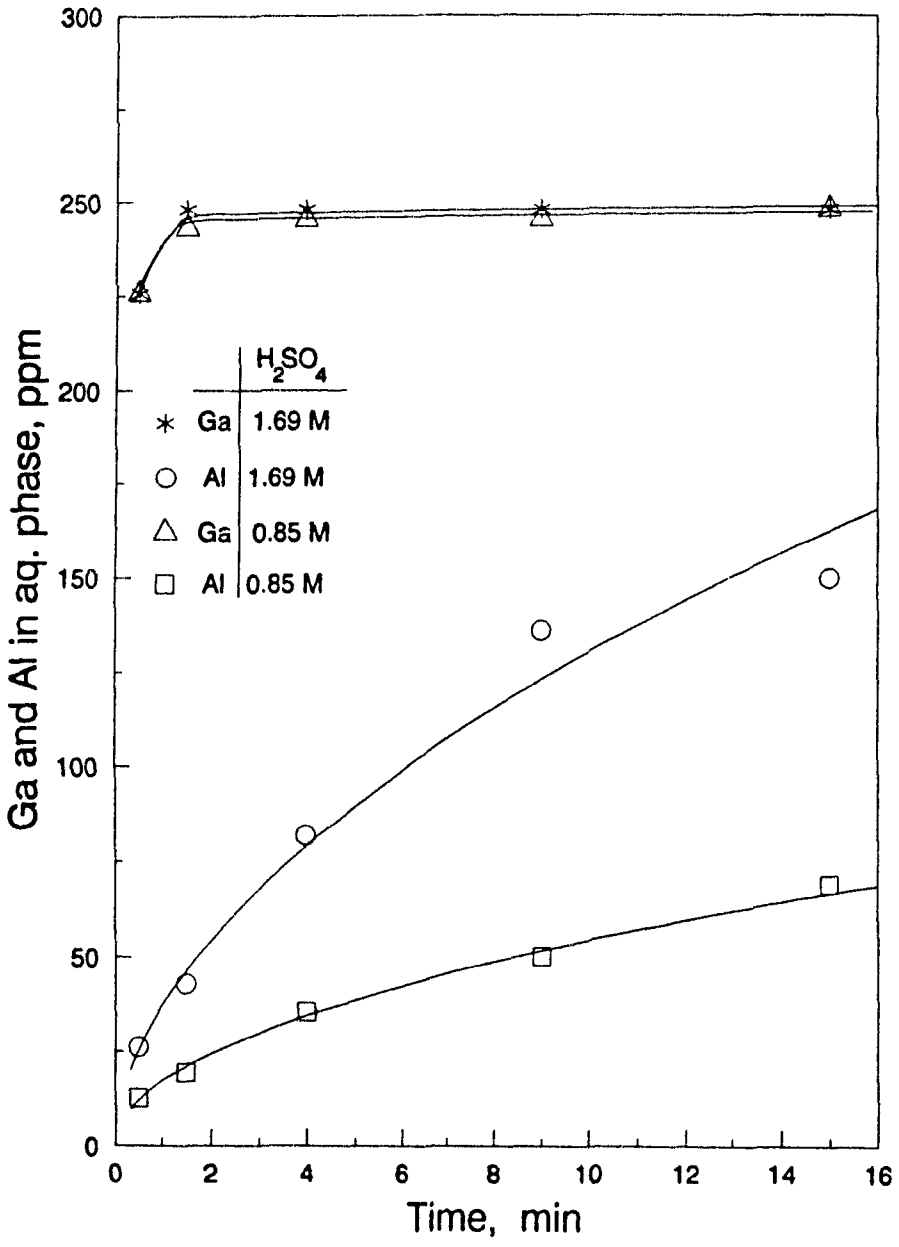

Figure 6.17: Stripping rates of gallium and aluminum. $Ga_{init\ (org)} = 3.56 \times 10^{-3}$ g-ion/l, $Al_{init\ (org)} = 1.48 \times 10^{-2}$ g-ion/l, 5 vol% D2EHPA.

These similarities between the extraction equilibrium parameters for two metals are considered to result from their similar chemical behaviour in general. Hence, it is reasonable to expect that they will also follow the same extraction mechanism.

Results for the rate of extraction (fig. 6.16) display, however, quite a different picture—despite the similar gallium and aluminum loadings at equilibrium, it is reached at much different rates for the two metals The same is similarly valid if the process is to start from organic phase pre loaded with the metals (fig 6.17).

The rates of gallium extraction and stripping appear to be much higher than those for aluminum, even though for the results on fig. 6.16 the initial gallium concentration in the aqueous phase is 22-23 times less than the one for aluminum. In fact, fig. 6.16 also shows that the equilibrium for gallium is established approximately in the first 5 minutes of phase contact, for the particular conditions. Similar conclusions can also be made for the rates of stripping.

The results from figs. 6.16 and 6 17 clearly demonstrate that the extraction and stripping rate constants for the two metals are considerably different. It is highly probable that this is due to their different rate constants of ligand exchange.

Furthermore, these observations—higher rate constants for the gallium extraction and stripping reactions (i.e., forward and backward reactions, resp.) together with the similar extraction equilibrium constants--are all inter-related and self-consistent: from the definition of an equilibrium constant as the ratio of the two rate constants (cf eqn 6.23) it follows that as long as the equilibrium constants for two metals are equal, or similar, the ratio of their forward reaction constants will be equal, or similar, to the ratio of their backward reaction rate constants This is what is indeed observed.

If now the conclusions and comparisons made with respect to gallium extraction equilibrium and kinetics with D2EHPA and OPAP reagents are brought together in the same perspective as those for gallium and aluminum extraction with D2EHPA, it can be seen that the resulting phenomena pertinent to the latter system are, in

a sense, reciprocal to those in the former In gallium extractions with D2EHPA and OPAP, considerably different equilibrium states, depending on the extractant, are achieved—but at similar rates. On the other hand, for the two chemically similar metals, gallium and aluminum, the equilibrium states established for the same extractant (D2EHPA) are close, but they are achieved at significantly different rates.

These remarks serve to emphasize the point that while the kinetics of the process is especially dependent on the metal itself, the established equilibrium state depends much on the extractant. The stability of the metal-extractant complex will depend on the strength of electrostatic interactions [50] between extractant and metal species as well as their suitability to fit into a close 'host'-'guest' [207] match, the uniqueness of which will be directly related to extractant's selectivity.

Since their extractive abilities are mostly based on electrostatic interactions, the organophosphorus acid extractants are not particularly selective, as compared with the class of chelating reagents. Thus, the above observations and conclusions are viewed as important for metal separation in the context of the type of extractants employed in this work. It is seen how existing difference in rate constants of ligand exchange can be used to facilitate separation— not only during extraction, but also during stripping, which is especially valuable if the two metals in question happen to be of similar nature, like gallium and aluminum.

It may well be expected that similar difference in rates will be observed if another alkylphosphoric acid extractant is used instead of D2EHPA, as long as the extraction mechanism remains the same. This will be especially the case if the two extractants have similar acidity. Therefore, in doing so, not much improvement in rates for a particular metal can be gained, if desired. Such results follow from the role of the rate constant of ligand exchange and its minor dependence on the nature of the extractant.

Furthermore, if equilibrium is to be established, the small differences existing between gallium and aluminum loadings in such conditions are likely to remain simi-

lar, if OPAP reagents, for example, are used instead of D2EHPA. Therefore, in order to achieve separation in the difficult cases of chemically similar metals, taking full advantage of their possibly different rates should be considered, especially when this type of extractants is to be employed.

6.6 Summary

The subject of this Chapter was the quantitative description of the reactions involved in gallium solvent extraction with organophosphorus acid reagents, and in particular D2EHPA, which would lead to better understanding of this type of systems, hence prediction of their behaviour.

Existing models, and particularly their reasoning when assuming an interfacial or aqueous phase chemical reaction, for solvent extraction systems, were reviewed with an emphasis given to the available criteria and arguments for determination of reaction site from experimental data. This was necessary in order to select as accurately as possible the model which would presumably most closely approach the real physico-chemical processes in the system.

Based on the experimental results on gallium extraction kinetics with D2EHPA, the above-mentioned criteria, and the considerations about the metal and extractant's solution chemistry, the model of mass-transfer with chemical reaction (MTWCR), developed originally by Hughes and Rod for the case of copper extraction with chelating reagents, and based on the two-film theory, was selected as the most appropriate.

The model was further developed to account for the much stronger acidic nature of the organophosphorus extractants, in comparison with the chelating reagents, as well as the extractant's existence predominantly as dimer in the bulk organic phase, but as monomer—at the interface.

The model's parameters were estimated, based on the extraction kinetics results for gallium-D2EHPA system. Hence, the model was able to describe these

results well. More importantly, when the estimated model parameters were compared with those obtained in similar studies elsewhere in literature, they appeared to have reasonable values.

The estimation of model's parameters, based on extraction kinetics data, also resulted in the conclusion that the first organic ligand addition is the rate-limiting step in the reaction scheme.

A number of assumptions and approximations were by necessity incorporated in the model. However, the most significant phenomenon that had *not* been quantitatively incorporated in the model, is the extent of extractant's de-dimerization in the interfacial region under the influence of polar water molecules there, which is expected to be different from the known dimer/monomer equilibrium in the bulk organic solution. At present, the model assumes equal extents.

Model's predictions were tested for considerably different conditions—with the experimental data from gallium stripping kinetics, and a reasonably good agreement was found. Next, based on model's predictions, diagrams were constructed depicting the gradual change in reaction rate as equilibrium is approached—by extraction or stripping of metal. Thus, the model-predicted state of equilibrium could readily be identified. When these model's predictions were compared with earlier experimental results from gallium extraction equilibria with D2EHPA, the agreement found was satisfactory—and to some extent surprising. This was considered as another indication for validity of the model. Alternatively, the agreement was regarded as a display of consistency of the experimental data—since they reflect different aspects, and yet of the same system.

The equilibrium and kinetic aspects of gallium extraction with D2EHPA and OPAP reagents were then discussed in terms of the model's implications for separation of metals. These were further linked with the importance of the rate constant of ligand exchange for kinetics-based separation, particularly for chemically similar metals, illustrated with the example of gallium and aluminum and D2EHPA as an

organophosphorus acid extractant.

In the next final Chapter, the overall conclusions from this work will be presented, along with some of its contributions considered to be original. Suggestions for further developments will also be offered.

Chapter 7

Epilogue

The purpose of this work was to study the extraction of gallium from acidic sulphate solutions, which are an important additional source of this metal, resulting from hydrometallurgical zinc production. The organophosphorus acid extractants have long been known as generally suitable, while D2EHPA is used in most of the existing technological schemes involving gallium. Its main disadvantage is the relatively low metal loadings at the acid levels of these solutions. In addition, the selectivity of this class of reagents is not very good in comparison, for example, with most chelating reagents. Many of the commercially available chelating extractants, however, have been specifically designed for copper, and thus they are mostly unsuitable in solving the above particular problems.

Hence, the present work emphasized on the equilibrium and kinetic aspects of gallium extraction together with the sulphate complexation phenomena in the aqueous phase, so aiming at their better understanding in order to allow prediction of behaviour and suggestions for improved extraction and metal separation. D2EHPA and OPAP were selected as extractants for this work.

In this concluding Chapter, the important results from the present work will be summarized along with the relevant conclusions. While some are specific to gallium extraction and solution chemistry, others are regarded as significant for extraction of metals with this type of reagents, in general. The developments and contributions

of this study, that are considered new and original, will then be presented. Finally, suggestions for further investigations will be outlined.

7.1 Conclusions

Gallium is extracted from acidic solutions by D2EHPA and OPAP extractants *via* cation-exchange mechanism and the chemical reaction rate-limiting step is the first organic ligand addition (step 4).

Sulphates from the aqueous solution are not coextracted. This means that extraction by solvation does not take place for the acidity range (pH > 0.4) of experimental conditions.

The reacting species is the metal cation. The analysis based on distribution of gallium species in the aqueous solution has shown that the rate of extraction is directly dependent on the concentration of Ga^{3+}, and not on any other gallium containing species.

Reaction 4.10 represents the overall stoichiometry that has been determined for gallium extraction reaction with D2EHPA, dissolved in kerosene. From the equilibrium data K'_{ex} was found to be equal to 0.757 mol/l (for $I = 0.5$).

In accordance with reaction 4.10, $GaR_3 \cdot HR$ has been determined as the predominant gallium-D2EHPA complex. However, experimental evidence also suggests that at high loading levels gallium exist as complexes with monomeric formula GaR_3, while at low loadings—as solvated species of the type $GaR_3 \cdot 3HR$.

Since OPAP is a mixture of two extractants—mono- and di-OPAP, a method was required and thus developed for separation of the two components. This led to OPAP reagents with varying compositions, thence a study of their effects on extractive properties. Furthermore, this makes it possible to prepare a mixed extractant to achieve desired distribution coefficients for a given metal.

Addition of an alcohol modifier (here, *n*-decanol) was required for the OPAP

systems in order to improve extractant's solubility in the organic solution as well as phase separation. At the same time, however, the alcohol causes monomerization of otherwise dimeric molecules of the extractant.

The analysis of the results from gallium extraction equilibria with OPAP reagents having different compositions lead to the conclusion that there are four simultaneously proceeding extraction reactions involving mono- and di-OPAP which result in the formation of four complexes: GaM_3, GaM_2D, $GaMD_2$, and GaD_3; with the respective reactions and equilibrium constants being defined by eqns (4.37)-(4.44) and the values given in Table 4-5. The obtained values for the constants appear to be reasonable and are in a good agreement with the predictions of the probability theory for ligand occupancy of a given site. Similar reactions are expected for other metals in the same system.

Based on the four extraction reactions, it is possible to describe well and predict the resulting values for D_{Ga} for variable extractant compositions, as well as their concentrations and pH of solution. Small changes in composition do not affect significantly the extraction performance Because of different aqueous solubilities of its components, this is especially important in the case when OPAP is to be used in continuous operation. Due to higher formula weight, it is not expected that OPAP reagents have much higher solubility than D2EHPA in water, even though they are more acidic.

The D_{Ga} values increase with increasing mole fraction of mono-OPAP in extractant's composition. Comparisons between D2EHPA and di-OPAP show that significantly higher values for D_{Ga} are obtained for di-OPAP under otherwise the same conditions.

Gallium complexation in aqueous solutions, when sulphates are present, has a significant effect on the equilibrium and kinetics of gallium extraction. The values of D_{Ga} as well as the extraction rate decrease considerably as the sulphate concentration is increased because it leads to decrease in concentration of the reacting species.

The effect of complexation on extraction remains the same regardless of the extractant as long as the mechanism and the reacting species are the same. In order to be taken into account quantitatively, the concentration of the reacting species has to be known.

Based on available literature data on gallium complexes in aqueous sulphate solution, an algorithm was developed for determination of complexes distribution under conditions and solution parameters that can be readily found. The principles remain the same whether one or more metals are present in the solution. The algorithm takes into account two gallium sulphate and four hydroxy complexes as well as the second dissociation reaction of H_2SO_4. The calculated distributions allow for changing ionic strengths of the solution which is crucially important for solutions in practice. The calculated distributions always refer to a constant temperature of 25 °C; if necessary, the algorithm can be further developed to cover the range of higher temperatures.

The results from species distribution were checked with available experimental data for the effect of sulphates on gallium extraction equilibria and extraction rates with D2EHPA. Reasonably good agreement was obtained. The crucial point in any such problem is the reliability of available data for the complexes; critical evaluation and caution is required. When reliable, the results may be used as an additional tool for identification of the reacting species.

The model of simultaneous mass-transfer with chemical reaction (MTWCR) was found to describe well the kinetic results in the gallium-D2EHPA system. The model was further developed to account for the strongly acidic nature, in comparison to most chelating reagents, of the organophosphorus acid extractants like those used in this work, as well as their existence in non-polar solvents predominantly as dimers but distributing to the aqueous phase as monomers.

Among the estimated model parameters is the chemical reaction rate constant. Its value ($k_f = 5.5 \times 10^6$ $m^3.kmol^{-1}.s^{-1}$) compares well with those obtained in similar

studies for other metals, available in literature, taking into account the data for the respective rate constants of water ligand exchange. These data are also consistent with the other results pointing towards a predominant chemical reaction controlling regime—independence of the rate on stirring, high values of E_a.

The model's predictions were verified with the experimental data from gallium stripping kinetics with D2EHPA. The obtained values were in a reasonably good agreement with those predicted by the model.

Simulation diagrams, depicting the pace of the reaction and based on model's predictions, were constructed thus allowing for precise determination of equilibrium conditions. Such diagrams made it possible to compare the model's predictions of the equilibrium state (defined as a condition of zero rate) with the results on gallium extraction equilibria with D2EHPA. The comparisons showed a satisfactory close agreement, and were regarded as another indication for the model's predicting ability.

Although the model was not applied to gallium-OPAP kinetic results, the apparent similarities with the data for D2EHPA suggest the reaction mechanism remains the same.

The differences in extraction rates between OPAP with varying compositions as well as between D2EHPA and OPAP reagents are due to, and can be explained mostly with their different acidity.

These differences in rates are relatively smaller in comparison to those found between the respective values of D_{Ga}. The reason is in the same, or almost the same, value of the chemical reaction rate constant k_f. This, in turn, is considered to result from the ligand independent rate constant of exchange.

While the established state of equilibrium differs significantly as the extractant is changed from D2EHPA to mono-OPAP, the rate at which it is achieved does not, although the order of increase remains the same for both D_{Ga} and extraction rates.

The possibility for separation of metals based on their different extraction rates, following different water ligand exchange rate constants, was demonstrated

with the example of gallium and aluminum.

The distribution coefficients for gallium and aluminum with D2EHPA are very close, which is explained with their generally similar chemical, and in particular acid-base properties, which are of primary importance in complex formation with organophosphorus acid extractants.

Thus, using different extraction rates, whenever possible, as a basis for metal separation with this type of extractants becomes a valuable option, especially when the metals in question have close chemical properties. A similarity in extraction equilibrium constants will then result in having almost equally different stripping rates too, provided that the extraction mechanism remains the same, and this is an additional option for separation of metals.

7.2 Claims to Originality

In the author's opinion, this is the first work to investigate and link together the equilibrium and kinetic aspects and the associated complexation phenomena of gallium solvent extraction with organophosphorus acid reagents from acidic sulphate and nitrate solutions.

Among the novel developments in this work, those considered to be distinct contributions to knowledge are the following.

- The analysis and interpretation of extraction equilibria of gallium with the OPAP reagents with varying composition; they should be similarly applicable for other metals too
- The account of gallium complexation in aqueous sulphate solutions, which allows its effects on extraction equilibrium and kinetics to be satisfactorily predicted quantitatively.
- The developments of the MTWCR model to account for the strongly acidic nature of most organophosphorus acid extractants, and in particular D2EHPA,

as well as the dimerization of the extractant in non-polar organic solvents, but distribution to the aqueous phase as monomer.

- The analysis, based on the developed model, which allows linkage of the results referring to extraction and stripping rates with the equilibrium state of the system.
- The use of different extraction/stripping rates to separate chemically similar metals with comparable distribution coefficients.
- The application of the RDC technique for studies of extraction kinetics at very low pH as well as for studies of stripping kinetics.
- The development of the method for separation of mono-OPAP from di-OPAP, based in part on a previously known method for purification of D2EHPA from M2EHPA.

7.3 Suggestions for Further Investigations

Following the developments on gallium extraction in this work, the appropriate next step is to apply the results in further studies on extraction from acidic sulphate solutions, but in presence of the metals found in the zinc production solutions—iron, zinc, germanium, indium, etc.

The presence of iron is one of the main problems in treating these solutions. While most of it is separated by precipitation (e.g., in the jarosite method), its concentration is still significant in the solution for solvent extraction. The standard approach is to reduce the ferric iron to ferrous and in such a form it is not extracted by the organophosphorus acid extractants used. It is possible that profound effects of ferrous iron on extraction of other metals present will not be observed. Whether they exist and how they influence the extraction equilibria and kinetics, even indirectly—by affecting complexation equilibria in the aqueous solution, should be one subject of further investigations in the system.

OPAP reagents extract more gallium and at lower acidities than D2EHPA. However, further studies should be focused on how this affects the extractant's selectivity with respect to the other metals present in the solution during extraction as well as stripping. One advantage of OPAP is that its extractive abilities can be deliberately varied by changes in its composition. This may allow selection of an optimal composition with respect not only to gallium loadings but also to the other metals in order to obtain the best possible separation. Therefore, this approach should be investigated as well. On the other hand, the same advantage of OPAP may also be used for extraction of metals in similar systems too.

Important for process application of OPAP will be the results from prolonged continuous operation with respect to extractant losses to the raffinate, and the costs of their further treatment. The losses, however, are not expected to be more problematic for OPAP than for D2EHPA and M2EHPA.

With the example of D2EHPA and OPAP, the present work has emphasized the importance of extractant's acidity (expressed by K_a) for achieving high metal loadings at equilibrium. The higher acidity of OPAP reagents has been explained with the presence of the phenyl- instead of alkyl group as in D2EHPA and M2EHPA. Furthermore, it is known that increase in selectivity for some important metal couples (e.g., Ni/Co) is observed as the alkylphosphoric extractant is replaced with an alkylphosphonic, and then with an alkylphosphinic reagent. However, extractant's acidity decreases in the same order, which leads to having the lowest metal loadings with the best reagent in terms of selectivity. It can be expected that the same order will be followed for extractants where the alkyl group is replaced with a phenyl group as, for example, in OPAP. In other words, a phenyl phosphinic reagent will be expected to yield similar selectivity to its alkyl counterpart (because the selectivity depends mostly on the spacial environment around the central phosphorus atom) but with higher loading levels. This is another approach following the present work, that may be worth investigating, although it will have to employ extractants not

commercially available at present.

Another potential possibility to improve selectivity with the presently available extractants suitable for acidic sulphate solutions, especially if based on different reaction rates, refers to employing the so-called 'phase-transfer catalysts'. These are reagents which serve as a phase-bridge to facilitate the transport of the extracted species from one to the other phase by reacting very fast with them. These reagents would certainly have selectivity on their own which can be used as an additional tool for improved metal separation.

Appendix A

Separation of mono-OPAP and di-OPAP

The method is based on the fact that monoalkyl phosphoric esters can be separated from dialkyl phosphoric esters by selective precipitation as barium salts [91]. The procedure, adopted here, differs from the one proposed for D2EHPA and M2EHPA separation [82] in the preparation of the homogeneous OPAP containing solution before the addition of soluble barium salt solution as well as in treatment of the filtrate after precipitation.

A sample of 27 g OPAP is taken and fully dissolved in 300 ml acetone (reagent grade) under continuous stirring. Then 180 ml distilled water are added. The obtained solution is clear, with pH of 1.3–1.4. Small portions of 2 M NaOH are then slowly added under stirring until pH reaches a value of 11.4-11.5 Up to this point, the procedure is, in fact, a potentiometric titration of the OPAP sample, and it is intended to be so, because the purpose is to obtain full dissociation of mono-OPAP. The choice of end pH value here is based on pH of the second equivalent point—for mono-OPAP (i.e., pH 11.0–11.1), as determined from the titration curve (fig. 3.3). Both di- and mono-OPAP dissociate, di-OPAP:

$$(CH_3(CH_2)_6CH_2C_6H_4O)_2P(O)OH \longrightarrow (CH_3(CH_2)_6CH_2C_6H_4O)_2P(O)O^- + H^+ \quad (A.1)$$

and mono-OPAP—first,

$$CH_3(CH_2)_6CH_2C_6H_4OP(O)(OH)_2 \longrightarrow CH_3(CH_2)_6CH_2C_6H_4OP(O)(OH)O^- + H^+ \quad (A.2)$$

and second dissociation:

$$CH_3(CH_2)_6CH_2C_6H_4OP(O)(OH)O^- \longrightarrow CH_3(CH_2)_6CH_2C_6H_4OP(O)(O)_2^- + H^+ \quad (A.3)$$

The solution is still visibly clear though with a slight yellowish colour. Under continued stirring (but with pH electrode now removed), a slow addition of 60 ml 0.5 M $BaCl_2$ solution starts. Immediately a white precipitate of barium mono-OPAP salt forms. The amount of $BaCl_2$ is approximately half that required for full mono-OPAP precipitation based on stoichiometry. If more is added, coprecipitation of the respective di-OPAP salt will become significant.

The precipitate is filtered (preferably with the help of vacuum) and collected (precipitate I). Filtration here is difficult because of slow formation of viscous organic liquid ('third phase'), heavier than water, containing mostly di-OPAP. Its formation is probably due to salting-out effects. It reports into the filtrate and can be then readily separated. After doing so, a new portion of 0.5 M $BaCl_2$ solution is added to the filtrate in order to precipitate completely the rest of mono- and di-OPAP. This second precipitate is filtered more easily (precipitate II).

Each precipitate is transferred into a separatory funnel and then di-ethyl ether is added in. Any water, if present, easily separates and is removed. The mixture in the funnel is then contacted with 1 M HCl solution, the white precipitate disappears—barium (and sodium) is stripped and the extractant is thus regenerated. A second contact with HCl solution follows in order to assure complete stripping—the acid solution is then checked for presence of Ba^{2+} by testing with soluble sulphate.

The same procedure is followed for the organic liquid ('third phase'), separated from the first filtrate—it is readily dissolved into di-ethyl ether, and then the extractant is regenerated by contacting with HCl solution.

The ether solutions are then washed several times with distilled water in order to remove any acid remaining. Finally, the ether is slowly evaporated to leave the extractant, containing mono- and di-OPAP in different proportions.

Typically, the extractant regenerated from precipitate **I** contains more than 96 mol % mono-OPAP, and from the 'third phase'---more than 85 mol % di-OPAP. Precipitate **II** yields mono- and di-OPAP in approximately 1:1 molar ratio. Examples of potentiometric titration curves for the products are given on figures A.1, A.2, A.3, respectively.

If a reagent with composition beyond the limits of those already obtained is needed (i.e., > 96 mol % mono-OPAP or > 85 mol % di-OPAP), then the respective reagent may be subjected to a second stage separation by selective precipitation. Any composition within the above limits can be produced by mixing the obtained reagents in an appropriate proportion.

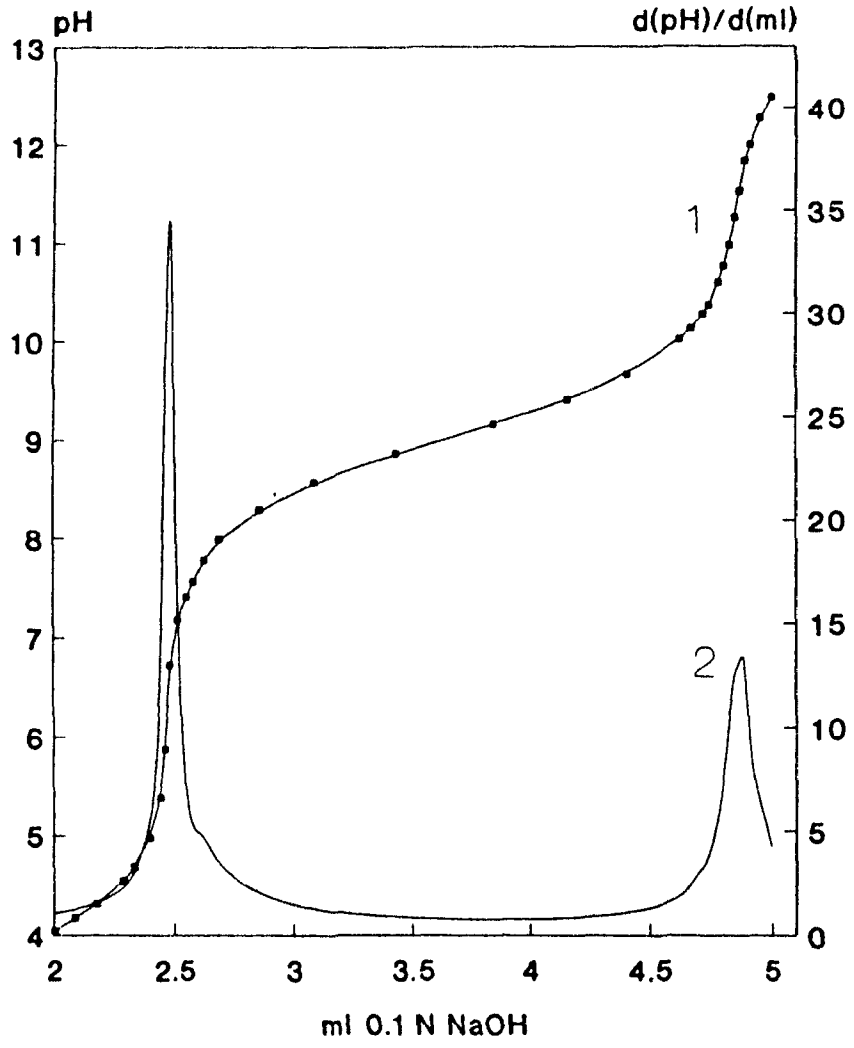

Figure A.1: Potentiometric titration of OPAP produced from precipitate I. Composition: 97.1 mol % mono-OPAP, 2.9 mol % di-OPAP.

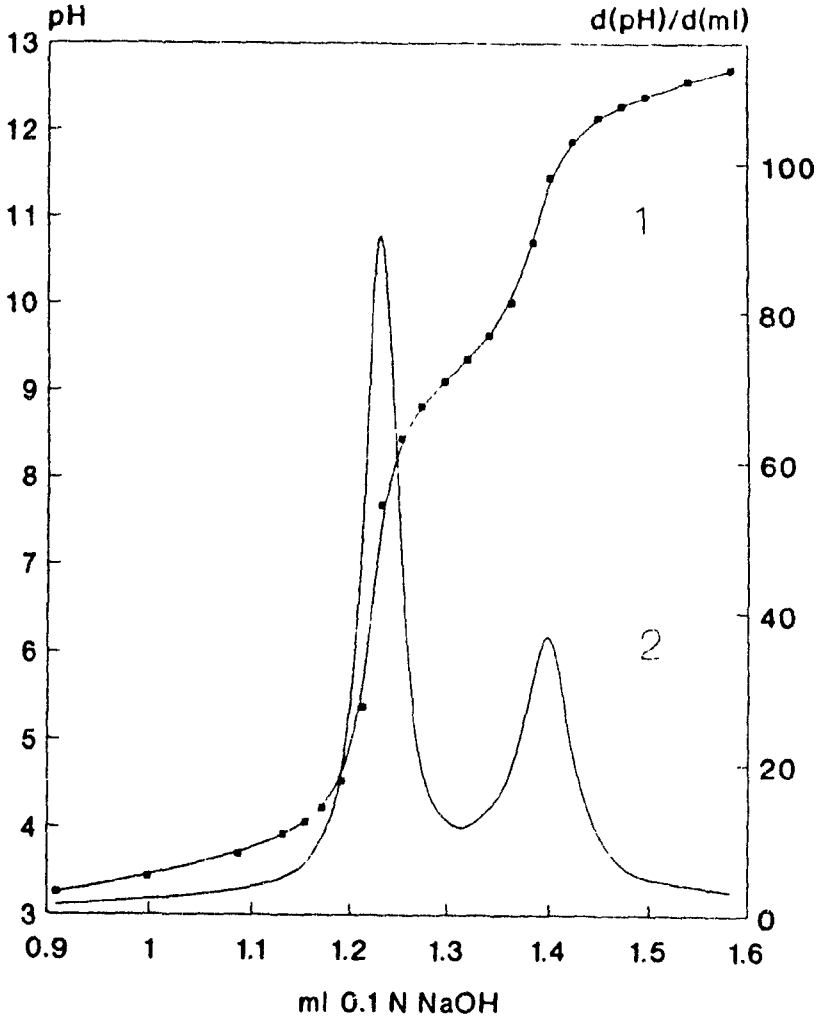

Figure A.2: Potentiometric titration of OPAP produced from the 'third phase'. Composition: 13.3 mol % mono-OPAP, 86.7 mol % di-OPAP.

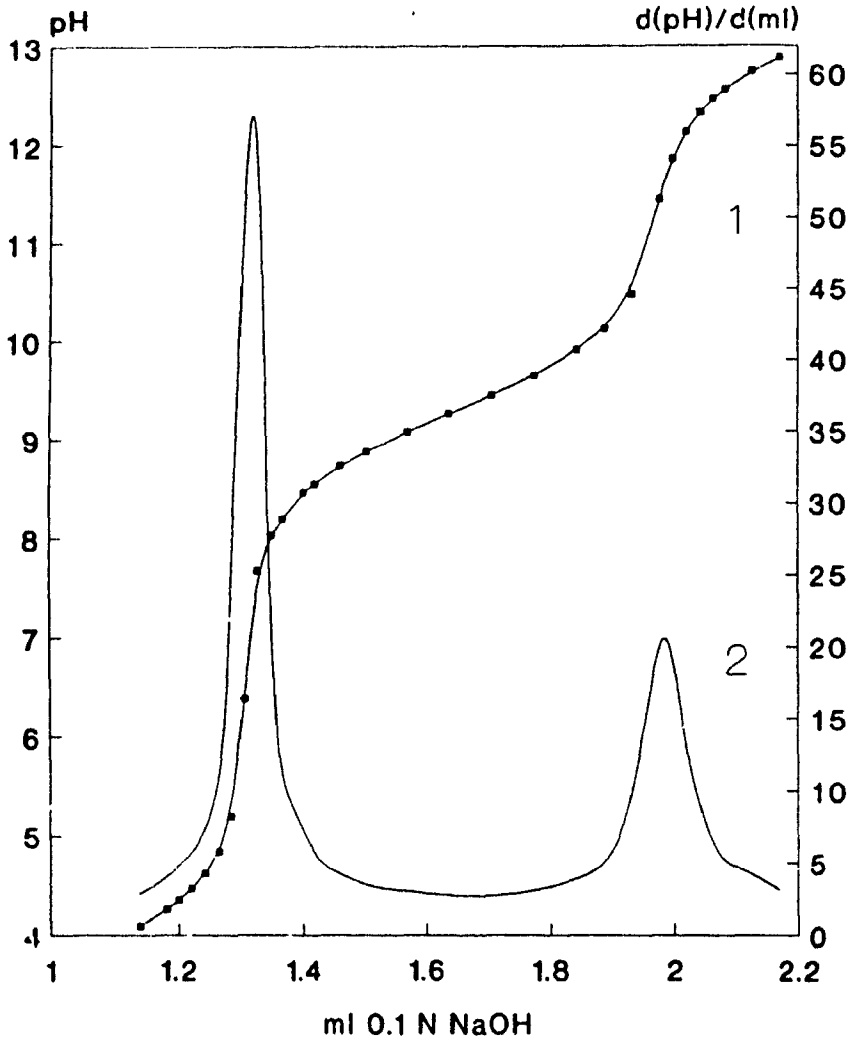

Figure A.3: Potentiometric titration of OPAP produced from the precipitate **II**. Composition: 50.8 mol % mono-OPAP, 49.2 mol % di-OPAP.

Appendix B

Equations for Species Distribution in Solution

The data given in Table 5-1 refer to the mass-stability constants, defined according to eqn (5.1) as

$$\beta_1 = \frac{[Ga(SO_4)^+]}{[Ga^{3+}][SO_4^{2-}]} \tag{B.1}$$

$$\beta_2 = \frac{[Ga(SO_4)_2^-]}{[Ga^{3+}][SO_4^{2-}]^2} \tag{B.2}$$

$$\beta_3 = \frac{[Ga(OH)^{2+}]}{[Ga^{3+}][OH^-]} \tag{B.3}$$

$$\beta_4 = \frac{[Ga(OH)_2^+]}{[Ga^{3+}][OH^-]^2} \tag{B.4}$$

$$\beta_5 = \frac{[Ga(OH)_3]}{[Ga^{3+}][OH^-]^3} \tag{B.5}$$

$$\beta_6 = \frac{[Ga(OH)_4^-]}{[Ga^{3+}][OH^-]^4} \tag{B.6}$$

For convenience, the second dissociation constant of sulphuric acid (eqn 5.5) is introduced in the calculations as stability constant of the HSO_4^- complex:[1]

$$\beta_7 = \frac{[HSO_4^-]}{[H^+][SO_4^{2-}]} \tag{B.7}$$

i.e., $\beta_7 = K_2^{-1}$. Finally, the dissociation constant of water, K_w is defined in its usual form as

$$K_w = [H^+][OH^-] \tag{B.8}$$

If $[Ga]^T$ and $[SO_4]^T$ are the total concentrations of gallium and sulphates in the aqueous solution, respectively, then the corresponding mass-balance equations are:

$$\begin{aligned}[Ga]^T \;=\; & [Ga^{3+}] + [Ga(SO_4)^+] + [Ga(SO_4)_2^-] + \\ & [Ga(OH)^{2+}] + [Ga(OH)_2^+] + [Ga(OH)_3] + [Ga(OH)_4^-]\end{aligned} \tag{B.9}$$

$$[SO_4]^T \;=\; [SO_4^{2-}] + [Ga(SO_4)^+] + 2[Ga(SO_4)_2^-] + [HSO_4^-] \tag{B.10}$$

From the condition for electroneutrality of the solution it follows that[2]

$$\begin{aligned}3[Ga^{3+}] + [Ga(SO_4)^+] + 2[Ga(OH)^{2+}] + [Ga(OH)_2^+] + [H^+] \;=\; \\ 2[SO_4^{2-}] + [HSO_4^-] + [Ga(SO_4)_2^-] + [Ga(OH)_4^-] + [OH^-]\end{aligned} \tag{B.11}$$

After substituting for the complexes concentrations from eqns (B.1)-(B.8) into the above mass- and charge-balance equations, and rearrangement, the following three equations with three unknowns—the three key components—$[Ga^{3+}]$, $[SO_4^{2-}]$, and $[H^+]$, are obtained:

$$\begin{aligned}&[Ga^{3+}] + \beta_1[Ga^{3+}][SO_4^{2-}] + \beta_2[Ga^{3+}][SO_4^{2-}]^2 + \\ &\beta_3 K_w[Ga^{3+}][H^+]^{-1} + \beta_4 K_w^2[Ga^{3+}][H^+]^{-2} + \beta_5 K_w^3[Ga^{3+}][H^+]^{-3} + \\ &\beta_6 K_w^4[Ga^{3+}][H^+]^{-4} - [Ga]^T = 0\end{aligned} \tag{B.12}$$

[1]Concentrations in molality units For further discussion see page 234

[2]Written for the case when the system is $Ga_2(SO_4)_3$-H_2SO_4-H_2O

$$[SO_4^{2-}] + \beta_1[Ga^{3+}][SO_4^{2-}] + 2\beta_2[Ga^{3+}][SO_4^{2-}]^2 + \beta_7[SO_4^{2-}][H^+] - [SO_4]^T = 0 \quad \text{(B.13)}$$

$$3[Ga^{3+}] + \beta_1[Ga^{3+}][SO_4^{2-}] + 2\beta_3 K_w[Ga^{3+}][H^+]^{-1} + \beta_4 K_w^2[Ga^{3+}][H^+]^{-2} + [H^+] - 2[SO_4^{2-}] - K_w[H^+]^{-1} - \beta_6 K_w^4[Ga^{3+}][H^+]^{-4} - \beta_7[SO_4^{2-}][H^+] - \beta_3[Ga^{3+}][SO_4^{2-}]^2 = 0 \quad \text{(B.14)}$$

Thus, the problem is to solve the above system of three non-linear equations for the three unknowns. For that purpose, the Newton-Raphson method is used with a modified iteration formula in order to avoid negative roots [146].

Once this is achieved, the concentrations of all species in the solution are calculated using the definition equations (B.1)-(B.8) and the values of the mass-stability constants. The latter, however, are valid only for the initially assumed ionic strength. Therefore, a separate iteration loop for I is required, where the ionic strength, found from species distribution at the current step and using eqn (5.10), becomes the value used for the next step.

From the concentration of H^+ and the ionic strength, found from the distribution of species, it is possible to estimate the single ion activity of H^+, and therefore—the pH. The method, proposed by Das and successfully applied for sulphuric acid solutions [147], was also used here. The single ion activity coefficient, γ_{H^+}, is found from

$$\log \gamma_{H^+} = -\frac{0.509\sqrt{I}}{1 + 1.87\sqrt{I}} + 0.0479I - \log\left\{1 + \frac{0.001 M_w \sum_{j=1}^{n} m_j}{1 - 0.001 h M_w m_{H^+}}\right\} \quad \text{(B.15)}$$

where M_w is the molecular weight of water, h is the hydration number of H^+ ($h = 4$ is assumed by Das), m denotes molal concentrations, and $\sum_{j=1}^{n} m_j$ is the sum of the molalities of all n-species present in the solution. The activity of H^+ is calculated as the product of γ_{H^+} and m_{H^+}.

Equation (B.15) requires conversion of species concentrations from molarities to molalities, and accordingly the ionic strength is expressed in terms of molality. The following formula, written for species i, has been used [148] for the conversion:

$$m_i = \frac{1000\, c_i}{1000\, \rho - \sum_{j=1}^{n} c_j M_j} \tag{B.16}$$

where c, m, and M denote molarity (moles per litre solution), molality (moles per kg solvent), and molecular weight (in grams per mole), respectively, n is the total number of species, and ρ is the density (in g/cm^3) of the solution. For this work, it has been assumed that ρ is constant and equal to one. It is possible, however, to introduce the density as a known analytical or empirical function of species concentrations or io. ic strength.

Although not explicitly discussed above, a similar conversion of concentration units is also required, and is included in the computer program, whenever the concentration of HSO_4^- is involved. The reason is that in the expressions for its stability constant and dependence on I (eqns 5.5 or B.7, and 5.6), the concentrations are expressed in molalities (see page 117), and not molarities. Thus, based on eqns (B.7) and (B.16) the expression for the molarity of HSO_4^- in terms of the molarities of H^+ and SO_4^{2-} becomes

$$[HSO_4^-] = \beta_7 [H^+][SO_4^{2-}] \frac{1000}{1000\, \rho - \sum_{j=1}^{n} c_j M_j} \tag{B.17}$$

Equation (B.17) is subsequently used to substitute $[HSO_4^-]$ in eqns (B.10) and (B.11) and in the calculations further in the program. For simplicity, however, this is not shown here in the resulting eqns (B.13) and (B.14), resp., in which the simple substitution from eqn (B.7) is used instead.

Appendix C

MTWCR Model: Derivation of the Equations

C.1 Introduction

The expressions for calculation of species concentration are derived from the appropriate flux equations (6.30)-(6.32), written for the aqueous diffusion layer and subject to the boundary conditions (6.33) and (6.34) These will be considered in the following section C.2.

Similar flux equations but written for the organic diffusion layer with their relevant boundary conditions and involving the metal-extractant complex, or complexes, must also be included in the model thus allowing calculation of species concentrations there. These will be presented in section C 3.

Finally, the expression for the flux of extractant through the interface, J_{HR}, will be derived for the limiting cases of instantaneous reversible and reversible pseudo-first order reactions for step 4 (first organic ligand addition) being the rate-limiting step. The resulting expressions when step 5 or step 6 are rate-limiting will also be given.

C.2 Aqueous Diffusion Layer

Calculation of $C_{i_{H^+}}$

From eqns (6.30) and (6.32) it follows that

$$\mathcal{D}_{HR}\frac{dC_{HR}}{dx} + \mathcal{D}_{R^-}\frac{dC_{R^-}}{dx} + \mathcal{D}_{H^+}\frac{dC_{H^+}}{dx} = -J_{i_{HR}} \tag{C.1}$$

This equation can be integrated for x from zero to δ, provided that the concentrations of species involved are continuous functions of x in this interval. With the respective boundary conditions (6.33) and (6.34) introduced, the integration yields

$$\mathcal{D}_{HR}\left(C_{0_{HR}} - C_{i_{HR}}\right) + \mathcal{D}_{R^-}\left(C_{0_{R^-}} - C_{i_{R^-}}\right) + \mathcal{D}_{H^+}\left(C_{0_{H^+}} - C_{i_{H^+}}\right) = -J_{i_{HR}}\delta \tag{C.2}$$

As discussed in Chapter 6 (page 163), all reaction steps, except the rate-limiting one, are considered to be at equilibrium. This also applies to the acid dissociation of the extractant, and therefore

$$K_a = \frac{C_{0_{H^+}}C_{0_{R^-}}}{C_{0_{HR}}} = \frac{C_{i_{H^+}}C_{i_{R^-}}}{C_{i_{HR}}} \tag{C.3}$$

After substitution for $C_{0_{R^-}}$ and $C_{i_{R^-}}$ from eqn (C.3) into eqn (C.2) and rearrangement, a quadratic equation for $C_{i_{H^+}}$ is obtained:

$$C_{i_{H^+}}^2 - \mathcal{A}C_{i_{H^+}} + \frac{\mathcal{D}_{R^-}}{\mathcal{D}_{H^+}}K_a C_{i_{HR}} = 0 \tag{C.4}$$

where

$$\mathcal{A} = C_{0_{H^+}} + \frac{J_{i_{HR}}}{\kappa_{H^+}} + \frac{\mathcal{D}_{R^-}C_{0_{HR}}K_a}{\mathcal{D}_{H^+}C_{0_{H^+}}} + \frac{\mathcal{D}_{HR}}{\mathcal{D}_{H^+}}\left(C_{0_{HR}} - C_{i_{HR}}\right) \tag{C.5}$$

and κ_{H^+} is the aqueous-side mass-transfer coefficient for H^+

$$\kappa_{H^+} = \frac{\mathcal{D}_{H^+}}{\delta} \tag{C.6}$$

Solving eqn (C.4) for $C_{i_{H^+}}$ yields[1]

$$C_{i_{H^+}} = \frac{\mathcal{A} + \sqrt{\mathcal{A}^2 - 4\frac{\mathcal{D}_{R^-}}{\mathcal{D}_{H^+}}K_a C_{i_{HR}}}}{2} \tag{C.7}$$

[1] Taking only the physically significant positive root. The other root would yield $C_{i_{H^+}} = 0$ in the case of $K_a \to 0$ (see eqn C.9)

Equation (C.7) represents the expression used to calculate the $C_{i_{H+}}$ values. It is clear that in the case of weak acid extractant, i.e., when $K_a \rightarrow 0$, the expression for $\mathcal{A}$ will become

$$\mathcal{A}' = C_{0_{H+}} + \frac{J_{i_{HR}}}{\kappa_{H+}} + \frac{\mathcal{D}_{HR}}{\mathcal{D}_{H+}}\left(C_{0_{HR}} - C_{i_{HR}}\right) \tag{C.8}$$

which, in such case, is equal to $C_{i_{H+}}$ because then eqn (C.7) transforms to

$$C_{i_{H+}} = \frac{\mathcal{A}' + \sqrt{\mathcal{A}'^2}}{2} \tag{C.9}$$

Finally, it should also be noted that most experiments have been carried out at relatively high acidities since this is the area of interest for gallium extraction. As a result, the difference between $C_{0_{H+}}$ and the calculated $C_{i_{H+}}$ was in most cases very small, thus essentially justifying the simplification assumption of the limiting regimes that $C_{i_{H+}} \approx C_{0_{H+}}$.

Calculation of $C_{i_{Ga^{3+}}}$

The expression for $C_{i_{Ga^{3+}}}$ is similarly derived. Integration of eqn (6.32) for x from $x = 0$ to $x = \delta$ yields

$$\mathcal{D}_{HR}\left(C_{0_{HR}} - C_{i_{HR}}\right) + \mathcal{D}_{R^-}\left(C_{0_{R^-}} - C_{i_{R^-}}\right) - 3\mathcal{D}_{Ga^{3+}}\left(C_{0_{Ga^{3+}}} - C_{i_{Ga^{3+}}}\right) = -J_{i_{HR}}\delta \tag{C.10}$$

After substitution for $C_{0_{R^-}}$ and $C_{i_{R^-}}$ and solving for $C_{i_{Ga^{3+}}}$ the following equation is obtained:

$$C_{i_{Ga^{3+}}} = C_{0_{Ga^{3+}}} - \frac{J_{i_{HR}}}{3\kappa_{Ga^{3+}}} + \frac{\mathcal{D}_{HR}}{3\mathcal{D}_{Ga^{3+}}}\left(C_{i_{HR}} - C_{0_{HR}}\right) + \frac{\mathcal{D}_{R^-}K_a}{3\mathcal{D}_{Ga^{3+}}}\left(\frac{C_{i_{HR}}}{C_{i_{H+}}} - \frac{C_{0_{HR}}}{C_{0_{H+}}}\right) \tag{C.11}$$

where $\kappa_{Ga^{3+}} = (\mathcal{D}_{Ga^{3+}}/\delta)$ is the mass-transfer coefficient for the metal in the aqueous diffusion layer.

Again, when the extractant is a weak acid, and therefore $K_a \rightarrow 0$, eqn (C.11) is simplified and thus becomes

$$C_{i_{Ga^{3+}}} = C_{0_{Ga^{3+}}} - \frac{J_{i_{HR}}}{3\kappa_{Ga^{3+}}} + \frac{\mathcal{D}_{HR}}{3\mathcal{D}_{Ga^{3+}}}\left(C_{i_{HR}} - C_{0_{HR}}\right) \tag{C.12}$$

Calculation of $C_{0_{HR}}$

In the same way as outlined above, the integration of eqn (6.31) for x from $x = 0$ to $x = \delta$ and then substitution for $C_{0_{R^-}}$ and $C_{i_{R^-}}$ from eqn (C.3) gives

$$\mathcal{D}_{HR}\left(C_{0_{HR}} - C_{i_{HR}}\right) + \mathcal{D}_{R^-} K_a \left(\frac{C_{0_{HR}}}{C_{0_{H^+}}} - \frac{C_{i_{HR}}}{C_{i_{H^+}}}\right) + 3\mathcal{D}_{GaR_3}\left(C_{0_{GaR_3}} - C_{i_{GaR_3}}\right) = 0 \tag{C.13}$$

The concentration of GaR_3 in the bulk aqueous phase, $C_{0_{GaR_3}}$, is then expressed from eqn (6.35) and substituted into eqn (C.13). Furthermore, since steps 2 and 7b, which represent the partitioning of HR and GaR_3, resp., at the aqueous-organic interface, are considered to be at equilibrium, as are all other steps except the RLS, it follows that

$$P_{HR} = \frac{\overline{C}_{i_{HR}}}{C_{i_{HR}}} \qquad \text{and} \qquad P_{GaR_3} = \frac{\overline{C}_{i_{GaR_3}}}{C_{i_{GaR_3}}} \tag{C.14}$$

Thus, after substitution for $C_{i_{HR}}$ and $C_{i_{GaR_3}}$ from eqns (C.14) into eqn (C.13) and rearrangement, the latter becomes

$$C_{0_{HR}}^3 + C_{0_{HR}}\mathcal{B}\left(\mathcal{D}_{HR} + \frac{\mathcal{D}_{R^-}K_a}{C_{0_{H^+}}}\right) - \mathcal{B}\left[\frac{\overline{C}_{i_{HR}}}{P_{HR}}\left(\mathcal{D}_{HR} + \frac{\mathcal{D}_{R^-}K_a}{C_{i_{H^+}}}\right) + \frac{3\mathcal{D}_{GaR_3}\overline{C}_{i_{GaR_3}}}{P_{GaR_3}}\right] = 0 \tag{C.15}$$

where

$$\mathcal{B} = \frac{C_{0_{H^+}}^3}{3\mathcal{D}_{GaR_3}K_{eq}C_{0_{Ga^{3+}}}} \tag{C.16}$$

Clearly, in the particular case of weakly acidic extractant, when $K_a \rightarrow 0$, eqn (C.15) will become

$$C_{0_{HR}}^3 + C_{0_{HR}}\mathcal{B}\mathcal{D}_{HR} - \mathcal{B}\left[\frac{\overline{C}_{i_{HR}}}{P_{HR}}\mathcal{D}_{HR} + \frac{3\mathcal{D}_{GaR_3}\overline{C}_{i_{GaR_3}}}{P_{GaR_3}}\right] = 0 \tag{C.17}$$

The derived eqn (C.15) for $C_{0_{HR}}$ is a cubic equation of the type

$$x^3 + px + q = 0$$

and has one real root when

$$\mathcal{E} = \left(\frac{p}{3}\right)^3 + \left(\frac{q}{2}\right)^2 > 0$$

It is obvious from eqn (C.16) that $\mathcal{B}$, and therefore the term equivalent to p in eqns (C.15) or (C.17), is always positive. Thus the condition $\mathcal{E} > 0$ will be always fulfilled. The one real root then is calculated as[2]

$$x = \sqrt[3]{-\frac{q}{2} + \sqrt{\mathcal{E}}} + \sqrt[3]{-\frac{q}{2} - \sqrt{\mathcal{E}}}$$

As derived, eqn (C.15) was used in the model to calculate $C_{0_{HR}}$, without any problems as far as the extraction kinetics was concerned. However, when the model was to be verified with the stripping kinetics experimental results, it appeared that the form of eqn (C.15) with the expression for $\mathcal{B}$, given by eqn (C.16), was not appropriate. The reason was that in this case the metal concentration in the bulk aqueous phase $C_{0_{Ga^{3+}}}$ was zero. Hence, $\mathcal{B} \to \infty$ and eqn (C.15) could not be solved for $C_{0_{HR}}$ in its present form. In the derivation of eqn (C.15), after substitution for $C_{0_{GaR_3}}$ from eqn (6.35) into eqn (C.13) the result is

$$\mathcal{D}_{HR}(C_{0_{HR}} - C_{i_{HR}}) + \mathcal{D}_R\text{-}K_a\left(\frac{C_{0_{HR}}}{C_{0_{H^+}}} - \frac{C_{i_{HR}}}{C_{i_{H^+}}}\right) + 3\mathcal{D}_{GaR_3}\left(\frac{C_{0_{Ga^{3+}}} C^3_{0_{HR}} K_{eq}}{C^3_{0_{H^+}}} - C_{i_{GaR_3}}\right) = 0 \tag{C.18}$$

and after rearrangement eqn (C.15) is obtained. In the case of stripping kinetics experiments $C_{0_{Ga^{3+}}} = 0$ and therefore eqn (C.18) simplifies to

$$\mathcal{D}_{HR}(C_{0_{HR}} - C_{i_{HR}}) + \mathcal{D}_R\text{-}K_a\left(\frac{C_{0_{HR}}}{C_{0_{H^+}}} - \frac{C_{i_{HR}}}{C_{i_{H^+}}}\right) - 3\mathcal{D}_{GaR_3} C_{i_{GaR_3}} = 0 \tag{C.19}$$

Strictly speaking, in a typical experiment for stripping kinetics it is only initially that $C_{0_{Ga^{3+}}} = 0$, and according to the assumptions made and those of the film theory, equilibrium between reactants and products in the bulk phase do exist. Nevertheless, under such conditions $C_{0_{Ga^{3+}}}$ will be so small (as well as $C_{0_{GaR_3}}$ in the first place) that the respective term in eqn (C.18) can be assumed to be zero.

From eqn (C.19), following the same procedure as for eqn (C.15) of substitution for $C_{i_{HR}}$ and $C_{i_{GaR_3}}$ from eqns (C.14) and rearrangement, the result for $C_{0_{HR}}$ is

$$C_{0_{HR}} = \frac{1}{\left(\mathcal{D}_{HR} + \frac{\mathcal{D}_R\text{-}K_a}{C_{0_{H^+}}}\right)}\left[\frac{\overline{C}_{i_{HR}}}{P_{HR}}\left(\mathcal{D}_{HR} + \frac{\mathcal{D}_R\text{-}K_a}{C_{i_{H^+}}}\right) + \frac{3\mathcal{D}_{GaR_3}\overline{C}_{i_{GaR_3}}}{P_{GaR_3}}\right] \tag{C.20}$$

[2]These are the Cardano's formulae for solving cubic equations

Clearly, eqn (C.20) will become

$$C_{0_{HR}} = \frac{\overline{C}_{t_{HR}}}{P_{HR}} + 3\frac{\mathcal{D}_{GaR_3}}{\mathcal{D}_{HR}}\frac{\overline{C}_{t_{GaR_3}}}{P_{GaR_3}} \tag{C.21}$$

in the case of weak acid extractant with $K_a \to 0$.

Expression for $J_{t_{HR}}$

From the equation for the acid dissociation constant of the extractant

$$K_a = \frac{C_{H^+}C_{R^-}}{C_{HR}}$$

by differentiating with respect to x the following equation is obtained:

$$\frac{dC_{R^-}}{dx} = K_a\frac{1}{C_{H^+}}\frac{dC_{HR}}{dx} - K_a\frac{C_{HR}}{C_{H^+}^2}\frac{dC_{H^+}}{dx} \tag{C.22}$$

After substitution for (dC_{R^-}/dx) from eqn (C.22) into eqn (C.1) and rearranging, the resulting differential equation is

$$\left(\mathcal{D}_{HR} + \frac{\mathcal{D}_{R^-}K_a}{C_{H^+}}\right)\frac{dC_{HR}}{dx} + \left(\mathcal{D}_{H^+} - \frac{\mathcal{D}_{R^-}K_aC_{HR}}{C_{H^+}^2}\right)\frac{dC_{H^+}}{dx} = -J_{t_{HR}} \tag{C.23}$$

Equation (C.23) is valid within the aqueous diffusion layer—from $x = 0$ to $x = \delta$. Written for $x = 0$ it gives

$$\left(\mathcal{D}_{HR} + \frac{\mathcal{D}_{R^-}K_a}{C_{t_{H^+}}}\right)\left(\frac{dC_{HR}}{dx}\right)_{x=0} + \left(\mathcal{D}_{H^+} - \frac{\mathcal{D}_{R^-}K_aC_{t_{HR}}}{C_{t_{H^+}}^2}\right)\left(\frac{dC_{H^+}}{dx}\right)_{x=0} = -J_{t_{HR}} \tag{C.24}$$

According to the boundary conditions (eqn 6.33), however, at $x = 0$

$$\left(\frac{dC_{H^+}}{dx}\right)_{x=0} = 0$$

and thus the following expression for $J_{t_{HR}}$ is obtained from eqn (C.24):

$$J_{t_{HR}} = -\left(\mathcal{D}_{HR} + \frac{\mathcal{D}_{R^-}K_a}{C_{t_{H^+}}}\right)\left(\frac{dC_{HR}}{dx}\right)_{x=0} \tag{C.25}$$

When $K_a \to 0$ eqn (C.25) will then become

$$J_{t_{HR}} = -\mathcal{D}_{HR}\left(\frac{dC_{HR}}{dx}\right)_{x=0} \tag{C.26}$$

which is the equation used in the original MTWCR model [197], and is justified since the model there applies exclusively to extraction with chelating reagents. However, in the present work eqn (C.25) is used, which is obviously more general and will reduce to eqn (C.26) only in the particular case of a weakly acidic extractant.

C.3 Organic Diffusion Layer

One of the assumptions in the model development, discussed in Chapter 6, is that four species exist in the organic phase, namely $(HR)_2$, HR, GaR_3, and $GaR_3 \cdot HR$, which concentrations are inter-related by the equilibria of steps 1 and 8b. With respect to the organic diffusion layer, the film-theory assumption of steady-state (i.e., no accumulation) implies that the combined flux of extractant in its both forms monomer and dimer—from the bulk to the interface is equal to the flux of products- GaR_3, and $GaR_3 \cdot HR$—in the opposite direction. Thus, the appropriate differential equation to describe this is

$$\overline{\mathcal{D}}_{HR}\frac{d\overline{C}_{HR}}{dx} + 2\overline{\mathcal{D}}_{(HR)_2}\frac{d\overline{C}_{(HR)_2}}{dx} + 3\overline{\mathcal{D}}_{GaR_3}\frac{d\overline{C}_{GaR_3}}{dx} + 4\overline{\mathcal{D}}_{GaR_3\,HR}\frac{d\overline{C}_{GaR_3\,HR}}{dx} = 0 \quad \text{(C.27)}$$

where $\overline{\mathcal{D}}$ denotes diffusion coefficients of species in the organic phase.

Calculation of $\overline{C}_{i_{HR}}$

From the same assumptions above, it follows that $J_{i_{HR}}$ can be expressed with organic phase concentrations of the extractant [158]:

$$J_{i_{HR}} = \overline{\kappa}_{HR}\left(\overline{C}_{0_{HR}} - \overline{C}_{i_{HR}}\right) + 2\overline{\kappa}_{(HR)_2}\left(\overline{C}_{0_{(HR)_2}} - \overline{C}_{i_{(HR)_2}}\right) \quad \text{(C.28)}$$

or with those of the reaction products:

$$J_{i_{HR}} = -\left[3\overline{\kappa}_{GaR_3}\left(\overline{C}_{0_{GaR_3}} - \overline{C}_{i_{GaR_3}}\right) + 4\overline{\kappa}_{GaR_3\,HR}\left(\overline{C}_{0_{GaR_3\,HR}} - \overline{C}_{i_{GaR_3\,HR}}\right)\right] \quad \text{(C.29)}$$

where $\overline{\kappa}$ is the respective mass-transfer coefficient of species in the organic phase.[3] Equation (C.28) expresses mathematically the argument that although extractant

[3]For the particular experimental set-up of the RDC technique, the effects of additional diffusion through the organic-impregnated porous membrane are reflected in the values of $\overline{\kappa}$

dimers do not distribute *as such* to the aqueous phase, they nevertheless contribute to the flux of extractant through the interface. This contribution is due to existing gradient in dimer concentration in the layer following transfer of monomer through the interface and dedimerization there.

Equation (C.29) represents the idea that once GaR_3 is formed in the aqueous diffusion layer and/or the interface, its transfer through the interface[4] is followed by formation and distribution of one (or more) other metal-extractant complexes, an example of which is step 8b.

From eqn (C.28) after substitution for the concentrations of $(HR)_2$ according to the equation for K_d (eqn 6.6) and rearrangement, a quadratic equation for $\overline{C}_{i_{HR}}$ is obtained:

$$\overline{C}_{i_{HR}}^2 + \frac{\overline{\kappa}_{HR}}{2\overline{\kappa}_{(HR)_2}K_d}\overline{C}_{i_{HR}} - \mathcal{F} = 0 \qquad \text{(C.30)}$$

where

$$\mathcal{F} = \overline{C}_{0_{HR}}^2 + \frac{\overline{\kappa}_{HR}}{2\overline{\kappa}_{(HR)_2}K_d}\overline{C}_{0_{HR}} - \frac{J_{i_{HR}}}{2\overline{\kappa}_{(HR)_2}K_d}$$

with the positive root being

$$\overline{C}_{i_{HR}} = -\frac{\overline{\kappa}_{HR}}{4\overline{\kappa}_{(HR)_2}K_d} + \frac{1}{2}\sqrt{\left(\frac{\overline{\kappa}_{HR}}{2\overline{\kappa}_{(HR)_2}K_d}\right)^2 + 4\mathcal{F}} \qquad \text{(C.31)}$$

Equation (C.31) is used in the model to calculate $\overline{C}_{i_{HR}}$.

Calculation of $\overline{C}_{i_{GaR_3}}$

From the equations for K_d (6.6) and K_G (6.16) it follows that

$$\overline{C}_{GaR_3 \cdot HR} = \overline{C}_{HR}\overline{C}_{GaR_3}\sqrt{K_d K_G} \qquad \text{(C.32)}$$

which is valid also for concentrations within the organic diffusion layer because the reactions involved are considered to be at equilibrium. Thus, after substitution for $\overline{C}_{0_{GaR_3\,HR}}$ and $\overline{C}_{i_{GaR_3\,HR}}$ from eqn (C.32) in eqn (C.29) and solving for $\overline{C}_{i_{GaR_3}}$ the

[4]Described by $J_{i_{GaR_3}}$, which is related to $J_{i_{HR}}$ by eqn (6.12) $J_{i_{HR}} = -3J_{i_{GaR_3}}$

following expression is obtained:

$$\overline{C}_{i_{GaR_3}} = \frac{\overline{C}_{0_{GaR_3}}\left(3\overline{\kappa}_{GaR_3} + 4\overline{\kappa}_{GaR_3\,HR}\overline{C}_{0_{HR}}\sqrt{K_d K_G}\right) + J_{i_{HR}}}{3\overline{\kappa}_{GaR_3} + 4\overline{\kappa}_{GaR_3\,HR}\overline{C}_{i_{HR}}\sqrt{K_d K_G}} \qquad (C.33)$$

This equation (C.33) is used in the model for calculation of $\overline{C}_{i_{GaR_3}}$.

Gallium-extractant complexes in the organic phase

The concentrations of the four complexes in the bulk organic solution are related by the monomer/dimer and step 8b equilibria, and described by eqns (6.6) and (6.16). In addition, the following mass-balance equations are formulated:

$$[Ga]^T_{org} = \overline{C}_{GaR_3} + \overline{C}_{GaR_3\,HR} \qquad (C.34)$$

for the total gallium concentration in the organic phase, and

$$[HR]^T_{org} = 3\overline{C}_{GaR_3} + 4\overline{C}_{GaR_3\,HR} + \overline{C}_{HR} + 2\overline{C}_{(HR)_2} \qquad (C.35)$$

for the total extractant concentration in all forms. Both $[Ga]^T_{org}$ and $[HR]^T_{org}$ are known or can be found.

Hence, eqns (C.34) and (C.35) together with eqns (6.6) and (6.16) represent a system of four equations with four unknowns—the concentrations of the four species. From these equations, after substitutions and rearrangement, the following expression can be obtained:

$$[HR]^T_{org} = \frac{[Ga]^T_{org}}{1 + \sqrt{K_G\overline{C}_{(HR)_2}}}\left(3 + 4\sqrt{K_G\overline{C}_{(HR)_2}}\right) + \sqrt{\frac{\overline{C}_{(HR)_2}}{K_d}} + 2\overline{C}_{(HR)_2} \qquad (C.36)$$

which is only with one unknown—$\overline{C}_{(HR)_2}$. Equation (C.36) can be solved for $\overline{C}_{(HR)_2}$ by the secant method, after which the concentrations of the other species are found.

C.4 Flux through the Interface, $J_{i_{HR}}$

The derivation of the equations for $J_{i_{HR}}$ for the two limiting regimes of instantaneous reversible and reversible pseudo-first order reactions will be presented for the reaction

scheme where the first organic ligand addition (step 4) is rate-determining as well as the resulting analogous equations for steps 5 and 6.

To simplify the notation, in the following derivations $\mathcal{D}'$ will be used to denote the expression

$$\mathcal{D}' = \mathcal{D}_{\mathrm{HR}} + \frac{\mathcal{D}_{\mathrm{R}} \cdot K_a}{C_{i_{\mathrm{H}^+}}} \tag{C.37}$$

Instantaneous Reversible Reaction

The respective equation for this regime is eqn (6.39):

$$\mathcal{D}_{\mathrm{HR}} \frac{d^2 C_{\mathrm{HR}}}{dx^2} = k_f K_a \frac{C_{\mathrm{HR}}}{C_{i_{\mathrm{H}^+}}} \left(C_{i_{\mathrm{Ga}^{3+}}} - \frac{1}{K_{\mathrm{eq}}} \frac{C_{i_{\mathrm{GaR_3}}} C^3_{i_{\mathrm{H}^+}}}{C^3_{i_{\mathrm{HR}}}} \right) \tag{C.38}$$

and it has to be integrated. For that purpose, a new variable, ψ, is defined:

$$\psi = \frac{dC_{\mathrm{HR}}}{dx}$$

and the following transformation holds:

$$\frac{d^2 C_{\mathrm{HR}}}{dx^2} = \psi \frac{d\psi}{dC_{\mathrm{HR}}} \tag{C.39}$$

Thus, eqn (C.38) can be written in a simplified form as

$$\mathcal{D}_{\mathrm{HR}} \psi \frac{d\psi}{dC_{\mathrm{HR}}} = \mathcal{G} C_{\mathrm{HR}} \tag{C.40}$$

where

$$\mathcal{G} = k_f K_a \frac{1}{C_{i_{\mathrm{H}^+}}} \left(C_{i_{\mathrm{Ga}^{3+}}} - \frac{1}{K_{\mathrm{eq}}} \frac{C_{i_{\mathrm{GaR_3}}} C^3_{i_{\mathrm{H}^+}}}{C^3_{i_{\mathrm{HR}}}} \right)$$

The boundary conditions for ψ are:

$$\text{at } x = 0 \qquad \psi = \left(\frac{dC_{\mathrm{HR}}}{dx} \right)_{x=0} = - \frac{J_{i_{\mathrm{HR}}}}{\mathcal{D}'} \tag{C.41}$$

following eqn (C.25) and

$$\text{at } x = \delta \qquad \psi = \left(\frac{dC_{\mathrm{HR}}}{dx} \right)_{x=\delta} = 0 \tag{C.42}$$

according to boundary conditions eqn (6.31).

Thus, integration of eqn (C.40) for x from $x = 0$ to $x = \delta$

$$\mathcal{D}_{\mathrm{HR}} \int_{-(J_{i_{\mathrm{HR}}}/\mathcal{D}')}^{0} \psi \, d\psi = \mathcal{G} \int_{C_{i_{\mathrm{HR}}}}^{C_{0_{\mathrm{HR}}}} C_{\mathrm{HR}} \, dC_{\mathrm{HR}} \tag{C.43}$$

results in

$$J_{i_{\mathrm{HR}}} = \sqrt{\frac{\mathcal{D}'^2}{\mathcal{D}_{\mathrm{HR}}} \mathcal{G} \left(C_{i_{\mathrm{HR}}}^2 - C_{0_{\mathrm{HR}}}^2 \right)} \tag{C.44}$$

and after substitution with the expression for $\mathcal{G}$ and rearranging the following equation is obtained:

$$J_{i_{\mathrm{HR}}} = \sqrt{\frac{\mathcal{D}'^2}{\mathcal{D}_{\mathrm{HR}}} k_f K_a \frac{C_{i_{\mathrm{Ga}^{3+}}}}{C_{i_{\mathrm{H}^+}}} \left(1 - \frac{1}{K_{\mathrm{eq}}} \frac{C_{i_{\mathrm{GaR_3}}} C_{i_{\mathrm{H}^+}}^3}{C_{i_{\mathrm{Ga}^{3+}}} C_{i_{\mathrm{HR}}}^3} \right) \left(C_{i_{\mathrm{HR}}}^2 - C_{0_{\mathrm{HR}}}^2 \right)} \tag{C.45}$$

Substituting for $C_{i_{\mathrm{HR}}}$ and $C_{i_{\mathrm{GaR_3}}}$ from eqns (C 14) and introducing then K' from eqn (6.21), the result is

$$J_{i_{\mathrm{HR}}} = \sqrt{\frac{\mathcal{D}'^2}{\mathcal{D}_{\mathrm{HR}} P_{\mathrm{HR}}^2} k_f K_a \frac{C_{i_{\mathrm{Ga}^{3+}}}}{C_{i_{\mathrm{H}^+}}} \left(1 - \frac{1}{K'} \frac{\overline{C}_{i_{\mathrm{GaR_3}}} C_{i_{\mathrm{H}^+}}^3}{C_{i_{\mathrm{Ga}^{3+}}} \overline{C}_{i_{\mathrm{HR}}}^3} \right) \left(\overline{C}_{i_{\mathrm{HR}}}^2 - P_{\mathrm{HR}}^2 C_{0_{\mathrm{HR}}}^2 \right)} \tag{C.46}$$

or, when the expression for $\mathcal{D}'$ (eqn C 37) is substituted:

$$J_{i_{\mathrm{HR}}} = \sqrt{\frac{\left(\mathcal{D}_{\mathrm{HR}} + \frac{\mathcal{D}_{\mathrm{R}^-} K_a}{C_{i_{\mathrm{H}^+}}} \right)^2}{\mathcal{D}_{\mathrm{HR}} P_{\mathrm{HR}}^2} k_f K_a \frac{C_{i_{\mathrm{Ga}^{3+}}}}{C_{i_{\mathrm{H}^+}}} \left(1 - \frac{1}{K'} \frac{\overline{C}_{i_{\mathrm{GaR_3}}} C_{i_{\mathrm{H}^+}}^3}{C_{i_{\mathrm{Ga}^{3+}}} \overline{C}_{i_{\mathrm{HR}}}^3} \right) \left(\overline{C}_{i_{\mathrm{HR}}}^2 - P_{\mathrm{HR}}^2 C_{0_{\mathrm{HR}}}^2 \right)} \tag{C.47}$$

Equation (C.47) is analogous to the main equation for the flux through the interface in the original MTWCR model [158], but here it refers to extraction of a three-valent metal with strongly acidic extractant. It is clear, that in the case of weak acid extractant, when $K_a \to 0$, the term

$$\frac{\mathcal{D}_{\mathrm{R}^-} K_a}{C_{i_{\mathrm{H}^+}}}$$

will be negligibly small compared to $\mathcal{D}_{\mathrm{HR}}$ since $\mathcal{D}_{\mathrm{R}^-}$ and $\mathcal{D}_{\mathrm{HR}}$ are of the same order of magnitude. Hence, eqn (C.47) will become the same as the originally developed flux equation [158], but for a three-valent metal:

$$J_{i_{\mathrm{HR}}} = \sqrt{\frac{k_f K_a \mathcal{D}_{\mathrm{HR}}}{P_{\mathrm{HR}}^2} \frac{C_{i_{\mathrm{Ga}^{3+}}}}{C_{i_{\mathrm{H}^+}}} \left(1 - \frac{1}{K'} \frac{\overline{C}_{i_{\mathrm{GaR_3}}} C_{i_{\mathrm{H}^+}}^3}{C_{i_{\mathrm{Ga}^{3+}}} \overline{C}_{i_{\mathrm{HR}}}^3} \right) \left(\overline{C}_{i_{\mathrm{HR}}}^2 - P_{\mathrm{HR}}^2 C_{0_{\mathrm{HR}}}^2 \right)} \tag{C.48}$$

Pseudo-first Order Reversible Reaction

From eqns (6.31), (6.37), and (C.22) it follows that

$$\left(\mathcal{D}_{\mathrm{HR}} + \frac{\mathcal{D}_{\mathrm{R}} - K_a}{C_{\mathrm{H}^+}}\right)\frac{dC_{\mathrm{HR}}}{dx} + 3\mathcal{D}_{\mathrm{GaR_3}}\frac{dC_{\mathrm{GaR_3}}}{dx} = 0 \tag{C.49}$$

Integrating eqn (C.49) for x from zero to $0 < x < \delta$ and solving for $C_{\mathrm{GaR_3}}$ yields

$$C_{\mathrm{GaR_3}} = C_{\mathrm{GaR_3}} + \frac{\left(\mathcal{D}_{\mathrm{HR}} + \frac{\mathcal{D}_{\mathrm{R}} - K_a}{C_{\mathrm{H}^+}}\right)}{3\mathcal{D}_{\mathrm{GaR_3}}}(C_{\mathrm{HR}} - C_{\mathrm{HR}}) \tag{C.50}$$

In the case when $K_a \rightarrow 0$ eqn (C.50) will become

$$C_{\mathrm{GaR_3}} = C_{\mathrm{GaR_3}} + \frac{\mathcal{D}_{\mathrm{HR}}}{3\mathcal{D}_{\mathrm{GaR_3}}}(C_{\mathrm{HR}} - C_{\mathrm{HR}}) \tag{C.51}$$

Substitution of $C_{\mathrm{GaR_3}}$ from eqn (C.50) in eqn (6.38), which applies to the pseudo-first order reaction regime, gives

$$\mathcal{D}_{\mathrm{HR}}\frac{d^2C_{\mathrm{HR}}}{dx^2} = k_f K_a \frac{C_{\mathrm{HR}}}{C_{\mathrm{H}^+}}\left\{C_{\mathrm{Ga^{3+}}} - \frac{\left[C_{\mathrm{GaR_3}} + \frac{\mathcal{D}'}{3\mathcal{D}_{\mathrm{GaR_3}}}(C_{\mathrm{HR}} - C_{\mathrm{HR}})\right]C^3_{\mathrm{H}^+}}{K_{\mathrm{eq}}C^3_{\mathrm{HR}}}\right\} \tag{C.52}$$

and then after rearranging for C_{HR} in a convenient for integration form:

$$\mathcal{D}_{\mathrm{HR}}\frac{d^2C_{\mathrm{HR}}}{dx^2} = uC_{\mathrm{HR}} - v\frac{1}{C^2_{\mathrm{HR}}} + w\frac{1}{C_{\mathrm{HR}}} \tag{C.53}$$

where

$$u = \frac{k_f K_a C_{\mathrm{Ga^{3+}}}}{C_{\mathrm{H}^+}}$$

$$v = \frac{k_f K_a C^2_{\mathrm{H}^+}}{K_{\mathrm{eq}}}\left(C_{\mathrm{GaR_3}} + \frac{\mathcal{D}'C_{\mathrm{HR}}}{3\mathcal{D}_{\mathrm{GaR_3}}}\right)$$

$$w = \frac{k_f K_a \mathcal{D}' C^2_{\mathrm{H}^+}}{3\mathcal{D}_{\mathrm{GaR_3}}K_{\mathrm{eq}}}$$

Using again the same transformation of variables (eqn C.39), and boundary conditions for ψ (eqns C.41 and C.42) and C_{HR} (eqns 6.33 and 6.34) integration of eqn (C.53) yields

$$J^2_{\mathrm{HR}} = \frac{\mathcal{D}'^2 u}{\mathcal{D}_{\mathrm{HR}}}\left(C^2_{\mathrm{HR}} - C^2_{0_{\mathrm{HR}}}\right) - \frac{2\mathcal{D}'^2 v}{\mathcal{D}_{\mathrm{HR}}}\left(\frac{1}{C_{0_{\mathrm{HR}}}} - \frac{1}{C_{\mathrm{HR}}}\right) + \frac{2\mathcal{D}'^2 w}{\mathcal{D}_{\mathrm{HR}}}\ln\frac{C_{\mathrm{HR}}}{C_{0_{\mathrm{HR}}}} \tag{C.54}$$

From this eqn (C.54) after rearrangement, the result for $J_{t_{HR}}$ is

$$J_{t_{HR}} = \sqrt{\frac{\mathcal{D}'^2}{\mathcal{D}_{HR}}\left[u\left(C^2_{t_{HR}} - C^2_{0_{HR}}\right) + 2w\ln\frac{C_{t_{HR}}}{C_{0_{HR}}} - 2v\left(\frac{1}{C_{0_{HR}}} - \frac{1}{C_{t_{HR}}}\right)\right]} \qquad \text{(C.55)}$$

where, again, $C_{t_{HR}}$ and $C_{t_{GaR_3}}$ can be substituted from eqn (C.14) and K_{eq} expressed by K', introduced from eqn (6.21). Also, in the case when $K_a \to 0$, eqn (C.55) will become

$$J_{t_{HR}} = \sqrt{\mathcal{D}_{HR}\left[u\left(C^2_{t_{HR}} - C^2_{0_{HR}}\right) + 2w\ln\frac{C_{t_{HR}}}{C_{0_{HR}}} - 2v\left(\frac{1}{C_{0_{HR}}} - \frac{1}{C_{t_{HR}}}\right)\right]} \qquad \text{(C.56)}$$

Finally, in the case when only the forward reaction is considered and the backward reaction neglected, which is possible under conditions of initial extraction rates, then the expression for $J_{t_{HR}}$ can be derived in the same way as eqn (C.47) starting from eqn (6.40). After integration of eqn (6.40) the end result is

$$J_{t_{HR}} = \sqrt{\frac{\left(\mathcal{D}_{HR} + \frac{\mathcal{D}_R - K_a}{C_{t_{H+}}}\right)^2}{\mathcal{D}_{HR}P^2_{HR}} k_f K_a \frac{C_{t_{Ga^{3+}}}}{C_{t_{H+}}}\left(\overline{C}^2_{t_{HR}} - P^2_{HR}C^2_{0_{HR}}\right)} \qquad \text{(C.57)}$$

Since eqn (6.40) is the same for both limiting regimes, it follows that the resulting eqn (C.57) will also be applicable to both of them as far as the conditions of initial extraction rates are met.

Steps 5 or 6 being rate-limiting

In a similar way, as demonstrated above, for the reaction schemes where step 5 or step 6 are rate-limiting, the appropriate expressions for $J_{t_{HR}}$ can be obtained from the derived rate equations (6 27) and (eqn 6.28), respectively

Thus, for the limiting regime of instantaneous reversible reaction the following equations result—when the second organic ligand addition (step 5) is the rate-limiting step—

$$J_{t_{HR}} = \sqrt{\frac{2\mathcal{D}'^2}{3\mathcal{D}_{HR}P^3_{HR}} k_f K_I K_a^2 \frac{C_{t_{Ga^{3+}}}}{C^2_{t_{H+}}}\left(1 - \frac{1}{K'}\frac{\overline{C}_{t_{GaR_3}}C^3_{t_{H+}}}{C_{t_{Ga^{3+}}}\overline{C}^3_{t_{HR}}}\right)\left(\overline{C}^3_{t_{HR}} - P^3_{HR}C^3_{0_{HR}}\right)} \qquad \text{(C.58)}$$

and in the case of third organic ligand addition (step 6) being rate-limiting:

$$J_{i_{HR}} = \sqrt{\frac{\mathcal{D}'^2}{2\mathcal{D}_{HR}P_{HR}^4}\frac{k_f K_{eq}}{K_{III}}\frac{C_{i_{Ga^{3+}}}}{C_{i_{H+}}^3}\left(1-\frac{1}{K'}\frac{\overline{C}_{i_{GaR_3}}C_{i_{H+}}^3}{C_{i_{Ga^{3+}}}\overline{C}_{i_{HR}}^3}\right)\left(\overline{C}_{i_{HR}}^4 - P_{HR}^4 C_{0_{HR}}^4\right)} \quad \text{(C.59)}$$

The comparison between the respective flux equations (C.46), (C.58), and (C.59) for a certain step being RLS show that the main differences are in the dependence of the flux $J_{i_{HR}}$ on acidity and extractant concentration

Furthermore, when the backward reaction is neglected, i.e., initial extraction rates are experimentally considered, then expressions for $J_{i_{HR}}$ when steps 5 or 6 are RLS can be developed in a way similar to the derivation of eqn (C.57). Thus, when step 5 is the RLS then the resulting expression for $J_{i_{HR}}$ is

$$J_{i_{HR}} = \sqrt{\frac{2\mathcal{D}'^2}{3\mathcal{D}_{HR}P_{HR}^3}k_f K_1 K_a^2\frac{C_{i_{Ga^{3+}}}}{C_{i_{H+}}^2}\left(\overline{C}_{i_{HR}}^3 - P_{HR}^3 C_{0_{HR}}^3\right)} \quad \text{(C.60)}$$

and when step 6 is rate-limiting:

$$J_{i_{HR}} = \sqrt{\frac{\mathcal{D}'^2}{2\mathcal{D}_{HR}P_{HR}^4}\frac{k_f K_{eq}}{K_{III}}\frac{C_{i_{Ga^{3+}}}}{C_{i_{H+}}^3}\left(\overline{C}_{i_{HR}}^4 - P_{HR}^4 C_{0_{HR}}^4\right)} \quad \text{(C.61)}$$

References

[1] Peaker, A.R., 1990. In: *Properties of Gallium Arsenide*, EMIS Datareviews Series No.2, publ. by INSPEC, The Institution of Electrical Engineers, London and New York, 1990, p. iv.

[2] Grant, I., 1988. *Trans. IMM sect. C*, 97: C48-C52

[3] Katrak, F. and Agarwal, J., 1981. *J. Metals*, 33(9): 33-36

[4] Highley, D., Slater, D. and Chapman, G., 1988. *Trans. IMM section C*, 97: C34-C42.

[5] Olsen, T.M., Voelker, D.E. and Smith, R.A., 1988. In: *Symp. on Precious and Rare Metal Technology*, Albuquerque, N.M., pp. 531-545

[6] Sheka, I.A., Chaus, I.S. and Mityureva, T.T., 1966. *The Chemistry of Gallium*, Elsevier, Amsterdam, pp. 8-14, 220-223.

[7] Neylan, D.L., Walters, C.P. and Haynes, B.W., 1985. In: *Symp. on Recycle and Secondary Recovery of Metals*, AIME, Fort Lauderdale, Florida, pp. 727-733.

[8] Michelsen, O.B., 1988. In: *Proc. Int. Solv. Extr. Conf.*, ISEC'88, Moscow, 4: pp. 259-264.

[9] Cotton, F.A. and Wilkinson, G.W., 1966. *Advanced Inorganic Chemistry*, 2nd ed., Interscience Publishers, pp. 103, 152-165, 443-444.

[10] Hudson, L.K., 1965. *J. Metals*, 17(9): 948-951

[11] Bretèque, P., 1956. *J. Metals*, 8(11) 1528-1529.

[12] Helgorsky, J. and Leveque, A., 1976 U.S Pat 3,971,843

[13] Monhemius, A.J., 1980. In: *Topics in non-ferrous extractive metallurgy*, A.R. Burkin (Editor), Blackwell Scientific Publications, pp. 104-130.

[14] Hoffmann, J E , 1989. In: *24th Sir Julius Wernher Memorial Lecture, 'Extraction Metallurgy'89*, IMM, London, pp. 5-16.

[15] Zhou, T., Zhong, X and Zheng, L , 1989 *J. Metals*, 41(6): 36-40.

[16] Baldwin, W G., Bock, E , Chow, A , Gesser, H.D., McBride, D.W. and Vaidya, O., 1980. *Hydrometallurgy*, 5: 213-225.

[17] Tsuboi, I., Kasai, S., Kunugita, E. and Komasawa, I., 1991. *J. Chem. Eng. Japan*, 24(1): 15-20.

[18] Leveque, A. and Helgorsky, J., 1977. In: *Proc. Int. Solv. Extr. Conf.*, ISEC'77, Toronto, pp. 439-442.

[19] Sato, T., 1986. In: *Int. Conf. Sep. Sci. Technol.*, New York, N.Y., 1: pp. 285-294.

[20] Sato, T. and Oishi, H., 1986. *Hydrometallurgy*, 16. 315-324.

[21] Sato, T., Nakamura, T. and Oishi, H., 1984. *Solv. Extn. Ion Exch.*, 2(1): 45-60.

[22] Sato, T., Nakamura, T., Yabuta, M. and Oishi, H., 1982. *Chem. Lett.*, 591-592.

[23] Sato, T., Nakamura, T., Oishi, H. and Yabuta, M , 1984. In: *Symp. on Solv. Extr.*, Hamamatsu, Japan, pp. 13-18

[24] Bauer, D. and Coté, G., 1988. In: *Proc Int. Conf Hydrometallurgy*, ICHM'88, Zheng Yulian and Xu Jiazhong (Editors), China, pp. 545-549

[25] Coté, G. and Bauer, D., 1986 In *Proc Int Solv Extr Conf*. ISEC'86, Munich, pp. 463-470.

[26] Pesic, B and Zhou, T., 1988. *J. Metals*, 40(7): 24 26.

[27] Helgorsky, J. and Leveque, A., 1981. Can Pat 1,099,522

[28] Helgorsky, J. and Leveque, A., 1982 Can Pat 1,117,767

[29] Fourré, P., Bauer, D. and Lemerle, J., 1983. *Anal. Chem* , 55 662 667

[30] Fourré, P. and Bauer, D., 1983 *Solv Extn. Ion Exch* , 1(3) 465 483.

[31] Helgorsky, J. and Leveque, A., 1981 Can Pat 1,106,611

[32] Bauer, D., Fourré, P. and Sabot, J , 1985. U S Pat. 4,559,203

[33] Wynn, N P. and Zabelka, M., 1985 Eur Pat. Appl. EP 143,719 *Chemical Abstracts*, 103. 57200q.

[34] Bauer, D., Fourré, P. and Sabot, J , 1985 Can Pat. 1,203.386.

[35] Uhlemann, E. and Mickler, W., 1981. *Anal Chim. Acta*, 130 177 182

[36] Bauer, D. and Pescher-Cluzeau, Y., 1987. *Hydrometallurgy*. 18 243 253.

[37] Pescher-Cluzeau, Y. and Bauer, D., 1986. In: *Proc. Int Solv Extr. Conf.*, ISEC'86, Munich, pp. 503–509.

[38] Uhlemann, E. and Weber, W., 1984. *Anal Chim. Acta*, 156 201-206

[39] De La Bretèque, P. and Beerli, M , 1975 U S. Pat 3,887,681

[40] Swift, E.H , 1924. *J. Am. Chem Soc* , 46: 2375-2381.

[41] Brooks, R.R and Lloyd, P.J., 1961. *Nature*, 189 375-376

[42] Irving, H.M. and Rossotti, F.J.C., 1952 *Analyst*, 77: 801 812

[43] Nachtrieb, N H. and Fryxell, R E , 1949. *J Am. Chem Soc.*, 71: 4035-4039.

[44] Powell, A.R , 1954 *Nature*, # 4431: 627-629.

[45] Powell, A.R , Lever, F.M. and Walpole, R E , 1951. *J. Appl Chem.*, 1: 541-551.

[46] Thompson, A P. and Harner, H R., 1951 *J Metals*, 191: 91-94.

[47] Good, M L and Holland, F.F , 1961. *J. Inorg Nucl Chem.*, 26: 321-327.

[48] Good, M.L. and Srivastava, S C., 1965. *J. Inorg. Nucl. Chem.*, 27: 2429-2436.

[49] Sato, T , Nakamura, T. and Ishikawa, S , 1984. *Solv. Extn Ion Exch.*, 2(2): 201 212.

[50] Sekine, T. and Hasegawa, Y., 1977. *Solvent Extraction Chemistry: Fundamentals and Applications*, Marcel Dekker, pp 219, 233-235, 432.

[51] Good, M.L., Srivastava, S.C. and Holland, F F., 1964 *Anal Chim. Acta*, 31: 534-544.

[52] Bhat, T.R and Sundararajan, S., 1967. *J Less Common Metals*, 12: 231-238.

[53] De, A K. and Sen, A.K., 1967. *Talanta*, 14. 629-635.

[54] Ishimori, T., Watanabe, K. and Nakamura, E., 1960 *Bull. Chem. Soc. Japan*, 33: 636-644.

[55] Reznik, A.M., Glubokov, Y.M. and Dimitrova, I.A., 1976. *Russ. J. Inorg. Chem* , 21. 1688-1689.

[56] Reznik, A.M. and Zekel, L , 1979 *Russ. J Inorg Chem.*, 24: 567-571.

[57] Judin, V.P. and Bautista, R.G., 1986. *Metall. Trans. B*, 17B: 259-265.

[58] Hasegawa, Y., Shimada, T. and Nitsu, M., 1980. *J. Inorg. Nucl Chem.*, 42: 1487 1489.

[59] Mitchell, J.W. and Riley, J E , 1975 *Talanta*, 22 567 570

[60] Levin, I.S., Shatalova, A A , Azarenko, T G , Vorsina, I A , Burtovaya-Balakireva, N.A. and Rodina, T.F., 1967. *Talanta*, 14 801 808.

[61] Levin, I.S., Burtovaya-Balakireva, N A and Vorsina, I A , 1968 *Russ J Inorg. Chem.*, 13(3): 450-451.

[62] Levin, I. and Balakireva, N , 1970 Talanta, 17 915 921.

[63] Sato, T., Horie, J. and Nishimura, T , 1987. In *Symp on Solv Extr* , Osaka, Japan, pp 131-136

[64] Kimura, K., 1960. *Bull. Chem. Soc. Japan*, 33: 1038 1046

[65] Kimura, K., 1961. *Bull. Chem Soc. Japan*, 34 63 68.

[66] De, A.K. and Ray, U.S., 1972. *Sep. Sci.*, 7 409-417.

[67] Katsura, T. and Abe, H., 1975. U.S Pat 3,920,450.

[68] Milner, G.W.C , Wood, A.J. and Woodhead, J.L., 1954. *Analyst*, 79: 272-279.

[69] Rafaeloff, R., 1971. *Anal. Chem.*, 43 272-274.

[70] Zangen, M. and Rafaeloff, R., 1970. *J Inorg Nucl Chem* , 32 2753 2758.

[71] Inoue, K., Baba, Y. and Yoshizuka, K , 1988. *Solv Extn Ion Exch.*, 6(3): 381-392.

[72] Inoue, K., Baba, Y. and Yoshizuka, K., 1988. In: *Symp. on Solv. Extr.*, Tokyo, Japan, pp. 31-36.

[73] Inoue, K. and Nakayama, D., 1984 In *Symp on Solv. Extr.*, Hamamatsu, Japan, pp. 19-24.

[74] Sato, T. and Sato, K., 1988. In: *Symp. on Solv. Extr.*, Tokyo, Japan, pp. 85-90.

[75] Tian Run-cang, Zou Jia-yan and Zhou Ling-zhi, 1981 In. *Symp on Mineral Processing and Extractive Metallurgy*. IMM, Kunming, China, pp. 615-624.

[76] Kikuchi, S. and Kamagami, S., 1984 In *Symp on Solv. Extr.*, Hamamatsu, Japan, pp. 25-28

[77] Kikuchi, S. and Kamagami, S., 1987. In. *Symp. on Solv. Extr* , Osaka, Japan, pp. 127 130.

[78] Judd, J.C. and Harbuck, D.D., 1990. SME Annual Meeting, Salt Lake City, Utah, Paper 90-147.

[79] Haraguchi, K and Freiser, H., 1983 *Inorg Chem.*, 22: 1187–1190.

[80] Slater, M.J., 1987. *The Possible Use of D2EHPA/Metal as a Liquid-liquid Extraction Test System*, Paper presented to the EFCE Working Party meeting, Prague, April 1987.

[81] Partridge, J., and Jensen, R., 1969 *J Inorg Nucl Chem.*, 31: 2587–2589.

[82] Acharya, S. and Nayak, A , 1988 *Hydrometallurgy*, 19. 309–320.

[83] Albery, W.J. and Fisk, P.R., 1981 In *Hydrometallurgy'81*, Soc. Chem. Ind., London, F5. 1-15.

[84] Albery, W.J., Choudhery, R.A. and Fisk, P.R., 1984. *Faraday Discuss. Chem. Soc.*, 77: 53-65.

[85] Albery, W.J., Burke, J F., Leffler, E.B. and Hadgraft, J., 1976. *J. Chem. Soc., Faraday Trans. 1*, 72. 1618-1626

[86] Dreisinger, D B and Cooper, W.C , 1986. *Solv. Extn. Ion Exch.*, 4(1): 135–147.

[87] Dreisinger, D.B and Cooper, W.C., 1986. *Solv. Extn. Ion Exch.*, 4(2): 317–344.

[88] Dreisinger, D.B., Cooper, W.C. and Distin, P A., 1989. *Int. Conf. Sep. Sci. Technol.*, Hamilton, Ontario, Paper No S3-1b

[89] Dreisinger, D.B. and Cooper, W.C , 1989. *Solv. Extn Ion Exch* , 7(2): 335 360.

[90] Chow, A. and Lipinsky, W., 1975. *Anal Chim Acta*, 75 87 91

[91] Meites, L. (Editor) 1963. *Handbook of Analytical Chemistry*, McGraw-Hill, New York, NY, pp. 146-149.

[92] Peppard, D.F., Ferraro, J.R. and Mason, G W., 1958 *J Inory Nucl. Chem.*, 7: 231-244.

[93] Peppard, D.F., Ferraro, J.R. and Mason, G.W., 1959. *J Inory. Nucl. Chem.*, 12: 60-70.

[94] Ferraro, J.R., Mason, G.W. and Peppard, D F., 1961. *J. Inory Nucl. Chem.*, 22: 285-291.

[95] Rao, G.S., Mason, G.W. and Peppard, D.F., 1966. *J. Inorg Nucl. Chem.*, 28: 887-897.

[96] Ritcey, G.M. and Ashbrook, A W., 1984. *Solvent Extraction Principles and Applications to Process Metallurgy*, Part I, Elsevier, Amsterdam, pp. 73 76.

[97] Danesi, P.R. and Vandegrift, G.F., 1981, *Inorg Nucl Chem Letters*, 17(3/4): 109-115.

[98] Sastre, A.M. and Muhammed, M., 1984. *Hydrometallurgy*, 12: 177-193.

[99] Sastre, A.M., Miralles, N. and Figuerola, E., 1990 *Solv. Extn. Ion Exch.*, 8(4&5): 597-614.

[100] McDowell, W.J. and Coleman, C.F., 1965. *J Inorg. Nucl. Chem.*, 27: 1117-1139.

[101] Sekine, T. and Dyrssen, D., 1964. *J. Inorg. Nucl Chem* , 26: 2013-2022.

[102] Sekine, T. and Dyrssen, D., 1967. *J. Inorg. Nucl Chem.*, 29 1489 1498

[103] Hála, J., 1979. *J. Radioanal Chem.*, 51(1) 15-25.

[104] Högfeldt, E. (compiled by) 1982. *Stability Constants of Metal-Ion Complexes. Part A: Inorganic Ligands*, IUPAC Chemical Data Series, No. 21, Pergamon Press, pp. 119-127.

[105] Hildebrand, J.H , Prausnitz, J M and Scott, R.L., 1970. *Regular and Related Solutions The Solubility of Gases, Liquids, and Solids*, Van Nostrand Reinhold Co., pp 85 88.

[106] Teng Teng, Li Yi-gui, Han Jin-wen and Ding Hong-bing, 1983. In: *Proc. Int. Solv. Extr Conf.*, ISEC'83, Denver, Colorado, pp 546-547.

[107] Teng Teng, Yi-Gue Li, Zhen-Hua Cheng and Liang-Ping Zhang, 1983. In: *Chemical Engineering Thermodynamics*, S. Newman (Editor), Ann Arbor Science, pp. 417-428.

[108] Yi-gui Li, Jiu fang Lu, Zong-cheng Li, Tie-zhu Bao, Ji-ding Li and Teng Teng, 1987. In. *Separation Processes in Hydrometallurgy*, G.A. Davies (Editor), E. Horwood Ltd , pp. 238-247

[109] Yi-gui Li, Jiu-fang Lu, Zong-cheng Li, Ji-ding Li, Gang Chen and Teng Teng, 1988 In: *Proc Int Conf. Hydrometallurgy*, ICHM'88, Zheng Yuhan and Xu Jiazhong (Editors), China, pp. 32–36.

[110] Fredenslund, A., Jones, R.L. and Prausnitz, J M., 1975. *AIChE J.*, 21(6): 1086–1099.

[111] March, J., 1968 *Advanced Organic Chemistry: Reactions, Mechanisms, and Structure*, McGraw-Hill Co., pp. 3-27, 217–230.

[112] Peppard, D.F., Mason, G.W. and Hucher, I , 1961. *J. Inorg. Nucl. Chem.*, 18: 245–258.

[113] Blake, C.A. Jr, Baes, C F. Jr, Brown, K B , Coleman,C F and White, J.C , 1958. In: *Proc. U.N. 2nd Int Conf Peaceful Uses Atomic Energy*, Geneva, vol. 28, pp. 289-298.

[114] Smith, J.M., 1981. *Chemical Engineering Kinetics*, McGraw-Hill Co , pp. 392 394.

[115] Sato, T., Yoshino, T., Nakamura, T. and Kudo, T , 1978 *J Inorg Nucl. Chem.*, 40: 1571–1574.

[116] Sato, T., Yoshino, T., Nakamura, T. and Kudo, T , 1979. *J Inorg. Nucl. Chem.*, 41: 731–734.

[117] Flett, D.S., Okuhara, D.N. and Spink, D R., 1973 *J Inorg Nucl. Chem.*, 35: 2471–2487.

[118] Baes, C.F. Jr and Mesmer, R.E., 1976. *The Hydrolysis of Cations*, Wiley Interscience, New York, pp. 313–319.

[119] Kotrlý, S. and Šucha, L., 1985. *Handbook of Chemical Equilibria in Analytical Chemistry*, E. Horwood Ltd , p. 128.

[120] Dean, J.A. (Editor), 1979. *Lange's Handbook of Chemistry*, 12th ed , McGraw-Hill Co., p. 5-51.

[121] Smith, R.M. and Martell, A.E., 1974 *Critical Stability Constants. Volume 4: Inorganic Complexes*, Plenum Press, New York, p. 11

[122] Nazarenko, V A, Antonovich, V P and Nevskaya, E M , 1968 *Russ J Inorg Chem* , 13(6): 825–828.

[123] Biryuk, E.A. and Nazarenko, V.A, 1973. *Russ J Inorg. Chem* , 18(11): 1576 1578.

[124] Harris, W.R. and Martell, A E , 1976 *Inorg Chem* , 15(3): 713 720

[125] Martell, A.E., Motekaitis, R J and Smith, R.M , 1990. *Polyhedron*, 9(2/3): 171-187.

[126] Öhman L.O., 1990. *Polyhedron*, 9(2/3) 199-205.

[127] Izatt, R.M., Eatough, D., Christensen, J.J and Bartholomew, C.H., 1969. *J. Chem. Soc. (A)*: 47-53.

[128] Kalidas, C., Knoche, W. and Papadopoulos, D., 1971. *Ber. Bunsen-Gesellschaft*, 75(2): 106-110.

[129] Nanda, R.K. and Aditya, S., 1962 *Z. Physik Chem.* (Frankfurt), 35: 139-145. *Chemical Abstracts*, 58, 8452f.

[130] Shishkova, L., 1978 *Dokl. Bolg. Acad. Nauk*, 31(7): 845-848.

[131] Shishkova, L., 1978. *God. Vissh. Minno-Geol. Inst., Sofia*, 24 (Pt. 3): 369-376.

[132] Shishkova, L., 1980. *Dokl. Bolg. Acad Nauk*, 33(6): 815-818.

[133] Marshall, W.L. and Jones, E V , 1966 *J Phys. Chem.*, 70(12): 4028-4040.

[134] Crundwell, F.K., 1987 *Hydrometallurgy*, 19: 227-234.

[135] Pouillon, D. and Doyle, F.M , 1987 *Metall Trans. B*, 18B 743-746.

[136] Tananaev, I.V. and Bolshakova, N K, 1962. *Russ. J. Inorg. Chem.*, 7(9): 1159-1162, 1162-1165.

[137] Fiat, D. and Connick, R.E., 1968. *J. Am. Chem. Soc.*, 90(3): 608-615.

[138] Miceli, J. and Stuehr, J., 1968. *J. Am Chem. Soc.*, 90(25): 6967-6972.

[139] Yamada, S., Iwanaga, A., Funahashi, S. and Tanaka, M., 1984. *Inorg. Chem.*, 23(22): 3528-3532.

[140] Akitt, J.W., Greenwood, N.N. and Khandelwal, B.L., 1972. *J. Chem. Soc., Dalton Trans* : 1226-1229

[141] Akitt, J.W. and Farnsworth, J.A., 1985 *J Chem. Soc , Faraday Trans 1*, 81: 193-205

[142] Zangen, M. and Rafaeloff, R., 1970. *J. Inorg Nucl. Chem* , 32: 2753 2758.

[143] Zangen, M. and Rafaeloff, R., 1970 *Sep Sci* , 5(1): 77-81.

[144] Vasilev, V.P., 1962. *Russ. J Inorg Chem.*, 7(8) 921 927

[145] Vasilev, V.P. and Vasileva, V.N., 1977. *Russ. J Inorg Chem* , 22(5) 633 636.

[146] Ting-Po I and Nancollas, G.H., 1972. *Anal. Chem* , 44(12)· 1910-1950.

[147] Das, K., 1988. *J. Solution Chem* , 17(4)· 327-336

[148] Weast, R.C. (Editor), 1987. *CRC Handbook of Chemistry and Physics*, 67th ed., CRC Press Inc., p. D-151.

[149] Nitsch, W., 1984. *Faraday Discuss. Chem Soc* , 77· 85 96

[150] Osseo-Asare, K., 1984. In: *Hydrometallurgical Process Fundamentals*, R.G. Bautista (Editor), Plenum Press, New York, pp. 357 405

[151] Whewell, R.J., Hughes, M.A. and Hanson, C , 1977. In *Proc Int Solv. Extr. Conf* , ISEC'77, Toronto, pp 185 192

[152] Carter, S.P. and Freiser, H , 1980 *Anal Chem.*, 52 511-514

[153] Akiba, K. and Freiser, H., 1982. *Anal. Chim. Acta*, 136. 329-337.

[154] Perez de Ortiz, E S., Cox, M and Flett, D.S., 1977. In *Proc. Int Solv. Extr. Conf.*, ISEC'77, Toronto, pp. 198-203

[155] Miyake, Y., Takenoshita, Y. and Teramoto, M., 1983. *J. Chem. Eng. Japan*, 16(3): 203–209.

[156] Harada, M., Miyake, Y., and Kayahara, Y., 1989. *J Chem. Eng. Japan*, 22(2): 168–177

[157] Freiser, H., 1988. *Chem Rev*, 88 611-616.

[158] Hughes, M A and Rod, V, 1984 *Faraday Discuss. Chem Soc.*, 77: 75-84.

[159] Watarai, H, Takahashi, M. and Shibata, K., 1986. *Bull. Chem. Soc. Japan*, 59: 3469 3173

[160] Chaiko, D.J and Osseo-Asare, K, 1988. *Sep Sci. Technol*, 23(12&13): 1423-1434.

[161] Szymanowski, J. and Prochaska, K., 1987. In: *Separation Processes in Hydrometallurgy*, G.A. Davies (Editor), E. Horwood Ltd., pp 199-206.

[162] Prochaska, K and Szymanowski, J, 1988. In. *Proc. Int Conf. Hydrometallurgy*, ICHM'88, Zheng Yuhan and Xu Jiazhong (Editors), China, pp. 189-193.

[163] Stepniak-Biniakiewicz, D., Szymanowski, J, Alejski, K. and Prochaska, K., 1990. *Solv. Extn Ion Exch*, 8(3): 425-444.

[164] Vandegrift, G.F. and Horwitz, E P., 1980. *J. Inorg. Nucl. Chem.*, 42: 119-125.

[165] Danesi, P.R and Vandegrift, G F., 1981. *J. Phys. Chem.*, 85. 3646-3651.

[166] Qian Yu, Jing-fen Yu, Jiufang Lu and Teng Teng 1988 In: *Proc. Int. Conf. Hydrometallurgy*, ICHM'88, Zheng Yulian and Xu Jiazhong (Editors), China, pp. 83-87.

[167] Danesi, P.R, 1984. *Solv. Extn. Ion Exch.*, 2(1): 29-44.

[168] Osseo-Asare, K., 1988 In: *Proc. Int. Conf. Hydrometallurgy*, ICHM'88, Zheng Yuhan and Xu Jiazhong (Editors), China, pp. 6-10.

[169] Gaonkar, A.G. and Neuman, R.D., 1987. *J. Colloid Interface Sci.*, 119(1): 251-261.

[170] Atkins, P.W., 1980. *Physical Chemistry*, Russ. Transl., Mir, Moscow, vol. 1, p. 265.

[171] Gaonkar, A.G. and Neuman, R.D., 1984. *J Colloid Interface Sci*, 98(1): 112-119.

[172] Danesi, P.R. and Chiarizia, R., 1977. In *Proc Int Solv. Extr Conf.*, ISEC'77, Toronto, pp. 219-227.

[173] Harada, M. and Miyake, Y., 1986. *J. Chem Eng. Japan*, 19(3). 196-207.

[174] Yoshizuka, K., Kondo, K. and Nakashio, F., 1985. *J Chem Eng. Japan*, 18(2): 163-168.

[175] Sato, Y., Akiyoshi, Y., Kondo, K. and Nakashio, F., 1989. *J Chem. Eng. Japan*, 22(2): 182-189.

[176] Kondo, K., Tsuneyuki, T., Hiramatsu, K. and Nakashio, F., 1990. *Sep. Sci Technol.*, 25(11&12): 1213-1224

[177] Atkins, P.W., 1980. *Physical Chemistry*, Russ. Transl., Mir, Moscow, vol. 2, p. 509.

[178] Ajawin, L.A., Perez de Ortiz, E.S and Sawistowski, H., 1983 *Chem Eng Res. Des.*, 61: 62-66.

[179] Ajawin, L.A., Demetriou, J., Perez de Ortiz, E S and Sawistowski, H., 1984. In: *Extraction'84*, The Institution of Chemical Engineers, Symp. Ser. No. 88, pp. 183-191.

[180] Hirato, T. and Toguri, J.M., 1988. In: *Symp. on Precious and Rare Metal Technology*, Albuquerque, N.M., pp. 461-471

[181] Hughes, M.A and Biswas, R.K., 1991. *Hydrometallurgy*, 26: 281-297.

[182] Miyake, Y., Matsuyama, H., Nishida, M., Nakai, M, Nagase, N and Teramoto, M., 1990. *Hydrometallurgy*, 23: 19-35.

[183] Matsuyama, H., Miyake, Y., Izumo, Y. and Teramoto, M., 1990. *Hydrometallurgy*, 24: 37–51.

[184] Ipinmoroti, K.O. and Hughes, M.A., 1990. *Hydrometallurgy*, 21: 255-262.

[185] Hughes, M.A. and Rod, V., 1984. *Hydrometallurgy*, 12: 267–273.

[186] Rod, V., 1988. In: *Proc. Int Solv. Extr. Conf*, ISEC'88, Moscow, 3: pp. 4–9.

[187] Harada, M., Mori, M., Adachi, M., and Eguchi, W., 1983. *J. Chem. Eng. Japan*, 16(3): 193–202.

[188] Danesi, P.R., Chiarizia, R. and Saltelli, A., 1976. *J. Inorg. Nucl. Chem.*, 38: 1687–1693.

[189] Cianetti, C. and Danesi, P.R., 1983. *Solv. Extn. Ion Exch.*, 1(1): 9–26.

[190] Komasawa, I., Otake, T. and Higaki, Y., 1981. *J. Inorg. Nucl. Chem.*, 43(12): 3351–3356.

[191] Ting-Chia Huang and Ruey-Shin Juang, 1986. *Ind. Eng. Chem. Fundam.*, 25: 752–757.

[192] Xun Fu, Zhengshui Hu, Yide Liu and Golding, J.A., 1990. *Solv Extn. Ion Exch.*, 8(4&5): 573–595.

[193] Savastano, C.A., Perez de Ortiz, E.S. and Osseo-Asare, K., 1990. *Solv. Extn. Ion Exch.*, 8(3): 401–423.

[194] Osseo-Asare, K., 1988. *Colloids and Surfaces*, 33. 209–215.

[195] Mendes Tatsis, M.A. and Perez de Ortiz, E.S., 1986. In: *Proc. Int. Solv. Extr. Conf.*, ISEC'86, Munich, pp. 27–33.

[196] Eigen, M., 1963. *Pure and Appl. Chem.*, 6: 97–115.

[197] Rod, V., 1980. *Chem. Eng. J.*, 20: 131–137.

[198] Rod, V., Strnadová, L., Hančil, V. and Šír, Z., 1981. *Chem. Eng. J.*, 21: 187–193.

[199] Sherwood, T.K., Pigford, R.L. and Wilke, C.R., 1982. *Mass Transfer*, Russ. Transl., Chimia, Moscow, pp. 342–355.

[200] Astarita, G., 1967. *Mass Transfer with Chemical Reaction*, Elsevier, Amsterdam, pp. 4–22, 63–76.

[201] Cussler, E.L., 1984. *Diffusion: Mass Transfer in Fluid Systems*, Cambridge University Press, Cambridge, pp. 346–350.

[202] Perry, J.H., 1973. *Chemical Engineers' Handbook*, 5th ed., McGraw Hill, 3-225-3-235.

[203] Hughes, M.A. and Abid, K.H., 1988. In: *Proc. Int. Conf. Hydrometallurgy*, ICHM'88, Zheng Yulian and Xu Jiazhong (Editors), China, pp. 163–167.

[204] Basolo, F. and Johnson, R.C., 1986. *Coordination Chemistry*, 2nd ed., Science Reviews, pp. 97–111.

[205] Hugi-Cleary, D., Helm, L. and Merbach, A.E., 1987. *J. Am. Chem. Soc.*, 109: 4444–4450.

[206] Richardson, D. and Alger, T.D., 1975. *J. Phys. Chem.*, 79(16): 1733–1739.

[207] Danesi, P.R., 1990. *Solv. Extn. Ion Exch.*, 8(6): 741–757.